DESIGN OF TYPE-2 FUZZY LOGIC CONTROLLERS USING META-HEURISTIC OPTIMIZATION ALGORITHMS FOR ROTARY INVERTED PENDULUM

MUKHTAR FATIHU HAMZA

FACULTY OF ENGINEERING
UNIVERSITY OF MALAYA
KUALA LUMPUR

2017

DESIGN OF TYPE-2 FUZZY LOGIC CONTROLLERS USING META-HEURISTIC OPTIMIZATION ALGORITHMS FOR ROTARY INVERTED PENDULUM

MUKHTAR FATIHU HAMZA

THESIS SUBMITTED IN FULFILMENT OF THE REQUIREMENTS FOR THE DEGREE OF DOCTOR OF PHILOSOPHY

FACULTY OF ENGINEERING
UNIVERSITY OF MALAYA
KUALA LUMPUR

2017

UNIVERSITY OF MALAYA

ORIGINAL LITERARY WORK DECLARATION

Name of Candidate: Mukhtar Fatihu Hamza

Registration/Matric No: KHA140046

Name of Degree: Doctor of Philosophy

Title of Thesis: Design of Type-2 Fuzzy Logic Controllers Using Meta-Heuristic Optimization Algorithms for Rotary Inverted Pendulum

Field of Study: Automation, Control, and Robotics

I do solemnly and sincerely declare that:

(1) I am the sole author/writer of this Work;
(2) This Work is original;
(3) Any use of any work in which copyright exists was done by way of fair dealing and for permitted purposes and any excerpt or extract from, or reference to or reproduction of any copyright work has been disclosed expressly and sufficiently and the title of the Work and its authorship have been acknowledged in this Work;
(4) I do not have any actual knowledge nor do I ought reasonably to know that the making of this work constitutes an infringement of any copyright work;
(5) I hereby assign all and every rights in the copyright to this Work to the University of Malaya ("UM"), who henceforth shall be owner of the copyright in this Work and that any reproduction or use in any form or by any means whatsoever is prohibited without the written consent of UM having been first had and obtained;
(6) I am fully aware that if in the course of making this Work I have infringed any copyright whether intentionally or otherwise, I may be subject to legal action or any other action as may be determined by UM.

Candidate's Signature Date:

Subscribed and solemnly declared before,

Witness's Signature Date:

Name:

Designation:

ABSTRACT

The type-2 fuzzy set (T2FS) is introduced to circumvent the limitations of the type-1 fuzzy set (T1FS). The main characteristic of type-2 fuzzy logic controller (T2FLC) is that, its Membership functions (MFs) are fuzzy. Therefore, it has more degree of freedom in designing varieties of systems with uncertainties. The control performance of type-1 fuzzy logic controller (T1FLC) can be improved by T2FLC because it has the advantage of footprint of uncertainty (FOU) that can be used to improve the corresponding MFs. Searching the suitable values of parameters and structure of type-2 fuzzy logic systems is a complex task. Many types of meta-heuristic algorithms have been proposed in the literature to solve this complex problem. This is presently attracting tremendous attention from researchers in this area of research. The Genetic algorithm (GA), Particle Swarm Optimization (PSO) and Cuckoo Search (CS) were considered in this research as three different paradigms that can be used in designing the optimized T2FLCs. In this research, the design of an optimized Interval Type-2 Fuzzy Proportional Derivative Integral Controller (IT2FPIDC) in cascade form for Rotary Inverted Pendulum (RIP) system is reported. The Type-1 Fuzzy Proportional Derivative Integral Controller (T1FPIDC) in cascade form was also designed using the same procedure for IT2FPIDC for fair comparisons. The parameters of the T1FPIDC and IT2FPIDC are optimized using GA, PSO and CS. This was also done to enable the comparisons between these types of meta-heuristic optimization algorithms. The goal is to stabilized the RIP at upright unstable equilibrium position and control it to follow a desired time varying trajectory. The performance indexes considered for the proposed controllers are steady state error (E_{ss}), settling time (t_s), rise time (t_r) and maximum overshoot (M_p). Experimental and simulation results indicated that the effectiveness and robustness of the proposed IT2FPIDCs on the RIP with respect to load disturbances, parameter variation and noise effects has been improved over its T1FPIDC counterpart. For example, the IT2FPIDC

has improvement between 6.1% to 33.3%, 5.7% to 35.2% and 6.6% to 20.8% in term of t_r,t_s, and E_{ss} respectively compared to optimized T1FPIDC. Also, the performance of CS base IT2FPIDC and T1FPIDC were improved with respect to some performance indexes over GA based and PSO based IT2FPIDC and T1FPIDC respectively. For example, the CS based IT2FPIDC has lower t_r,t_s, and M_p of 0.41sec, 0.76sec and 0.17degree respectively compared with GA and PSO based IT2FPIDC. Similarly, the CS based T1FPIDC has lower t_r,t_s, and M_p of 0.56sec, 1.18sec and 0.19degree respectably compared with GA and PSO based T1FPIDC. Though in all the cases the E_{ss} is all most similar. The proposed control strategy can be regarded as a promising strategy for controlling different uncertain, unstable and nonlinear systems especially in presence of noise and disturbances.

ABSTRAK

Jenis-2 set kabur (T2FS) diperkenalkan untuk memintas batasan jenis-1 set kabur (T1FS). Ciri utama dari jenis-2 kabur pengawal logik (T2FLC) adalah bahawa, fungsi Keahlian yang (MFS) adalah kabur. Oleh itu, ia mempunyai lebih darjah kebebasan dalam mereka bentuk jenis sistem dengan ketidaktentuan. Prestasi kawalan jenis-1 fuzzy logik pengawal (T1FLC) boleh diperbaiki dengan T2FLC kerana ia mempunyai kelebihan jejak yang tidak menentu (FOU) yang boleh digunakan untuk meningkatkan yang sepadan MFS. Mencari nilai yang sesuai parameter dan struktur jenis-2 sistem logik kabur adalah satu tugas yang kompleks. Banyak jenis algoritma meta-heuristik telah dicadangkan dalam kesusasteraan untuk menyelesaikan masalah yang kompleks ini. Ini kini menarik perhatian yang besar dari penyelidik dalam bidang ini penyelidikan. Algoritma Genetik (GA), Particle Swarm Optimization (PSO) dan carian cuckoo (CS) telah dipertimbangkan dalam kajian ini tiga paradigma yang berbeza yang boleh digunakan dalam mereka bentuk T2FLCs dioptimumkan. Dalam kajian ini, reka bentuk dioptimumkan Interval Type-2 Fuzzy berkadar Pengawal Integral Derivative (IT2FPIDC) dalam bentuk lata untuk sistem RIP dilaporkan. The Type-1 Kabur berkadar derivatif Pengawal Integral (T1FPIDC) dalam bentuk lata juga direka dengan menggunakan prosedur yang sama untuk IT2FPIDC untuk perbandingan yang adil. Parameter T1FPIDC dan IT2FPIDC dioptimumkan menggunakan GA, PSO dan CS. Ini juga telah dilakukan bagi membolehkan perbandingan antara jenis algoritma pengoptimuman meta-heuristik. Matlamatnya adalah untuk stabil RIP pada kedudukan keseimbangan stabil tegak dan mengawalnya untuk mengikuti pelbagai trajektori masa yang dikehendaki. Indeks prestasi dipertimbangkan untuk pengawal yang dicadangkan adalah ralat mantap negeri (E_{ss}), menetap masa (t_s), masa naik (t_r) dan terlajak maksimum. Keputusan eksperimen dan simulasi menunjukkan bahawa keberkesanan dan keteguhan IT2FPIDCs yang dicadangkan pada RIP berkenaan dengan memuatkan gangguan, perubahan parameter

dan kesan bunyi yang telah diperbaiki dari rakan sejawatannya T1FPIDC itu. Sebagai contoh, IT2FPIDC mempunyai peningkatan antara 6.1% kepada 33.3%, 5.7% kepada 35.2% dan 6.6% kepada 20.8% dalam tempoh t_r,t_s, dan E_{ss} masing-masing berbanding dioptimumkan T1FPIDC. Juga, prestasi CS asas IT2FPIDC dan T1FPIDC telah bertambah baik berkenaan dengan beberapa indeks prestasi lebih IT2FPIDC GA berasaskan dan PSO berasaskan dan T1FPIDC masing-masing. Sebagai contoh, IT2FPIDC CS berasaskan mempunyai t_r, lebih rendah, t_s, dan M_p daripada 0.41sec, 0.76sec dan 0.17degree masing-masing berbanding dengan IT2FPIDC GA dan PSO berasaskan. Begitu juga dengan T1FPIDC CS berasaskan mempunyai t_r, lebih rendah, t_s, dan M_p daripada 0.56sec, 1.18sec dan 0.19degree sopan berbanding dengan T1FPIDC GA dan PSO berasaskan. Walaupun dalam semua kes-kes yang E_{ss} adalah semua yang paling serupa juga. strategi kawalan yang dicadangkan boleh dianggap sebagai strategi menjanjikan untuk mengawal sistem yang tidak menentu, tidak stabil dan tak linear yang berbeza terutamanya dalam kehadiran bunyi dan gangguan.

ACKNOWLEDGEMENT

First of all, I would like to express my highest appreciation to Allah S.W.T the Almighty and Merciful for giving me life, strength, health, and opportunity to complete this thesis.

I would like to express my appreciations to my two eminent supervisors Professor. Dr. Imtiaz Ahmed Choudhury and Asso. Prof. Dr. Hwa Jen Yap for the excellent guidance throughout the execution of this work. I would also like to thanks, Dr. Tufan Kunbasar for his tremendous help. I would also like to demonstrate my appreciations to the management of Bayero University Kano and the TETFund for their support throughout the work. My vote of thanks also goes to Alh. Fatihu Hamza, Haj Khadija Abdullahi, Aisha Murtala and rest of my family for their prayers, for always being there for me, and motivation.

TABLE OF CONTENT

LIST OF FIGURES

LIST OF TABLES

LIST OF SYMBOLS AND ABBREVIATIONS

Abbreviations	Description
E_{ss}	steady-state error
M_p	overshoot
t_r	rise time
t_s	settling time
α_r	Reference pendulum angle
ACO	Ant Colony Optimization
ADRC	active disturbance rejection control
ALM	average linkage methods
ANFIS	Adaptive Neuro Fuzzy Inference System
ANFIS	Adaptive Neuro Fuzzy Inference
BB-BC	big bang-big crunch
BP	Back propagation
CS	Cuckoo search
DE	Differential evaluation
DOF	Degree of freedom
EM	Electromagnetism-like mechanism
FA	Firefly Algorithm
FCM	fuzzy c-mean
FLC	Fuzzy Logic Controller
FLS	Fuzzy Logic System
FOU	Footprint of Uncertainty
FPGA	Field programmable gate array
FPIDC	Fuzzy proportional integral derivative controller

GA	Genetic Algorithm
GT2FLS	General Type-2 Fuzzy Logic system
GT2FS	General Type-2 Fuzzy Set
HO	Hybrid Optimization
IAE	Integral absolute error
IP	Inverted pendulum
ISE	Integral square error
IT2FLC	Interval Type-2 Fuzzy Logic Controller
IT2FLS	Interval Type-2 Fuzzy Logic System
IT2F-PDC	Interval Type-2 Fuzzy Proportional Derivative Controller
IT2FPIDC	Interval type 2 fuzzy proportional integral derivative controller
ITAE	Integral of time weighted absolute value of error
ITSE	Integral time square error
LC	limit cycles
LMF	Lower membership function
LMI	linear Matrix Inequalities
LQG	Linear Quadratic Gaussian
LQR	Linear Quadratic Regulator
LQR	Linear quadratic regulation
LuGre	Lund Institute and Grenoble Laboratory
MF	Membership Function
MIMO	Multiple Input and Multiple Output
MSE	Mean square error
N	Negative
NM	Negative medium
NN	Neural network

P	Positive
PD	Proportional Derivative
PI	Proportional Integral
PID	Proportional Integral Derivative
PM	Positive medium
PP	Pole Placement
PP	Pole placement
PSO	Particle Swarm Optimization
RIP	Rotary Inverted Pendulum
RMSE	Root mean square error
ROLSA	Recursive orthogonal least squares algorithm
SA	Simulated Annealing
SDE-CACO	Species-Differential-Evolution and Continues ant colony optimization
SDRE	Dependent Riccati Equation
SMC	Sliding Mode Control
STA	Simple Tuning Algorithm
STP	Solid Transportation Problem
T1FCM	type-1 fuzzy clustering method
T1FLC	Type-1 Fuzzy Logic Controller
T1FLS	Type-1 Fuzzy Logic System
T1FPIDC	Type 1 fuzzy proportional integral derivative controller
T1FS	Type-1 Fuzzy Set
T1-MF	Type one fuzzy membership function
T2FLC	Type-2 Fuzzy Logic Controller
T2FLS	Type-2 Fuzzy Logic System

T2FS	Type-2 Fuzzy Set
T2-MF	Type two fuzzy membership function
TSA	Tabu Search Algorithm
TSK	Takagi segino king
UMF	Upper membership function
WSN	wireless sensor network
Z	Zero
γ	weighing factor
λ	mean value
σ	standard deviation
Φ	Arm angle
$\boldsymbol{\alpha}$	Pendulum angle

CHAPTER 1: INTRODUCTION

1.1 Background

The data available in many real-world problems such as control, time series forecasting, pattern recognition, decision making, system identification and modeling are quite associated with uncertainties in nature (Mendel, 2007). This is due to a deficiency in information which may be imprecise, incomplete, contradictory, vague, unreliable, fragmentary or deficient in some other way. Uncertainty is an inherent characteristic of information (Zadeh, 1974). In particular, most real industrial systems are nonlinear in nature and exhibit some level of uncertainty (Martinez-Soto et al., 2015). Some modern control, such as nonlinear, adaptive, variable structure and optimal control have been proposed for the past decades (Castillo & Melin, 2014). Although these control strategies exhibit a good performance, but they are complex and difficult to implement (Z. Zhang & Zhang, 2012). The conventional Proportional Integral Derivative (PID) controller exhibits good performance for linear system, and it is widely employed in the industry due to its simple structure and robustness in different operation conditions. However, the tuning of the parameters of PID accurately becomes difficult because most of the industrial plants are highly complex and have some issues such as nonlinearities, time delay, and higher order (Hassanzadeh & Mobayen, 2011). Due to the complexity of most industrial plants and the limitation of PID controller, an unprecedented interest was diverted to the applications of the Fuzzy Logic Controller (FLC). This is because it uses the expert knowledge and linguistic rules describe its control action. Also, the FLC does not require the complete mathematical model of the system to be controlled and it can work properly with nonlinearities and uncertainties (Mendel et al., 2014).

The fuzzy logic theory increased the ability of systems to cope with the uncertainty problems. The basic feature of fuzzy reasoning allows for handling a different kind of uncertainties (Zadeh, 1965). The Fuzzy Logic System (FLS) are of two types viz.:

Type 1 Fuzzy Logic System (T1FLS) and Type 2 Fuzzy Logic System (T2FLS) (Zadeh, 1974). In T1FLS, the uncertainty is represented by a precise number in a range of (0, 1) interpreted as a degree of Membership Function (MF). Given the fact that it is too difficult to know a precise value for uncertainty, working with T1FLS is more reasonable. However, some researchers argued that in cases where there is a high level of uncertainty, T1FLS has limited ability to handle it because its membership degree for each input is a crisp number (Bellman & Zadeh, 1970).

The T2FLS which uses the Type-2 Fuzzy Set (T2FS) was introduced to circumvent the limitations of the T1FLS. The main characteristic of T2FLS is that its MFs are fuzzy. Therefore, it has more Degree of Freedom (DOF) in designing verities of systems with uncertainties (Karnik et al., 1999). The control performance of T1FLS can be improved by T2FLS because it has the advantage of Footprint of Uncertainty (FOU) that can be used to improve the corresponding MF (Mendel, 2007). The T2FLS is of two types, namely, Interval Type-2 Fuzzy Logic System (IT2FLS) that uses Interval Type-2 Fuzzy Sets (IT2FSs) and General Type-2 Fuzzy Logic System (GT2FLS) that uses General Type-2 Fuzzy Sets (GT2FS) (Mendel, 2014). It was argued that in the presence of uncertainty, T2FLS is preferred over the T1FLS (Castillo & Melin, 2012). Similarly, there are several records of experimental evidence illustrating some significant improvements regarding accuracy of T2FLS over T1FLS counterpart (Baklouti & Alimi, 2013; Fayek et al., 2014; Wang, & Bi, 2015).

The design of type-2 fuzzy model based on experimental data can be categorized into two; the first is constructing the type-2 fuzzy model from the existing optimal type-1 fuzzy model, and the second is the direct design of type-2 fuzzy model from the experimental data. In both of the methods, the manual design and tuning of the MFs of T2FLS to give a proper response is a difficult task (Castillo & Melin, 2014).

Rotary Inverted Pendulum (RIP) will be used as a benchmark for testing the proposed controllers. Looking at RIP from the control point of view it exhibits many interesting and challenging properties, such as nonlinearities and instability. The RIP is in the class of underactuated mechanical systems. These features make RIP to be known widely as an experimental setup for testing a different kind of control algorithms (Ramírez-Neria et al., 2014). The RIP consists of a rotational servo motor system which drives the output gear, rotational arm, and a pendulum. The RIP has some real application such as in robotics, pointing control, aerospace systems, marine systems, mobile systems, flexible systems, and locomotive systems. At hanging position, the RIP represents a real model of the simplified industry crane application. This means that any controller works properly on RIP is expected to work properly in the field of robotics, pointing control, aerospace systems, marine systems, mobile systems, flexible systems, and locomotive systems (Chen & Huang, 2014). The main control objectives of the RIP are Swing-up control, stabilization control, switching control and trajectory tracking control.

To the best of the author's knowledge, at this moment there is no any GA or PSO or CS optimized type-2 fuzzy logic control applied to RIP. A cascade control method is effective for a system with high level of disturbances and large time error such as the RIP (Oh et al., 2009). Also, as mentioned earlier that there are many records that shows the type-2 fuzzy control strategy is effective and give robust control response for systems with high level of uncertainty and/or inaccurate model. Putting the type-2 fuzzy in cascade topology will have the advantages of type-2 fuzzy control and cascade control structure which will eventually give more robust controller for a system with uncertainties and large time error.

This study proposed the design of Interval Type-2 Fuzzy Proportional Derivative Integral Controller (IT2FPIDC) in cascaded form for control of RIP. The parameters of

the IT2FPIDC will be optimized using GA, PSO, and CS. The GA and PSO were chosen in this research in view of the fact that these algorithms are more established in the literature than other evolutionary algorithms. In addition, the GA and PSO have proven to improve performance over other algorithms in solving optimization problems (Castillo & Melin, 2012; Civicioglu & Besdok, 2013). On the other hand, CS is selected due to the pact that at this moment there is no record of the use of CS to optimized the T2FLC. Also, there is some record for other applications which shows that CS outperformed the GA and PSO (Abdelaziz & Ali, 2015; Gandomi et al., 2013). As such these three meta-heuristic optimization algorithm will be used to optimized some parameters of T2FLC and compare their performances.

The goal is to stabilize the pendulum in an upright position. The servo behavior (trajectory tracking control) of RIP is analyzed. Disturbances rejection of the proposed controller is analyzed by adding the internal noise and external disturbance to the system. Also, the controller is applied on the RIP in real time to validate the simulation results. The performances of GA, PSO and CS, is compared. Also, the designing of IT2FPIDC as an optimization dilemma that slightly altered four performance indices was formulated which includes steady state error, settling time, rise time and maximum overshoot of the response.

1.2 Problem Statement

The FLS has numerous attractive features which include easy incorporation of expert knowledge into the control law, less model dependent, robustness and easily used to model the linguistic rules. Moreover, the FLS can work properly with system uncertainties and nonlinearities (Mendel, 2007). The model of both T1FS and T2FS are described by their parameters. The T1FS is described by fewer parameters than T2FS. The FLS design DOF depends on the number of parameters associated with the FLS;

therefore, the T1FLS has less design DOF than T2FLS. The possibilities of T2FLS to outperform a T1FLS is likely based on the increase in the number of design DOF that can be used properly at a high level of uncertainty (Mendel, 2014).

Despite the importance of T2FLS, there is no systematic and comprehensive methodology for the design of T2FLS. The main problem in the design of T2FLS is the process of tuning becomes more difficult and much time consuming for increasing number of input and output of the controller. The structural and tuning parameters are required to be correctly determined for FLS to work properly (Castillo & Melin, 2012). These parameters include: MF parameters, scaling factors, inference mechanism, fuzzy rule, type of MF, fuzzy linguistic set and input/output variables to the fuzzy inference. Trial-and-error can be used to find values for these parameters, but it is not feasible especially for a high number of input and output to the controller (Maldonado et al., 2014). Due to this, there is a need of using a systematic procedure which is easier for finding the optimized values of the T2FLS design parameters. These stated problems which serve as the driving force that motivated this research.

The use of meta-heuristic optimization algorithms is proposed in this research to help in obtaining an optimal T2FLC design parameters. Meta-heuristic optimization algorithms refer to a class of soft computing techniques that relate to the searching of optimal, satisfactory or best solution for a particular problem. The solution can be the absolute best out of other alternative solutions (Martínez-Soto et al., 2014). Recently, many meta-heuristic optimization algorithms such as Genetic Algorithm (GA), Particle Swarm Optimization (PSO), Ant Colony Optimization (ACO), big-bang big-crunch optimization, bacterial foraging optimization, biogeography optimization, Chemical optimization, back propagation algorithm, simulated annealing, firefly algorithm, Tabu Search optimization, and hybrid optimization (HO) have been used for the design of a T2FLC for different applications. Nevertheless, there is some meta-heuristic algorithm

that are yet to be applied in this domain of research. Also, most of the previous work address the issue of optimizing the controller gain (scaling factor) only or optimizing the MF parameters only. The optimization of the scaling factors together with the MF parameters are ignored. Also, the optimization of inference mechanism, fuzzy rule, type of MF, fuzzy linguistic set and input/output variables to the fuzzy inference are disregarded in most cases. Moreover, most of the proposed optimal T2FLC are tested by simulation studied only. While the real-world experiment to validate the simulation work is ignored. Furthermore, the previous method normally used the objective functions which minimized one or two performance indexes. The common objective function used in the literature are Integral of the time-weighted absolute value of error (ITAE), Integral absolute error (IAE), Integral time square error (ITSE), Mean square error (MSE), Root mean square error (RMSE) and Integral square error (ISE). There is a need to have a single objective function that can minimize all the four important performance indexes (i.e. steady state error, settling time, rise time and maximum overshoot).

This study is different from the Fuzzy neural networks (FNN) which are widely known as the combination of the fuzzy logic system (FLS) and NN in which an NN expresses FLS. Basically, FNN is a learning machine that can be used to find the FLS parameters (i.e., fuzzy rules, fuzzy sets) by using approximation techniques as in NN.

1.3 Research Questions

I. Can meta-heuristic optimization algorithms be used to obtain an optimal T2FLC design parameters?

II. What will be the performance of T2FLC when the best controller scaling factor and the best membership function parameters are used?

III. Is there any improvement in performance of optimized T2FLC over T1FLC under load disturbances, parameter variation and noise effects?

IV. Can the performance of optimal T2FLC be tested using simulation and experimental studies for validation?

V. Can the single objective function be used to minimized the four important performance indexes (i.e. steady state error, settling time, rise time and maximum overshoot)?

VI. What will be the performance of GA-based, PSO-based and CS-based T2FLC at normal condition and in the presence of disturbances?

VII. What are the limitation of the controllers applied on RIP in the past?

VIII. What will be the performance of the optimal T2FLC when it applies to RIP?

1.4 Aim

The main aim of this study is to design the type-2 fuzzy logic controllers using meta-heuristic optimization algorithms for non-linear control systems. To realize the aim, the following research objectives are identified.

1.4.1 Research Objectives

I. To develop a mathematical model of rotary inverted pendulum

II. To design and develop a GA based, PSO based and CS optimization based type-2 fuzzy logic controller type-1 fuzzy logic controller for the rotary inverted pendulum.

III. To simulate the developed controllers and compare their performance under different disturbance conditions.

IV. To evaluate the Performance of the controllers experimentally and compare with the simulation results for validation.

1.5 Scope and Limitations

Within the framework of this research, the IT2FS is used. This is because the computational complexity is manageable in IT2FS compared with its GT2FS counterpart,

and the IT2FLS is more practicable. The design parameters considered for optimization in this research are the antecedent MFs parameters and scaling factor (controller gains). The GA, PSO, and CS are the three meta-heuristic optimization algorithms paradigms considered for the design of T2FLS in this research. This is because the GA and PSO are more established in the literature than other evolutionary algorithms in this domain. Also, CS is the novel metaheuristic optimization algorithms in this domain. The proposed controllers are applied on RIP for both the simulation and experiment.

1.6 Contributions

The main contribution of this study is the novel design of optimal Interval Type-2 Fuzzy PID Controller (IT2FPIDC) in cascade structure for RIP control. This contribution and the other contributions to the present study are presented as follows:

I. The novel design of optimal IT2FPIDC is proposed using CS algorithm. Also, the design of optimal IT2FPIDC using GA and PSO are proposed for comparisons of the performance of CS based IT2PIDLC.

II. Unlike previous Objective functions used in design the IT2FLC which commonly minimized one or two performance index proposed by researchers, this research proposed the objective function that can compromise between four important performance indexes namely: steady state error, settling time, rise time and maximum overshoot.

III. The optimized T1FPIDCs are designed using the same method used in IT2FPIDC (i.e. in cascade structure using GA, PSO, and CS) for fair comparisons to demonstrate the advantages of IT2FPIDC

IV. Provides analysis and synthesis of the published articles from 2012 to 2015 in the area of applying meta-heuristic optimization algorithms in the design of IT2FLS for different applications. The insight on proposed algorithms, algorithms

compared with, other controllers compared with IT2FLC, and major findings are highlighted.

V. The review on the application of RIP as a benchmark for testing different types of the controller is provided. This include the friction analysis in the joints, linear controllers, nonlinear time-invariant controllers, self-learning and adaptive controllers.

VI. The research has proposed linear and nonlinear mathematical model of RIP using both Newton's Euler-Lagrange and Kane's methods. The proposed models are found to be more accurate than the previous model provided by the researchers. The Matlab model for both mathematical models are also provided.

VII. The proposed intelligent optimal IT2FLC has been added as an alternative to the controllers for RIP that are already discussed by researchers in the literature.

VIII. The experimental and simulation results of the proposed IT2FPIDC indicate the advantages and disadvantages of GA, PSO and CS algorithms based on the performance index used.

IX. This study used energy based controller to explain all the control objectives of the RIP

1.7 Flowchart of Research activities

The research activities are executed based on the following flowchart.

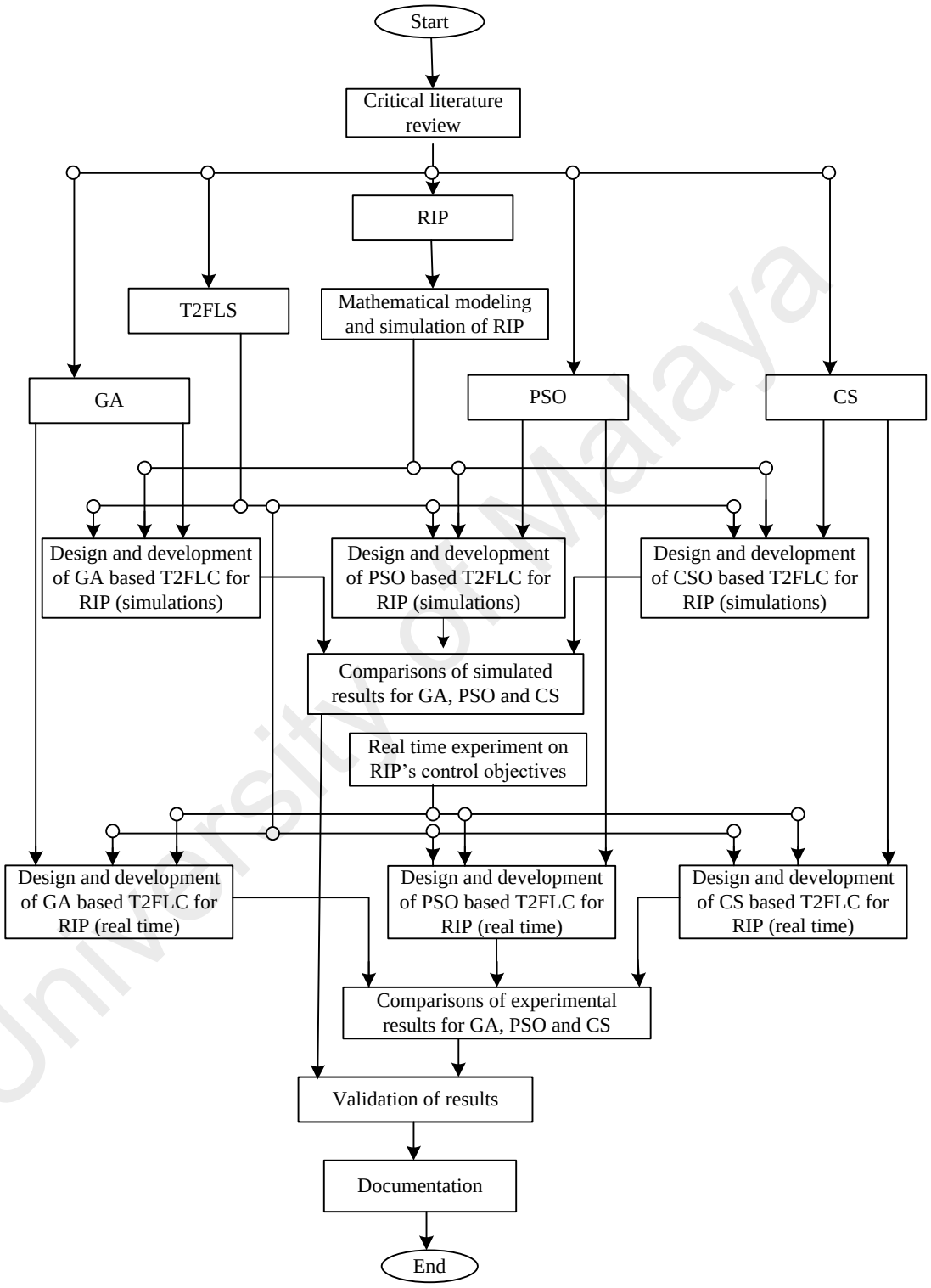

Figure 1.1: Flowchart of project activities

1.8 Thesis Organization

1.8.1 Chapter 1: Introduction

This chapter introduced the general research background, including problem statement, research questions, aim of the research, objectives, scope and limitation, Contribution of the studies, motivation, and the flowchart for the research activities.

1.8.2 Chapter 2: Meta-heuristic Optimization Algorithms in Design T2FLS

The recent advances in the use of meta-heuristic optimization algorithms in design T2FLS in intelligent control, prediction, classification, clustering and pattern recognition is provided in this chapter. This include the brief overview of T2FLS, structure of general fuzzy PID controller, review on optimization of T2FLS using HO, GA, PSO and other meta heuristic optimization algorithms. Future trend and a general overview of this domain of research were also presented. The gap of the research was found.

1.8.3 Chapter 3: Rotary Inverted Pendulum as a Benchmark for Testing Control Algorithms

The Current development on using Rotary Inverted Pendulum as a benchmark for testing linear and nonlinear control algorithms based on simulations and experiments was provided in this chapter. The linear and nonlinear mathematical model of RIP was developed. This is based on Kane's and Newton-Euler Lagrange method including the Matlab model. The energy based controller for RIP was used to explain the control objectives of RIP. The effect of friction and friction compensation in RIP is provided. Resent review on different types of controllers applied to RIP was discussed. The limitation of the previous approach and the gap for the research was also provided.

1.8.4 Chapter 4: Methodology

The method used for modeling and simulation was explained in this chapter. This include the mathematical model and cascade control method. The problem formulation

including the parameter setting for GA, PSO and SC was explained for both simulation and experiment. The performance index, cost value standard deviation and mean value for GA, PSO and CS was discussed. The method for experiments and validation was provided in this chapter.

1.8.5 Chapter 5: Results and Discussions

The best simulation and experimental results found for GA based, PSO based and CS based IT2FLC is presented in this chapter. This include the comparisons for different weighing factor. Reference tracking and disturbance rejection ability of the proposed controllers was analyzed. The validation of the simulation with experiments are presented. The meaning and the impact of the result found was discussed.

1.8.6 Chapter 6: Conclusion and Recommendations

This chapter discusses the general conclusions made from the findings of this research. The future work to be conducted was highlighted. Recommendation are also made.

CHAPTER 2: META-HEURISTIC OPTIMIZATION ALGORITHMS IN DESIGN T2FLS

2.1 Introduction

This chapter presents a review of the recent advances in the use of meta-heuristic optimization algorithms in optimizing the design of T2FLS in intelligent control, prediction, classification, clustering and pattern recognition. The comprehensive literature review of the studies in this domain was conducted to provide a state-of-the-art review to prevent replication of what has already been accomplished. Additionally, the clear perspective with a broad and in-depth review of the research studies in this domain was provided. Moreover, the brief overview of T2FLS, structure of general fuzzy PID controller, review on optimization of T2FLS using hybrid optimization (HO), GA, PSO and other meta heuristic optimization algorithms was presented. Future trend and a general overview of this domain of research were also presented. The gap of the research based on optimization of T2FLC was highlighted.

2.2 Type-2 Fuzzy Logic Systems

The idea of FLS and T2FS was pioneered by Zadeh in 1965 and 1975 respectively (Zadeh, 1965, 1974). A concise overview of T2FLS was presented in this section with the intention of providing readers with the basic knowledge of how T2FLS operates to achieve its objective.

Imagine blurring the type-1 membership function (T1-MF) as shown in Figure 1(a) by moving the points on the triangle from left to right. Type-2 membership function (T2-MF) was formed as shown in Figure 1(b).

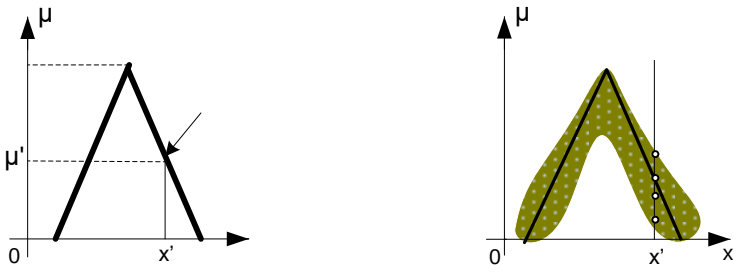

(a) (b)

Figure 2.1: (a) Type-1 MF, (b) Blurred type-1 MF

Considering a specific value of x, say *x'*, in T1-MF has a specific crisp value μ. On the other hand, in blurred T1-MF, it does not have a single value. Instead, the MF has many values with different weight at all the point where the vertical line intersects the blur. The amplitude distribution can be assigned to all these points. Doing this for all $x \in X$, a three dimensional MF was created that characterised a T2FS (Mendel et al., 2006). A T2FS $\tilde{A}$, is charaterised by T2-MF $\mu_{\tilde{A}}(x,y)$, for $x \in X$ and $u \in J_x \subseteq [1,0]$, that is.,

$$\tilde{A} = \left\{\left((x,y),\mu_{\tilde{A}}(x,y)\right) \middle|\ \forall\, x \in X, \forall\, y \in J_x \subseteq [0,1]\right\} \tag{2.1}$$

in which $0 \leq \mu_{\tilde{A}}(x,u) \leq 1$

The primary membership of x can be represented as: $J_x \subseteq [0,1]$ and the secondary set is $\mu_{\tilde{A}}(x,u)$ which is T1FS. Therefore, a type-2 membership grade should lie between or be equal to 0 and 1 (Karnik et al., 1999). Each primary membership has its corresponding secondary membership (also lies in [1,0]) that defines its possibilities. The uncertainty can be represented by foot print of uncertainty (FOU) region (Karnik & Mendel, 1998a).

As stated earlier, the T2FLS are of two types, namely IT2FLS and GT2FLS. The scope of this research is on IT2FS. All the secondary grades of the IT2FS are equal to 1,

and it is completely described by upper MF and lower MF (UMF and LMF) as shown in Figure 2.2.

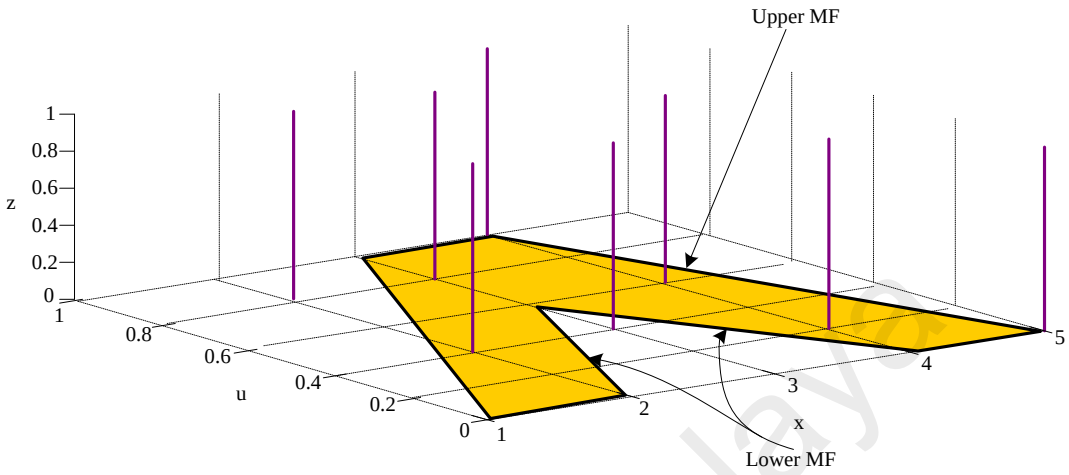

Figure 2.2: Interval type-2 fuzzy set

The primary membership is called J_x, and its associated possible secondary MFs that can be trapezoidal, triangular, interval, etc. When the interval secondary MF is employed an Interval T2FS (IT2FS) is obtained (Karnik & Mendel, 1998a). In other words, when $\mu_{\tilde{A}}(x,u) = 1$ for $\forall u \in J_x \subseteq [0,1]$, an IT2FS is constructed as shown in Figure 2.3. Detailed explanation and formulation of IT2FSs can be found in (Kumbasar & Hagras, 2015; Mendel et al., 2014).

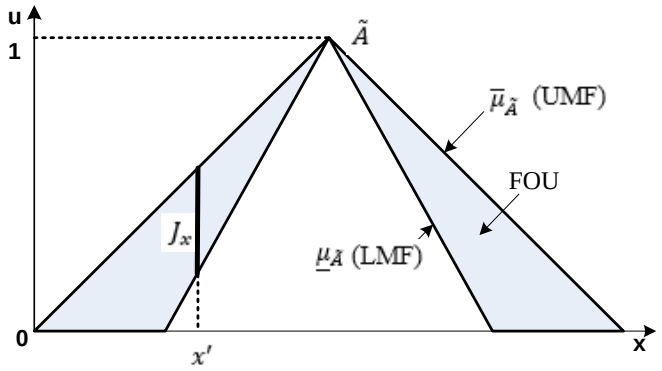

Figure 2.3: Illustration of an IT2FS

In the case when $\mu_{\tilde{A}}(x,u) \neq 1$ for $\forall u \in J_x \subseteq [0,1]$, then a General T2FS (GT2FS) is obtained. Detailed explanation and formulation of GT2FSs are presented in (Kumbasar & Hagras, 2015; Mendel et al., 2014). The triangular MF and its corresponding secondary MF for T1FS, IT2FS and GT2FS are shown in Figure 2.4.

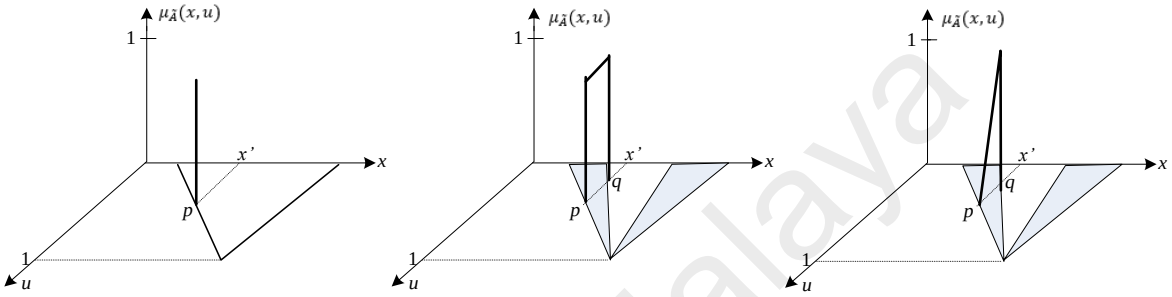

(a) (b) (c)

Figure 2.4: Secondary MF at $x = x'$ for (a) a T1FS, (b) an IT2FS, (c) a GT2FS

In type-2 fuzzy logic literature, the main research focus is on IT2FSs and thus on IT2FLSs. This lies because IT2FSs are computationally less expensive in comparison with its General counterpart and can be defined easily by only its UMF and LMF. The generation of the IT2FSs is usually accomplished by extending/blurring its T1 counterpart (Mendel et al., 2014). In Figure 2.5, various IT2FSs are generated with respect to their baseline T1FSs. In Figure 2.5 (a), the IT2FS is constructed by providing uncertainty at the end points of its T1 counterpart while in Figure 2.5 (b) the uncertainty is provided at the core of the T1FSs. The IT2FSs sketched in Figure 2.5 (c) is the general case where both the end points and the core of the T1FS is blurred. It can be easily observed from Figure 2.5; the IT2FS has more design parameters to be determined in comparison with its T1 counterpart. The IT2FS construction methods can be roughly categorized into two, the first is to construct the type-2 fuzzy sets from an existing T1FS, and the second is the direct design of IT2FSs from either collected experimental data by employing clustering

methods or NN structures. Recently, various meta-heuristic optimization algorithms are employed to construct the optimal IT2FSs.

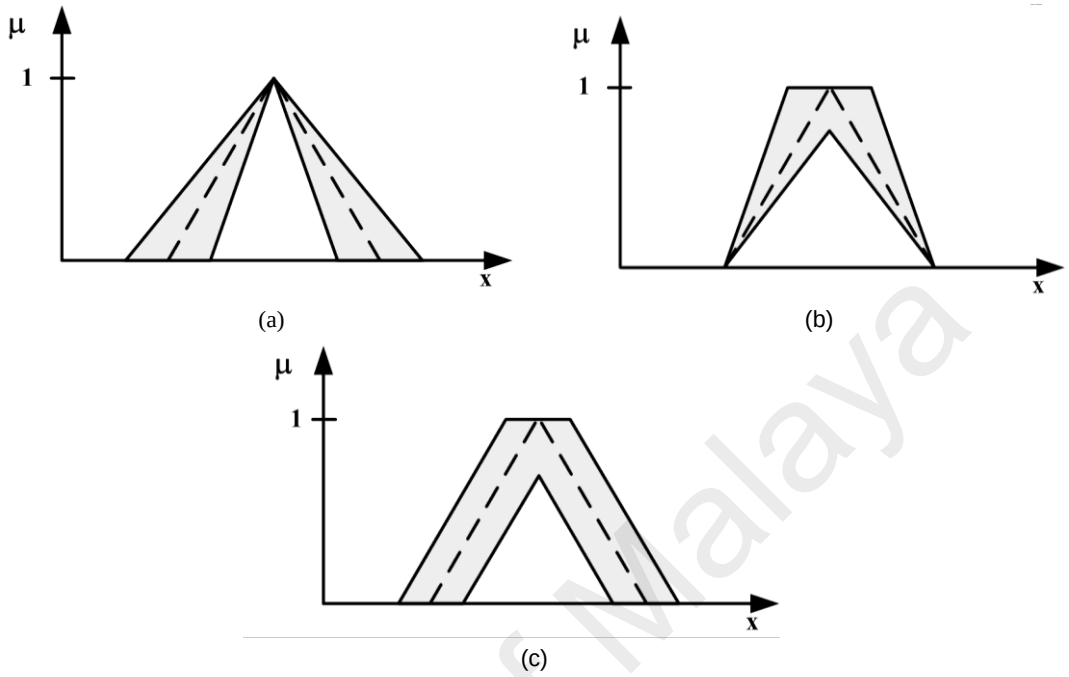

Figure 2.5: Illustration of various IT2FS with their baseline T1FSs (dashed line)

Like T1FLS, the T2FLS is using IF-THEN rules but its antecedent and/or consequent sets are type-2. The type-2 Takagi-sugeno-king (TSK) FLS are of three different models based on their structure (Baron, & Balazinski, 2006) as describe in Table 2.1.

Table 2.1: Structure of type-2 fuzzy TSK

Type-2 TSK FLS	Antecedents	Consequents
Model I	Type-2 fuzzy set	Type-1 fuzzy set
Model II	Type-2 fuzzy set	Crisp number
Model III	Type-1 fuzzy set	Type-1 fuzzy set

Furthermore, T2FLS consist of the following blocks: fuzzification, inference, and output processing. The output processing block comprises of the type reduction and the defuzzification blocks as shown in Figure 2.6. For a better illustration, a fuzzy system with two crisp inputs and one crisp output was used in Figure 2.6, which is the same for

both IT2FLS and GT2FLS. Each of the blocks is explained in brief in sections 2.2.1 to 2.2.4. In this research, the interval type-2 fuzzy Mamdani system with centre-of-set type reduction was used for illustration (IT2FS TSK, GT2FS Mamdani, and GT2FS TSK also exist) (Mendel, 2007).

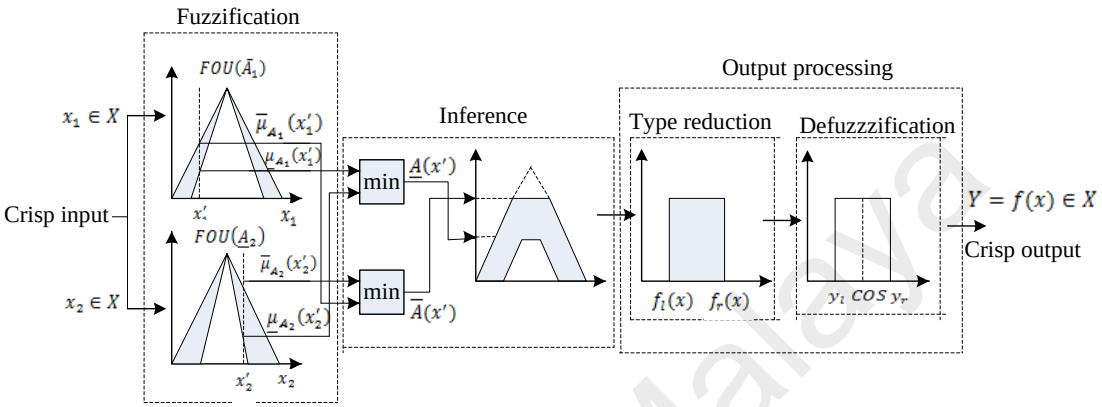

Figure 2.6: Type-2 fuzzy logic system structure

2.2.1 Fuzzification

The fuzzifier in T1FLS and T2FLS are doing the same work, which is transforming numeric vector entries $X = (x_1 \dots x_p)^T \in X_1 * X_1 * \dots * X_p \equiv X$ in to $\tilde{A}_x$ (T2FS) defined in X. Given the singleton numeric inputs, the mapping can be performed as follows (Mendel, 2007):

$$\left.\begin{array}{l} \mu_{\tilde{A}_x}(x) = 1/1 \text{ with } \; X = X', \\ \mu_{\tilde{A}_x}(x) = 1/0 \text{ , for } \forall X \in X \text{ with } x \neq x' \end{array}\right\} \tag{2.2}$$

Equation (2.2) shows that $\mu_{\tilde{x}_i}(x_i) = 1/1$ when $x_i = x_i'$ and $\mu_{\tilde{x}_i}(x_i) = 1/0$ when $x_i \neq x'_i$ for all $i = 1, \dots, p$.

2.2.2 Rules

Both T1FLS and T2FLS use IF-THEN rules. In T2FLS, the antecedent and/or consequent MFs are represented by T2FSs. For T2FLS characterized by M number of

rulas with p inputs $x_1 \in X_1, \ldots, x_p \in X_p$ and one output $y \in Y$. The i^{th} rule can be expressed as Equation (2.3), (Mendel et al., 2014).

$$\mathrm{R}^i : \text{IF } x_1 \text{ is } \tilde{\mathrm{F}}_1^i \text{ and} \ldots \text{and } x_p \text{ is } \tilde{\mathrm{F}}_p^i, \text{ THEN } y \text{ is } \tilde{\mathrm{Y}}^i \tag{2.3}$$

where $\tilde{F}_k^i$ $(k = 1, \ldots p)$ are type -2 antecedent fuzzy sets, $i = 1, \ldots, M$, and $\tilde{\mathrm{Y}}^i$ the output of the i^{th} rule. The assumption here is that, all antecedent and consequent fuzzy set in mamdani rules are type-2.

2.2.3 Inference

The inference mechanism in T2FLS is same as that in T1FLS. It is a rule combination to produce a mapping from some input T2FSs to output T2FSs. It is necessary to calculate the intersection, union, and composition of type-2 relations to realize this mapping (Mendel, 2001). Equation (2.3) can be rewritten as:

$$\mathrm{R}^i : \tilde{F}_1^i \times \ldots \times \tilde{F}_p^i \to \tilde{Y}^i = \tilde{A}^i \to \tilde{Y}^i, \; i = 1, \ldots, M \tag{2.4}$$

$R^i$is described by the MF $\mu_{R^i}(X, y)$ for $X = (x_1, \ldots, x_p)$,

where

$$\mu_{R^i}(X, y) = \mu_{\tilde{A}^i \to \tilde{Y}^i}(X, y) = \mu_{\tilde{F}_1^i}(x_1) \prod \ldots \prod \mu_{\tilde{F}_p^i}(x_p) \prod \mu_{\tilde{Y}^i}(y) =$$

$$\left[\prod_{l=1}^{p} \mu_{\tilde{F}_l^i}(x_l)\right] \prod \mu_{\tilde{Y}^i}(y) \tag{2.5}$$

The p-diamentional input to $R^i$is given by T2FS $\tilde{A}_x$ whose MF is

$$\mu_{\tilde{A}_x}(X) = \mu_{\tilde{x}_1}(x_1) \prod \ldots \prod \mu_{\tilde{x}_p}(x_p) = \prod_{l=1}^{p} \mu_{\tilde{x}_l}(x_l) \tag{2.6}$$

where $\tilde{X}_l (l = 1, \ldots, p)$ are the labels of the fuzzy sets describing the inputs. Each rule determines the T2FS $\tilde{B}^i = \tilde{A}_x \circ R^i$ such that:

$$\mu_{\tilde{B}^i}(y) = \mu_{\tilde{A}_x \circ R^i} = \coprod_{x \in X} \left[\mu_{\tilde{A}_x}(X) \prod \mu_{R^i}(X, y)\right] y \epsilon G i = 1, \ldots, M \quad (2.7)$$

this Equation is the input-output relation in Figure 2.6 between the T2FS that excite a single rule in the inference engine and the T2FS at the output of that engine.

In this study, the IT2FS was used in the FLS and meet under product *t*-norm. Therefore, the result of the input and antecedent operations which are contained in the firing set $\prod_{l=1}^{p} \mu_{F_{l_l}}(x_l' \equiv F^i(X'))$, is an interval T1FS (Castillo, 2012):

$$F^i(X') = \left[\underline{f}^i(X'), \overline{f}^i(X')\right] \equiv \left[\underline{f}^i, \overline{f}^i\right], \quad (2.8)$$

where

$$\underline{f}^i(X') = \underline{\mu}_{\tilde{F}_1^i}(x_1') * \ldots * \underline{\mu}_{\tilde{F}_p^i}(x_p') \quad (2.9)$$

and

$$\overline{f}^i(X') = \overline{\mu}_{F_1^i}(x_1') * \ldots * \overline{\mu}_{F_p^i}(x_p') \quad (2.10)$$

2.2.4 Output Processing

The output processing constitutes the type reduction that generates the T1FS, and fuzzifier that converts the generated T1FS to the crisp output (Dongrui, 2013). There are many kinds of type-reduction in literature, which includes centre-of-sets, centroid, height, and modified height (Karnik & Mendel, 1998; Karnik & Mendel, 1998b; Mendel, 2015). In this study, the centre-of-set type reduction will be used as follows (Karnik et al., 1999; Qilian & Mendel, 2000).

$$Y_{cos}(Y^1, \ldots, Y^M, F^1, \ldots, F^M) = [y_l, y_r] = \int_{y^1}^{\cdot} \ldots \int_{y^M}^{\cdot} . \int_{f^1}^{\cdot} \ldots \int_{f^M}^{\cdot} . 1 \Big/ \frac{\sum_{i=1}^{M} f^i y^i}{\sum_{i=1}^{M} f^i} \quad (2.11)$$

where Y_{cos} is the interval set determind by y_l and y_r (two end points); $f^i \epsilon F^i = \left[\underline{f}^i, \overline{f}^i\right]$; $y^i \epsilon Y^i = \left[\underline{y}^i, \overline{y}^i\right]$; $i = 1, \ldots, M$; and M is the number of rules.

It can be observed that each set on the right-hand side of Equation (2.11) is an interval T1FS, hence the left hand of that Equation($Y_{cos}(Y^1, \ldots, Y^M, F^1, \ldots, F^M)$) is also interval T1FS. Therefore, $Y_{cos}(Y^1, \ldots, Y^M, F^1, \ldots, F^M)$ can be found by just computing the y_l and y_r(Qilian & Mendel, 2000). Karnik and Mendel (Karnik & Mendel, 1998a; Karnik & Mendel, 1998) have shown that, y_l and y_r depend on maximum of $\underline{f}^i$ or $\overline{f}^i$ values as follows:

$$y_l = \frac{\sum_{i=1}^{M} f_l^i y_l^i}{\sum_{i=1}^{M} f_l^i}, \tag{2.12}$$

and

$$y_r = \frac{\sum_{i=1}^{M} f_r^i y_r^i}{\sum_{i=1}^{M} f_r^i} \tag{2.13}$$

where f_l^i and f_r^i denotes the firing strength membership grade [either $\underline{f}^i$ or $\overline{f}^i$] contributing to the left-most point y_l and right most point y_r respectively.

The fuzzifier of an interval type-2 Fuzzy can be calculated as follows (Qilian & Mendel, 2000):

$$y(x) = \frac{y_l + y_r}{2} \tag{2.14}$$

2.3 Structure of General Fuzzy PID Controller

For easy demonstration, the two inputs (error $e(t)$ and the error variation$\Delta e(t)$,)) and one output u direct action type of fuzzy PID controller (FPIDC) is used as shown in Figure 2.7. The number of input/output depends on the problem to be solved. In most real

applications, the inputs are more than two. Detailed on fuzzy PID, fuzzy PD and fuzzy PI structures and their relationships are presented in literatures (Aliasghary et al., 2013; Mendel et al., 2014). The structure of FPIDC was formed from fuzzy PD controller with an integrator at the output. The output u is the control signal and is define by the following equation 2.15 (Kumbasar & Hagras, 2015).

$$u = \delta U + \gamma \int U dt \tag{2.15}$$

The scaling factors K_p, K_D, γ, δ are used to normalise the input/output of the FLC. The $e(t)$ and $\Delta e(t)$ are normalized by the scaling factor (K_p, K_D) to the common interval (-1, 1) in which the MFs of the input are defined. After the normalization, $e(t)$ and $\Delta e(t)$ are converted to E and ΔE respectively. γ and δ are used to map the output U onto the actual output domain u. In Figure 2.7, there are two blocks that can be used to introduce the uncertainty in the system either in series with controller and plant or in the feedback or both. The structure in Figure 2.7 is the same for T1FLC, IT2FLC and GT2FLC.

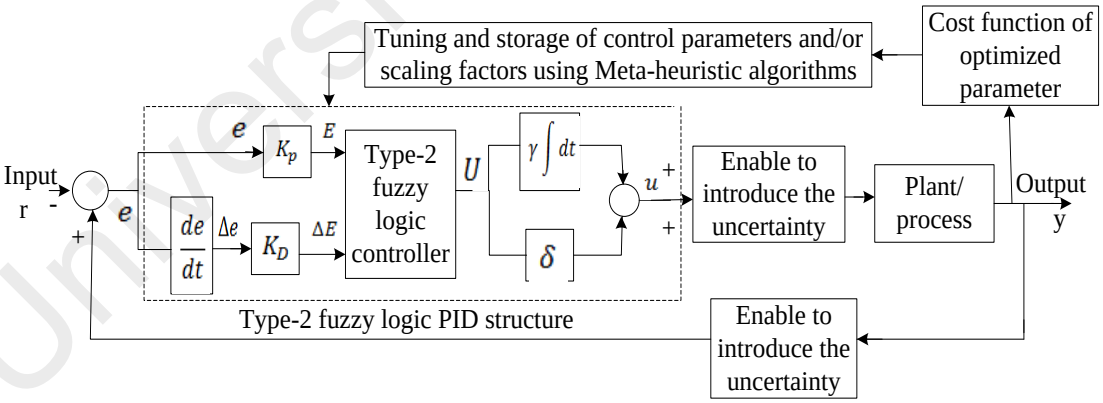

Figure 2.7: Comprehensive block diagram of FLC (FLPIDC)

The design parameters of FLC can be categorized into two, namely: tuning parameters and structural parameters as illustrated in Figure 2.8. The tuning parameters include MF parameters and scaling factors, and are to be adjusted offline at the design

phase. Subsequently, the optimal parameters are fixed during the operation phase except in a case of continuous adaptation (Kumbasar & Hagras, 2015; Mendel et al., 2014). The structural parameters include the inference mechanism, fuzzy rule, type of MF, fuzzy linguistic set and input/output variables to the fuzzy inference. Normally, the structural parameters are determined during the offline design phase (Mendel & Rajati, 2015; Sánchez et al., 2015).

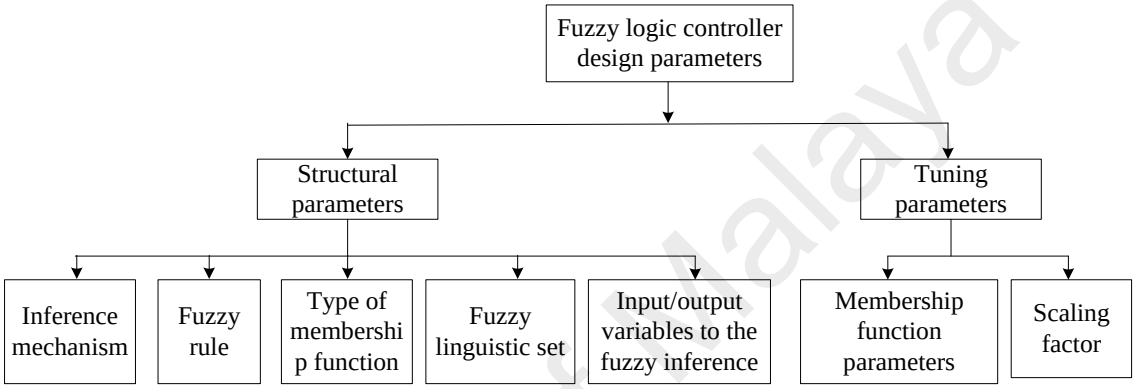

Figure 2.8: Design parameters of FLC

2.4 Meta-heuristic Optimization Algorithms

The meta-heuristic optimization algorithm refers to a searching algorithm that can give a significantly good solution to an optimization problem particularly the problem with limited computation capability or imperfect or incomplete information. It samples a set of solutions which is tremendous to be completely sampled and make some assumption about the given optimization problem. There are many types of meta-heuristic optimization algorithm which include GA, PSO, ant colony optimization, Big-Bang Big-Crunch optimization, Bacterial foraging optimization, biogeography optimization, Chemical optimization, back propagation algorithm, simulated annealing, firefly algorithm and tabu Search optimization among others. The brief introduction on GA, PSO and CS are presented in the following sections.

The critical issues in these optimization algorithms on the design of FLS are as follows (Nguyen & Meesad, 2013):

I. Encoding (representation) of fuzzy logic in the corresponding optimization paradigm, for example, the feature of FLS has to be encoded in the form of chromosome for GA, particle for PSO, Firefly for firefly algorithm, etc.;

II. Determination of the boundaries of parameters to be optimized (solution space);

III. Choosing a suitable objective function.

2.4.1 Genetic Algorithm (GA)

The basic foundation of GAs was proposed in 1975 by John Holland in Haupt & Haupt (2004). It is based on Darwin's ideas. Darwin's stated that in a computing environment, the stronger individuals are more likely to be the winners. GA is a meta-heuristic search algorithm based on natural selection and genetic process (Sivanandam & Deepa, 2008). In GA, the potential solution to a problem is an individual which can be represented by a set of parameters. These parameters are just like a gene of a chromosome and can be represented by the string of values in binary form (Herrera, 2008). The fitness value is used to test the degree of goodness of the chromosome for solving a problem that is directly related to the objective value. The operators employed in a simple GA include selection, crossover, and mutation (Herrera, 2008). GAs are often regarded as function optimizers, and they have been applied in many optimization problems. In particular, the use of GAs for fuzzy systems design equip them with the adaptation and learning capabilities which brought about genetic fuzzy systems (GFSs) (Herrera, 2008). Genetic learning processes cover different levels of complexity according to the structural changes created by the algorithm (Jong, 1988), from optimization of parameters (simplest case) to learning the rule set of a rule-based system (highest level of complexity) (Goldberg, 2002). The optimization of the parameter is the approach used to adapt a different variety of fuzzy system, as in genetic neuro-fuzzy systems or genetic fuzzy clustering (Tang, & Kwong, 2012). It was reported in Cordón et al. (2001) that genetic fuzzy rule-based systems is the most well-known types of GFSs. It is essential to differentiate between

learning and adaptation (tuning) problems in fuzzy systems. The Learning process performs a more elaborated search in the space of possible rule-base or entire knowledge base, irrespective of the predefined set of rules. Also, learning involves the process of automated fuzzy rule sets design that starts from scratch. On the other hand, the adaptation process assumes a predefined rule-base and have the objective of searching a set of optimal parameters for the data-base, scaling function, and MF. Also, adaptation includes the optimization of existing fuzzy rule-based systems.

The flowchart for simple GA for optimization of T2FLS is shown in Figure 2.6.

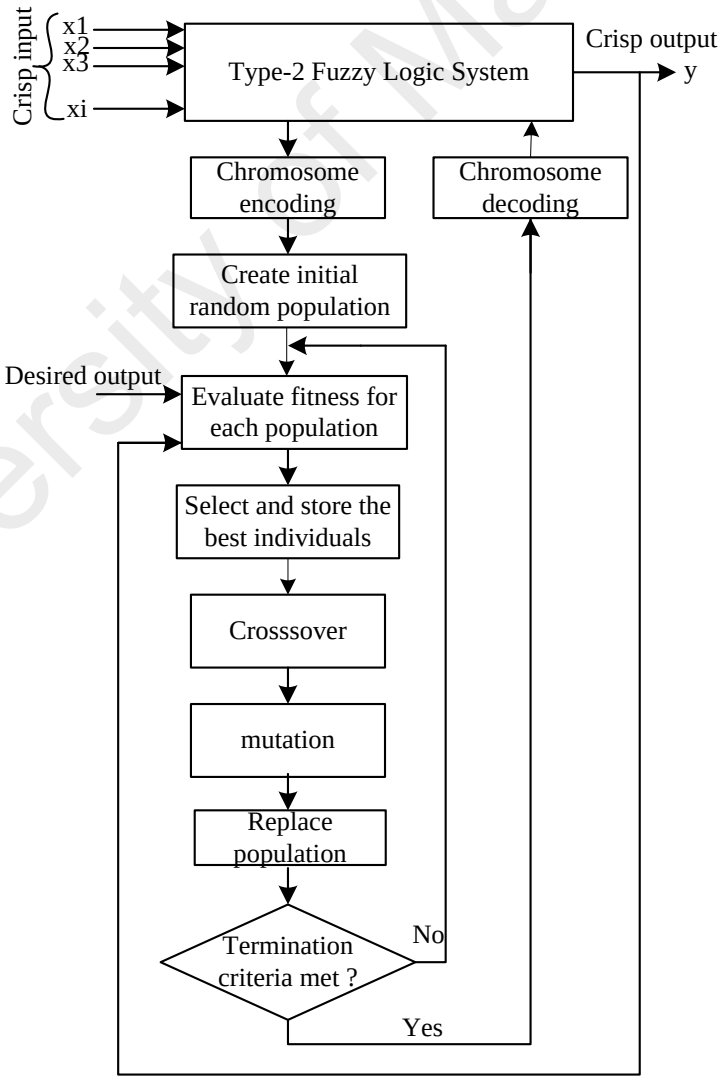

Figure 2.9: Flowchart of simple GA for optimization of T2FLS

2.4.2 Particle Swarm Optimization (PSO)

The PSO was introduced in 1995 by Kennedy and Eberhart (1995). It is an optimization algorithm based on social and population behaviour, just like flocking of bird or fish schooling. The population in PSO is called swarm that can contain many particles. At each iteration t, the position P_t^i of the i^{th}particle is updated based on Equation (2.16). The set S is updated to the next iteration using Equation (2.16) Dehuri et al. (2009).

$$\left.\begin{aligned} V_{t+1}^i &= V_t^i + c_1 r_1\left(P_{best}^i - P_t^i\right) + c_2 r_2\left(g_{best} - P_t^i\right), \\ P_{t+1}^i &= P_t^i + V_{t+1}^i \end{aligned}\right\} \tag{2.16}$$

where P_{best}^i is the best position attained for the individual particle and g_{best} is the best position attained for the particle among all the population. r_1 and r_2 are random numbers between 0 and 1, while c_1 and c_2 are position constants learning rate.

Modified PSO in the form of a constriction factor X, was introduced in literature (Clerc & Kennedy, 2002; Russell & Shi, 2001) and is given by Equations (2.17) and (2.18). In this, X controls the entire three components in the update velocity rule, inorder to reduce the velocity as search progresses.

$$V_{t+1}^i = X\left[V_t^i + c_1 r_1 (P_{best}^i - P_t^i) + c_2 r_2 (g_{best} - P_t^i)\right] \tag{2.17}$$

$$X = \frac{2}{\left|2-\beta-\sqrt{\beta^2-4\beta}\right|},\ \beta = c_1 + c_2 > 4. \tag{2.18}$$

The velocity is restricted within $[-V_{max}, +V_{max}]$. If the velocity deviates from this range it has to be forced to be within the range (Eberhart & Shi, 2001).

PSO algorithm can be implemented easily and demonstrates stable convergence when compared with other optimization algorithms as reported in the following literatures

(Chiou & Liu, 2009; Maldonado et al., 2013; Oh et al., 2011). The following advantages of PSO over other conventional optimization method was discussed in literature Oh et al. (2011) as follows: PSO is less vulnerable to being trapped in local minima because it is population-based search algorithm and exhibits implicit parallelism. PSO can also easily deal with non-differentiable and nonlinear objective functions. In addition, PSO is more robust and flexible than conventional methods, this is because it uses probabilistic transition rules rather than deterministic ones (Oh et al., 2011). Moreover, PSO has a unique feature of the suppleness to accomplish a sound balance between the local and global exploration of the search space. This enhances the overall search capabilities and overcomes the premature convergence problem, unlike GA and other heuristic algorithms. The quality of the solution in PSO is independent of the initial population, unlike the traditional methods (Shahsadeghi et al., 2014). The flowchart for simple PSO applied to a T2FLS is shown in Figure 2.7.

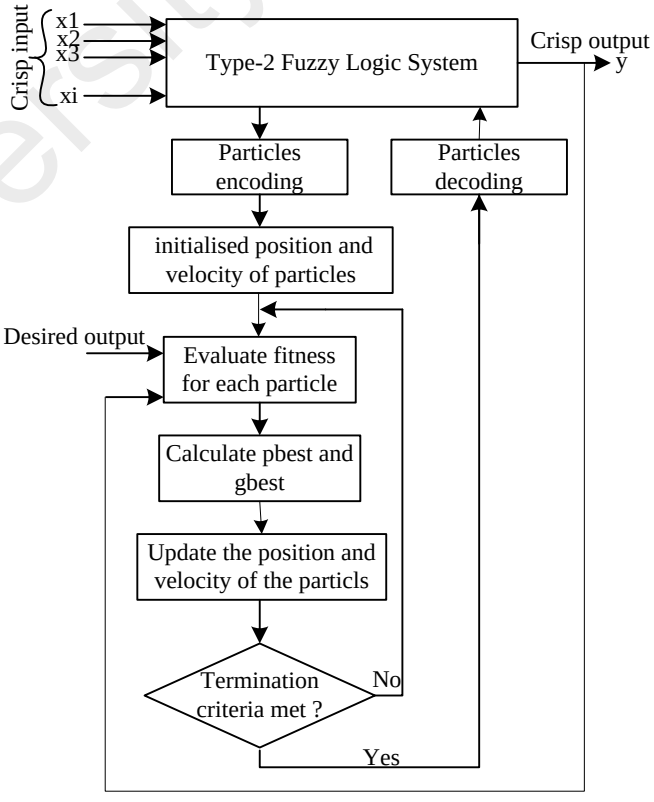

Figure 2.10: Flowchart for simple PSO for optimization of T2FLS.

2.4.3 Cuckoo Search Optimization

The CS algorithm is developed by Yang and Deb (2009, 2010). The CS currently draws attention from researchers that are using meta-heuristic algorithms for solving optimization problems. Investigations on CS are growing quickly within the literature with applications covering many areas (Yang & Deb, 2014). Recently, CS has been applied in numerous areas with encouraging performances e.g., power system stabilization (Elazim & Ali, 2016), forecasting (Sun et al., 2016), Intelligent controllers (Dash et al., 2015), etc. The global search of CS uses Lévy flights non-standard random distribution with infinite mean and variance. Therefore, exploration of search space by CS is closer to the Nature, where resources are distributed non-uniformly. Hence, a global convergence can be better guaranteed (Yang, 2014).

2.4.3.1 Origin of the Cuckoo Search Algorithm

The origin and basic theoretical background of CS are described in this section, specifically, the origin of the algorithm, common characteristics, representation of solutions, the generation of new solutions, evaluation function, replacement and termination condition.

The beautiful sounds and aggressive reproduction strategy of a cuckoo makes it a fascinating bird. Within a broader view, the cuckoo family of birds are divided in three major species, i.e., Musophagidae, Cuculidae and Opisthocomidae. Cuckoos can be found across the globe. There are over 100 different species worldwide, whereas only Cuculidae can be found in Europe. Typically, cuckoos feed on caterpillars. Interestingly, the Ani and Guira cuckoo species can lay eggs in a communal nest. In order to increase their hatching probability, these two cuckoo species remove eggs from other nests. Some other cuckoo species engage the obligate brood parasitism by laying their eggs in the nests of other host birds. It has been estimated that half of the cuckoos do not hatch their own eggs

but rather resort to parasitism. The aggressive reproduction strategies of the cuckoo's breeding parasitism are summarized as follows: Typically, a female cuckoo lays between 6 to 22 eggs with color matching the host eggs. In nature, different species produce different colored eggs. The size of the eggs varies within 16.3 mm to 21.9 mm. A female cuckoo hides close to an appropriate host nest in order to use the opportunity by dumping her eggs in the host nest. Typically, the new host birds are aggressively evicted by the new born cuckoos (Davies, 2010). The three types of breeding cuckoo parasitism strategies are as follows: (1) intraspecific breeding parasitism, (2) cooperative breeding, and (3) nest takeover. Direct conflict between the host birds and cuckoos is however possible. The host birds either abandon the nest or throw the alien eggs out of the nest to produce new eggs.

2.4.3.2 Cuckoo Search Algorithm

The behavior of the cuckoo is simulated in CS optimization to provide better performances than other distribution-based random walks when exploring large scale search spaces. The three major ideas of cuckoo's behavior are proposed by Yang & Deb (2009) for rules governing the CS optimization algorithm as follows:

1. Each cuckoo lays one egg at a time and dumps it into a randomly-chosen nest.
2. Nests with the eggs of optimal quality will move to the next generation.
3. The available host nest is fixed and the egg laid by a cuckoo is discovered by the host bird with the probability of the worst nests being abandoned ($pa \in [0,1]$).

In the CS algorithm, the quality or fitness of a solution is modelled proportional to the objective function value. Without difficulties, getting an optimized solution to a complete problem using CS does not require a comprehensive search. Each individual solution corresponding the host *nest* represents the position of the cuckoo's egg in the CS algorithm. Generally, the position is defined as (Yang & Deb, 2014):

$$X_i^{(t)} = \left\{x_{i,j}^{(t)}\right\}, \qquad \text{for } i = 1 \ldots n \quad \text{and} \quad j = 1 \ldots D \tag{2.19}$$

where t denotes the current generation, n the number of host nests within the population and D the dimensionality of the problem. In the CS algorithm, the initial value of the j^{th} attributes in the i^{th} particle $x_{i,j}^{(0)}$ is typically determined as follows:

$$x_{i,j}^{(0)} = U(0,1).\left(u_j - l_j\right) + l_j \tag{2.20}$$

where $U(0,1)$ determines the random value drawn from the uniform distribution within the interval [0,1], u_j and l_j are the upper and lower boundaries of the j^{th} attributes, respectively. In each generation, the CS algorithm controls these boundaries as follows: If the value of the attributes underflows, this value is updated with the corresponding lower bound, while if this value overflows, it is updated with the corresponding upper bound. The general form of the CS algorithm which is based on a global random-walk appropriate for exploration of the search space through Lévy flights is described as follows:

$$X_i^{(t+1)} = X_i^{(t)} + \vartheta \oplus \text{Lévy}\,(\mathrm{S}, \lambda) \qquad \mathrm{S} \gg S_0 > 0, \tag{2.21}$$

where $t \in [1, MaxGeneration]$ is the number of current generation, where the *MaxGeneration* is the predetermined number of maximum generations, ϑ is the step size scale factor, s the step size, λ is the standard deviation, and Lévy flight is expressed as follows:

$$\text{Lévy}\,(\mathrm{S}, \lambda) = \frac{\lambda\Gamma(\lambda)\sin(\pi\lambda/2)}{\pi}\frac{1}{S^{1+\lambda}} \tag{2.22}$$

Naturally, the flight movements of many animals and insects are recognized as being random. Commonly, a foraging path of animals has a characteristic that their next move's base on the current state and the variation probability of the next state. Anyway, it chooses

the path to be determined indirectly on a probability which can be modelled mathematically. Lévy flight is a random distribution that enables a series of straight jumps chosen from a heavy-tailed probability density function (Brown et al., 2007). In statistical terms, when the distribution is used within a stochastic algorithm for global optimization, like CS, this corresponding algorithm is capable of finding the global optimum (Pavlyukevich, 2007). The Lévy flight process step size can be calculated as follows:

$$S = \frac{u}{|v|^{\frac{1}{\beta}}}, \tag{2.23}$$

where u and v are two random values drawn from normal distribution with mean zero and their standard deviations φ_u^2 and φ_v^2 as follows:

$$u \sim N(0, \varphi_u^2),\ v \sim N(0, \varphi_v^2), \tag{2.24}$$

and

$$\varphi_u = \left\{ \frac{\Gamma(1+\beta)\sin(\tau\beta/2)}{\Gamma\left[\frac{1+\beta}{2}\right]\beta 2^{(\beta-1)^2}} \right\}^{\frac{1}{\beta}},\ \varphi_v = 1. \tag{2.25}$$

The original CS is used in this research. This has the capability of interleaving the global search (according to Eqn. (2.19)) with the local search (according to Eqn. (2.20)). This interleaving is controlled by a switching parameter p_a which determines a fraction of the worst nests needed to be abandoned and new one to be built in order to discover new probably and more promising regions of the search space. In summary, all the mentioned features of the CS are assembled within a pseudo-code of the original CS algorithm which is illustrated in Fig. 2.8 (Yang & Deb, 2009):

Cuckoo Search via Lévy Flights

begin
Objective function $f(\mathbf{x}),\ \mathbf{x} = (x_1, ..., x_d)^T$
Generate initial population of
n host nests $\mathbf{x}_i\ (i = 1, 2, ..., n)$
while *(t <MaxGeneration) or (stop criterion)*
Get a cuckoo randomly by Lévy flights
evaluate its quality/fitness F_i
Choose a nest among n (say, j) randomly
if $(F_i > F_j)$,
replace j by the new solution;
end
A fraction (p_a) *of worse nests*
are abandoned and new ones are built;
Keep the best solutions
(or nests with quality solutions);
Rank the solutions and find the current best
end while
Postprocess results and visualization
end

Figure 2.11: Pseudo-code of the original CS algorithm

Some of well-known CS algorithm modifications, that are wrongly treated as the original one, use an explicit balancing among the exploration/exploitation components of the search process via the switching parameter p_a. This balancing is mathematically expressed as

$$X_i^{(t+1)} = \begin{cases} U(0,1).\left(u_j - l_j\right) + l_j, & \text{if } U(0,1) \le p_a, \\ X_i^{(t)} + \alpha \oplus \text{Lévy } (S, \lambda), & \text{otherwise.} \end{cases} \tag{2.26}$$

Note that the global random walk is performed only when $U(0,1) \le p_a$. The selection of better solutions in CS can be expressed as

$$X_{best}^{(t+1)} = \begin{cases} X_i^{(t+1)}, & if\ f\left(X_i^{(t+1)}\right) \le f\left(X_{best}^{(t)}\right), \\ X_{best}^{(t)}, & otherwise. \end{cases} \tag{2.27}$$

The flowchart for CS applied for optimization of T2FLS is shown in Figure 2.9.

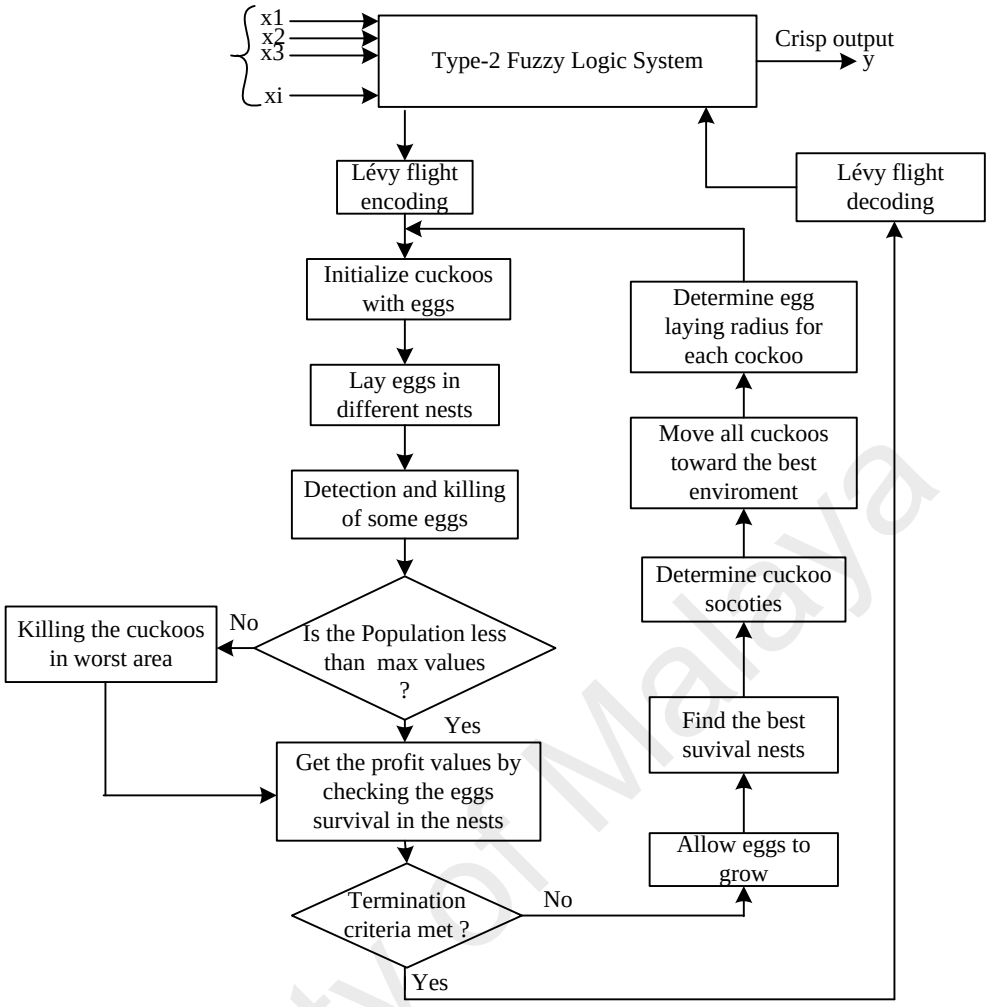

Figure 2.12: Flowchart of Lévy flight CS algorithm

2.5 Literature Review on the Use of Meta-Heuristic Optimization Algorithms in Design T2FLS

This section presents a review on recent advances (2012 to 2015) on the application of meta-heuristic algorithms for the optimization of type-2 fuzzy logic systems for intelligent control, time series prediction, classification, clustering and pattern recognition. The Hybrid optimization, GA and PSO are the three different paradigm considered in this research.

2.5.1 Hybrid Optimization (HO) Based T2FLS

Hybrid optimization method in T2FLS design refers to a combination of two or more meta-heuristic optimization algorithms for adjusting the parameters associated with

T2FLS to speed up the optimization task by getting lower complexity in computation, faster convergence and global optimization (Chaparro et al., 2008). In some cases, achieving an optimal solution to a problem using conventional optimization techniques that have high computational complexity is quite difficult (Xia & Wu, 2005). Recently, the applications of hybrid optimization techniques in automatic design of T2FLS for different complex applications have attracted interest from many researchers (Kao & Zahara, 2008; Kim, 2007; Kim et al., 2007). Taking the advantages of two or more optimization techniques, a hybrid optimization which gives better convergent rates and solution quality can be found. More explanation about the automatic switching among the constituent optimizers in hybrid optimization can be found in literature (Dulikravich & Colaço, 2015)

There are many researches on the optimization of T2FLS using hybrid optimization algorithms. Success was recorded in most of these researches. The review of these literatures is discussed in this section. The review in this section demonstrates the effectiveness of using the hybrid optimization algorithms for automatic design of the T2FLS.

Martínez-Soto et al. (2015) presented automatic design of FLC using Hybrid PSO-GA method for minimizing a steady state error of a plant's response. Three different plants were used as a benchmark, namely, stable system, unstable system and trajectory tracking control for autonomous mobile robot. Hybrid PSO-GA method was used to adjust the parameters of the FLC. To demonstrate the effectiveness and robustness of the hybrid PSO-GA based FLC, comparison was made between GA, PSO and Hybrid PSO-GA based FLC in different plant. The simulation results show that the IT2FLC and T1FLC obtained using hybrid PSO-GA was better than that of GA and PSO. In addition, the results obtained by IT2FLC are better than that of T1FLC in presence of disturbances.

They used objective function that minimizes the steady state error using the average of the absolute error represented with the following Equation:

$$EP_T = \sum_{i=n} \frac{abs(rf(i)-cr(i))}{2} \tag{2.28}$$

where rf is the trajectory reference, cr is the control response and EP_T is the average absolute error.

The species-based hybrid electromagnetism-like mechanism (EM) and back propagation (BP) algorithm (SEMBP) were hybridize for the design of interval type-2 neural systems with asymmetric MF (AIT2FNS) in literature Li et al. (2014). The interval type-2 symmetric MF and the TSK-type consequents part are adopted for the implementation of the network structure in AIT2FNS. The SEMBP was used to train AIT2FNS. The simulation results obtained by nonlinear tracking control and bath temperature control show the performance and effectiveness of the proposed method over the traditional PSO, GA, EM and SEM. They used the objective function defined as:

$$E(i) = \frac{1}{2}\sum_k (y_r(k) - y(k))^2 \tag{2.29}$$

where$y_r(k)$is the desired trajectory, $y(k)$ is the system output and k is the discrete time index.

Fayek et al. (2014) presented the systematic design and hybrid optimization whereby PSO and GA optimise different parameters in the same system and real time implementation of IT2FLCfor control of position of DC servo motor. PSO and GA were used for the optimization of controller input/output gains, and MFs parameters respectively. It was reported that the proposed controller outperformed the T1FLC and PI controller in terms of efficiency and effectiveness under noise and disturbances. The

objective function used in both stages of the design process is a multiple- objective function defined as:

$$FE = O_1 - 0.5O_2 \tag{2.30}$$

where $O_i = IAE = \sum_{k=1}^{n} |e(k)|$

$O_1$is the first objective function, O_2 is the second objective function, $e(k)$ is the error at k^{th} point, and n is the number of points in the run

Hsu & Juang (2013) hybridized a Species-Differential-Evolution and Continues Ant Colony Optimization (SDE-CACO) algorithms for improvement of IT2FLC performance. New species SDE mutation operation was introduced into a continuous ACO algorithm in order to improve its explorative ability. The clustering-based approach was used to generate all the IT2FLC rules online during the evaluating leaning process. The SDE-CACO was used to optimize the free generated parameters of IT2FLC online. The proposed algorithm was applied for simultaneous wall-following control and speed control of mobile robot. Comparison was made between the continuous ACO, PSO and DE. Based on the real-world experiments and simulation results obtained, it was reported that the proposed algorithm showed higher efficiency and effectiveness in wall-following control and speed control over comparative algorithms. They introduced the new objective function that includes the following three principle factors for successful wall-following control strategy: (1) making smooth changes in steering angle; (2) moving at high speed; (3) maintaining a proper distance from the wall being followed. The overall control consists of two training stages. Each stage has different objective function C_1 and C_2 for stage one and stage two respectively as follows:

$$C_1 = f_1 + f_2 + f_3 \tag{2.31}$$

and

$$C_2 = f_1 + f_2 + f_3 + f_4 \tag{2.32}$$

where

$$f_1 = \frac{\sum_{t=1}^{T_{Total}} |RD(t)-1|}{T_{Total}}; \tag{2.33}$$

$$RD(t) = \frac{S_4(t)}{d_{wall}}; \tag{2.34}$$

$$f_2 = \alpha_2 \times \frac{\sum_{t=1}^{T_{Total}} |\phi(t)|}{T_{Total}}; \tag{2.35}$$

$$f_3 = \alpha_3 \times (T_{Total} - T_{stop}); \tag{2.36}$$

$$f_4 = \alpha_4 \times \frac{1}{\sum_{t=1}^{T_{Total}} d(t)/T_{Total}}. \tag{2.37}$$

f_1 is the average of the relative RD values occurring over all T_{Total} time steps. f_2 describes the included angle φ between the robot front direction and the wall. f_3 describes the difference between T_{Total} and the time step number T_{stop} when a collision occurs. f_4 is defined as the inverse of the average moving speed. α_2, α_3 and α_4 are weighting coefficients.

Hernandez et al. (2015) hybridized the BP algorithm and recursive orthogonal least squares algorithm (ROLSA) for interval A2-C1 type-1 non-singleton type-2 TSK FLS. The ROLSA was used to tune the type-1 consequent parameters while the parameters of the antecedent part of the interval type-2 were tuned by BP algorithm. The proposed method was compared with a non-hybrid method (that only used BP algorithm for tuning both the antecedent and consequent parameters) which shows that, the proposed hybrid method outperformed the non-hybrid method in nonlinear adaptation, which enables the

interval type-2 fuzzy model to optimally match the nonlinear behaviour of the process. The proposed method was applied to the modelling and prediction of the transfer bar surface temperature in an industrial hot strip mill facility. The performance of each of the IT2TSK NSFLS1 system is evaluated based on the RMSE. The experimental results show improvement in the prediction.

Nguyen et al. (2015) presented the wavelet transformation and IT2FLS for automated medical data classification. The wavelet coefficient served as an input to the IT2FLS. The IT2FLS utilizes a hybrid learning process comprising supervised parameters tuning by GA and unsupervised structure learning by fuzzy c-mean (FCM) clustering. The experiments are implemented on Wisconsin breast cancer and Cleveland heart disease. The obtained results demonstrate the significant dominance of the proposed method compared to the ANFIS, fuzzy ARTMAP, support vector machine and probabilistic neural network, in terms of accuracy and specificity. The accuracy measure was used as an objective function as follows:

$$Acc = \frac{P}{N} \tag{2.38}$$

where N denotes the number of predicted cases and P is the number of cases being predicted correctly.

Long and Meesad (2014) presented an optimal design of IT2FLS for prediction of short-term and long-term horizontal sea water level. The structure of fuzzy rule and number of rules are determined by c-means clustering algorithm, while the desirable parameters of MF and consequents parameters of FLS are found by using the hybrid Chaos firefly algorithm and GA (CFGA). The result obtained demonstrates that IT2FLS designed by hybrid CFGA outperformed the one designed by standalone GA and FA based on RMSE and scatter index. Hosseini et al. (2012) presented an automatic design

and tuning of Gaussian IT2MF for multidimensional pattern classification problems. The combination of GA and Cross-validation technique (GA-CVT) is used to tune the MFs and their FOU. In GA-CVT, the chromosome structure has fewer genes than ordinary GA and it has more precise initialization of chromosome than ordinary GA. The proposed method was applied to nodule classification in a lung computer-aided detection system. The proposed method outperformed T1FLS by more than 30% in terms of classification accuracy.

The GA and PSO optimizations of type-2 fuzzy inference system for IT2FLS weight in neural network were presented in literature Gaxiola et al., (2013). GA and PSO were used to tune the two IT2FLS that work in back-propagation leaning method with type-2 fuzzy weight adjustment. The proposed method was applied to Mackey-Glass time series benchmark. Satisfactory results were obtained for both GA and PSO. However, the result obtained by GA is better than the one obtained by PSO. Kim et al. (2013) presented a design of an optimal FCM based IT2FNN classifier. The premise part of the proposed classifier rules was realized from two versions of FCM clustering with different fuzzification coefficients values in order to form the interval T2-MF. The coefficients of the linear function in the consequent part were updated by using back propagation algorithm. PSO was used to optimize the momentum coefficient, learning rate and fuzzification coefficients. The machine learning data was used for the experiment and it was carried out in the 5 fold cross validation mode. It was concluded that the proposed classifier obtained the desirable performance. Juang and Jang (2014) presented the type-2 neural fuzzy system leaned through type-1 (T2NFS-T1) and its implementation in FPGA chip. The antecedent part of each rule in T2NFS-T1 used IT2FSs while the consequent part used TSK type with interval combination weight. To reduce the cost of hardware implementation and training time, the T2NFS-T1 used the simplified type reduction. The consequent rule and antecedent parameters of T2NFS-T1 were tuned using

a hybrid of gradient decent (GD) and rule-order (RO) recursive least square (RLS) algorithm. Simulation results show the effectiveness and efficiency of the proposed system for modelling and prediction problem over type-1.

A summary of presented publications where HO has been used to optimize the T2FLS is presented in Table 2.3

Table 2.2 Hybrid meta-heuristic algorithms use for designing T2FLS

Reference	Problem domain	Hybrid optimization	Algorithm compared with the hybrid	Other system (s) compared with T2FLS	Result
Martinez-Soto et al. (2015)	Control	PSO+GA	GA and PSO	T1FLC	PSO+GA better than GA and PSO. T2FLC outperform T1FLC
Li et al. (2014)	Control	EM+BP	PSO, GA and EM	IT2FNS	EM+BP better than PSO and GA. AIT2FNS better than IT2FNS
Fayek et al. (2014)	Control	PSO+GA	Not compared	T1FLC and PI	T2FLC better than T1FLC and PI
Hsu and Juang (2013)	Control	SDE+CACO	ACO, PSO and DE	Not Compared	SDE+CACO better than ACO, PSO and DE
Hernandez et al. (2015)	Modelling and prediction	BPA+ROSLA	BPA	Not compared	Hybrid better than BPA
Nguyen et al. (2015)	Classification	GA+FCM	Not compared	ANFIS, fuzzy ARTMAP and probabilistic FNN	T2FLS better than ANFIS ,fuzzy ARTMAP and probabilistic FNN
Long and Meesad (2014)	Prediction	FA+GA	FA and GA	Not compared	Hybrid better than FA and GA
Hosseini et al. (2012)	Classification	GA+CVT	Not compared	T1FLS	T2FLS better than T1FLS
Gaxiola et al. (2013)	Prediction	BPA+GA and BPA+PSO	Not compared	Not compared	Hybrid BPA-GA better than Hybrid BPA-PSO
Kim et al. (2013)	Classification	BPA+PSO	Not compared	Not compared	No comparison
Juang and Jang (2014)	Modelling and prediction	GD+RO RLS	Not compared	T1FLS	T2FLS better than T1FLS

2.5.2 GAs Based T2FLS

Several studies have been done on optimization of T2FLS using different variant of GA. Success was reported in most of these works in different area of applications. Thus, this section presents the state-of-the-art review.

Sun et al. (2015) proposed RNA genetic algorithm (RNA-GA) for the optimization of MFs parameters associated with T2FLC and T1FLC. Five nonlinear functions constraints were used to test the searching capability of the RNA-GA. The performance of the optimised T2FLC and T1FLC using RNA-GA and GA were tested on control of the double inverted pendulum system under unexpected disturbances. The ITAE was used as objective function. Based on the experimental results obtained, it was found that the optimized T2FLC demonstrates superiority perfomance in the elimination of obstinate vibrations and oscillations over the optimized T1FLC. In addition, comparative simulations show that the RNA-GA optimized T2FLC better than the comparative algorithms. Lu (2015) proposes an IT2FLC with GA-based type reduction algorithm for reduction of IT2FS as well as to obtain the optimal defuzzified output from type reduced set. The RMSE was used as an objective function. The proposed type reduction was executed offline which reduced the computational cost significantly and facilitate the design of IT2FLC operation in real time. The proposed controller was applied on truck backing control problem. The proposed IT2FLC outperformed the conventional IT2FLC in terms of robustness, computational cost and speed. Cervantes and Castillo (2015) proposed a novel method for complex control by combining several FLC. The proposed method is particularly useful for multivariable control system. The method has two levels of hierarchical architecture (individual FLC and a superior control to adjust the global result). Flight controls that require several individual controller was used to test the behaviour of the proposed method. GA was used to adjust the parameter

of the T2FLC.The fitness function that quantifies the errors of each controller was used as follows:

$$f(Y) = \frac{\left(\sum_{i=1}^{n} \frac{|y_{ref_1}^i|}{n} - \frac{|y_{fs_1}^i|}{n} + \sum_{i=1}^{n} \frac{|y_{ref_2}^i|}{n} - \frac{|y_{fs_2}^i|}{n} + \sum_{i=1}^{n} \frac{|y_{ref_m}^i|}{n} - \frac{|y_{fs_m}^i|}{n}\right)}{m} \quad (2.39)$$

where y_{ref} is the reference, y_{fs} is the output of the controller and n is the number of points of the dynamic response used in the comparison. m stands for the number of the individual controllers used. Based on the simulation result obtained, it was concluded that the proposed method uses T2FLC and it decreases the control error and improve the overall behaviour of the plant when compared with the T1FLC.

Maldonado et al. (2014) optimized the average approximation of an interval type-2 fuzzy logic controller (AT2FLC) using multi-objective GA for hardware applications such as speed control of DC motor in a FPGAs. The researchers considered the combination of triangular and trapezoidal T2-MFs of an AT2FLC such that the GA needs to optimize some parameters (adaptable) of the T2-MFs in order to have less execution time. The composite objective function that compromise between the minimum overshoot, undershoot and steady state error was used as shown in equation (2.40). The optimised AT2FLC was compared with the optimised T1FLC as well as the PID controller tuned by Ziegler-Nichols method. The real world experiment's results show that AT2FLC outperformed the T1FLC and PID controller by observing the lower error in presence of uncertainty.

$$U = \sum_{i=1} \omega_i f_i(x); \quad (2.40)$$

where ω is the positive value.

Castillo and Cervantes (2014) used GA in the design of a T1FLC and T2FLC for airplane longitudinal control. They used three inputs (stick, rate of elevation and angle of attack) to the controller. GA was applied for the optimization of MFs of the fuzzy systems. The fitness function used is based on the average error between the output of PID and fuzzy controllers as shown in equation (2.41). Based on the simulation results obtained, it was concluded that at higher levels of disturbances in the plant, the GA-based T2FLC outperform the T1FLC as well as the PID controller.

$$Error = \sum_{i=1}^{n} \frac{\left| y_{PID}^{i} - y_{fuzzy}^{i} \right|}{n} \tag{2.41}$$

where y_{PID} is the output of the PID controller and y_{fuzzy} is the output of the fuzzy controller.

Melendez et al. (2013) proposed the GA for the optimization of an interval type-2 fuzzy reactive controller for autonomous mobile robot. The hierarchical genetic algorithm (HGA) was used for the optimization of fuzzy MF, fuzzy rules and mobile robot power usage. To overcome the problem of loop trajectory, the new module was added to the system which consists of a monolithic neural network that is used for detecting patterns of loop on the robot trajectory. Based on the simulation results obtained, it was concluded that HGA shows its effectiveness on multi objective task and the proposed type-2 neuro-fuzzy allowed the HGA to optimise the forward movement of the robot through the maze and refrain from any type of collision with obstacles. Cervantes and Castillo (2013) presented statistical comparisons of T1FLC and T2FLC for control of water level in three tanks. GA was used for optimization of MFs for both controllers. MSE was used as an objective function. Three different paradigms, namely, empirical T1FLC, GA based T1FLC and GA based T2FLC were used for comparisons. It was concluded that based on the simulation results obtained, the GA based T2FLC shows better performance

compared to empirical T1FLC and GA based T1FLC. In the work of presented in Bi et al. (2013), a GA based T2FLC for single intersection signal control was proposed. GA was used to optimise the MFs parameters of T2FLC. The comparison results (simulation) show the superiority of GA based T2FLC over T1FLC as well as fixed time control in terms of reduction of vehicular delay and queue length at the traffic intersection. The objective function used is as follows:

$$OF = \sum_{l=1}^{n} \frac{D_{Rn}^{l} + D_{GN}^{l}}{qg^{l} + qr^{l} + lqg^{l-1} + lqr^{l-1}} \tag{2.42}$$

where D_{Rn}^{l} and D_{GN}^{l} are the total delay time of the vehicles in red phase and total wait time at green phase of l cycle respectively. qg^{l} and qr^{l} Are the number of arrival vehicles at green phase and red phase. lqg^{l-1} and lqr^{l-1} Are the staying number of vehicles at different phase in the previous cycle.

Shill et al. (2012) applied a real coded quantum GA for simultaneous optimization of T2FS and rule sets for control of robot manipulators with unstructured dynamical uncertainties. The main aim of their study is to make the design of IT2FLC automatic. It was concluded that based on the real world experiment and simulation, Quantum GA based T2FLC resisted noisy unstructured environment and succeeded in having higher control performance better than the Quantum GA based T1FLC, traditional T1FLC, and neural coded FLCs. Moldonado and Castillo (2012) described the automatic design of an AT2FLC for DC motor speed control. The GA and PSO were employed for optimization of parameters of AT2FLC. The objective function of PSO and GA considers three characteristics that makes them to be multi - objective type as follows:

minimum overshoot: if $y_{(t)} > r_{(t)} \rightarrow o_1 = \min\left(y_{(t)}\right) - r_{(t)}$; (2.43)

minimum undershoot: $o_2 = \left|min\left(y_{(t)}\right) - r_{(t)}\right|$; (2.44)

minimum output steady state error: $sse = \sum_{t=201}^{1000} y_{(t)} - r_{(t)}$. (2.45)

where $y_{(t)}$ is the output of the system and $r_{(t)}$ is the reference signal. Simulation was carried out in FPGA using the xilinx system generator. Satisfactory results were obtained for both GA and PSO. However, the result obtained by GA was better than the results obtained by PSO. In another work, Moldonado and Castillo (2012) used GA based T2FLC for velocity regulation in DC motor. Xilinx system generator of xilinxISE, and Matlabsimulink for synthesizing the T2FLC in a very high description language (VHDL) code for a field programmable gate array (FPGA) was used. GA was used to optimize trapezoidal and triangular MFs of T2FLC and T1FLC for hardware application such as FPGA. The same objective function as the one presented in literature Yazmin Maldonado & Oscar Castillo (2012) was used. The GA based T2FLC, GA based T1FLC and PID controller tuned by Ziegler-Nichols method was compared. It was reported that, GA based T2FLC outperformed GA based T1FLC as well as PID controller.

Chengdong et al. (2012) applied a Single Input Rule Modules (SIRM) -connected T2FLC scheme for baking up control of the truck-trailer system. The two most important tasks for designing such SIRM-connected T2FLC are: Design a suitable SIRM for each input item, and determine the parameters of SIRM-connected T2FLC such as important degree of input items, scaling factors and MF of T2FLC in each SIRM. GA was used to optimise these parameters. The control objective is to force the vertical position y, trailer angle β, and relative angle α to be zero. The following objective function was used:

$$J = \sum_{s=1}^{S} \left(\gamma_\alpha IAE_s(\alpha) + \gamma_\beta IAE_s(\beta) + \gamma_y IAE_s(y) \right) \quad (2.46)$$

where S is the number of initial conditions used. γ_α, γ_β and γ_y are scaling factors. The comparison betweenT2FLC and T1FLC was made. The simulation results show that the proposed scheme with optimised T2FLC outperformed the scheme with optimised

T1FLC and gave less time backing up the truck-trailer system from initial state to expected state. Ghaemi et al. (2012) presented the hybrid combination of adaptive T2FLC and sliding mode control (SMC) called Adaptive Interval Type-2 Fuzzy Proportional Integral Sliding Mode Controller (AIT2FPISMC) for the design of a robust control system with high level of uncertainties and nonlinearity. The T2FLS was used to approximate unknown nonlinear terms, PI was used to eliminate chattering effect in SMC and SMC was used to address the issue of noise and disturbances. GA was employed to tune the parameters of AIT2FPISMC. Mean squire error (MSE) for the closed loop control was considered as the fitness function. It was found that based on the simulation results, the proposed controller has good performance and was improved with GA.

In the study presented by Soto et al. (2014) the GA optimization of an interval type-2 fuzzy logic integrator (IT2FLI) and type-1 fuzzy logic integrator (T1FLI) in ensembles of ANFIS models for the forecasting of the Dow Jones time series (DJTS) was proposed. GA was used for adjusting the MFs of each integrator. Both T2FLI and T1FLI have three input variables and one output variable (forecast). Three different MFs (Gaussian, Generalized Bell and Triangular) were used to test the performance of IT2FLI and T1FLI. The architecture of the work was divided into four phases First, the DJTS historical data was simulated in Ensemble of ANFIS, and secondly, the training and validation was sequentially performed in each ANFIS model. The third phase used the optimized T2FLI and T1FLI to integrate the whole results of Ensemble of ANFIS model. Finally, the desired prediction was compared with the forecast output determined by the architecture. It was reported that IT2FLI outperformed the T1FLI with 98% accuracy. The objective function that can minimize the forecasting error was used as follows:

$$f(t) = \sqrt{\frac{\sum_{t=1}^{n}(a_t - p_t)^2}{n}} \tag{2.47}$$

where a_t, is the real data of the time series, p_t is the output of each fuzzy integrator, t and n are the sequence time series and the number of data in time series respectively.

Nguyen et al. (2014) presented an optimal design of an IT2FLS that can deal with the issue of uncertainty in noisy data and training set. The researchers used clustering data space to set up the T1FLS and a suitable method to transform T1FLS to IT2FLS. GA was used to adjust the parameters of an IT2FLS. The proposed method was tested on different forms of experiments comprising of time series prediction and nonlinear systems identification. The objective function used in this research is the same as that one used in literature Soto et al. (2014). Based on the obtained results, it was concluded that the proposed method can deal with difficulties of uncertainty of training set. Melin and Pulido (2014) provided the details of a GA based optimization method for design ensemble neural network with fuzzy integration for complex time series forecasting. GA was used to find the number of modules, neurons, layers and the parameters associated with IT2FLS. They used the DJTS as the benchmark. The proposed method obtained 99% prediction accuracy and its performance was increased with IT2FLS.

Sanchez and Melin (2013b) proposed an optimization method for modular neural network using the multi-objective hierarchical GA (MOHGA). The data set was divided into granules. MOHGA was used to optimize the parameters associated with IT2FLI, error goals, learning algorithm, number of hidden layer, granules and neurons per hidden layer. The proposed method was applied for pattern recognition problem. The proposed method with IT2FLI creates a system with better results and behaviour. Sánchez and Melin (2013a) presented a new model of Hierarchical GA (HGA) for optimization of T2FLI. The method combines the T2FLI and modular neural network (MNN) for pattern recognition. HGA can deal with complex systems that cannot be handled by simple GA

easily. In this work, HGA was used to optimize the type of the system, number of MF and their parameters. Better results were obtained when the proposed HGA was used.

In the work presented by Pulido et al. (2013), a hybrid approach of ensemble neural network with T2FLI and its optimization with GA for time series prediction was studied. The GA was used to optimize parameters of T2FLI and the network architecture. The researchers used Mackey-Glass time series as the benchmark. It was proved that, optimized T2FLI give a better result with less error than its T1FLI counterpart under the noise in training network. Nguyen et al. (2013) presented the hybrid method for prediction of stock price which comprises of feed forward neural network (FFNN) and IT2FLS. GA was used for optimization of variable of IT2FLS. K-means clustering method was used for initialization of GA instead of a traditional random initialization. Enhancement on the iterative algorithm with stop condition (EIASC) was used for type-reduction as an alternative to Karnik-Mendel procedure which was found to be time consuming. It was concluded that, optimized IT2FLS produces forecasting results with higher accuracy than T1FLS as well as FFNN models. The GA also becomes more efficient and converges faster when it is initialized in a more knowledgeable way rather than random initialization. The RMSE was used as an objective function. In literature Gaxiola et al. (2013b), the GA optimization of T2FLS and BP learning algorithm with T2FLS weight adjustment for pattern recognition and time series prediction was presented. The proposed algorithm uses T2FLS to allow neural network to handle the uncertainties. The GA was used to optimise the T2FIS to be used in the hidden and outer layers as well as the number of neurons in the hidden layer to get the T2FLS weight for each neural network forming the ensemble. The proposed algorithm was tested on Mackey Glass time series and the human iris biometric measure for time series prediction and pattern recognition respectively. A very good result with less error was recorded for both tests.

Melin et al. (2012) presented the hybrid method combining the FLS and the neural networks for accurate and efficient solution of pattern recognition problem. The proposed method consists of modular neural network mode which uses FLS for integration of the response. The proposed algorithm was applied on human recognition based on 3 biometric measures (voice, iris and ear). Two GAs were used to optimise the entire model. One GA for adjusting the parameters of modules of neural network. The other GA optimised the fuzzy logic integrator which have the ability to select the number and type of MFs to be used, combine different types of MF, decide the type of logic (type-1 or type-2 fuzzy logic) to be used and create a fuzzy rule. In all the cases they considered, a better rate of recognition was obtained when an optimized T2FLI was used in the presence of noise. Mahmoodian (2012) presented the hybrid TSK model of T2FLS rule mining based on support vector machine (SVM) for prediction of breast cancer relapse time on a continuous scale. The parameters of T2FLS were optimised by GA. It was concluded that the use of optimised T2FLS indicates a better performance and copes with a lot of uncertainty in the model. In (Hidalgo et al., 2012), the optimization strategy for design of Type-2 fuzzy inference system (T2FIS) based on the size of FOU of MFs was presented. Three cases were considered, namely: 1. Equal values of uncertainty of all MFs, 2. Different values of uncertainty in each input 3. Different values of uncertainty for each MF. The researchers compared the simple GA for optimization of each of the different cases separately, and the proposed complete GA where all the cases are included in an objective function used to find optimal T2FIS. Adaptive Noise Cancellation and Miles per Gallon were used as the benchmark. It was concluded that the proposed complete GA gives better result for more complex problems.

A summary of review through which GAs has been used to optimize the T2FLS is presented in Table 2.4.

Table 2.3: Genetic algorithms use for designing T2FLS

Reference	Problem domain	Algorithm compared with GA	Other system (s) compared with T2FLS	Result
Sun et al. (2015)	Control	RNA-GA	T1FLC	RNA-GA better than GA. T2FLC better than T1FLC
Lu (2015)	Control	Not compared	Conventional IT2FLC	Proposed IT2FLC outperformed conventional IT2FLC
Leticia et al. (2015)	Control	Not compared	T1FLC	T2FLC better than T1FLC
Maldonado et al. (2014)	Control	Not compared	T1FLC and PID	AT2FLC better than T1FLC and PID
Castillo & Cervantes (2014)	Control	Not compared	T1FLC and PID	T2FLC better than T1FLC and PID
Melendez et al. (2013)	Control	Not compared	Not compared	Not compared
Cervantes & Castillo (2013)	Control	Not compared	T1FLC	T2FLC better than T1FLC
Bi et al. (2013)	Control	Not compared	T1FLC and fixt time control	T2FLC better than T1FLC and fixed time control
Shill et al. (2012)	Control	Not compared	No, T1FLC and neural coded FLS	T2FLC better than T1FLC and neural coded FLS
Maldonado & Oscar Castillo (2012)	Control	PSO	Not compared	GA better than PSO
Maldonado & Castillo (2012)	Control	Not compared	T1FLC	T2FLC better than T1FLC
Li et al. (2012)	Control	Not compared	T1FLC	T2FLC better than T1FLC
Ghaemi et al. (2012)	Control	Not compared	Not compared	Not compared
Soto et al. (2014)	Prediction	Not compared	T1FLS	T2FLS better than T1FLS
Nguyen et al. (2014)	Prediction	Not compared	T1FLS	T2FLS better than T1FLS
Melin & Pulido (2014)	Prediction	Not compared	T1FLS	T2FLS better than T1FLS
Sanchez & Melin, (2013b)	Pattern recognition	Not compared	Not compared	Not compared
Sanchez & Melin (2013a)	Pattern recognition	Not compared	Not compared	Not compared
Pulido et al. (2013)	Prediction	Not compared	T1FLS	T2FLS better than T1FLS
Nguyen et al. (2013)	Prediction	Not compared	T1FLS and FFNN	T2FLS better thanT1FLS and FFNN
Gaxiola et al., et al. (2013b)	Pattern recognition	Not compared	Not compared	Not compared
Melin et al. (2012)	Pattern recognition	Not compared	Not compared	Not compared
Mahmoodian (2012)	Prediction	Not compared	Not compared	Not compared
Hidalgo et al. (2012)	Prediction	Not compared	Not compared	Not compared

2.5.3 PSO Based T2FLS

Many publications on optimization of T2FLC using different kinds of PSO exist in the literature. Thus, a review of the literature that used PSO for the optimization design of T2FLS is presented in this section.

Shahsadeghi et al. (2014) presented an optimal type-2 fuzzy sliding mode (OT2FSM) controller for control of general chaotic systems. The Random Inertia Weigh PSO (RNW-PSO) was used to adjust the parameters of the controller including the input and output MFs coefficients of type-2 fuzzy. The inertia weight enhances the efficiency of the PSO by equilibrating the local exploitation and the global exploration capabilities of the swarm. The MSE for the closed loop control was considered as the fitness function. The simulation results obtained by the proposed controller were compared with that of optimal type-2 fuzzy PID controller and optimal H-infinity adaptive PID controller. It was found that the proposed controller performs better than the comparatives controllers. Niknam et al. (2014) presented an optimal type-2 sliding mode controller for class of nonlinear uncertain systems under external disturbances. RNW-PSO was used to adjust the parameters of the controller as well as the input and output MFs coefficients of type-2 fuzzy. The RMSE was used as an objective function. Inverted pendulum system was used as case study. Based on the simulation results, it was concluded that the proposed controller is free of chattering effect, robust and obtained the desired performance. Khooban et al. (2014) proposed the design of an optimal type-2 fuzzy PID controller for air supply pressure of air-conditioning, heating and ventilation systems. The coefficient of PID and the input and output MFs parameters of IT2FLC were simultaneously optimized by RNW-PSO. MSE was considered as the objective function. The simulation result shows that the proposed controller outperformed the PID, ANF and STFPIC controllers under the presence of the uncertainties in the parameters of the model.

Allawi and Abdallah (2014) proposed an IT2FLC for multiple mobile robots. The researchers considered the control of robot cooperation, target reaching task and avoidance of collision during navigation. The parameter of the proposed controller was adjusted using PSO. The objective function which constitutes the number of robots and collision time was used as follows:

$$fitness_i = \frac{1}{2}\sum_{j=1, j\neq i}^{n}\left(\frac{k}{tc_{ij}}\right)^2 \quad (2.48)$$

where n is the number of robots, tc_{ij} is the collision time between robot i and robot j and k is the constant. Hybrid reciprocal velocity obstacles were used for avoidance of collision. They used two real E-peck mobile robots for experimental testing. It was concluded that the robot navigation efficiency was increased for optimized IT2FLC in both simulation and experimental results compared with conventional IT2FLC. Maldonado et al. (2013) presented the optimization of MFs of AT2FLC using PSO. To minimize the running time, the fuzzy rules were not modified and only certain point of MFs were considered. The proposed method was applied for regulation of speed of DC motor, and it is coded in VHDL for a FPGA xilinxspartan 3A. The experimental results obtained by PSO were compared with the one obtained by GA which indicated that, PSO has faster running time than GA. Baklouti and Alimi (2013) proposes a new adaptive learning procedure of IT2FLC for design of robot navigation planning task. Real time PSO technique was used to instantaneously optimise the MFs of the IT2FLC.The fitness function that minimise the angular velocity smoothness index was used. The "iRobot create" was used as benchmark. It was concluded that based on the real world experimental results found, the proposed method gives a free collision trajectory and smooth path for navigation of the robot. Panda et al. (2012) presented a PSO-based IT2FLC for the design of power system stabilizer for damping oscillations in power transmission line. The proposed controller was tested on the single machine infinite bus

and multiple machine infinite bus. PSO algorithm was used to optimise the MFs of the IT2FLC. The proposed controller was compared with the optimal T1FLC and optimal lead-lag controller. Based on the simulation results obtained, it was reported that the proposed controller was found to be more robust with respect to the different disturbances and system parameters variations.

Son (2014) presented the novel clustering algorithm called Context Fuzzy Geographically Weighted Clustering (CFGWC) on IT2FLS for the enhancement of the clustering quality of state-of-the-art clustering algorithm called FGEC for geo-demographic analysis. PSO was used to optimize the parameters of the IT2FLS, and to find the best initial centres for CFGWC. In addition to the significance of these optimizations, it avoids initialization which may cause other type-2 fuzzy clustering algorithm accelerates the convergence of the algorithm. It was reported that the proposed algorithm obtained a higher clustering quality compared to other algorithms. They used the following objective function:

$$J = \sum_{k=1}^{N} \sum_{j=1}^{C} \left\| X_k - V_j \right\|^2 \rightarrow min \tag{2.49}$$

Singh and Borah (2014) presented a new T2FLS based time series model that can effectively use more observations in forecasting. PSO was used to optimize the parameters of the proposed model. The performance of the proposed model was tested on a daily stock index price data set of the state bank of India. In comparison with a conventional time series models and existing fuzzy time series model, the proposed model obtained results that are more effective and more robust than T1FLS. Pulido et al. (2014) presented the PSO based ensemble neural networks with fuzzy integrator for time series prediction of Mexican stock exchange. PSO was used for tuning the structure of ensemble neural networks as well as T1FLI and T2FLI. Simulation results indicated that the use of T2FLI outperformed T1FLI. It was concluded that based on the prediction results found,

the use of ensemble neural networks with optimized T2FLI could be a good choice in predicting complex time series.

Sanchez et al. (2013) presented a novel method for design of an interval type-2 fuzzy inference system (IT2FIS). Two different methodologies were used. The first method is by using the principle of granularity where the antecedent's uncertainty was calculated directly. The second method is by using two T1 TSK first order function, where the consequents which are interval type-2 (IT2) TSK were calculated directly. PSO was used to obtain the spread of each IT2 TSK function so as to adjust the FOU convergence. Based on the final result of convergence of FOU in the presence of noise, the proposed IT2FISs are both robust and not very wide which cannot capture noise beyond the level of output. Khosla et al. (2012) presented the PSO-base IT2FLS for time series forecasting. The PSO was used to adjust the MFs, FOU and rule set of the IT2FLS. The proposed design approach was applied to Macky-Glass time series forecasting benchmark. Four different experiments were performed for different corrupted chaotic time-series data set. It was concluded that the proposed method obtained a desirable forecasting result with less error.

Chakravarty and Dash (2012) presented an integrated functional link interval type-2 fuzzy neural network system (IFLIT2FNNS) for stock market indices prediction. T2FS was employed in the antecedent part and the consequent part was the output from the functional link artificial neural network (FLANN). PSO and back-propagation methods were used independently for optimization of all the forecasting model's parameters. Three benchmarks were used to test the proposed method, namely: Standard's and Poor's 500, Bombay stock exchange and Dow jones industrial average. The proposed method was compared with integrated FLANN, T1FLS and local linear wavelet neural

network (LLWNN). The comparison indicates the better performance of the proposed method.

A summary of the publications in which PSO was applied for the optimization of the T2FLC is presented in Table 2.5.

Table 2.4: PSO used for designing T2FLS

Reference	Problem domain	Algorithm compared with PSO	Other system (s) compared with T2FLS	Result
Shahsadeghi et al. (2014)	Control	Not compared	PID	T2FLC better than PID
Niknam et al. (2014)	Control	Not compared	Not compared	Not compared
Khooban et al. (2014)	Control	Not compared	PID, ANF and STFPIC	T2FLC better than PID, ANF and STFPIC
Allawi and Abdalla (2014)	Control	Not compared	Un optimized T2FLC	optimal T2FLC better than un-optimised T2FLC
Maldonado et al. (2013)	Control	GA	Not compared	PSO better than GA
Baklouti and Alimi (2013)	Control	Not compared	T1FLC	T2FLC better than T1FLC
Panda et al. (2012)	Control	Not compared	T1FLC and lead lag controller	T2FLC better than T1FLC and lead lag controller
Son (2014)	Clustering	Not compared	FGWC	T2FLS better than FGWC
Singh and Borah, 2014)	Prediction	Not compared	T1FLS	T2FLS better than T1FLS
Pulido et al. (2014)	Prediction	Not compared	T1FLS	T2FLS better than T1FLS
Sanchez et al. (2013)	Clustering	Not compared	Not compared	Not compared
Khosla et al. (2012)	Prediction	Not compared	Not compared	Not compared
Chakravarty and Dash (2012)	Prediction	Not compared	T1FLS, IFLANN and LLWNN	T2FLS better than T1FLS, IFLANN and LLWNN

2.5.4 Other Meta-heuristic Optimization Algorithms Based T2FLS

Several works on optimization of T2FLC using different types of meta-heuristic optimization algorithms have been reported in literature. Success was recorded in most of these researches in different areas of applications. The review of the representative of these types of research was presented in this section to demonstrate the effectiveness of using the corresponding optimization method for automatic design of T2FLS.

Castillo et al. (2012) presented an ACO and PSO method for adjusting the MFs parameters of an IT2FLC for design of an optimal intelligent controller for trajectory tracking control of autonomous mobile robot. The MSE for the closed loop control was considered as the objective function. The statistical analysis shows that the ACO outperformed PSO and GA in this particular control and IT2FLC outperformed T1FLC. Yesil (2014) propose a big bang-big crunch (BB-BC) optimization design strategy of IT2FPIDC for load frequency control in power systems. The BB-BC optimization was used to adjust the FOU, MFs and the scaling factor of IT2FPID controllers. The ITAE was used as objective function. Four area interconnected power system was used as a benchmark. Based on the simulation results, the comparisons were made between the proposed method, T1FLPID and conventional PID, while all the controllers were optimized using BB-BC. The IT2FPID controllers operate 51.5% and 76.5% better than the T1FPID and PID respectively. A novel application of BB-BC for optimization of cascade structure of IT2FPID and its antecedent MF parameters was presented in literature Kumbasar and Hagras (2014). The proposed controller was applied for the path tracking control of PIONEER3-DX mobile robot. Several experiments in both simulation and real world were performed. IAE was used as a performance measure for both inner and outer loop. The proposed controller was compared with self-tuning T1FPID structure

as well as PID and T1FPID counterpart which were optimised using BB-BC. The results obtained illustrate that, the IT2FPID structure enhanced the control performance significantly in the presence of disturbances and uncertainties when compared with self-tuning, BB-BC based PID and BB-BC based T1FPID structures. In addition, they also show that the reason for superior control performance of IT2FPID controller is not just because it has extra parameters, but rather is in the way it is dealing with noise and uncertainty present in real world compared with self-tuning T1FPIDC. In addition, BB-BC gives high quality solution with less computational time when compared with PSO.

El-Nagar and El-Bardini (2014) proposed the IT2FNN controller for hardware-in-the-loop simulation to simulate the control of a multivariable anaesthesia system. The antecedent part consists of IT2F linguistic process while the consequent part consists of interval neural network. The BP algorithm was used for online training of parameters of IT2FNN. The performance criteria used are ISE, ITAE and RMSE. The experimental result obtained by the proposed controller outperformed the one obtained by the adaptive IT2FLC and T1FNN controller under uncertainties in terms of settling time and overshoot. Kiani et al. (2013) presented the optimal design of IT2FLC for automatic voltage regulator system. Bacterial foraging optimization algorithm (BFOA) was used for tuning the MFs of IT2FLC. They consider the following fitness function in the simulation:

$$^{min}_{k}J(k) = G_e \int_0^T e^2(t)dt + G_u \int_0^T u^2(t)dt + G_M M_p \tag{2.50}$$

where $e(t)$ is the error, $u(t)$ is the control signal, T is the running time, M_p is the overshoot, and G_e, G_u, and G_M are the weighted constants. The simulation results obtained indicated that the BFOA outperform the extended discrete action reinforcement learning automata (EDARLA) under noise. Sayed et al. (2013a) presented a modified biogeography-based optimization algorithm (MBBO) for design of an IT2FLC for the improvement of the performance of Egyptian second testing nuclear research reactor.

MBBO was employed in designing the IT2FLC in order to get optimal parameters of MFs of the controller. ISE was used as an objective function. In the simulation,IT2FLC obtained the best performance and ISE index compared to PD controller. In another work by Sayed et al. (2013b), an optimal design of IT2FLC for performance improvement of the plant control systems was presented. The MBBO and PSO were used for tuning the MFs parameters of IT2FLC.ISE was used as an OF. The proposed controller was tested on two plants with different complexity (stable and unstable). The simulation results obtained by MBBO are better than the PSO based on running time and overshoot. Melin et al. (2013) presented an optimal design of FLC for tracking problem of the dynamic model of a unicycle mobile robot under perturbed torques. Chemical optimization (CO) was used for searching the optimal parameters of IT2FLC and T1FLC. ISE was used as an objective function. Both experimental and simulation results show that the CO outperform the GA, PSO and ACO. Also CO based IT2FLC outperformed the CO based T1FLC. Astudillo et al. (2012, 2013) applied the Chemical Reaction Optimization (CRO) method for optimal design of IT2FLC for tracking control of unicycle autonomous mobile robot. CRO was used to search for the gain constants and MFs parameters involved in the tracking controller. ISE was used as an OF. Both experimental and simulation results show that the best error obtained by CRO was similar with the one obtained with GA with less running time.

Li et al. (2013) proposed IT2FLS based data-driven strategy for modelling and optimization of thermal comfort words and energy consumption. The multi-objective optimization was used to optimize the temperature range through energy consumption and balancing the thermal comfort including MFs of the FLS. The results found in the simulation indicated that the specific room showed the robustness and effectiveness of the proposed method. Cortes-Rios et al. (2014) propose the parallel model implementation of Simple Tuning Algorithm (STA) for IT2FLC. The effect of AND/OR

operators' combinations on fuzzy rules, new integral criteria parameters, and mechanism to calculate the feedback gain are included to improve the algorithm applicability and performance. ISE, IAE, ITSE and ITAE were consider as performance criteria. The STA based IT2FLC was tested using Hagglund and Astrom benchmark systems and their performance were compared with that of PID controllers. Good performance of the proposed method was achieved compared to PID controller based on simulation and experimental results.

Liu et al. (2014) presented an optimal solution to a Solid Transportation Problem (STP) with Tabu Search Algorithm (TSA) based type-2 fuzzy variables. ISE was used as an objective function. Three types of new defuzzification criteria for type-2 fuzzy variables were proposed such as expected value, optimistic value and pessimistic value. The multi fold fuzzy STP is formulated as the chance-constrained programming model with minimum cost of expected transportation. The application and effectiveness of the proposed method was illustrated using numerical experiments and it was found to advance performance over state of the art methods. Zhang et al. (2014) presented a clustering routing protocol for wireless sensor networks based on T2FLS and ACO for lifetime prolonging and load balancing in wireless sensor network (WSN). T2FLS is used to handle the rule uncertainty and balance the network load. The number of neighbour nodes, residual energy and the distance to the base station was considered as the input to the T2FLS while candidate Cluster Head (CH) competition radius and CH are considered as output of T2FLS. ACO was used for adjusting these input and output of T2FLS. It was reported that, the proposed routing protocol could reduce the transmissions energy consumption of CHs and balance the network load. Furthermore, it prolongs the lifetime of WSN.

Yao et al. (2013) presented the IT2FLS for robust human behaviour recognition using machine vision in intelligent environments. The big bang-big crunch(BB-BC) optimization was used to optimize the MFs parameters and rule based of IT2FLS. Weizmann dataset was used as a benchmark. In terms of overall average recognition accuracy, the proposed method outperformed the traditional IT2FS, optimal T1FLS and traditional T1FLS. Gaxiola et al. (2013a) proposed the upper and lower type-2 fuzzy weight adjustment for neural network performing the learning method. BP algorithm was used for updating the weight. The proposed method was applied to Mackey-Glass time series prediction. NN with greater robustness and less susceptibility under noisy time series data was provided by the proposed method. Doostparast et al. (2014) presented α-plane based automatic general type-2 fuzzy clustering method (GT2FCM) for gene expression data analysis. A two stage Simulated Annealing (SA) algorithm optimization was presented. In the first stage, the annealing process accompanied by its proposed perturbation mechanism was devoted. After the termination of this stage, its output was inserted to the second stage in order to check for possible local optima. The output of this stage was then reinserted to the first stage until no better solution is obtained. This optimization is based on the objective function using α-planes for general type-2 fuzzy c-means clustering algorithm. The proposed method was evaluated using different artificial datasets and three real gene expression datasets. The results of the experiments showed the flexibility and effectiveness of the proposed method under highly uncertain environment compared with type-1 fuzzy clustering method (T1FCM) and average linkage methods (ALM).

Nguyen and Meesad (2013) presented the optimal design of IT2FLS and T1FLS TSK for sea water level prediction using Firefly Algorithm (FA), PSO and GA. These optimization methods were used to optimise the MFs parameters for IT2FLS and T1FLS. The prediction results obtained by FA outperformed the one obtained by PSO, GA and

ANFIS. Additionally, the results obtained by optimal IT2FLS outperformed the one obtained by T1FLS. Almaraashi and Hedar (2014) presented the comparison between TSA and Directed TSA (DTSA) for better improvement of configuration of IT2FLSs. DTSA is the hybrid of TSA which have the ability of both local and global search while TSA is a pure global search. STA and DSTA were used to search for the best configuration of IT2FLS rule base and MFs parameters. The proposed method was applied on Iris flowers and Haberman classification data sets benchmark. The results obtained showed that, DTSA gives faster and better IT2FLS configuration than TSA.

A summary of presented publications in which other optimization methods that have been used to optimize the T2FLC is presented in Table 2.6.

Table 2.5: Other meta-heuristic algorithms used for designing of T2FLS

Reference	Problem domain	Proposed algorithm	Algorithm compared with the proposed algorithm	Other system (s) compared with T2FLS	Result
Castillo et al. (2012)	Control	Ant colony optimization	PSO and GA	T1FLC	T2FLC better than T1FLC and ACO better than PSO
Yesil (2014)	Control	Big bang-big crunch	Not compared	T1FLC and PID	T2FLC better than T1FLC and PID
Kumbasar and Hagras (2014)	Control	Big bang-big crunch	PSO	Self-tuning T1FPIDC, BB-BC based T1FPIDC and PID	T2FPID better than Self tuning T1FPIDC, BB-BC based T1FPIDC and PID
El-Nagar and El-Bardini (2014)	Control	Back propagation algorithm	Not compared	Adaptive IT2FLC and T1FLC	T2FLC better than adaptive IT2FLC and T1FLC
Kiani et al. (2013)	Control	Bacterial foraging optimization	EDARLA	Not compared	BFO better than EDARLA
Sayed et al. (2013a)	Control	Biogeography optimization	Not compared	PD	T2FLC better than PD
Sayed et al. (2013b)	Control	Biogeography optimization	PSO	Not compared	MBBO better than PSO
Melin et al. (2013)	Control	Chemical optimization	GA, PSO and ACO	T1FLC	T2FLC better than T1FLC and CO better than GA, PSO and ACO
Astudillo et al. (2012, 2013)	Control	Chemical optimization	GA	Not compared	CO better than GA
Li et al. (2013)	Control	Multi-objective optimization	Not compared	Not compared	Not compared
Cortes-Rios et al. (2014)	Control	Simple tuning optimization	Not compared	PID	T2FLC better than PID
Liu et al. (2014)	Control	Tabu search optimization	Not compared	Not compared	Not compared
Qi-Ye et al. (2014)	Clustering	ACO	Not compared	Not compared	Not compared
Yao et al. (2013)	Pattern recognition	BB-BC optimization	Not compared	T1FLS and other traditional non fuzzy systems	T2FLS better than T1FLS and other traditional non fuzzy system
Gaxiola et al. (2013a)	Prediction	BPA	Not compared	Not compared	Not compared
Doostparast Torshizi and Fazel Zarandi (2014)	Classification	SA	Not compared	T1FCM	GT2FCM better than T1FCM
Nguyen and Meesad (2013)	Prediction	FA	PSO and GA	T1FLS	T2FLS better than T1FLS. FA better than PSO and GA
Almaraashi and Hedar (2014)	Classification	TSA	DTSA	Not compared	DSTA better than STA

2.6 Future Trend and General Overview of the Research Area

The general summary of the area of this research i.e., the applications of Meta-heuristic Optimization Algorithms in the design of T2FLS is presented in this section. Based on the review of this area, the possible future trends that can be visualized were discussed. The complex problems of different kind of control (robotic, power systems, motor systems, mechanical systems etc.) as well as time series prediction, classification, clustering and pattern recognition with high level of noise and/or uncertainties can be handled properly by T2FLS. In recent years, the applications of T2FLS in intelligent control have become a common practice. It is widely known that the FLS design is not a simple task, particularly the design of T2FLS. This is due to the fact that T2FLS has more design parameters than the T1FLS. Meta-heuristic optimization algorithms have been used in automatic design of type-1 as well as type-2 systems that made it to become a standard practice as indicated in literature Castillo and Melin (2012). Now the trend has been extended to the use of the combination of more than one optimization algorithms in solving a problem. This method is referred to as hybrid optimization.

Based on this review it can be noted that the total number of publications for 2012 to 2015 in intelligent control is increasing per year (Figure 2.13 (a) and (b)). It can be stated that the trend in the area of design of T2FLS using optimization method is increasing yearly and this trend is expected to continue in the future because T2FLSs have been used more frequently in this area of research.

It is hard to declare one of applied optimization techniques as the best for optimization of T2FLS at the moment. This is because all of the reviewed methods have a record as successful methods of optimization of T2FLS in some applications. Although the HO method has outperformed some conventional optimization methods (such as GA, PSO and Firefly algorithm) in different applications, it cannot be declared as the best since it

is not compared with all of the methods. In any case, the need of application of optimization method in design of T2FLS was justified. This is due to the complexity in the design. Furthermore, it is advisable not to use gradient-based algorithms in optimizing T2FLS because the computations for MFs parameters will become much more complicated as stated in literature Mendel (2014) Therefore, researchers in this area should use the derivative free algorithms such as QPSO, SA, PSO, GA, CS etc. or their combination to form hybrid.

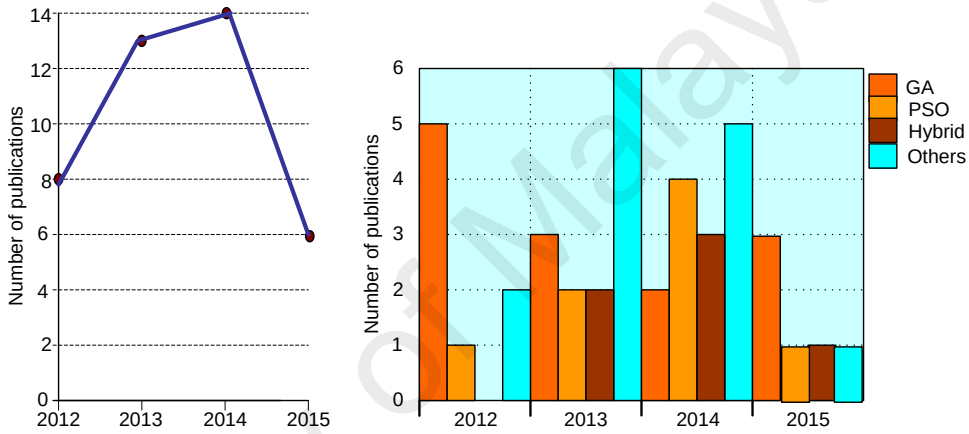

(a) (b)

Figure 2.13: (a) total number of publications per year, (b) distribution of publications per type of optimization method and year

2.6.1 Limitation of Previous T2FLS Design Methods and the Gap for future research

It is worth mentioning that based on this review, only few studies used the optimization based design to employ T2FLC in real-world environment. Also all the objective functions used by the researchers in this area are minimizing only one or two performance index. In addition, many studies do not compare the performance of their proposed optimization method with the state of the art optimization method. This is difficult or even impossible to measure the effectiveness of the proposed optimization method without any comparisons. To the best of my knowledge, there are many types of

optimization techniques that have not yet been applied to the optimization of T2FLC. These techniques include Grid search, cuckoo search optimization, genetic programming, harmony computing, membrane computing, bat algorithm etc. It is expected that, these optimization methods as well as those that will be proposed in the future will be applied in further studies in order to determine their effectiveness in the area of design of T2FLC.

CHAPTER 3: ROTARY INVERTED PENDULUM AS A BENCHMARK FOR TESTING CONTROL ALGORITHMS

3.1 Introduction

This chapter describe the four control objectives of RIP in detailed using energy based controller. It also, presented the review of the state of art work proposed by the researchers for each control objective of RIP. These comprise the linear, nonlinear time invariant, self-learning and adaptive nonlinear controllers. The dynamic model of RIP is developed based on Kane's and Newton-Euler Lagrange methods. The advantage and disadvantages of each model is exploit including the review of previous model developed by researchers. The Simulink model for both Kane's and Newton-Euler Lagrange methods are developed based on the derived equations. Comparisons between these methods was carried out using Matlab Simulink. Simulations was carried out to study the nonlinear behavior of the RIP. The trend of the studies in this area was point out from the year 2011 to date. Future research opportunities and challenges of the previous approaches in this area of research are presented. It is expected that expert researchers can use this chapter as starting point for further advancement while graduate scholars can use it as an initial point.

3.2 RIP

The initial motivation of studies of the inverted pendulum (IP) arose based on the need to design the balance controllers for the rockets during vertical take-off. The rocket is highly unstable at the instant of launching, thus, there is a need of a continuous alteration mechanism to stay at upright position in the open loop configuration Mathew et al. (2013). IP is an important member of nonlinear unstable under-actuated mechanical systems. The IP is a suitable benchmark system that can be used for training and experimental validation of new control strategies in robotics and control theory. The RIP which is also known as Furuta pendulum was proposed in 1992 by Furuta et al. (1992)

and since then it has been investigated by many researchers (Acosta, 2010; Carlos Aguilar-Avelar & Moreno-Valenzuela, 2015; Ferreira et al., 2011). The RIP is one of the available version of IP that can be found in most control laboratories. This study focuses on the RIP which inherits under-actuated, unstable, nonlinear and non-minimum phase system dynamics as shown in literiture Fairus et al. (2013). The experimental setup of the RIP produced by Quanser is shown in Figure 4.7 in chapter four.

The RIP systems perform in an extensive range in real life applications such as aerospace systems, robotics, marine systems, mobile systems, flexible systems, pointing control, and locomotive systems Ghorbani et al. (2013). In addition, the study of dynamic model and control algorithms in controlling the RIP plays an important role in controlling spacecraft, rockets, maintaining the equilibrium state for two legs robots and skyscraping buildings (Quyen et al., 2012). Moreover, when the pendulum of RIP is at hanging position, it represents real model of the simplified industry crane application (Ileš et al., 2011).

The control objectives of the RIP can be categorized into four categories:

I. Controlling the pendulum from downward stable position to upward unstable position known as Swing-up control (Oltean, 2014),
II. Regulating the pendulum to remain at the unstable position known as stabilization control (Chen & Huang, 2014),
III. The switching between swing-up control and stabilization control known as switching control (Nath et al., 2014),
IV. Controlling the RIP in such a way that the arm tracks a desired time varying trajectory while the pendulum remains at unstable position known as trajectory tracking control (Aguilar-Avelar & Moreno-Valenzuela, 2015).

In this context, different kinds of control algorithms have been applied for these control objectives. Other control problems associated with RIP that were investigated by the researchers include the friction compensation (Aguilar-Avelar & Moreno-Valenzuela, 2014; Gafvert et al., 2015), system identification (Chandran et al., 2015), synchronization problem (Ghorbani et al., 2013; Liu, 2014), decoupling of RIP to eliminate the under actuated problem (Chen & Huang, 2014; Rudra et al., 2013) and stability analysis (George et al., 2012).

3.3 Mathematical Modelling of RIP

Before designing a controller, the equations that characterize the behavior of the RIP system have to be developed as correctly as possible irrespective of the complexity of the equations.

Normally, the nonlinear dynamic equation of a RIP is derived using the Euler-Lagrange method (Antonio-Cruz et al., 2015) or Newton's laws of motion method (Oltean, 2014). Usually the following five assumptions are made:

I. The system consists of two ideal rigid bodies.
II. The position of the whole system is fixed in a horizontal and flat ground surface.
III. The motor inductance and friction on the armature are neglected.
IV. The equivalent frictional force of motor/arm is neglected.
V. The pendulum is rotating in a constant plane.

Subsequently, the nonlinear dynamic equation is linearized so as to simplify the design and analysis of the proposed controllers. This can be done using the linear approximation method which is based on the nonlinear model expansion in to Taylor series about the operating point and discarding the nonlinear terms (NøRgaard et al., 2000).

The free body diagram of RIP consisting of two connected rigid bodies actuated by a servomotor system is shown in Figure 3.1. These bodies are rotational arm and pendulum. Both arm and pendulum are one DOF. The arm is attached to the output gear of the motor and it can rotate around the fixed point B. The angle ϕ is the generalized coordinate for arm which is the angle between the arm and the horizontal x-axis (arm angle). The vectors $\hat{b}_1, \hat{b}_2, \hat{b}_3$ are the inertial earth fixed reference frame, in which $\hat{b}_3$ is away and perpendicular to the earth surface. The vectors $\hat{b}_r, \hat{b}_{\phi_1}, \hat{b}_3$ are the arm fixed reference in which $\hat{b}_r$ is away from fixed point B along the arm length. The pendulum is attached to free end of the rotating arm and has its mass centre at point C. The angle α is the generalized coordinate for pendulum, which is the angle between the pendulum and the vertical z-axis (pendulum angle). The pendulum has two plane of symmetry through $\hat{a}_1$ axis with normal direction $\hat{a}_2$ and $\hat{a}_3$ and it can rotate in a plane perpendicular to $\hat{b}_r = \hat{a}_3$. The pendulum fixed of reference are $\hat{a}_1, \hat{a}_2, a_3$ in which $\hat{a}_1$ point away from point A. The torque τ is applied at the fixed end of the arm by the motor and the direction of the torque depends on the direction of the voltage applied to the motor. The pendulum can move from 0 degree to 360 degrees about the arm axis in clockwise or anticlockwise directions. The arm is restricted to move from 0 to 75 degree about z-axis in clockwise or anticlockwise directions.

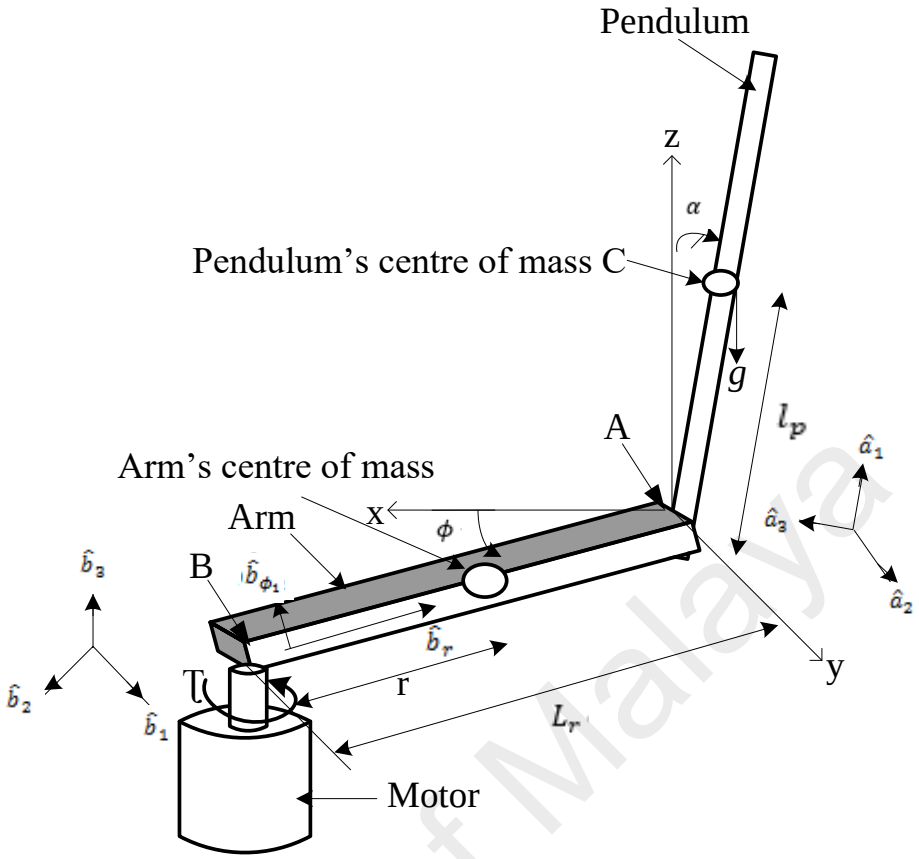

Figure 3.1: Free body diagram of RIP including the system's coordinates

3.3.1 Newton's Euler Lagrange Model of RIP

Most of literatures used Newton-Euler or Lagrange methods to find the dynamic equation of mechanical systems. The advantages of Newton-Euler Lagrange methods are: for simple systems this method is computationally efficient, quite intuitive and gives a normal extension from quasi-static analysis. The major drawback of this methods is that for complex configurations a significant effort is required to obtained a minimal (reduced) set of equations.

3.3.1.1 Nonlinear Newton's Euler Lagrange Model of RIP

Contrary to most literature were they simplify the generated model by assuming that, the pendulum is rotating in a constant plane as in literature (Ernest & Horacek, 2011; van Kats, 2004). In this study, we consider the rotary motion of the arm all together. That is,

it was assume that the actual plane pendulum is rotating in is different in every instant. Which means, the assumption number V in section 3.3 was nullified. This make the developed model to be more complex but with high accuracy. The newton's Euler Lagrange is used to developed the nonlinear model of RIP. The RIP model can be describe using the general motion equation of robot as follows:

$$D(\boldsymbol{q})\ddot{\boldsymbol{q}} + C(\boldsymbol{q}, \dot{\boldsymbol{q}})\dot{\boldsymbol{q}} + \boldsymbol{f}_C(\dot{\boldsymbol{q}}) + \boldsymbol{f}_v(\dot{\boldsymbol{q}}) + G(\boldsymbol{q}) = \boldsymbol{u} \quad (3.1)$$

Where $\boldsymbol{q} \in \mathbb{R}^2$ is the position coordinate that are represented by α and ϕ, the vectors $\dot{\boldsymbol{q}}$ and $\ddot{\boldsymbol{q}}$ are the velocity and acceleration respectively, $D(\boldsymbol{q}) \in \mathbb{R}^{2\times 2}$ is the symmetric and positive definite inertia matrix, $C(\boldsymbol{q}, \dot{\boldsymbol{q}})\dot{\boldsymbol{q}} \in \mathbb{R}^2$ are the Coriolis and centripetal forces, $\boldsymbol{f}_C(\dot{\boldsymbol{q}}) \in \mathbb{R}^2$ are the differentiable and continuous version of coulomb's frictional forces, $\boldsymbol{f}_v(\dot{\boldsymbol{q}}) \in \mathbb{R}^2$ are the viscous frictional forces, $G(\boldsymbol{q}) \in \mathbb{R}^2$ are the gravitational forces, $\boldsymbol{u} \in \mathbb{R}^2$ is the input torque. The step by step procedure of modelling of RIP is presented in Appendix A. The applied control torque and the position coordinate of the joints are considered in the present study. $\tau(t)$ is the control torque. The pendulum clockwise movement with respect to the upward position is considered as positive in this research

The model of RIP in equation (3.1) is given as follows:

$$\begin{bmatrix} u_1 + u_2 & -u_3 \\ -u_3 & u_6 \end{bmatrix}\begin{bmatrix} \ddot{\phi} \\ \ddot{\alpha} \end{bmatrix} + \begin{bmatrix} u_4\dot{\alpha} & u_5\dot{\alpha} \\ -\frac{u_4}{2}\dot{\phi} & 0 \end{bmatrix}\begin{bmatrix} \dot{\phi} \\ \dot{\alpha} \end{bmatrix} + \begin{bmatrix} B_r & 0 \\ 0 & B_p \end{bmatrix}\begin{bmatrix} \dot{\phi} \\ \dot{\alpha} \end{bmatrix} + \begin{bmatrix} 0 \\ -u_7 \end{bmatrix}[g] = \begin{bmatrix} 1 \\ 0 \end{bmatrix}[\tau] \quad (3.2)$$

where $u_1 = (J_r + mL_r^2)$, $u_2 = ml_p^2 sin^2\alpha$, $u_4 = ml_p^2 \sin 2\alpha$, $u_3 = mL_r l_p \cos\alpha$, $u_5 = mL_r l_p \sin\alpha$, $u_6 = \left(J_p + ml_p^2\right)$ $u_7 = ml_p \sin\alpha$, $\tau = \frac{\eta_m \eta_g k_t k_g}{R_m} V_m - \frac{\eta_m \eta_g k_t k_g^2 k_m}{R_m}\dot{\phi}$.

The description and values of these parameters are given in Table 3.1.

Table 3.1: Parameters of RIP

Symbol	Description	Value	Unit
m_p	Mass of pendulum	0.127	kg
L_p	Total length of Pendulum	0.337	m
J_p	Pendulum moment of inertia about its center of mass	0.0012	$kg.m^2$
B_p	Pendulum viscous damping coefficient as seen at the pivot axis	0.0024	N.m.s/rad
lp	Length of pendulum center of mass	0.156	m
L_r	Rotary arm length	0.168	m
B_r	Rotary arm viscous damping coefficient as seen at the pivot axis	0.0024	N.m.s/rad
J_r	Rotary arm moment of inertia about its center of mass	0.000998	$Kg.m^2$
R_m	Motor armature resistance	2.6	Ω
k_t	Motor current-torque constant	0.00768	N-m/A
k_m	Motor back-emf constant	0.00768	V/(rad/s)
K_g	High-gear total gear ratio	70	
η_m	Motor efficiency	69	%
η_g	Gearbox efficiency	90	%
J_{eq}	Equivalent moment of inertia as seen at the load	0.0036	kg.m2
B_{eq}	Equivalent viscous damping coefficient as seen at the load	0.004	Nms/rad

The detailed proof of these dynamic equations are presented in Appendix A:

3.3.1.2 Linear Newton's Euler-Lagrange Model of RIP

The linearization of the nonlinear dynamic equation is a common practice in control engineering design, especially for the design of linear controllers. This is to ease the complication of the dynamic equations. The nonlinearities in the equation of motion of RIP is arises from the trigonometric function present in the equation. Many types of linearization have been used in order to linearize the nonlinear model of RIP. This include Jacobian linearization, input-output feedback linearization, and optimal linearization. The small angle formula (at near equilibrium position of the pendulum) was used for linearization in literature (Mathew et al., 2013; Oltean, 2014). The Jacobian linearization was employed in literature (Al-Jodah et al., 2013). The linear model of RIP was found using partial feedback linearization in literature (Mandić et al., 2014). Feedback linearization method was used in literature (Chou & Chen, 2014). The resultant linear model of all the mentioned linearization method are local linear. That is, the linear model

has similar dynamic to nonlinear model around a specific operating point it was linearized. The weakness of the local linearization can be overcome using the optimal linearization method. This method gives a linear model that have the exact dynamic of the nonlinear model at any operating point with minimum approximation error. The optimal linearization of RIP was discussed in the literature (Zhang & Zhang, 2011). The nonlinear model can be approximated to linear model via the Taylor series expansion about the operating point and discarding the nonlinear terms as follows (The detailed proof of the equations is presented in Appendix B):

$$(J_r + mL_r^2)\ddot{\phi} - mL_r l_p \ddot{\alpha} = \tau - B_r\dot{\phi} \tag{3.3}$$

$$-mL_r l_p \ddot{\phi} + (J_p + ml_p^2)\ddot{\alpha} - mgl_p\alpha = -B_p\dot{\alpha} \tag{3.4}$$

In matrix form, the equation (3.3) and (3.4) can be written as:

$$\begin{bmatrix} J_r + mL_r^2 & -mL_r l_p \\ -mL_r l_p & J_p + ml_p^2 \end{bmatrix}\begin{bmatrix} \ddot{\phi} \\ \ddot{\alpha} \end{bmatrix} + \begin{bmatrix} B_r & 0 \\ 0 & B_p \end{bmatrix}\begin{bmatrix} \dot{\phi} \\ \dot{\alpha} \end{bmatrix} + \begin{bmatrix} 0 \\ -mgl_p\alpha \end{bmatrix} = \begin{bmatrix} \tau \\ 0 \end{bmatrix} \tag{3.5}$$

The linear state space equation is given by

$$\dot{x} = Ax + Bu \tag{3.6}$$

$$y = Cx + Du \tag{3.7}$$

where

$$A = \frac{1}{J}\begin{bmatrix} 0 & 0 & 1 & 0 \\ 0 & 0 & 0 & 1 \\ 0 & m^2 l_p^2 L_r g & -(J_p + ml_p^2)(\varsigma_2 + B_r) & -mL_r l_p B_p \\ 0 & (J_r + mL_r^2)mgl_p & -mL_r l_p(B_r + \varsigma_2) & -(J_r + mL_r^2)B_p \end{bmatrix}, \tag{3.8}$$

$$B = \frac{1}{J}\begin{bmatrix} 0 \\ 0 \\ ml_p^2\varsigma_1 \\ mL_r l_p \varsigma_1 \end{bmatrix}, \tag{3.9}$$

$$C = \begin{bmatrix} 1 & 0 & 0 & 0 \\ 0 & 1 & 0 & 0 \end{bmatrix}, \tag{3.10}$$

$$D = \begin{bmatrix} 0 \\ 0 \end{bmatrix}. \tag{3.11}$$

$$J = J_p m L_r^2 + J_r J_p + J_r m l_p^2 \tag{3.13}$$

$$\tau = \varsigma_1 V_m - \varsigma_2 \dot{\phi} \tag{3.14}$$

where

$$\varsigma_1 = \frac{\eta_m \eta_g k_t k_g}{R_m} \tag{3.15}$$

$$\varsigma_2 = \frac{\eta_m \eta_g k_t k_g^2 k_m}{R_m} \tag{3.16}$$

$$\begin{bmatrix} \dot{\phi} \\ \dot{\alpha} \\ \ddot{\phi} \\ \ddot{\alpha} \end{bmatrix} = \begin{bmatrix} 0 & 0 & 1 & 0 \\ 0 & 0 & 0 & 1 \\ 0 & 75.47 & -119.44 & -0.08945 \\ 0 & 103.91 & -4.429 & -1.2817 \end{bmatrix} \begin{bmatrix} \phi \\ \alpha \\ \dot{\phi} \\ \dot{\alpha} \end{bmatrix} + \begin{bmatrix} 0 \\ 0 \\ 53.57 \\ 2.678 \end{bmatrix} V_m \tag{3.17}$$

$$\begin{bmatrix} \phi \\ \alpha \end{bmatrix} = \begin{bmatrix} 1 & 0 & 0 & 0 \\ 0 & 1 & 0 & 0 \end{bmatrix} \begin{bmatrix} \phi \\ \alpha \\ \dot{\phi} \\ \dot{\alpha} \end{bmatrix} \tag{3.18}$$

The RIP system open loop poles are $w = [0,\ 9.447,\ -10.701,\ -119.467]$. It can be seen that the RIP system is unstable because it has one pole at the right hand side of *s*-plane. Hence there is a need to test for the system's controllability prior to any control action. This can be done by testing the rank of matrix

$R = [B, AB, A^2B, A^3B \ldots A^{n-1}B]$, using equation (3.17). If R has full rank then the system is fully controllable. The R has full rank when $rank(R) = 4$.

3.3.1.3 Matlab Model based on Newton's Euler-Lagrange Model of RIP

The Matlab model of RIP can be found based on the developed nonlinear mathematical model in equations (3.1) and (3.2). This is by substituting the values of the RIP parameters. The parameters of the used RIP and their description is presented in Table 3.1.

After the substitution and rearranging, the nonlinear equation of motion of RIP can be found as:

$$\ddot{\phi}(0.00458 + 0.006659\sin^2\alpha) + \dot{\phi}(0.07143 + 0.006659\dot{\alpha}\sin 2\alpha) - 0.0003328\ddot{\alpha}\cos\alpha + 0.0003328\dot{\alpha}^2\sin\alpha = 0.128V_m \quad (3.19)$$

$$0.0153286\ddot{\alpha} - 0.0003328\ddot{\phi}\cos\alpha - 0.0033295\dot{\phi}^2\sin 2\alpha + 0.0024\dot{\alpha} - 0.1946\sin\alpha = 0 \quad (3.20)$$

The Newton's Euler-Lagrange based Nonlinear Matlab model is developed using the equation (3.19) and (3.20) and its shown in Figure 3.2.

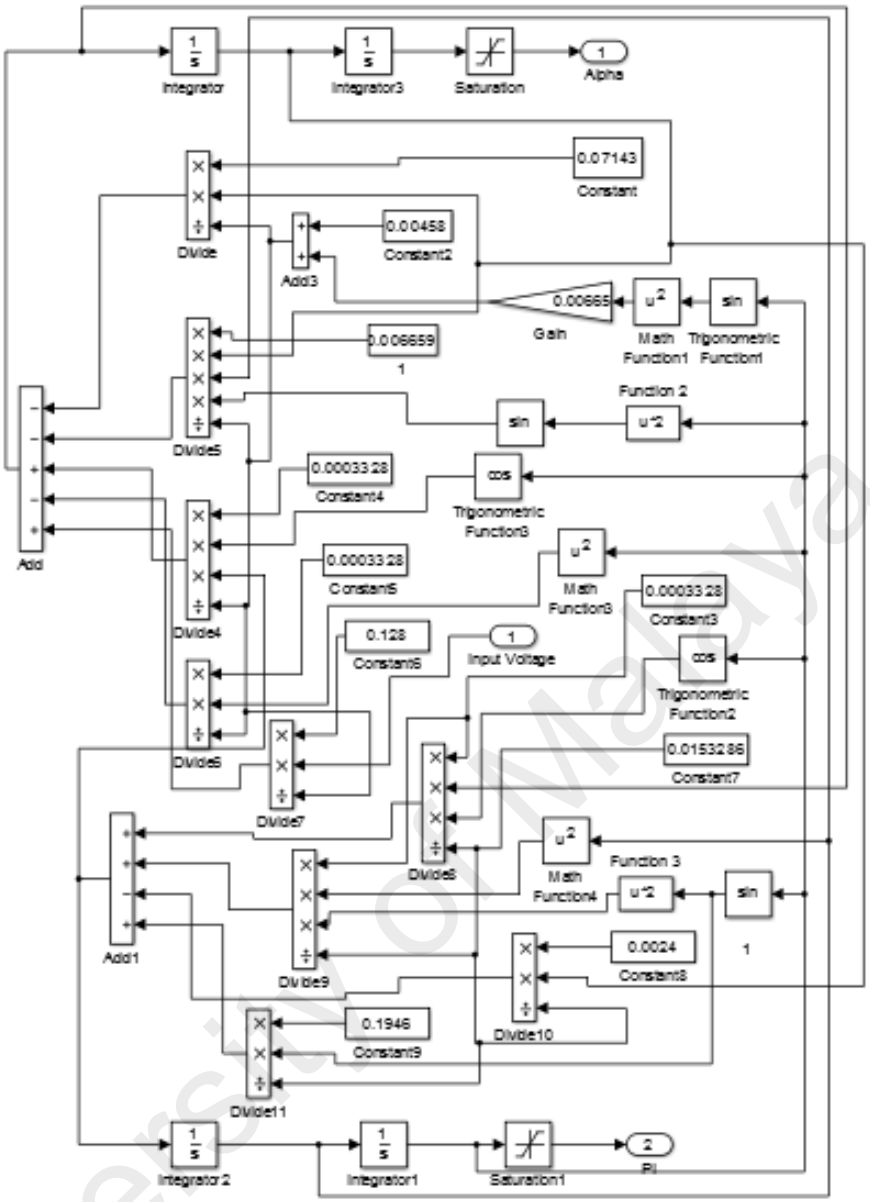

Figure 3.2: Newton's Euler-Lagrange based Nonlinear Matlab model of RIP

The Linear Matlab model of RIP can be found based on the developed linear mathematical model in equations (3.3) and (3.4). This is by substituting the values of the parameters in Table 3.1. After the substitution and rearranging, the linear equation of motion of RIP can be found as:

$$\ddot{\phi} = 0.07259\ddot{\alpha} - 28.539\dot{\phi} + 15.06V_m \tag{3.21}$$

$$\ddot{\alpha} = 0.04235\ddot{\phi} - 0.305\dot{\alpha} + 24.76\alpha \tag{3.22}$$

The Newton's Euler-Lagrange based linear Matlab model is developed using the equation (3.21) and (3.22) and its shown in Figure 3.3.

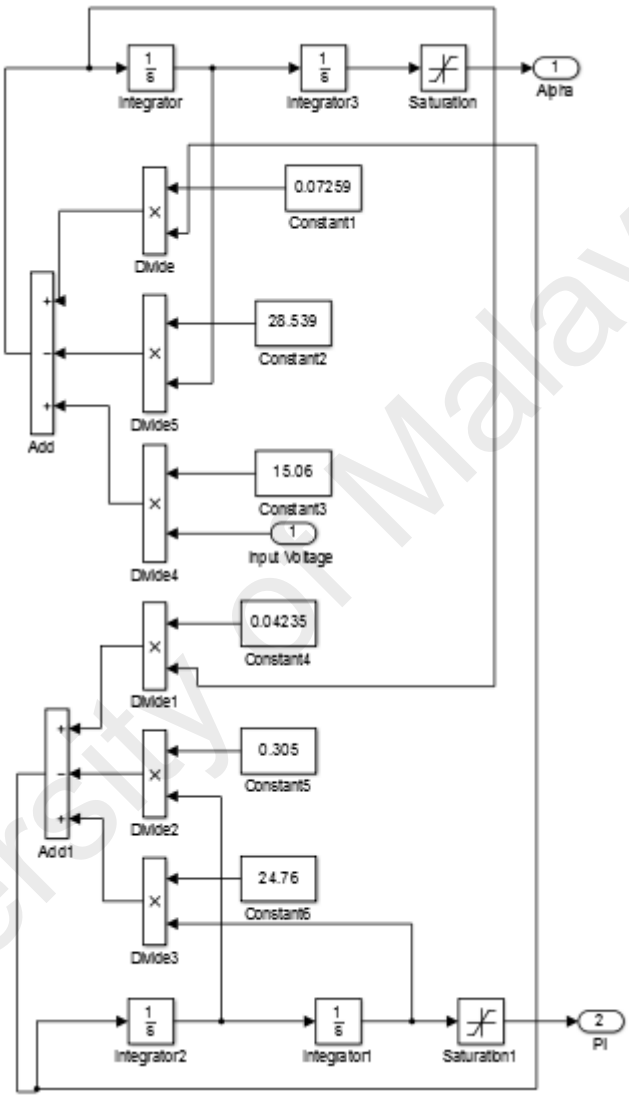

Figure 3.3: Newton's Euler-Lagrange based linear Matlab model of RIP

3.3.2 Kane's Method of Modelling RIP

Numerous researchers used Kane's method to developed the dynamic equation for different mechanical systems. Kane's method is suitable for developing the dynamic equations for systems consisting of multiple rigid bodies like spacecraft which is moving under the effect of some gravitational fields (Knutson, 2012). Lagrange multiplier was used in the derivation using Lagrange method, while the calculation of redundant forces

was involved in Newton method. As a result, Newton-Euler, Lagrage-Euler and Lagrange methods requisite complicated and tedious formulation for a large multi-body system Shamsudin et al. (2013). Consequently, they likely led to an inefficient computation. Kane's method can be regarded as an alternative method of modeling. This method does not require the calculation of multipliers or redundant forces. Kane method is based on the partial velocities of the constituents of the system (Komistek et al., 1997). Hence, Kane's method is more efficient than Lagrange and Newton-Euler methods in terms of computation for systems consisting of multiple rigid bodies (Nukulwuthiopas et al., 2002). In this section, a nonlinear dynamical equation of the RIP is derived using Kane's method.

3.3.2.1 Nonlinear Kane's Model of RIP

Using the same assumption as in the Newton's Euler-Lagrange, the nonlinear equation of motion of RIP can be derived using Kane's method as follows:

Consider the Free body diagram of RIP including the system's coordinates in Figure 3.2. The equation for $\hat{a}_3$ direction is the pendulum equation of motion and it can be express as follows:

$$ml(r\dot{u}_1 \cos\alpha + g \sin\alpha) = I_{33}\dot{u}_2 - (I_{22} - I_{11})u_1^2 \cos\alpha \sin\alpha \tag{3.23}$$

Equation (3.23) can be written in the following form

$$\varepsilon u_1^2 \cos\alpha \sin\alpha + \beta\dot{u}_1 \cos\alpha = \dot{u}_2 - \omega_n^2 \sin\alpha \tag{3.24}$$

where $\varepsilon = \frac{I_{22}-I_{11}}{I_{33}}$, $\beta = \frac{mrl}{I_{33}}$ and $\omega_n^2 = \frac{mgl}{I_{33}}$ in which the parameter ε is approximately equal to moment of inertia for thin rod and ω_n is the natural frequency of the pendulum. Based on parallel axis theorem (Bedford et al., 2008), $I_{33} = \bar{I}_{33} + ml^2$, $I_{22} = \bar{I}_{22} + ml^2$ and $I_{11} \equiv \bar{I}_{11}$.

The right-hand side of equation (3.24) is the expression of the standard pendulum on the cart while left-hand side is due to the additional rotation of the base on the circular arc.

The dynamic equation of arm can be found from its $\hat{b}_3$ component of moment equilibrium about the fixed point B as follows:

$$\tau = \overline{b}u_1 + I_0\dot{u}_i + T_1\cos\alpha - T_2\sin\alpha + rF_\phi \tag{3.25}$$

where $\overline{b}u_1$ is the equivalent frictional force of motor/arm, I_0 is the transverse moment of inertia for arm at the fixed point B, τ is the torque applied to the arm by the motor. Substituting for T_1, T_2 and F_ϕ at their directions we have the dynamic equation for arm as follows:

$$\tau_0 = (\gamma\sin^2\alpha + I)\dot{u}_1 - \beta\dot{u}_2\cos\alpha + \beta u_2^2\sin\alpha + \gamma u_1 u_2\sin 2\alpha + bu_1 \tag{3.26}$$

where $\tau_0 = \frac{\tau}{I_{33}}$, $I = \frac{I_0 + I_{11} + mr^2}{I_{33}}$ and $b = \frac{\overline{b}}{I_{33}}$

The detailed proof of these equations is presented in Appendix C.

3.3.2.2 Matlab model of RIP based on Kane's method

The parameters in Table 3.1 was used. By assuming the equivalent frictional force of motor/arm equal to zero. Substituting the values of the parameters and rearranging equations (3.24) and (3.26), the equation of motion of RIP can be found as

$$\ddot{\phi} = \frac{1}{0.8077\cos\alpha}\ddot{\alpha} - \frac{\sin\alpha}{0.8077}\dot{\phi}^2 + 58.4\tan\alpha \tag{3.27}$$

$$\ddot{\alpha} = \frac{1.112+\sin^2\alpha}{0.8077\cos\alpha}\ddot{\phi} + \frac{14.62+0.8077\sin\alpha}{0.8077\cos\alpha}\dot{\alpha}^2 - \frac{\sin 2\alpha}{0.8077\cos\alpha}\dot{\alpha}\dot{\phi} + \frac{31.06}{0.8077\cos\alpha}V_m \tag{3.28}$$

Based on the autonomous model in equation (3.27) and (3.28), the Matlab Simulink of RIP is developed as shown in Figure 3.4.

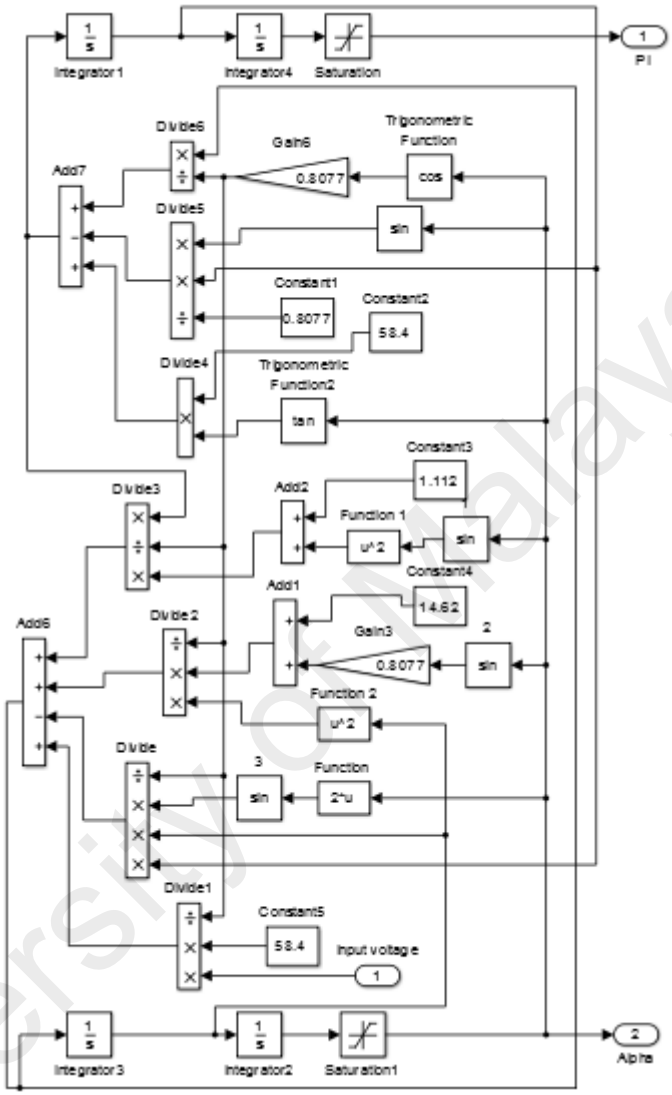

Figure 3.4: Kane's based Nonlinear Matlab model of RIP

3.3.2.3 Open loop response for the RIP model based on Kane's method

Initially, the pendulum is positioned in an inverted position with very small displacement say 0.05°, then it is allowed to fall by applying a pulse signal to the model. The open loop responses for pendulum and arm are shown in Figure 3.5 and Figure 3.6 respectively. This response of the Simulink model was revealed to be accurate in comparison with the widely known empirical observations of pendula characteristics as described in the following literature (Antonio-Cruz et al., 2015; Fairus et al., 2015;

Jadlovský & Sarnovský, 2013). Moreover, the adequate correctness of the simulation model was approved. The response shows that the whole system is nonlinear and unstable.

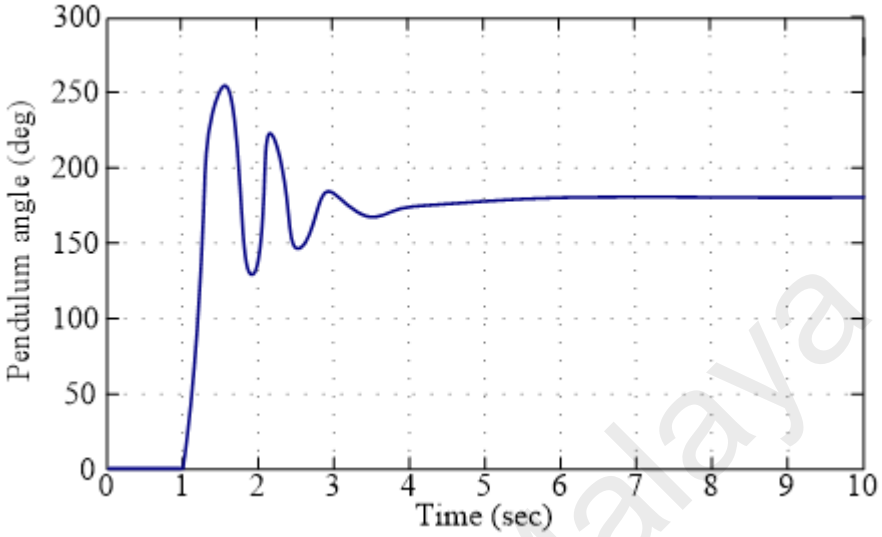

Figure 3.5: Open loop response for Pendulum

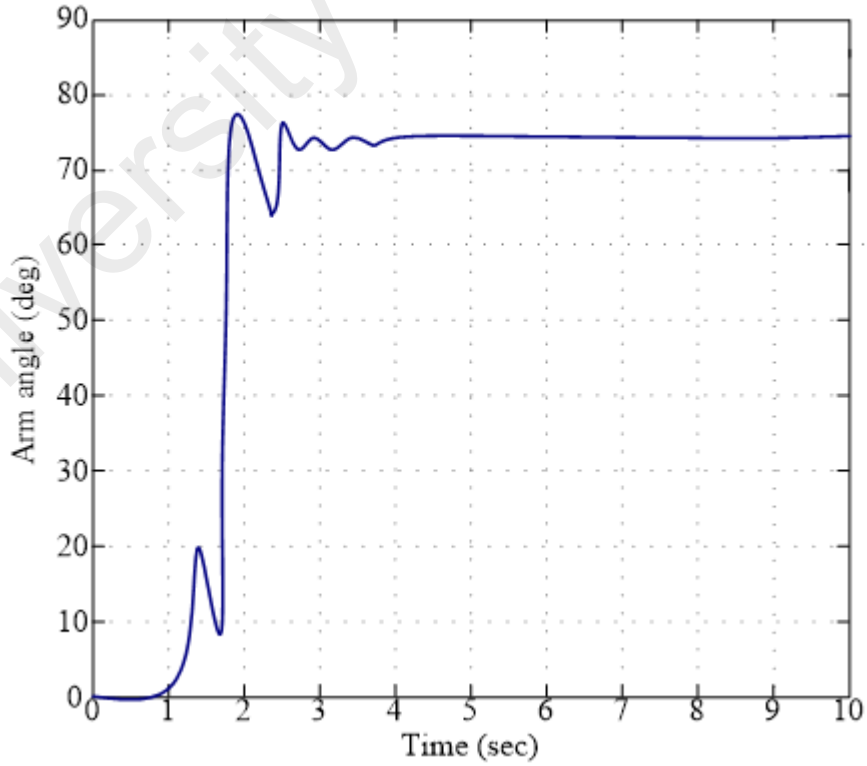

Figure 3.6: Open loop response for Arm

3.3.3 Comparisons of the developed models

The open loop response for the nonlinear dynamic equation of RIP developed using Kane's method is compared with the nonlinear dynamic equation of RIP developed using Newton-Euler Lagrange method as shown in Figure 3.7. This is by applying a pulse signal to the models. The simulation result for pendulum and arm are shown in Figure 3.8 and 3.9 respectively. The simulation results show that the Kane's and Newton-Euler Lagrange responses are similar and their behaviors are closely the same for both pendulum angle and arm angle.

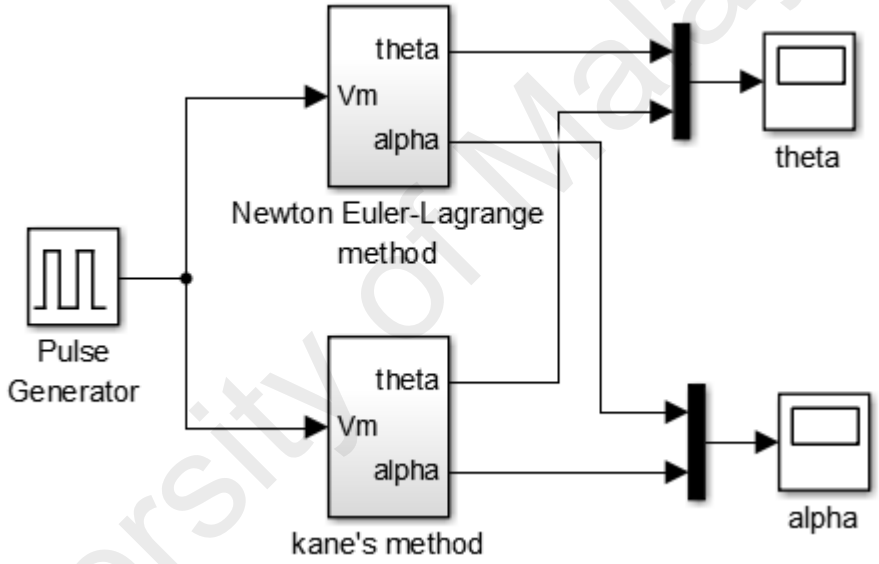

Figure 3.7: Comparison of Newton-Euler Lagrange and Kane's methods

It can be seen that for the Kane's based model, the pendulum falls in about 1.4-second while for Newton-Euler Lagrange based model the pendulum falls in more than 1.75 seconds. Also for the arm, it can be seen that for the Kane's based model the arm moves from 0° to about 22.33° and come back to about 9° within 1.75 seconds. However, within the same time, the Newton-Euler Lagrange based model can only move from 0° to about 23.33°. This demonstrate that Kane's model based is faster in respond compared to the Newton-Euler Lagrange based model. These simulation results agree with the theoretical results; therefore, the presented model is valid to some level.

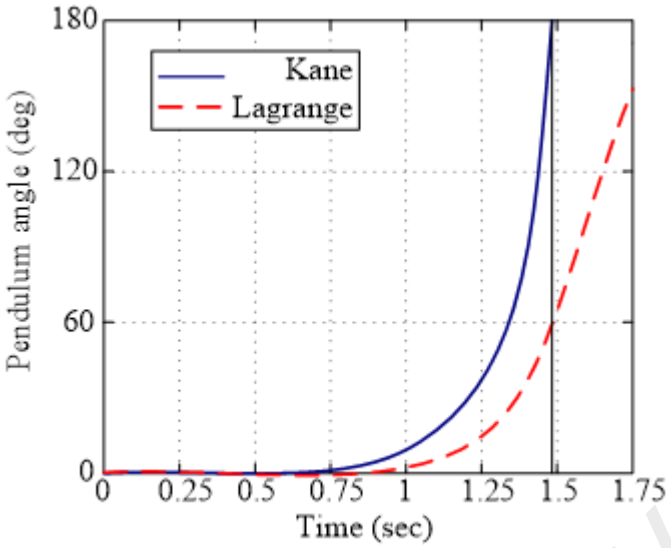

Figure 3.8: Comparison of pendulum's open loop response

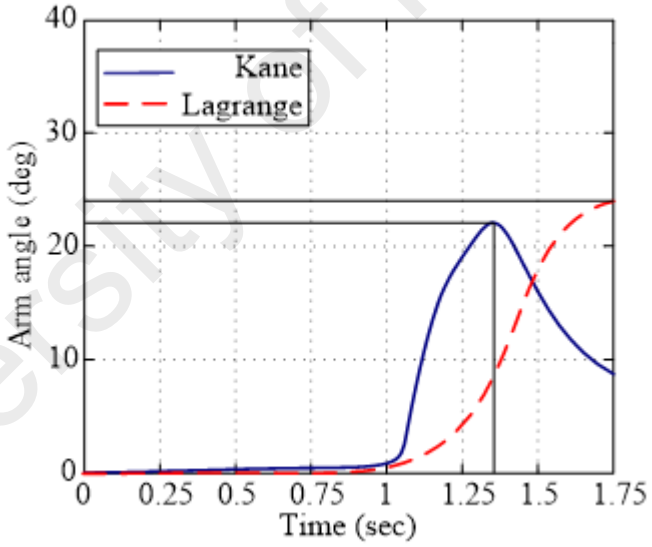

Figure 3.9: Comparison of arm's open loop response

3.3.4 Validation of the developed model with the state of art model

The open loop response for nonlinear-1 (developed using Newton's Euler-Lagrange in section 3.3.1.1), nonlinear-2 proposed in literature Oh et al. (2009) and linear (developed using Newton's Euler-Lagrange in section 3.3.1.2) dynamic models of RIP are compared to validate the proposed model with the state of art model. Originally the pendulum is placed in an inverted position with very small displacement; then it is allowed to fall by

applying a pulse signal to the model. The simulation results in Figure 3.10, and 3.11 show that the nonlinear-1 and nonlinear-2 are similar and their behaviors are the same for both pendulum angle and arm angle. This shows that nonlinear one can be considered as a nonlinear model of the RIP because the nonlinear two has already been proved and used in literature Oh et al. (2009). The linear model depicts the nonlinear pendulum motion for the first 1.3 seconds until it attains 21^0 then it began to deviate from the actual motion. The response shows that the whole system is nonlinear and unstable.

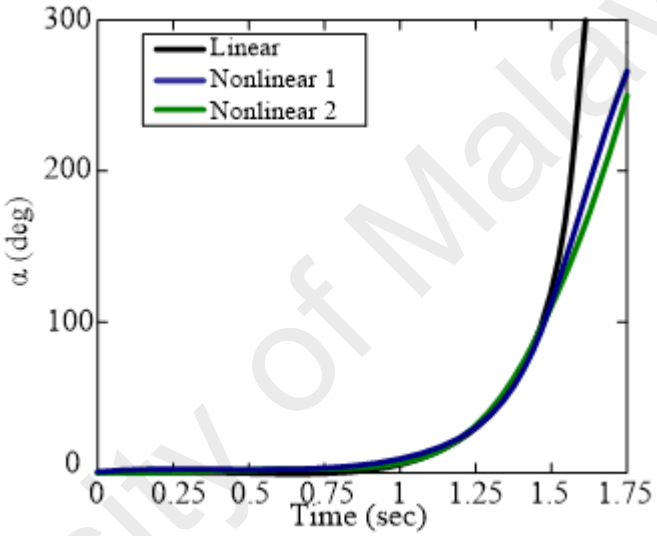

Figure 3.10: Open loop response for RIP (pendulum angle)

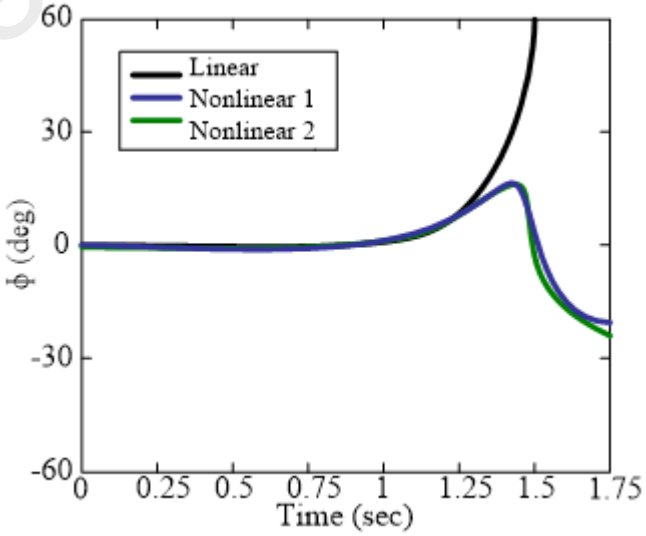

Figure 3.11: Open loop response of RIP (pivot arm angle)

3.4 Friction and Friction compensation in RIP system

The investigation of friction and friction compensation is very important in control engineering community. Friction can be seen as a highly nonlinear component which can result in limit cycles (LCs), steady state error and poor system performance. The RIP can be used to study the effect of friction and friction compensation since the frictional effects in RIP are so clearly visible. It can be shown that the friction in the driven arm might cause the LCs with high amplitude. The LCs can be predicted using widely known friction models such as LuGre model (Acosta, 2010), Coulomb friction model (Gafvert et al., 2015) and Coulomb friction with stiction model (Gäfvert, 1999). The amplitudes of the LCs and all other effects due to friction can be reduced using friction compensator based on these friction models (Gafvert et al., 2015). The friction phenomena in RIP happens in the joints (i.e. the pendulum and arm joints). The friction in both joints can be demonstrated as follows:

3.4.1 Pendulum joint

The friction in this joint can be demonstrated using a damping constant through a small ball bearing. Based on the Rayleigh's dissipation function (Ogata, 1998):

$$D = \frac{1}{2}(b_1\xi_1^2 + b_2\xi_2^2 + \cdots + b_i\xi_i^2) \tag{3.29}$$

where b_i is the i^{th} viscous damper coefficient and ξ_i is the velocity difference across the i^{th} viscous damper which can be express as a function of the generalized velocity. Therefore, for the RIP pendulum

$$D(\dot{\phi}) = \frac{1}{2}b_1\dot{\phi}^2 \tag{3.30}$$

The non-conservative torque τ_n is given by:

$$\tau_n = \frac{dD(\dot{\phi})}{d\dot{\phi}} = \frac{d}{d\dot{\phi}}\left(\frac{1}{2} b_1 \dot{\phi}^2\right) = b_1 \dot{\phi}^2 \tag{3.31}$$

The constant b_i is found to be 226×10^{-7} based on the free motion experiment (Acosta, 2010). This value is very small, that is why the friction in the pendulum joint is generally neglected.

3.4.2 Arm Joint

The frictional torque in the motor shaft comprised of the dynamic friction, static friction, and natural damping. The Coulomb friction model can be considered as a simple model given as:

$$\tau = \tau_c \text{sgn}\left(\frac{d\alpha}{dt}\right) \tag{3.32}$$

This model does not describe the friction at zero velocity (Gäfvert, 1999). The Lund Institute and Grenoble Laboratory (LuGre) model can be used to describe the friction at all points. The dynamic equation of LuGre model is as follows (Awtar et al., 2002):

$$\frac{dz}{dt} = v - \sigma_0 \frac{|v|}{g(v)} z \tag{3.33}$$

$$g(v) = \tau_c + (\tau_s - \tau_c) e^{-\left(\frac{v}{v_s}\right)^2} \tag{3.34}$$

$$\tau_r = \sigma_0 z + \sigma_1 \frac{dz}{dt} + \sigma_2 v \tag{3.35}$$

where z is the initial state of the model, v is the velocity at $\dot{\alpha} = \dot{\phi}$, v_s is the Stribek's velocity, σ_0 and σ_1 are the internal model parameters, σ_2 is the dynamic friction constant, τ_c is the Coulomb friction torque, τ_s is the static friction torque and τ_r is the estimated friction torque.

3.4.3 System Identification

The physical meaning of the parameters in equation (3.33)-(3.35) is explained in detail in (Altpeter, 1999). Also, the explanation and steps for identification of the parameters in equation (3.33)-(3.35) for RIP will be presented in this section. It can be stated that for the identification of all these parameters only the arm and the motor is needed, thus the pendulum is decoupled from the system. The open loop response is used in all these identifications. The least square algorithm can be used to identify σ_2 and τ_c by considering the first order system as follows:

$$J_a \frac{dv}{dt} + \sigma_2 = \tau - \tau_c \text{sgn}(v) \tag{3.36}$$

The moment of inertia of the arm and motor J_a can be estimated experimentally. To identify the τ_s the angle of the motor is feedback with a small PI action given in the form:

$$u = g_1 e + g_2 \int_0^t e(\tau) d\tau \tag{3.37}$$

where e is the error between the desired reference and measured state. $g_{1,2}$ are PI gains. The parameters τ_s, J_a and τ_c are required to be known for identification of v_s which can be known based on the above identification steps. By introducing a very small speed in the shaft of the motor (i.e. $\frac{dz}{dt} \approx 0$) the fictitious state z in equation (3.33) can be approximated as:

$$z \approx \frac{v}{|v|} \frac{g(v)}{\sigma_0} \tag{3.38}$$

Also, τ_r from (3.34) can be approximated as:

$$\tau_r = \left(\tau_c + (\tau_s - \tau_c) e^{-(v/v_s)^2}\right) \text{sgn}(v) \tag{3.39}$$

The equation

$$J_a \frac{dv}{dt} = \tau - \tau_r \tag{3.40}$$

can be linearized to

$$v(t) = v_s \sqrt{\ln \varepsilon(t)} \tag{3.41}$$

The ε is given by:

$$\varepsilon = \frac{\tau_s - \tau_c}{\left(\tau - J_a \frac{dv}{dt}\right)\text{sgn}(v) - \tau_c} \tag{3.42}$$

This approximation is valid for $\varepsilon \geq 1$ and $\tau_s > \tau_c$. The values of ε and v_s can be found by inputting the sinusoidal torque to the system. The parameter σ_0 can be estimated by inputting the ramp signal in such a way that the angle cross zero. The range of values of the ramp signal should be around $\pm \frac{4}{5}\tau_s$. Therefore $\sigma_0 \approx \frac{\Delta\tau}{\Delta\phi}$. For identification of σ_1 the small displacement is assumed and $g(v) \gg |z|$. hence $v = \dot{z} = \dot{\phi}$ from (3.33).

Consequently, the linear second order equation can be used as:

$$\tau = J_a \ddot{\phi} + (\sigma_1 + \sigma_2)\dot{\phi} + \sigma_0(\phi + \phi(0)) \tag{3.43}$$

Thus, the value of σ_1 can be estimated easily based on equation (3.44) since it is a linear second order system

$$\sigma_1 = 2\xi\sqrt{J_a \sigma_0} - \sigma_2 \tag{3.44}$$

where ξ is the linear model damping constant.

The identification result presented in literature Acosta (2010) indicates that the LuGre model can give a precise estimation of friction. This gives a chance to design a good friction compensator in the arm joint. Based on this, the control method can be

designed considering the RIP as a conservative system. The generic diagram for friction compensation model is presented in Figure 3.12.

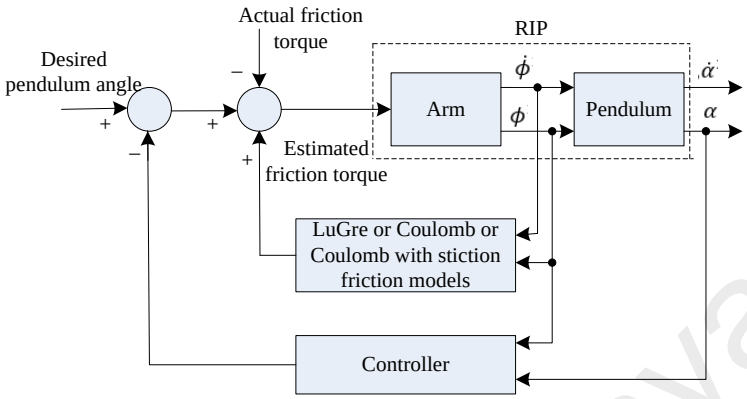

Figure 3.12: Friction compensation model for RIP

3.5 Review of Controllers applied on RIP system

The main goal of RIP control is to swing up the pendulum near to the upright unstable equilibrium position and balance it there. Afterward, the arm is controlled to track the desired time-varying trajectory while the pendulum remains at an unstable position. Different kinds of controllers have been used for these purposes. These include the linear controllers, nonlinear time-invariant controllers, self-learning, and adaptive nonlinear controllers. This section presents the review of the state of art work proposed by the researchers on the RIP control.

3.5.1 Linear Controllers Applied to RIP

Having a linear model of RIP, a linear controller can simply be linked for state reference tracking (Chan et al., 2013). The design of gain matrix *K* is the only requirement of this controller as shown in Figure 3.13.

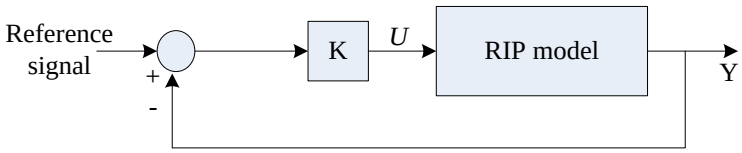

Figure 3.13: Linear controller for reference tracking

The assumptions made are: the system is full state controllable, the state variables can be measured and they are available for feedback, and the control input are unconstrained. Pole placement (PP) method can be used in this case to obtain suitable performance for control of overshoot and rise time. Given a linear closed loop system:

$$\left.\begin{aligned}\dot{X} &= AX + BU\\ Y &= CX\end{aligned}\right\} \tag{3.45}$$

The control vector U can be designed in a state feedback form as follows (Tewari, 2002):

$$U = -KX \tag{3.46}$$

therefore, equation (3.45) become

$$\dot{X} = (A - BK)X = A_{CL}X \tag{3.47}$$

The PP comprises evaluating a gain matrix K in such a way that the desired poles in linear model of RIP system are the eigenvalues of A_{CL}. The PP was used for stabilization control of RIP in literatures (Jadlovska & Sarnovsky, 2013; Lee et al., 2014), also Nath and Mitra (2014) presented the counter based controller and PP with integrator for swing up and stabilization controls respectively. They used energy criteria for the switching control.

Linear quadratic regulation (LQR) is slightly more complex than PP. The LQR provides an optimal control law for a linear system with a quadratic performance index J.

The design problem is that of finding a control input U, which minimizes the performance index given by Bemporad et al. (2002):

$$J = \int_0^\infty (X^T QX + U^T RU)dt \tag{3.48}$$

where R and Q are positive definite square matrices. The matrix R and Q are used to scale the relative contributions of the terms of the quadratic forms $U^T U$, and $X^T QX$, respectively. In this case, the K in equation (3.47) is given by:

$$K = R^{-1}B^T P \tag{3.49}$$

moreover, the symmetric definite matrix *P* is the solution to the algebraic Riccati equation given by

$$PA + A^T P + Q - PBR^{-1}B^T P = 0 \tag{3.50}$$

Many researchers employed the LQR approach to design controllers for RIP. This is likely because the LQR guarantee the optimal control law. For example, the stabilization problem of RIP was solved using LQR in literature (Barbosa et al., 2011; Fujita et al., 2014; Ghorbani et al., 2013; Mathew et al., 2013; Nguyen & Shen, 2011; Petchithai et al., 2015; Seman et al., 2013). The stabilization and swing-up control are implemented via a unified LQR controller in literature Zhang and Zhang (2011) which can efficiently evade switching control between the two stages. Some researchers compared the performance of LQR with other linear controllers. The findings for this comparisons are contradictory. This is because the LQR method is shown to have lower overshoot and settling time than PP in literature (Lee et al., 2014). However, the results reported in the literature (Jadlovska & Sarnovsky, 2013) shows that the PP has superior robustness than LQR. Also, the mix of H_2/H_∞ control is shown to be better than the LQR control. All these evaluations cannot be generalised because they are peculiar to the specific model of RIP and specific tuning of the corresponding controller. The controllers that can be designed using LQR or PP are considerably different. This is because LQR depends on the weighting matrices Q and R in literature (Ufnalski et al., 2015) while PP depends on

selected pole (Wei et al., 2016). Generally, a higher gain and better convergence can be achieved by selecting bigger Q gains for the LQR or poles that are more to the left half plane for PP controller. But this produced more vibrations at equilibrium (Chan et al., 2013). When faster settling time is required, the LQR is prepared in choosing those states which is impossible with PP. Thus LQR can be used to manage the trade-offs between actuators and states more accurately as stated in (Chan et al., 2013).

Linear Quadratic Gaussian (LQG) controller is another type of LQR that comprises the Kalman filter observer and optimal LQR controller as shown in Figure 3.14. The Kalman filter is used for noise immunity and state estimation. The detailed explanation on LQG is presented in (Videcoq et al., 2015). Measured states are used in LQR without a filter. Though LQR is a sufficient design approach that holds its phase margin assurances; this is in the case where by the observer dynamics are greatly faster than the system dynamics. The LQG was proposed in the literature (Chiluvuri et al., 2015) to ensure stabilization of pendulum with a minimal deviation of arm and pendulum angles. This is based on applying large penalties on arm and pendulum angles in the cost function of the optimal control law.

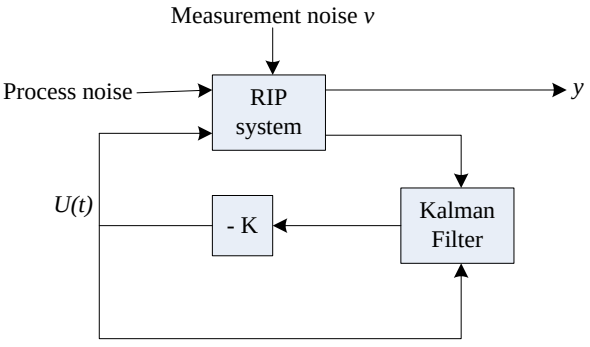

Figure 3.14: Linear quadratic Gaussian controller

The H_∞ and H_2 controllers are alternative robust and optimal controllers. These controllers are using different cost function and they are less sensitive to disturbances and

model errors (Hassibi et al., 1999). Al-Jodah et al. (2013) proposed the energy based controller for swing up and the mix of H_2 and H_∞ state feedback for stabilization control. The proposed stabilization controller was compared with the conventional full state feedback controller and LQR controller. The results showed that the proposed stabilization method is better than its comparatives.

The Proportional Integral Derivative (PID) controller shows an excellent performance for the linear system of RIP. The PID controller is commonly used in industries because of its simple structure and robustness in different operation conditions (Hassanzadeh & Mobayen, 2011). The PID controller alone, or in hybrid form with other controller, or PI controller (when the derivative gain is zero), or PD controller (when the integral gain is zero) have been widely applied to different control objectives of RIP in literature. The PID controller was employed for the swing up control, partial feedback linearization for stabilization and the angle threshold for switching control. The Genetic algorithm (GA) based PID controller, particle swarm optimization (PSO) based PID controller and ant colony optimization based PID controller are proposed for stabilization and reference tracking controls of RIP in literature (Hassanzadeh & Mobayen, 2011). Kharitnove polynomial based PI controller was designed for the same purpose in literature (George et al., 2012). The PD controller and fuzzy PD controller were used for swing up and stabilization respectively in literature (Oltean, 2014). The energy threshold method was employed for switching control while the fractional order PD was applied for stabilization control of RIP in literature (Mandic et al., 2014). The performances of PD and PD with the dead zone for RIP stabilization was compared in literature (Rubio et al., 2013).

The main issue in PID, PI, and PD controllers is finding the appropriate gains. The acceptable gains can be found simply from the experimentation via trial and error. Else,

Ziegler–Nichols method can be employed to set the initial gains. However, meta-heuristic algorithms can be used to find the best gains with respect to an objective function (Hassanzadeh & Mobayen, 2011).

Chou and Chen (2014) investigated the new swing-up control method for RIP using energy based control and the feedback linearization method. The energy function is chosen to design the control law in which the gain k is selected based on the trajectories in the phase-plane. The result found a show that the fast energy rate depends on the value of gain k. Seman et al. (2013) proposed two ways for swinging up control of RIP based on energy. The first way is the conventional method based on comparing the present total energy of the RIP system with the energy in its up-right position. The second way is by using an exponentiation operation over the pendulum position. The stabilization control is tackled using LQR. Mathew et al. (2013) studied the performances of energy based and PD controllers for swing up control of RIP and sliding mode controller and LQR controllers for stabilization control. The simulation results indicate that the energy based controller is better than PD controller with less number of oscillation to reach the equilibrium position. Also for stabilization, the LQR has less overshoot and a faster settling time, but the Sliding Mode Control (SMC) is more robust in the presence of parameter uncertainties. Nguyen and Shen (2011) proposed a hybrid control scheme for swing up and LQR control for the stabilization of RIP. The flexibility of the hybrid control scheme is based on the choice of energy based swing up the controller and heuristic swing up the controller at the different pendulum's positions. A novel composite control method for tracking control of RIP is reported in the literature (Aguilar-Avelar & Moreno-Valenzuela, 2015). This scheme comprises of an energy-based compensation and a feedback-linearization-based controller. The analysis of the closed loop system indicated that the system is uniformly ultimately bounded to the trajectories of error. The real-time experiments and numerical simulations show the viability of the proposed method. The

proposed control scheme is compared with the hybrid output tracking controller consisting of a differential flatness, nonlinear backstepping and small gain theorem proposed in in literature (Yan, 2003).

The trajectory tracking control of RIP using active disturbance rejection control (ADRC) method was studied in literature (Ramírez-Neria et al., 2014). A linear controller of the ADRC was designed based on the linear observer. This is done on the origin of the flat tangent system linearization around an arbitrary equilibrium. The proposed method was compared with the SMC in real time. The results show that the proposed method has superior performance over the SMC. Aguilar-Avelar and Moreno-Valenzuela (2014) compared a feedback linearization control method and output tracking nonlinear controller for tracking control of RIP. The results indicated the superiority of the feedback linearization method based on regulation and tracking error with slightly higher control torque.

3.5.2 Nonlinear Time Invariant Controllers

The SMC, fuzzy logic control and back-stepping are the most commonly employed nonlinear control strategies applied on RIP. It is widely known that SMC effectively provides robust control for the nonlinear system even in the presence of uncertainties and disturbances (Hung et al., 1993). This method has been applied successfully for RIP control due to its attractive features (Fairus et al., 2015). These features include easy realization, compatibility to Multiple Input and Multiple Output (MIMO) systems, good control performance for a nonlinear systems such as good transient response, fast response, and insensitivity to external disturbance and plant parameter variation (Faradja et al., 2014). Also, it is possible to guarantee the stability of SMC because it benefits from the merit of switching control law (Pan et al., 2012). However, the switching control law introduced chattering in the system. This is due to its

alternating switching, which occurs from its digital implementation (Feng, 2006). The stabilization problem of RIP was solved using a different kind of SMC. For example, Linear Matrix Inequalities (LMI) based multi-objective integral SMC is proposed in (Fairus et al., 2015). The proposed controller indicates the superior performance compared with the LQR. The SMC based on higher order differentiator observer was used for stabilization control of RIP in literature (Faradja et al., 2014) and conventional SMC was proposed in (Ashrafiuon & Whitman, 2012) for the same purpose. Stabilization problem of RIP was solved using SMC with time delay in literature (Pan et al., 2012). Cascade optimal SMC was proposed in the literature (Muske et al., 2012) for RIP stabilization control. The parameters of SMC were optimally updated using a discrete-time, nonlinear model predictive control structure. Kurode et al. (2011) proposed the SMC for both swing up and stabilization controls of RIP. The proposed method was compared with the PD swing up and LQR stabilization controllers. The results show that the SMC can swing up within a small period and it is more robust than PD and LQR controllers, respectively.

The proposed controller by Kurode et al., (2011) was shown to be better than PD controller swing-up and LQR stabilization. The integral SMC based on the observed values of the state variables is proposed in in literature (Ferreira et al., 2011). The novel algorithm outperformed its comparative in both pendulum stabilization and trajectory tracking control.

FLCs are often employed for nonlinear systems control. This due to its attractive features which include easy incorporation of expert knowledge into the control law, less model dependent, robustness and ease of use to model linguistic rules. FLC can approximate any nonlinear control law based on the number of the fuzzy sets. Yet, the stability of a general FLC is difficult to confirm. This is due to the piecewise nature of

the control law which makes it difficult to confirm the Lyapunov stability. Different types of FLC have been used for different control objective of RIP in literature. A stabilization control of RIP was tackled using robust FLC in cascade form (Alt et al., 2011). Both inner and outer FLCs in literature (Alt et al., 2011) are based on a uniform fuzzy set with a minimum number of rules. The Swing-up control, stabilization control, and trajectory tracking controls problems were solved using intelligent optimized cascade fuzzy-PD controller based on GA and differential evolution in literature (Oh et al., 2012). A parallel distributed compensation based FLC using LQR method is reported in (Fairus et al., 2013) for stabilization control of RIP system. The composite FLC (CFLC) for swing up and stabilization of RIP system is presented in literature (Li, 2013). This is essentially state feedback control by fuzzy summation of FLC and PD controls. In literature (Hassan et al., 2013), the performance of FLC was shown to be better in comparison with LQR for stabilizing the RIP system. The variable universe of discourse FLC (VUDFLC) was used for stabilization control of RIP in (Long et al., 2014). The simulation results indicate the robustness and effectiveness of VUDFLC over the general FLC. Fuzzy PD Controller was used for stabilization control in literature (Oltean, 2014; Oltean & Duka, 2014).

The SMC have been hybridised with other controllers, especially for suppressing chattering. For example, SMC and FLC were hybridized in literature (Ahangar-Asr et al., 2011) for stabilization control of RIP. This control scheme has the advantages of both constituents and deviates from the limitations of each constituent.

Nonlinear LQR was applied in the stabilization of nonlinear control of RIP called State-Dependent Riccati Equation (SDRE) method (Jadlovská & Sarnovský, 2013). This is based on the transformation of the nonlinear system into its equivalent form through extended linearization. The results found by SDRE indicate a better performance than the standard LQR in terms of settling time and overshoot. A novel swing up control of RIP

by means of the Speed-Gradient method which is based on the measured coordinates is reported in the literature (Aracil et al., 2013). A nonlinear stabilization based on the Forwarding method was presented, and shown to be better than LQR stabilization. Lyapunov-based switching method was used. In work reported in the literature (Casanova et al., 2015), the researchers investigated the real-time application of an event-based control method for tracking control of RIP. The communication between the plant and the controller is achieved via Ethernet, i.e. TCP/IP. This reduced the bandwidth used by control loop and led to a Networked Control System. The experimental results indicate how the proposed method can reach a substantial reduction of the bandwidth consumed with an insignificant worsening of the performance.

Aguilar-Avelar and Moreno-Valenzuela (2015) hybridized a feedback-linearization-based controller with an energy-based compensation for reference tracking control of RIP. The proposed method ensured that the closed-loop system is uniformly ultimately bounded. The proposed method demonstrate a better tracking performance than the combination of back-stepping, small gain theorem and differential flatness proposed in (Yan, 2003). Tsuge et al. (2014) developed nonlinear controller based on polynomial and non-polynomial representations using PSO and sum of squares methods for stabilization of RIP. The stability condition of polynomial and non-polynomial systems were derived by approximating the domain of attraction with input magnitude constraints. The tensor product model transformation based swing-up control of RIP was proposed using the LMI based control in literature (Ileš et al., 2011). The stabilization control of RIP was tackled using interconnection and damping assignment passivity- based control in literature (Ryalat & Laila, 2013). The energy shaping where the reference energy function to the passive map was allocated, and injection of damping to guarantee asymptotic stability. Fabbri et al. (2013) applied the Packet-Based Control method with the dynamic controller for swing-up and stabilization control of RIP. Ethernet network was used to implement

the network communication channel. The proposed controller was compared with the conventional local controller for divers time-varying actuation delays which indicate its effectiveness. Aracil et al. (2013) investigated a new nonlinear method for RIP control. The Speed-Gradient approach based on directly measured coordinates was used to swing-up the RIP. The nonlinear controller based on the Forwarding method was proposed for stabilization of RIP. Türker et al. (2012) proposed the stabilization control of RIP using a static feedback controller based on direct Lyapunov method and partial feedback linearization. The asymptotic stability of the system has a region of attraction containing nearly all points in the upper half-plane of the pendulum independent of the physical parameters. The direct Lyapunov stability method based on a set of transformations for stabilization of RIP is proposed in (Turker et al., 2013). Fabbri et al. (2013) investigated the packet-based control (PBC) method for swing up and stabilization controls of RIP in real time. The PBC was compared with a local micro-controller for diverse time-varying actuation delays. The results indicate the validity and robustness of PBC method in the presence of actuation delays.

3.5.3 Self-learning and Adaptive nonlinear controllers

Quyen et al. (2012) proposed a hybridization of a PID controller and ANN for the RIP. Here, the ANN was trained by using the input and output data via a supervised learning method. The training data is derived from the model of RIP with the PID controller of two variables. The output controller based on Attractive Ellipsoid Method (AEM) and adaptive state estimator was developed in (Ordaz & Poznyak, 2012) for the stabilization of RIP. This method guaranties the stabilization of the controlled system trajectories within an ellipsoid of a "minimal size." The same method was proposed in the literature (Ordaz & Poznyak, 2016) with some modification of the AEM idea that allows the use of online information acquired during the process. Azar and Serrano (Azar & Serrano, 2015) investigated the adaptive SMC, second order SMC and PD+SMC for stabilization control

of RIP. The variable structure design procedure and Lyapunov stability theorem are used to develop these control methods to obtain asymptotically stable system trajectories. The results obtained indicate the superiority of adaptive SMC aver second order SMC and PD+SMC. A novel adaptive NN-based control method for RIP was proposed in the literature (Moreno-Valenzuela et al., 2016). Based on the input and output weights adaptation laws, the proposed method can guarantee reference tracking of the signal for the arm while the pendulum remains at an unstable position. Three different reference tracking were tested namely: sinusoid trajectory with torque disturbances, complex trajectory and sinusoid trajectory with additive Gaussian noise in measured feedback signals torque. The proposed method was compared with linear PID controller, adaptive NN+PID, and adaptive NN+PD controller. The proposed control method was found to be more robust than the comparative methods. Lyapunov-based adaptive controller was proposed in the literature (Chen & Huang, 2014) to stabilize the RIP with time-varying uncertainties. The hierarchical adaptive back-stepping SMC was proposed in (Rudra et al., 2013) for balancing control of RIP subjected to the external disturbances. The RIP model was decoupled into two subsystems. To derive each subsystem to the desired sliding surface, an adaptive back-stepping based control law was designed for each subsystem. The balancing control of RIP using a Temporal Based NN (TBNN) model was proposed in (Hercus et al., 2013). The online training ability of TBNN controller makes it possible to control the RIP without the need of its exact model. The Adaptive Neuro-Fuzzy Inference (ANFIS) controller was presented in literature (Agrawal & Mitra, 2013) for balancing of RIP. The simulation results demonstrate that ANFIS controller is better when compared with FLC and PID controller in terms of overshoot, settling time and parameter variation. Singh et al. (2012). Studied the linear fusion function based on LQR mapping, and tuning of controller parameters adaptively using ANFIS for stabilization of RIP. The weights tuning and number of rule explosion which are the main

issues in FLC are eliminated by the proposed method. The proposed method is shown to be better in disturbances rejection, tracking performance and robustness against parameters variation than the classical LQR controller.

3.5.4 Disturbance Observer

The external disturbances or unmodelled system dynamics can cause law frequency disturbances in RIP control. The law frequency disturbances can be rejected by disturbance observer (Chen et al., 2000). The disturbance observer aids in improving the control action of the proposed controller. A disturbance observer is employed to estimate a state of the system. Then, the estimation of disturbance can be accomplished by comparing the measured and predicted system states. The resulting estimated disturbance is added to the proposed controller's output as shown in Figure 3.15. The generalized PI disturbance observer based control was used for stabilization of RIP in literature (Ramírez-Neria et al., 2014). Stamnes et al. (2011) confirm the presence of a globally exponentially convergent speed observer in closed loop form for general Euler–Lagrange systems. The complexity of the observer is reduced compared to the one proposed in the literature (Astolfi et al., 2010). The proposed observer is used to approximate the pendulum's velocities.

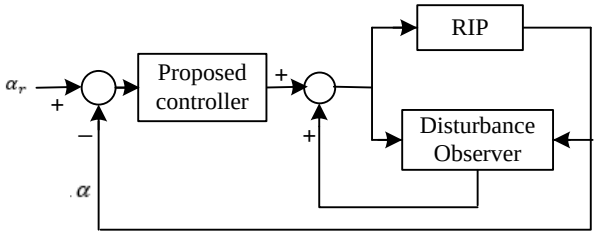

Figure 3.15: Control Objectives of the RIP

3.6 Control Objective of RIP

There are four main control objectives of RIP which include: Swing-up control, stabilization control, switching control and trajectory tracking control. The block diagram

in Figure 3.16 describes how these control objectives are implemented. These control objectives will be discussing in this section. The demonstration of the control objectives of RIP is done using energy based controller in Matlab Simulink environment.

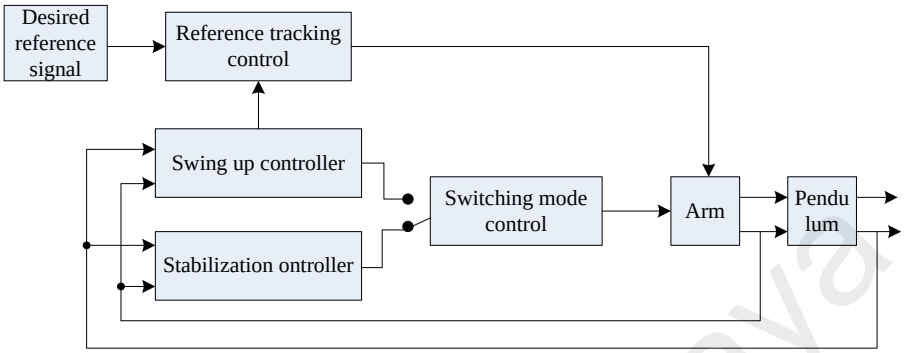

Figure 3.16: Description of the control objective of RIP

3.6.1 Swing up control

The swing-up control is the controlling the pendulum from downward stable position to upward unstable position. Normally this objective is implemented together with the stabilization control. When the swing up controller swing the pendulum near to the equilibrium position the stabilization controller is switch on by the switching mode controller.

3.6.1.1 Energy based swing up controller

The main control objective for RIP is to move the pendulum from the stable down position to the upright unstable position as quickly as possible and kept it there. Many types of control methods have been applied to solve this problem. For example, nonlinear, linear, SMC, partial feedback linearization has been used as disused in section 3.5.1 to 3.5.4. The energy based control strategy for under actuated systems has been studied by many researchers. This is by using the passivity and energy of the system. The major advantage of this method is the easiness in developing the controller from the function of energy storage, that adopts the system's mechanical energy. In addition, the energy based controller can confirm the asymptotic stability of the equilibrium, since it derived straight

from the total energy of the system. The energy based controller is the original back bone of many other intelligent control systems (Ordaz & Poznyak, 2016). Moreover, it is easier to used energy as a mode of switching between swing up and stabilization controller when energy based controller is used. Also, the implementation of energy based controller in real time is more realistic. This state the motivation of selecting the energy based controller to illustrate the control objectives of RIP.

Considering the nonlinear model of RIP as follows:

$$(J_r + mL_r^2)\ddot{\phi} + ml_p^2\ddot{\phi}sin^2\alpha + ml_p^2\dot{\phi}\dot{\alpha}\sin 2\alpha - mL_rl_p\ddot{\alpha}\cos\alpha + mL_rl_p\dot{\alpha}^2\sin\alpha = \tau - B_r\dot{\phi} \quad (3.51)$$

$$\left(J_p + ml_p^2\right)\ddot{\alpha} - m\ddot{\phi}L_rl_p\cos\alpha - \frac{1}{2}m\dot{\phi}^2l_p^2\sin 2\alpha - mgl_p\sin\alpha = -B_p\dot{\alpha} \quad (3.52)$$

The energy based swing up a controller can be designed for a pendulum in stable down position. The equation (3.52) can be re arrange and presented as follows:

$$\ddot{\alpha} = \Gamma^{-1}\left(\delta(\alpha)\ddot{\phi} + \sigma(\alpha)\dot{\phi}^2 + \varphi(\alpha) - B_p\dot{\alpha}\right) \quad (3.53)$$

where $\Gamma = J_p + ml_p^2,\ \Gamma > 0,\ \ \delta(\alpha) = mL_rl_p\cos\alpha,\quad \sigma(\alpha) = \frac{1}{2}ml_p^2\sin 2\alpha$ and $\varphi = mgl_p\sin\alpha$.

Now substituting equation (3.43) into equation (3.41), we have:

$$\ddot{\phi} = \frac{-2\sigma\dot{\phi}\dot{\alpha}\sin 2\alpha - B_r\dot{\phi} - mL_rl_p\dot{\alpha}^2\sin\alpha + \tau + \Gamma^{-1}\delta(\alpha)\sigma(\alpha)\dot{\phi}^2 + \Gamma^{-1}\delta(\alpha)\varphi(\alpha) - \Gamma^{-1}\delta(\alpha)B_p\dot{\alpha}}{J_r + m(L_r^2 + l_p^2sin^2\alpha) - \Gamma^{-1}\delta^2(\alpha)} \quad (3.54)$$

Therefore, the applied torque is:

$$\tau = 2\sigma\dot{\phi}\dot{\alpha}\sin 2\alpha + B_r\dot{\phi} + mL_rl_p\dot{\alpha}^2\sin\alpha - \Gamma^{-1}\delta(\alpha)\sigma(\alpha)\dot{\phi}^2 - \Gamma^{-1}\delta(\alpha)\varphi(\alpha) + \Gamma^{-1}\delta(\alpha)B_p\dot{\alpha} + \ddot{\phi}\left(J_r + m(L_r^2 + l_p^2sin^2\alpha) - \Gamma^{-1}\delta^2(\alpha)\right) \quad (3.55)$$

The pendulum dynamics in terms of pivot acceleration a can be defined as (Mathew et al., 2013):

$$J_p\ddot{\alpha} + \frac{1}{2}ml_p(g\sin\alpha - a\cos\alpha) \tag{3.56}$$

where a is the pendulum link base linear acceleration which is proportional to the arm torque and it can be expressed as:

$$\tau = m_r L_r a \tag{3.57}$$

The energy function of the RIP neglecting the linear velocity of the pendulum can be defining as:

$$E(t) = K(t) + P(t) = \frac{1}{2}J_p\dot{\alpha}^2 + \frac{1}{2}ml_p g(1-\cos\alpha) \tag{3.58}$$

$$\dot{E}(t) = J_p\dot{\alpha}\ddot{\alpha} + \frac{1}{2}ml_p g\dot{\alpha}\sin\alpha \tag{3.59}$$

from equation (3.46) the $\sin\alpha$ can be express as follows:

$$\sin\alpha = \frac{1}{mgl_p}\left(-2J_p\ddot{\alpha} + ml_p a\cos\alpha\right) \tag{3.60}$$

substituting equation (3.60) in equation (3.59) we have:

$$\dot{E}(t) = \frac{1}{2}ml_p a\dot{\alpha}\cos\alpha \tag{3.61}$$

Using the Lyapunov theory for stability, the Lyapunov function can be chosen as (Chou & Chen, 2014)

$$V = \frac{1}{2}E^2 \Rightarrow \dot{V} = E\dot{E} \tag{3.62}$$

$$\dot{V} = E\left(\frac{1}{2}ml_p a\dot{\alpha}\cos\alpha\right) \tag{3.63}$$

The proportional control can be used to swing up the pendulum to the desired reference energy E_r as:

$$a = (E - E_r)\dot{\alpha}\cos\alpha \tag{3.64}$$

By setting $E_r = E_p$, the link will swing to the upright position. Where E_p is the potential energy of the pendulum. The control signal magnitude should be large inorder to have quick energy change. As such the following energy based swing up controller is implemented

$$a = S_{a_{max}} k.(E - E_r)\text{sgn}(\dot{\alpha}\cos\alpha) \text{ for } k > 0 \tag{3.65}$$

where k is a control gain (tunable), all the routes initiating around the downward position will lastly converge to $E - E_r = 0$. Essentially, the speed of the convergence defends on the value of k, (i.e. the larger the value of k, the faster the convergence rate will be). $S_{a_{max}}$ is a function that saturate the control signal at maximum pendulum pivot acceleration a_{max}. The faster switching can be achiedved by taking the sign of $\dot{\alpha}\cos\alpha$

Let $\ddot{\phi} = \tau_1$. Therefore $\tau_1 = -\frac{l_p}{L_r}\dot{\phi}^2\sin\alpha + \frac{\tau_2}{L_r}$ and it can be shown that $\tau_2 = -L_r\ddot{\phi} + \dot{\phi}^2 l_p \sin\alpha\,\dot{\alpha}$

$$\dot{V} = -Eml_p\dot{\alpha}\cos\alpha\,\tau_2 \tag{3.66}$$

Obviously by selecting $\tau_2 = k.\text{sgn}(E\dot{\alpha}\cos\alpha)$. Therefore

$$\dot{V} = -k.ml_p|\dot{\alpha}E\cos\alpha| \leq 0 \tag{3.67}$$

From the expression in (3.57), it can be seen that the function V will stop at constant value or decrease to zero. As for the trajectory of E=0, it can be determined from (3.48) as follows:

$$\dot{\alpha}^2 = \frac{2ml_pg}{J_p}(1-\cos\alpha) = \frac{4ml_pg}{J_p}\sin^2\frac{\alpha}{2} \Rightarrow \dot{\alpha} = \pm 2\sqrt{\frac{ml_pg}{J_p}}\sin\frac{\alpha}{2} \quad (3.68)$$

The energy based controller for swing up is shown in Figure 3.17. This is based on equation (3.55). It is similar to the one used by Quanser RIP.

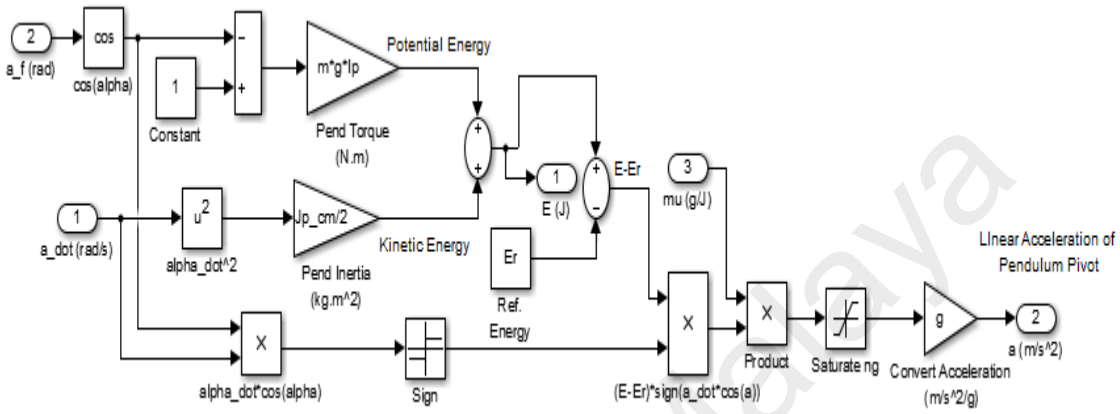

Figure 3.17: Energy based swing up controller

3.6.2 Switching control

The switching control is the criteria that is used to change the control action from one mode to another. Energy threshold and pendulum angle threshold are used for this purpose in the literature. In this study, both pendulum angle and energy criteria is proposed for switching between swing up and stabilization control as in equation (3.59)

$$\text{switching criteria} = \begin{cases} \text{Stabilization} & \begin{cases} |\alpha| < \frac{\pi}{9} \text{ and } \dot{\alpha} < 2.62\text{rad/sec} \\ |E - E_r| < 0.04 \text{ and } \dot{\alpha} < 2.62\text{rad/sec} \end{cases} \\ \text{swing up control} & \text{otherwise} \end{cases} \quad (3.69)$$

The Matlab switching strategy is shown in Figure 3.18.

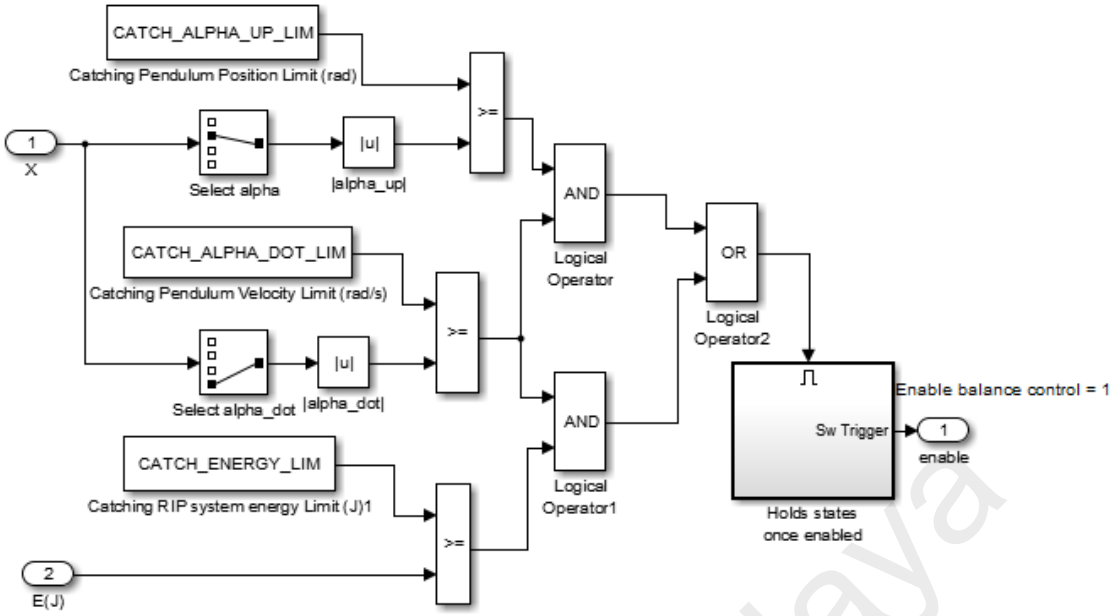

Figure 3.18: Mode switching

3.6.3 Trajectory tracking control

The trajectory tracking control of RIP is the controlling the RIP in such a way that the arm tracks the desired time-varying trajectory while the pendulum remains at an unstable position. This objective is similar to the reference tracking of the two-wheeled robot. The signal generator can be used to generates the type of desired signal (i.e. Square, sine, sawtooth, random, etc.). The set point for trajectory tracking can be implemented as in Figure 3.19.

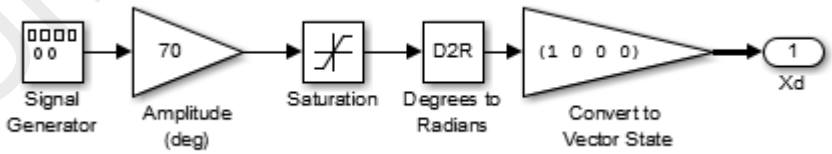

Figure 3.19: Set point for trajectory tracking

Recently, only few literature address this control objective using a different kind of controllers

3.6.4 Limitations of previous control methods applied on RIP and the opportunities for future research

Most of the proposed controllers applied for RIP control are model dependent since most of them are based on integral and/or invariant motion. So, it is essential to have the accurate mathematical model of RIP. In this context, many types of RIP have been developed together with their mathematical models (Antonio-Cruz et al., 2015; Driver & Thorpe, 2004; Jadlovský & Sarnovský, 2013). Newton-Euler, Lagrange-Euler, and Lagrange methods were used to develop the nonlinear mathematical model of RIP (Driver & Thorpe, 2004; Fairus et al., 2015; Shamsudin et al., 2013). Lagrange multiplier was used in the derivation using Lagrange method, while the calculation of redundant forces was involved in Newton method. As a result, Newton-Euler, Lagrange-Euler, and Lagrange methods require complicated and tedious formulation for a large multi-body system (Nukulwuthiopas et al., 2002). Consequently, they likely led to an inefficient computation. There is a need to find the most accurate model of RIP that is free from the stated limitations. Kane's method can be regarded as an alternative method of modeling. This method does not require the calculation of multipliers or redundant forces. It is based on the partial velocities of the constituents of the system (Komistek et al., 1997). Hence, Kane's method is likely to be more efficient than Lagrange and Newton-Euler methods regarding computation. On the other hand, it should be stated that most literature are simplifying the generated model by assuming that the pendulum is rotating in a constant plane. However, in actual sense, the rotary motion of the arm should be considered all together with a pendulum. That is, to consider the actual plane in which the pendulum is rotating is different in every instant. This can make the developed model be more complex but with high accuracy. Moreover, the frictional force effect in pendulum and arm joint are normally neglected in previous works. However, the effect of friction in RIP is clearly visible. It has been shown in (Gafvert et al., 2015) that the friction in the driven arm might

cause LCs with high amplitude. This can have a significant impact on the performance of the proposed controllers.

Most of the controllers proposed on RIP are for stabilization control objective of RIP. Though some other works deal with the stabilization control together with the swing up control objective which necessitate the introduction of switching control. But some of these work do not explain their switching control method. Another limitation is that most of the researchers applied their proposed intelligent self-learning or adaptive nonlinear controllers only on simulations. However, simulations studies can be used to demonstrate robustness to model uncertainties and disturbances. However, there may be some difficulties in practical implementation of such controllers. This includes the selection of the sampling time, sensor noise, and the total lag time for the real system. The experimental result would be more preferred to show the effectiveness and robustness of the controllers due to the real system effects mentioned. Also, the training of unstable ANN controller in real time is uncertain. It is expected that the simulation result should be validated with an experiment in real life settings. Many studies do not compare the performance of their proposed controller with the state of the art controllers. Therefore, it is difficult or even impossible to measure the effectiveness and robustness of the proposed controller over the state of the art controllers. Even for those who made the comparison, they could not make a general conclusion. Regarding the switching mode control, some researchers used pendulum angle threshold while others used the energy threshold. All these have the disadvantage of causing some oscillations in the system. There are many other intelligent controllers that are yet to be applied to the RIP, among which is a Type-2 fuzzy logic controller (T2FLC). Also, the hybrid T2FLC and SMC are yet to be tested on the RIP. Also, only a few works address the problem of trajectory tracking control. There is a need to have more research in this domain since it is one of the most important control objectives of RIP. Furthermore, the studies on the trajectory

tracking control have not included the swing up control. There is a need to have a comprehensive work that deals will all the control objectives with a detailed explanation to understand their relationship. All the proposed schemes used different controllers to achieve a single control objective (i.e. a controller for stabilization and another controller for swing up).

CHAPTER 4: METHODOLOGY

4.1 Introduction

The methodology used for designing the optimized T1FPIDC and IT2FPIDC is presented in this chapter. The parameters optimized include the scaling factors for fuzzy PID controller and the MFs parameters. The cascade control method is also discussed in this chapter. The method for designing the internal structure for both T1FPIDC and IT2FPIDC are presented based on the GA, PSO, and CS algorithms. Finally, the methodology for applying the proposed controllers in the real world is presented.

4.2 Cascade Control Method

The structure of the general cascade control including the optimization of controller's parameter as shown in Figure 4.1. Numerous researchers implemented a different kind of control of RIP system based on cascade method. Some used the two similar controllers in cascade form as in literature (Casanova et al., 2015; Oh et al., 2012; Oltean, 2014) while others used different controllers in cascade form as in literature (Chen & Huang, 2014; Muske et al., 2012).

In this context, the system to be controlled is represented by two sub-systems, that is sub-system 1 and sub-system two as shown in Figure 4.1. The structure of cascade control method consists of two control loops with a controller in each loop. The input to the outer controller is the error between the desired input signal y_{ref} and the output of the sub-system 2 y_0. The input to the inner controller is the difference between the output of the outer controller (r_0) and the output of sub-system 1 (y_i). The output signal from inner controller (r_i) serve as the control input to the sub-system 1, while the output of sub-system 1 (y_i) serve as the control input to sub-system 2. The tuning of the control parameters in cascade control strategy can be done individually as done in literature (Kumbasar & Hagras, 2014), i.e. to design the inner loop controller based on the propose

objective function firstly. Subsequently, the outer loop controller can be design after the tuning of the inner controller. However, the tuning can be done simultaneously since the two controller must be keep in touch to each other as done in literature (Oh et al. 2011). In this study, the optimization of the controller's parameters will be done in two phases. In phased 1, the optimization algorithm is used to optimised the parameter of inner loop controller based on the reference trajectory generated from the outer loop controller. In phase 2, the optimization algorithm is used to optimised the parameter of outer loop controller based on the desired reference trajectory set by the designer. At phase 2, the parameters of the inner controller are fixed. Both the two phases are performed to minimized the proposed performance criterion.

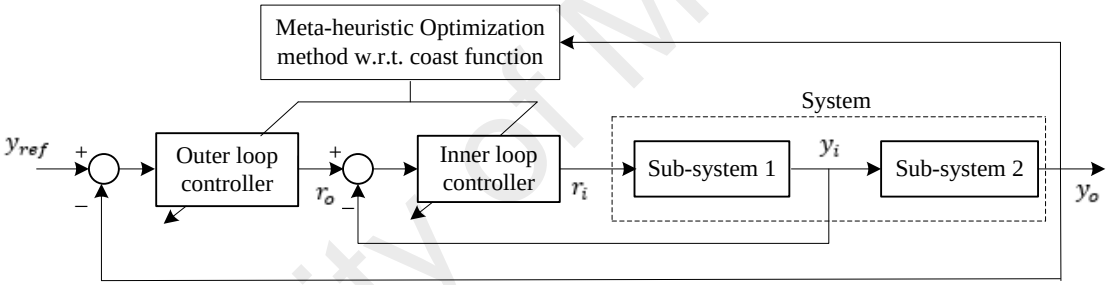

Figure 4.1: General cascade control structure with parameters optimization

4.3 Proposed cost function

In this research, the optimized T1FPIDC and optimized IT2FPIDC is implemented in cascade form. In this context, the design method for these controllers based on three different paradigms (i.e. GA, PSO and CS) will be presented. This will be done with respect to the new cost function presented as follows:

$$\text{cost}(t) = \frac{e^{-\gamma}}{2}(t_s - t_r) + \frac{1-e^{-\gamma}}{2}\left(E_{ss} + M_p\right) \tag{4.1}$$

where E_{ss} is the steady-state error, t_r is the rise time in second, t_s is the settling time in second, M_p is the percentage overshoot and γ is the weighing factor. Two different

values of γ is considered in the study (i.e. $\gamma = 1$ and 1.5). The steady-state error and overshoot are need to be reduced in this study. The γ was chose to be greater than 0.7 in this study because the main control of the RIP system defends on the stability of the servo motor. Looking at the characteristics of the servo motor at the initial state the maximum overshoot and the steady state error are higher. To have the smooth control action, the overshoot and the steady state error need to be small (Van de Straete, Degezelle, De Schutter, & Belmans, 1998). This is the reason why the the overshoot and the steady state error are given priority in this research. The values of the γ was taken precisely to be 1 and 1.5 becouse in all most all the literature using such kind of cost function with similar system as ours they take $\gamma = 1$ and $\gamma = 1.5$. (Hassanzadeh & Mobayen, 2011, Gaing, 2004). This is to investigate the effect of γ in the cost function and to study the possible different solutions.

The dynamic behavior and convergence characteristic of GA, PSO and CS will be examine using the mean value (λ) and standard deviation (σ) of the cost value of all individuals during the computation processes. The mean value is employed to measure the algorithm accuracy while the standard deviation is used to measure the convergence speed of the algorithm.

Equations (4.2) and (4.3) show the formula for calculating σ and λ respectively (Haupt & Haupt, 2004).

$$\sigma = \sqrt{\frac{1}{n}\sum_{i=1}^{n}\left(cost_{p_i} - \lambda\right)^2} \tag{4.2}$$

$$\lambda = \frac{\sum_{i=1}^{n} cost_{p_i}}{n} \tag{4.3}$$

where *n* is the population size and *cost* is the individual cost value.

4.4 Design of T1FPIDC in cascade form

4.4.1 Internal structure of T1FPIDC

The standard Fuzzy PID structure with two inputs and one output discussed in section 2.3 is used. The sigmatic diagram of proposed T1FPIDC is shown in Figure 4.2

The inputs of the outer controller are error $e_1(t)$ and change of error $\Delta e_1(t)$ while its output is U. These inputs are normalized to $E_1(t)$ and $\Delta E_1(t)$ in the range in which the input MFs of outer controller are define. This is done using the scaling factor K_{P_1} and K_{D_1}respectively. The output scaling factors K_{I_1}, K_{a_1} are used to convert the signal $U(t)$ in to $u(t)$. This normalization is done based on the following equations:

$$E_1(t) = K_{P_1} e_1(t) = K_{P_1}\big(\alpha_r(t) - \alpha(t)\big), \tag{4.4}$$

$$\Delta E_1(t) = K_{D_1} \Delta e_1(t) = K_{D_1}(e_1(t) - e_1(t-1)), \tag{4.5}$$

$$u(t) = K_{I_1} \int U(t)dt + K_{a_1} U(t). \tag{4.6}$$

in which the instant sampling time is t, the parameter $U(t)$ is the output of outer loop, $\alpha(t)$ and $\alpha_r(t)$ are the pendulum angle and reference signal respectively.

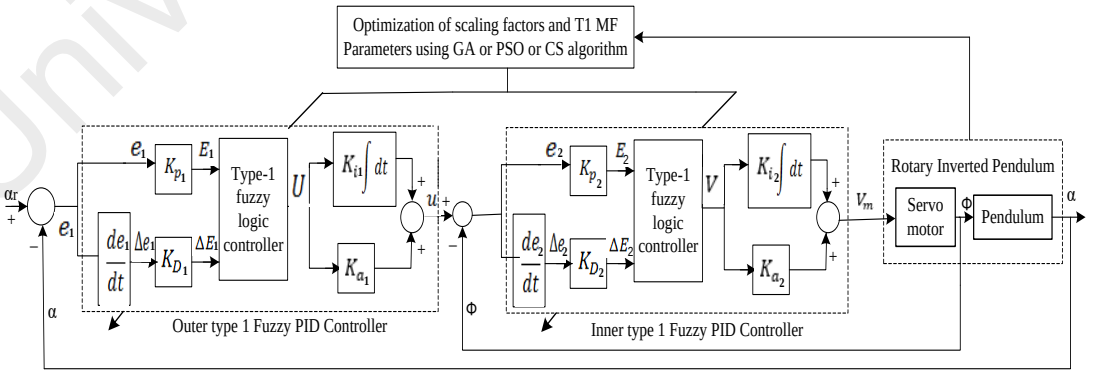

Figure 4.2 T1FPIDC in cascade form with parameter optimization

Similarly, the inputs of the inner controller are error $e_2(t)$ and change of error $\Delta e_2(t)$ while its output is V. These inputs are converted to $E_2(t)$ and $\Delta E_2(t)$ respectively. This will

be done through the normalization in the range in which the input MFs of inner controller are define based on the scaling factor K_{P_2} and K_{D_2}. The output V(t) is converted to the control voltage to the servo motor $v_m(t)$ by scaling factors K_{I_2} and K_{a_2}. This normalization is done based on equations following equations:

$$E_2(t) = K_{P_2} e_2(t) = K_{P_2}\big(u(t) - \phi(t)\big), \tag{4.7}$$

$$\Delta E_2(t) = K_{D_2} \Delta e_2(t) = K_{D_2}(e_2(t) - e_2(t-1)), \tag{4.8}$$

$$V_m(t) = K_{I_2} \int V(t)dt + K_{a_2} V(t). \tag{4.9}$$

where *V(t)* is the output of inner loop and $\phi(t)$ is the arm angle.

The $three$ by $three$ asymmetrical rule based is employed in handling the T1FPIDC as shown in Table 4.1.

Table 4.1 Rule base of T1FLC and IT2FLC with weights

$E/\Delta E$	N	Z	P
N	N(ζ_1)	NM(ζ_2)	Z(ζ_3)
Z	NM(ζ_4)	Z(ζ_5)	PM(ζ_6)
P	Z(ζ_7)	PM(ζ_8)	P(ζ_8)

The typical structure of this rule is as follows:

$$R_n: \text{IF E is } A_j^1 \text{ and } \Delta\text{E is } A_j^2 \text{ THEN y is } Y_n \text{ with } \zeta_n \tag{4.10}$$

where $n = 1, \ldots, 9$ is the number of rules, ζ_n is the weighing factor that is use to indicate the significant of corresponding rule and $\zeta_n \in [0,1]$. Three triangular MFs are used to defined the input of all T1FLC structure. This MFs are shown in Figure 4.3 and named N, Z and P that stand for negative, zero and positive respectively. Three parameters (l_{i_j}, c_{i_j} and r_{i_j}) are used to defined the T1FSs of the T1FLC as shown in Figure 4.3. Where

$i = 1,2\ and\ j = 1,2,3$. The T1FLC outputs are defined by five singleton crisp consequents MFs as shown in Figure 4.4. Where N, NM, Z, PM and P stand for negative, negative medium, zero, positive medium and positive respectively. The weighing factor and the output MFs are not optimised in this research. The weight for all rules are set to 1. The centre of sets type defuzzification and product implication are used in this study for T1FLC.

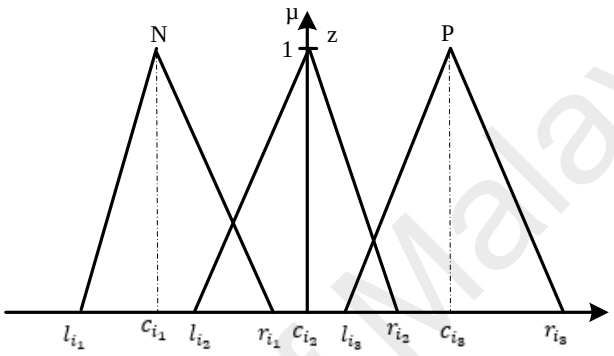

Figure 4.3: T1FS

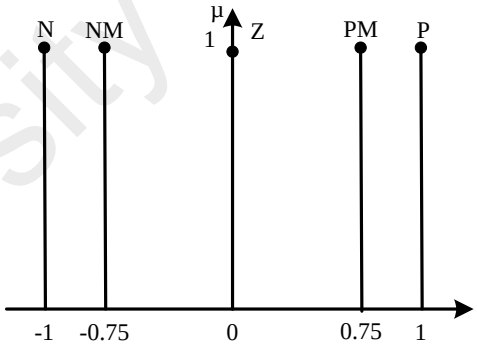

Figure 4.4: The consequent MFs for T1FC and IT2FC

4.4.2 Optimization of T1FPIDC cascade structure using Meta-heuristic optimization algorithms.

As stated in chapter 1 that three different type of meta-heuristic algorithm will be used for optimization in this research (i.e., GA, PSO and CS). These optimization algorithms are used to optimized the scaling factors and the antecedent MFs parameters for both outer and inner controllers to minimized the proposed performance criterion. All the three antecedent MFs of T1FLC (N, Z, and P) are defined with three parameters for each input.

These parameters are $l_{i_1}, c_{i_1}, r_{i_1}$ for N, $l_{i_2}, c_{i_2}, r_{i_2}$ for Z and $l_{i_3}, c_{i_3}, r_{i_3}$ for P ($i = 1,2$). Therefore, the total number of structural parameters of the antecedent MF to be optimized for two inputs T1FPIDC design are $9\times2 = 18$. Furthermore, four scaling factors for input and output of the T1FPIDC are need to be optimized. Hence the total parameters to be optimized using GA, PSO and CS for the design of T1FPIDC are $18 + 4 = 22$ to minimised the performance criterion. The optimization variables for GA, PSO and CS are defined as

$$x_{T1FPIDC_{\text{inner loop}}} = \big(l_{1_1}, c_{1_1}, r_{1_1}\ l_{1_2}, c_{1_2}, r_{1_2}\ l_{1_3}, c_{1_3}, r_{1_3},$$
$$l_{2_1}, c_{2_1}, r_{2_1}\ l_{2_2}, c_{2_2}, r_{2_2}\ l_{2_3}, c_{2_3}, r_{2_3}, K_{P_2}, K_{D_2}, K_{I_2}, K_{a_2}\big) \quad (4.11)$$

for the inner loop. Similar variables are optimized using GA, PSO and CS for the outer loop. The optimization of T1FPIDC is accomplished in two phase. In phased 1, the GA, PSO, and CS are used to optimized the parameter of inner loop controller based on the reference trajectory generated from the outer loop controller. In phase 2, the GA, PSO, and CS are used to optimized the parameter of outer loop controller based on the desired reference trajectory set by the designer. At this phase, the parameters of the inner controller are fixed. Both the two-phase are performed to minimized the performance criterion. To have the normal convex T1FSs, the parameters of the antecedent MFs of the outer and inner control loop are optimized based on the constraints given by the following equations:

$$c_{i_1} < c_{i_2} < c_{i_3} \quad (4.12)$$

$$l_{i_1} < c_{i_1} < r_{i_1} \quad (4.13)$$

$$l_{i_2} < c_{i_2} < r_{i_2} \quad (4.14)$$

$$l_{i_3} < c_{i_3} < r_{i_3} \quad (4.15)$$

The pseudo codes for GA, PSO and CS methods based T1FPIDC are given in Table 4.2, Table 4.3 and Table 4.4 respectively.

Table 4.2: Pseudo code of GA based cascade T1FPIDC and IT2FPIDC design

Step 1	Define the type of controller (T1FPIDC/IT2FPIDC) and its corresponding parameter setting i. Inner loop $x_{T1FPIDC_{\text{inner loop}}}$ / $x_{IT2FPIDC_{\text{inner loop}}}$ ii. Outer loop $x_{T1FPIDC_{\text{outer loop}}}$ / $x_{IT2FPIDC_{\text{outer loop}}}$
Step 2	Specify the upper and lower bounds of the controller parameter and define the population size P_n, number of generation G_n, type of crossover, crossover rate C_r, type of mutation and mutation rate M_r
Step 3	Generate the initial random population of individual of size P_n and evaluate the fitness of individual according to $t_s, t_r, M_p, E_{ss}, E_u$ via equation 4.1 the value of the performance criteria in time domain are calculated by sending each controller parameter (individual) to Matlab Simulink, after that, the performance criterion is evaluated for each individual
Step 4	IF $(G_n > \text{current\_generation})$ THEN generate new solution $C_r * P_n$ by selecting the new solution of two parents from the current population and generate the child solution using crossover
Step 5	IF $(M_r > \text{random\_range})$ THEN mutate the child solution
Step 6	Evaluate the child solution according to the performance criterion and add the child to the population. Now the population size become $P_n * (C_r + 1)$
Step 7	Remove the extra least fit solution $P_n * C_r$ from the population and return the best fit members of population until stopping criteria

Table 4.3: Pseudo code of PSO based cascade T1FPIDC and IT2FPIDC design

Step 1	Define the type of controller (T1FPIDC/IT2FPIDC) and its corresponding parameter setting iii. Inner loop $x_{T1FPIDC_{\text{inner loop}}}$ / $x_{IT2FPIDC_{\text{inner loop}}}$ iv. Outer loop $x_{T1FPIDC_{\text{outer loop}}}$ / $x_{IT2FPIDC_{\text{outer loop}}}$
Step 2	Specify the upper and lower bounds of the controller parameter and generate the initial particles randomly,

Step 3 the value of the performance criteria in the time domain are calculated iteratively by sending each controller parameter (particle) to Matlab Simulink, after that, the performance criterion is evaluated for each particle according to $t_s, t_r, M_p, E_{ss}, E_u$ via equation 4.1

Step 4 Then evaluate each particle in the initial population by using the objective function and search for p_{best} and g_{best} via equation 2.16

Step 5 Calculate the velocity and the constriction factor for the particles via equation 2.17 and 2.18 and check for the maximum velocity then, update the velocity and position of each particle.

Step 6 For each particle, *pbest* is reset in comparison with the previous p_{best} through fitness of objective function then g_{best} is updated in comparison with best p_{best}

Step 7 If one of the terminating condition is satisfied, then stop, else go to step 5

Step 8 The particle that has the latest g_{best} is an optimal parameter.

Table 4.4: Pseudo code of CS based cascade T1FPIDC and IT2FPIDC design

Step 1 Define the type of controller (T1FPIDC/IT2FPIDC) and its corresponding parameter setting

i. Inner loop $x_{T1FPIDC_{\text{inner loop}}}$ / $x_{IT2FPIDC_{\text{inner loop}}}$
ii. Outer loop $x_{T1FPIDC_{\text{outer loop}}}$ / $x_{IT2FPIDC_{\text{outer loop}}}$

Step 2 Specify the upper and lower bounds of the controller parameter and define the number of population *n*, host nest x_i for $i = 1,2, \dots, n$, step size s, step size scaling factor α and switching parameter P_a

Step 3 generate the initial population of n host nest x_i

Step 4 WHILE stopping criteria or (Max_generation > Current_generation) Get a cuckoo randomly via Lévy flights and evaluates its fitness F_i according to the performance criteria in time domain by sending each controller parameter to Matlab Simulink, after that, the performance criterion is evaluated for each nest according to $t_s, t_r, M_p, E_{ss}, E_u$ via equation 4.1

Step 5 Select the next F_j randomly out of n
IF$(F_j < F_i)$
Replace j by new solution

Step 6 Abandoned the worse nest according to a fraction P_a and build new ones

Step 7 Keep the nest with best solutions and find the current best by ranking the solutions

4.5 Design of IT2FPIDC in cascade form

4.5.1 Internal structure of T2FPIDC

The sigmatic diagram of the two inputs structure of IT2FPIDC is illustrated in Figure 4.5. This is similar to that of T1FPIDC regarding scaling factors.

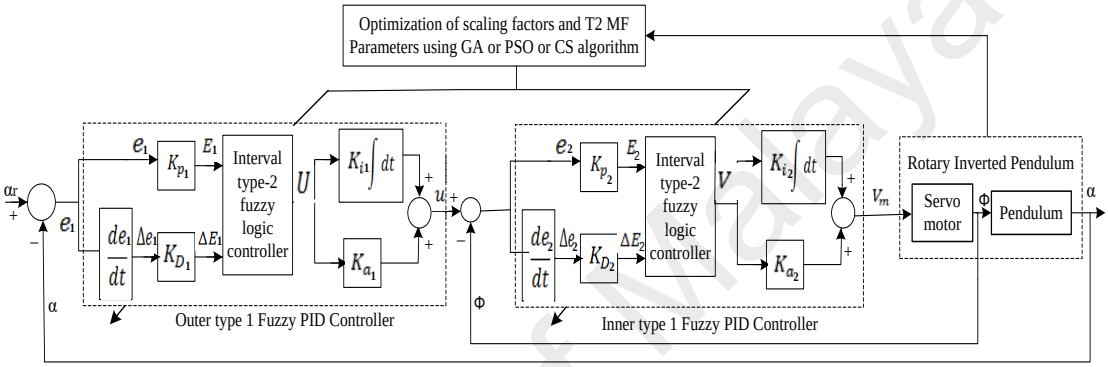

Figure 4.5: IT2FPIDC in cascade form with parameter optimization

The rule base used here is the same as that used in T1FPIDC which is 3×3 (given in Table 4.1). The typical structure of the IT2FPIDC rule is as follows:

$$R_n: \text{IF E is } \tilde{A}_j^1 \text{ and } \Delta\text{E is } \tilde{A}_j^2 \text{ THEN y is } Y_n \text{ with } \zeta_n \tag{4.16}$$

where $n = 1, \ldots, 9$ is the number of rules, $\zeta_n \in [0,1]$ is the weighing factor. Three triangular MFs are used to defined the input of all IT2FLC structure. This MFs are illustrated in Figure 4.6 and named N, Z and P that stand for negative, zero and positive respectively. Five parameters (l_{i_j}, l_{j_j} c_{i_j} r_{i_j} and r_{j_j}) are used to defined the antecedent IT2FSs of the IT2FLC as shown in Figure 4.6. Where $i = 1,2$ and $j = 1,2,3$. The upper and lower MF ($\overline{\mu}_{\tilde{A}}$ and $\underline{\mu}_{\tilde{A}}$) are used to described the IT2FS ($\tilde{A}$). In order to be fair in comparisons, the output of IT2FPIDC are the same as that of T1FPIDC (five singleton crisp consequents) as shown in Figure 4.4. Also, the weighing factor and the output MFs

are not optimised in this case. The weight for all rules are set to 1. The description of all the process involve in the used IT2FLC is presented in chapter two. This include the fuzzification, rules, inference, type reduction and defuzzification. The centre-of-set type reduction is used in this study. It has been shown that the IT2FLC defuzzification can be done as follows (Karnik & Mendel, 1998):

$$y = \frac{y_l + y_r}{2} \tag{4.17}$$

where y_l and y_r are the type reduced set's end points. These two end points can be calculated by reordering $Y_n\zeta_n$ such that $Y_1\zeta_1 \leq Y_2\zeta_2 \leq \cdots Y_N\zeta_N$ and matched the corresponding firing interval set. The y_l and y_r can be calculated as follows (Qilian & Mendel, 2000):

$$y_l = \frac{\sum_{n=1}^{L} \overline{f}_n Y_n\zeta_n + \sum_{L+1}^{N} \underline{f}_n Y_n\zeta_n}{\sum_{n=1}^{L} \overline{f}_n\zeta_n + \sum_{L+1}^{N} \underline{f}_n\zeta_n} \tag{4.18}$$

$$y_r = \frac{\sum_{n=1}^{R} \underline{f}_n Y_n\zeta_n + \sum_{R+1}^{N} \overline{f}_n Y_n\zeta_n}{\sum_{n=1}^{M} \underline{f}_n\zeta_n + \sum_{M+1}^{N} \overline{f}_n\zeta_n} \tag{4.19}$$

The switching points L and R are calculated using Karnik-Mendel type reduction method (Karnik & Mendel, 1998). The updated Matlab/Simulink toolbox for interval type-2 fuzzy logic system proposed by Taskin and Kumbasar (2015) is used to initialized the internal structure of the proposed optimized IT2FPIDC.

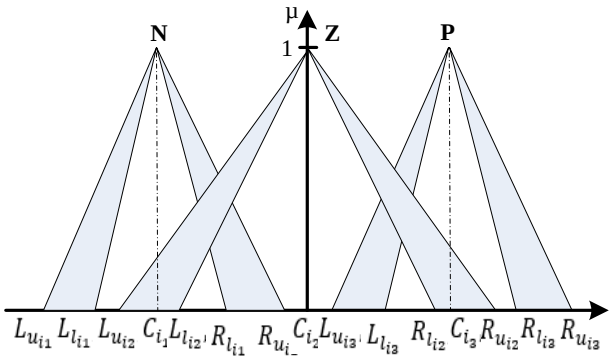

Figure 4.6: IT2FSs

4.5.2 Optimization of IT2FPIDC cascade structure using Meta-heuristic optimization algorithms.

The GA, PSO, and CS are used to optimized the scaling factors and the antecedent MFs parameters for both outer and inner controllers of IT2FPIDC to minimise the proposed performance criterion. All the three antecedent MFs of IT2FLC (N, Z, and P) are defined with five parameters for each input. These parameters are $L_{u_{i1}},\ L_{l_{i1}},\ C_{i_1},\ R_{l_{i1}},\ R_{u_{i1}}$ for N, $L_{u_{i2}},\ L_{l_{i2}},\ C_{i_2},\ R_{l_{i2}},\ R_{u_{i2}}$ for Z and $L_{u_{i3}},\ L_{l_{i3}},\ C_{i_3},\ R_{l_{i3}},\ R_{u_{i3}}$ for P ($i = 1,2$). Therefore, the total number of parameters of the antecedent MF to be optimized for two inputs IT2FPIDC design are $15\times2 = 30$. Obviously, it can be seen that T1FPIDC has less 12 structural parameters compared with IT2FPIDC. This means the IT2FPIDC has extra design DOF than T1FPIDC. Similar to T1FPIDC, the T2FPIDC has four scaling factors for input and output that are need to be optimized. Therefore, the total parameters to be optimized using GA, PSO and CS for the design of IT2FPIDC should be $30 = 34$ to minimised the performance criterion. The rules base and consequent MFs would not be optimized in the design of IT2FPID controller. This is for us to show the effectiveness of the extra DOF of IT2FSs provided by the FOU present in IT2FSs in a closed loop performance of a system. Hence the optimization variables for GA, PSO and CS are defined as

$$x_{IT2FPIDC_{\text{inner loop}}} = \left(L_{u_{11}},\ L_{l_{11}},\ C_{1_1},\ R_{l_{11}},\ R_{u_{11}}, L_{u_{12}},\ L_{l_{12}},\ C_{1_2},\ R_{l_{12}},\ R_{u_{12}}, L_{u_{13}},\right.$$

$$L_{l_{13}},\ C_{1_3},\ R_{l_{13}},\ R_{u_{13}},\ L_{u_{21}},\ L_{l_{21}},\ C_{2_1},\ R_{l_{21}},\ R_{u_{21}}, L_{u_{22}},\ L_{l_{22}},\ C_{2_2},\ R_{l_{22}},\ R_{u_{22}}, L_{u_{23}},$$

$$\left. L_{l_{23}},\ C_{2_3},\ R_{l_{23}},\ R_{u_{23}}, K_{P_2}, K_{D_2}, K_{I_2}, K_{a_2}\right) \quad (4.20)$$

Similar variables are to be optimised for the outer control loop. Moreover, the weighing factor ζ_n is not optimised and it is taken to be 1 for all the rules as in the case of T1FPIDC. The optimization of IT2FPIDC is accomplished in the same manner as described for T1FPIDC. Also have the normal convex IT2FSs, the parameters of the antecedent MFs of the outer and inner control loop are optimised based on the constraints given in the following equations:

$$L_{u_{i1}} < L_{l_{i1}} < C_{i_1} < R_{l_{i1}} < R_{u_{i1}} \quad (4.21)$$

$$C_{i_1} < C_{i_2} < C_{i_3} \quad (4.22)$$

$$L_{u_{i1}} < L_{l_{i1}} < C_{i_1} < R_{l_{i1}} < R_{u_{i1}} \quad (4.23)$$

$$L_{u_{i2}} < L_{l_{i2}} < C_{i_2} < R_{l_{i2}} < R_{u_{i2}} \quad (4.24)$$

$$L_{u_{i3}} < L_{l_{i3}} < C_{i_3} < R_{l_{i3}} < R_{u_{i3}} \quad (4.25)$$

The pseudo codes for GA, PSO and CS methods based IT2FPIDC are given in Table 4.2, Table 4.3 and Table 4.4 respectively. I t is the same with that of T1FPIDC is in step 1. For IT2FPIDC equation 4.20 will be used while for T1FPIDC equation 4.11 will be used.

4.6 Parameter settings for optimization algorithms

The number of particles in PSO, the population size in GA and the number of the nest in CS are taken to be the same (100). Also, their maximum number of iteration are taken to be the same (150). This is to have the fair comparisons between the proposed meta-heuristic algorithms. The formulation and theories for GA, PSO and CS are presented in sections 2.4.

The selection of the specific parameter values is as a result of rigorous experimentations. All the algorithms are implemented in Matlab, and each of the methods is tested in 60 independent runs with 60 distinct initial trial solutions. All these were done in Matlab R2013a, 2.4GHz processor with 8GB RAM. The Simulink diagram for the implementation of these optimized controllers in cascade form is shown in Figure 4.7. The RIP model developed using Kane's method was used for the simulation studies. This is the same for both T1FPIDC and IT2FPID; the only difference is in the controller. Also, the Matlab codes for IT2FPIDC optimized using the simple GA, PSO and CS used are shown in Appendix F. For the simulations, the initial arm, and pendulum angles are 0 and 0.97 degrees.

a. For GA method, population size = 100; crossover rate = 0.5; mutation rate = 0.1; maximum number of generation = 150, also the type of operators used for each population in GA are linear ranking selection algorithm, simple crossover and uniform mutation. The elitism method was used (i.e. to retained the best individual from present population to the next population).
b. For PSO method, number of particles = 100; position acceleration constant learning rate c_1 & c_2 are set to 2; maximum number of generation = 150 and constriction factor = 0.4; $\pm V_{max} = \pm 20\%$ of the search space.
c. For CS The number of nest n is chose to be 100. This is for us to be fair in the comparisons of the proposed meta-heuristic optimization method. Also it was stated in (Yang & Deb, 2009) that in multimodal system the nests are distributed at different local optima. Which means that if the number of local optima are much lower than the number of nest the CS can discover all the optima concurrently. This become advantageous and more important when dealing with multiobjective and multimodal optimization problems like in case of this research. step size scaling factor $\alpha = 1$, switching parameter $P_a = 0.25$

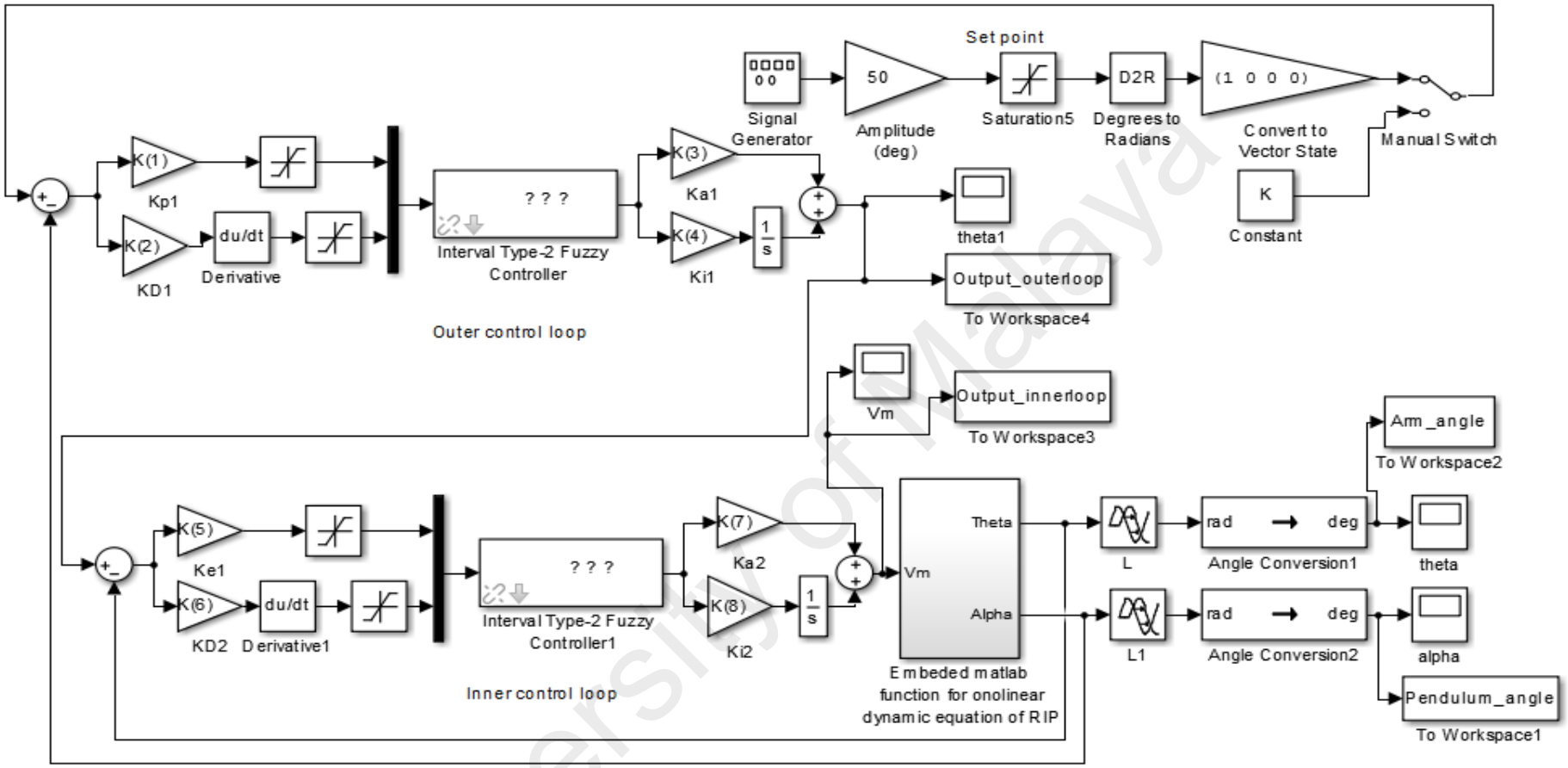

Figure 4.7: Simulink diagram for the simulation studies

4.7 Experiment

The RIP produced by Quanser is used in this research (Apkarian and collaborators 2011). The schematic diagram and experimental setup of the used RIP is shown in Figure 4.8 and 4.9 respectively. This setup consists of two optical encoders for measuring the pendulum's and arm's angles respectively. It also comprised of the data acquisition device for collecting the information from the encoders and give it to the computer. The data acquisition device also received the control signal from the computer and gives it to the power amplifier for the amplification of the signal before feeding to the servo motor. In this study, the counter clockwise direction is considered as positive direction for the arm and the clockwise direction is the positive direction for the pendulum. The initial angle for the arm and pendulum in real time are 0 and -180 degrees respectively. Also, the experimental sampling time is 0.01sec. The stabilization controller is set to operate when the pendulum angle reached $\pm 10°$.

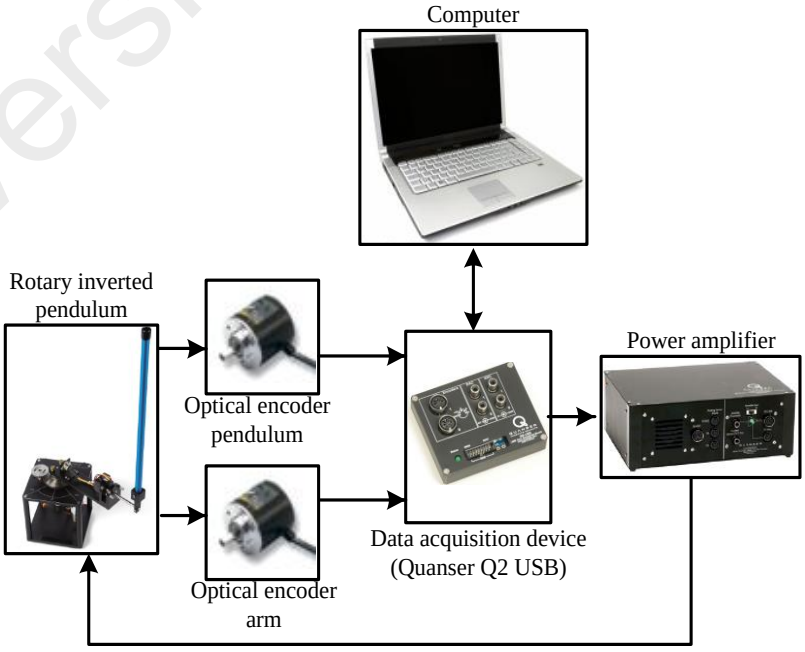

Figure 4.8: Schematic Diagram of RIP

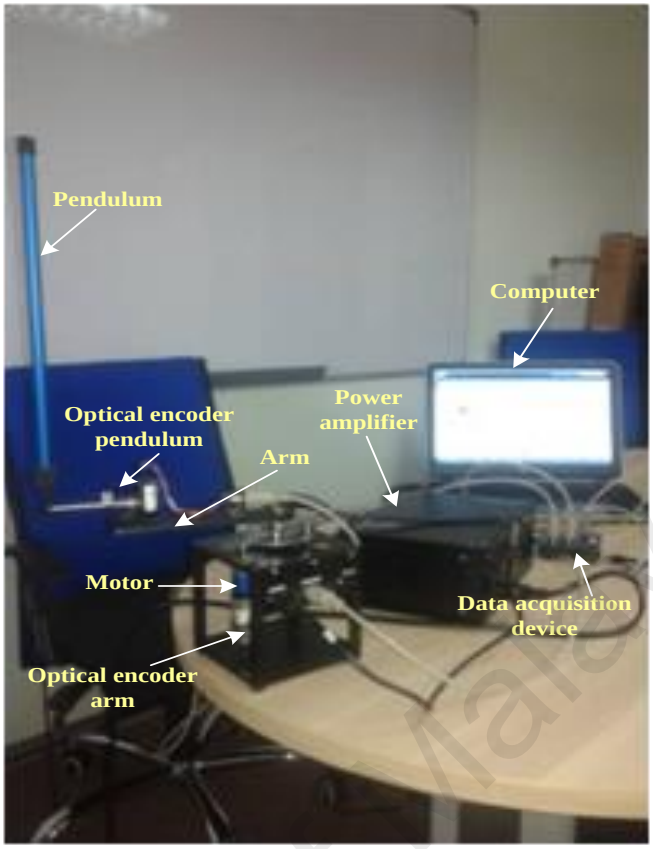

Figure 4.9: Experimental setup of RIP

All the control methods were implemented in Matlab/Simulink R2013a, 2.4GHz processor with 8GB RAM which interacts with practical RIP in real time through QUARC targets libraries. The experiments were performed on Quanser SRV02 RIP set up. The US Digital S1 single-ended optical shaft encoder that can offer a high resolution of 1024 lines per revolution (4096 counts per revolution in quadrature mode) was used for measuring both pendulum and arm angles. The Power Amplifier used was VoltPAQ-X1. The data acquisition device used was Quanser Q2-USB (hardware in loop board type). It should be noted that to have a good real-time results; the power limits should be respected by the applied torque. The main specification of SRV02 RIP is presented in Table 4.5. The gearhead and sensor specifications of SRV02 RIP are presented in Table 4.6 and Table 4.7 respectively (Apkarian and collaborators 2011). The Simulink diagram is shown in Figure 4.11.

Table 4.5: Main SRV02 RIP Specification

Description	Values	Variation
Motor nominal input voltage	6.0 V	
Motor armature resistance	2.6 Ω	±12%
Motor armature inductance	0.18 mH	
Motor current-torque constant	$7.68\times10^{-3}\mathrm{N-m/A}$	±12%
Motor back-emf constant	$7.68\times10^{-3}\mathrm{V/(rad/s)}$	±12%
High-gear total gear ratio	70	
Low-gear total gear ratio	14	
Motor efficiency	0.69	±5%
Geabox efficiency	0.9	±10%
Rotor moment of inertia	$3.90\times10^{-7}\mathrm{kgm^2}$	±10%
Tachometer moment of inertia	$7.06\times10^{-8}\mathrm{kgm^2}$	±10%
High-gear equivalent moment of inertia without external load	$9.76\times10^{-5}\mathrm{kgm^2}$	
Low-gear equivalent moment of inertia without external load	$2.08\times10^{-5}\mathrm{kgm^2}$	
High-gear Equivalent viscous damping coefficient	$0.015\mathrm{Nm/(rad/s)}$	
Low-Gear Equivalent viscous damping coefficient	$1.50\times10^{-4}\mathrm{Nm/(rad/s)}$	
Mass of bar load	0.038 kg	
Length of bar load	0.1525 m	
Mass of disc load	0.04 kg	
Radius of disc load	0.05 m	
Maximum load mass	5 kg	
Maximum input voltage frequency	50 Hz	
Maximum input current	1 A	
Maximum motor speed	628.3 rad/s	

Table 4.6: Gearhead specification of SRV02 RIP

Description	Values
Internal gearbox ratio	14
Internal gearbox ratio (low-gear)	1
Internal gearbox ratio (high-gear)	5
Mass of 24-tooth gear	0.005 kg
Mass of 72-tooth gear	0.030 kg
Mass of 120-tooth gear	0.083 kg
Radius of 24-tooth gear	6.35×10^{-3}m
Radius of 72-tooth gear	0.019 m
Radius of 120-tooth gear	0.032 m

Table 4.7: Sensor specification of SRV02 RIP

Description	Values	Variation
Potentiometer sensitivity	35.2 deg/V	$\pm$2%
Tachometer sensitivity	1.50 V/kRPM	$\pm$2%
SRV02-E encoder sensitivity	4096 counts/rev	
SRV02-EHR encoder sensitivity	8192 counts/rev	

The stabilization control and the trajectory tracking control will be examining in the experiments using optimized T1FPIDC and optimized IT2FPIDC. Also, the robustness of the proposed optimized controllers will be analyzed in real time. This will be done by attaching another rod to the free end of the pendulum. The additional rod has the weight and the length equal to the help of the length and the weight of the original pendulum (i.e. $L_{add} = 0.1685m$ and $m_{add} = 0.0635kg$). This is to temper the physical parameters of the pendulum and to alter the position of its center of mass.

4.8 Original Contributions in the Methodology of the present study

This section will precisely present the original contributions in the methodology proposed in this study as follows:

1. The performance index used in the design of T2FLCs using optimization methods are to minimize either the integral of squared-error (ISE), or the integrated absolute error (IAE), or the integrated of time-weighted-squared-error (ITSE). These performance indexes are often used in the design of control system due to their easy analytical evaluation in the frequency domain (Gaing, 2004). Nevertheless, these performance indexes have their individual advantages and disadvantages. Though the minimization of ISE and IAE can give the response with small overshoot but at the expense of long settling time. This is because the ISE weights all errors equally irrespective of time. The ITSE can overcome the shortcoming of the ISE. However, the processes of the derivation of the ITSE analytical formula are difficult and time-consuming (Krohling et al. 1997). In this research, a performance criterion in the time domain that includes four different control performance index is used. This performance criterion can fulfill the design requirements by manipulating with the value of γ. As stated by Gaing (2004) that to reduce the steady-state error and overshoot, the weighing factor is set to be $\gamma > 0.7$. While to reduce the settiling time and rise time, the weighing factor is set to be $\gamma < 0.7$. This was illustrated in Figure 4.10.

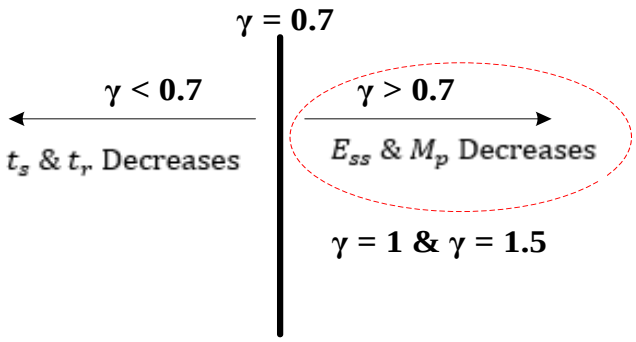

Figure 4.10: Impact of weighing factor variation

2. The dynamic behavior and convergence characteristic of the metaheuristic optimization algorithms was examine using the mean value and standard deviation of the cost value of all individuals during the computation processes. The mean value is employed to measure the accuracy of the corresponding algorithm while the standard deviation is used to determine the convergence speed of the algorithm.
3. The cascade control structure was used in this study due to the characteristics of RIP. The RIP is a single input multiple output (SIMO) system. In SIMO systems, change of one output by some disturbances affects the control of the other output (Oh et al. 2009). Considering the nonlinear behavior of RIP system, it is difficult to achieve the past settling time. Also, RIP has a high level of disturbances and large time constant. For a system like this, the best control strategy is cascade because it has the advantage of attenuating the effect of disturbances and improve the dynamics of the entire control loop (Kumbasar & Hagras, 2014).
4. The novel CS algorithm was proposed in this study. Recent studies have confirmed the effectiveness of CS over other meta-heuristic algorithms (Civicioglu & Besdok, 2013; Jr et al., 2014). The successful record of the CS is due to its outstanding balance between local and global searching. Also, the CS has the fewer number of parameters required for its execution. In addition, based on the literature review performed in this study, there is no any T2FLC design using CS algorithm before this research.

5. The optimization of the IT2FPIDC is accomplished in two phase. In phased 1, the meta-heuristic algorithm is used to optimized the parameter of inner loop controller based on the reference trajectory generated from the outer loop controller. In phase 2 the meta-heuristic algorithm is used to optimized the parameter of outer loop controller based on the desired reference trajectory set by the designer. At this phase, the parameters of the inner controller are fixed. Both the two-phase are performed to minimized the performance criterion. In this manner, the average computational time taking for the controller is reduced.

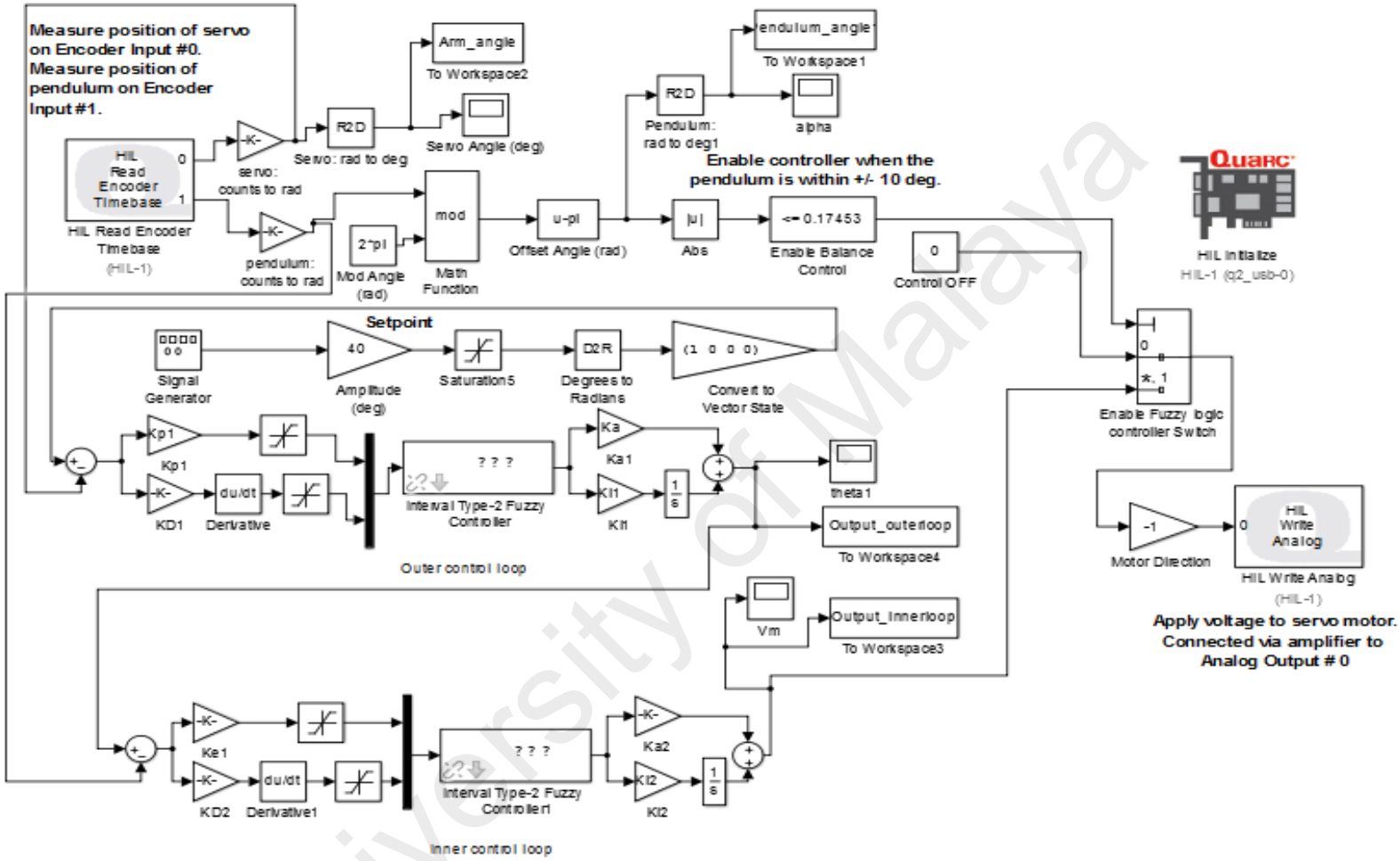

Figure 4.11: Simulink diagram of the Experimental setup

CHAPTER 5: RESULTS AND DISCUSSIONS

5.1 Introduction

The simulations and experimental results are presented in this chapter. The results include the optimized antecedent MFs and best values for the scaling factors for both optimized T1FPIDC and optimized IT2FPIDC. The convergence characteristics of the proposed optimization algorithms are also presented. The stabilization control, disturbance rejection analysis, trajectory tracking control and validation of the simulation results with experimental results are also presented. The GA based, PSO based and CS based T1FPIDC results will be presented before presenting the GA based PSO based and CS based IT2FPIDC. At the end of the chapter the comparisons between the proposed controllers will be presented.

5.2 Simulation results for optimized cascade T1FPIDC

5.2.1 Optimized antecedent MFs for T1FPIDC

As stated in the methodology that for fair comparisons of the performance of the optimization algorithms, the size of the population and the maximum number of iterations for all T1FPIDC (GA-based, PSO-based and CS-based) design methods are chosen to be the same. That is the number of iteration and population size are 150 and 100 for all cases. The inner and the outer controllers are optimized to minimize the coast function in equation (4.1). By setting the weighing factor $\gamma = 1$, the optimized antecedent MFs for T1FPIDC inner loop E_2 and ΔE_2, and outer loop E_1 and ΔE_1 for GA-based, PSO based and CS-based are shown in Figure 5.1, 5.2 and 5.3 respectively. Also, by setting the weighing factor $\gamma = 1.5$, the optimized antecedent MFs for T1FPIDC inner loop E_2 and ΔE_2, and outer loop E_1 and ΔE_1 for GA-based, PSO based and CS-based are shown in Figure 5.4, 5.5 and 5.6 respectively.

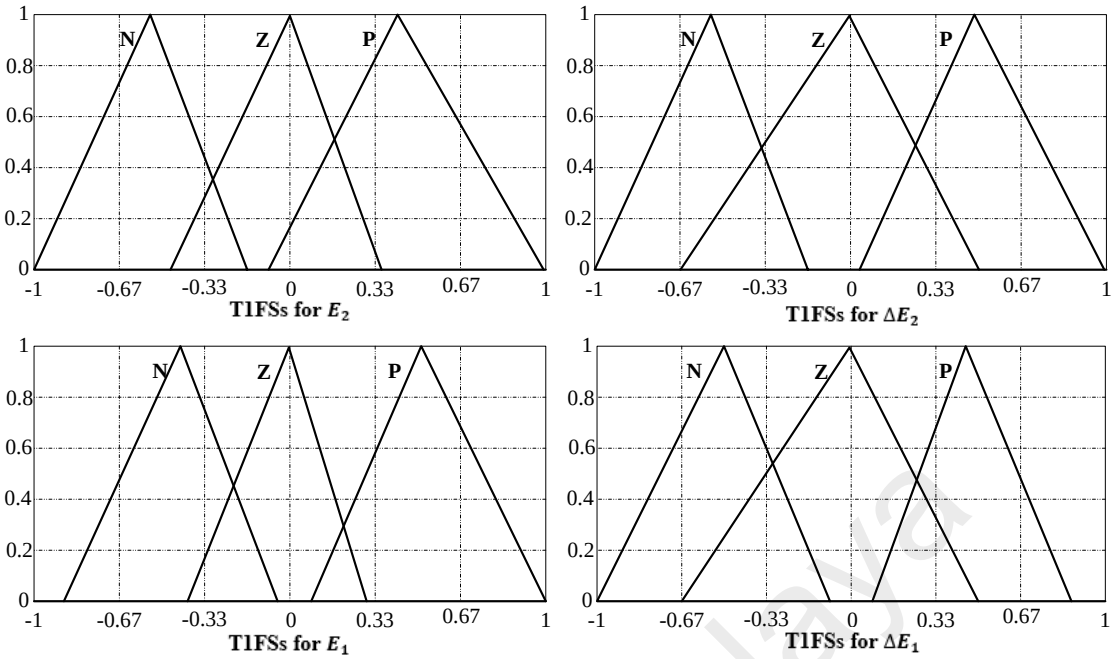

Figure 5.1: Optimized antecedent MFs of T1FPIDC (GA-based), $\gamma = 1$

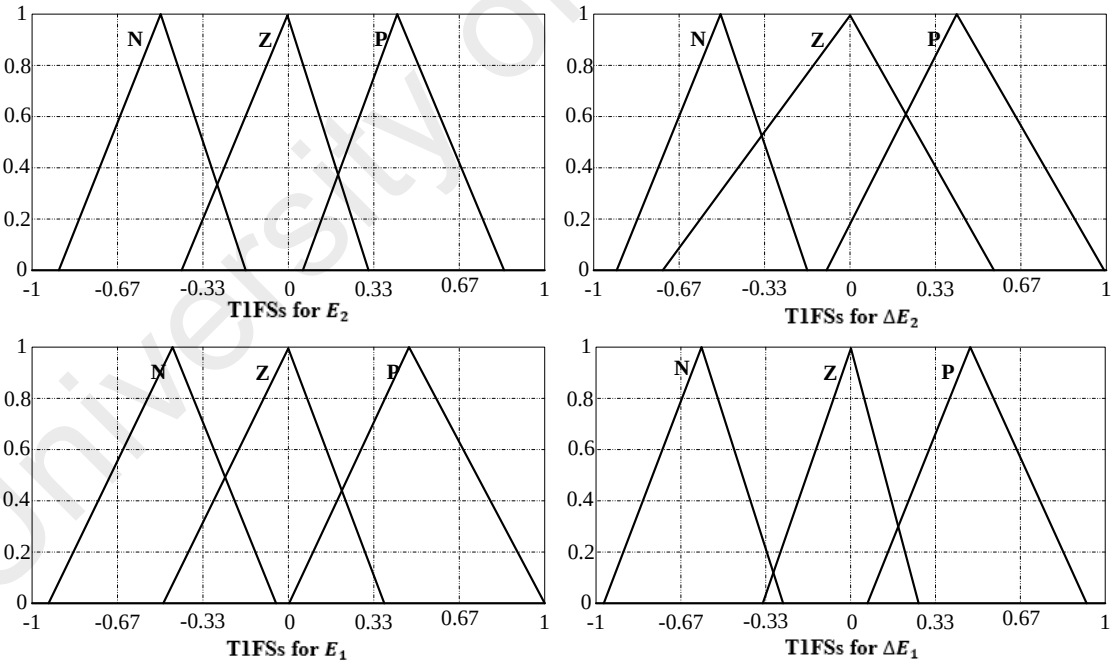

Figure 5.2: Optimized antecedent MFs of T1FPIDC (PSO-based), $\gamma = 1$

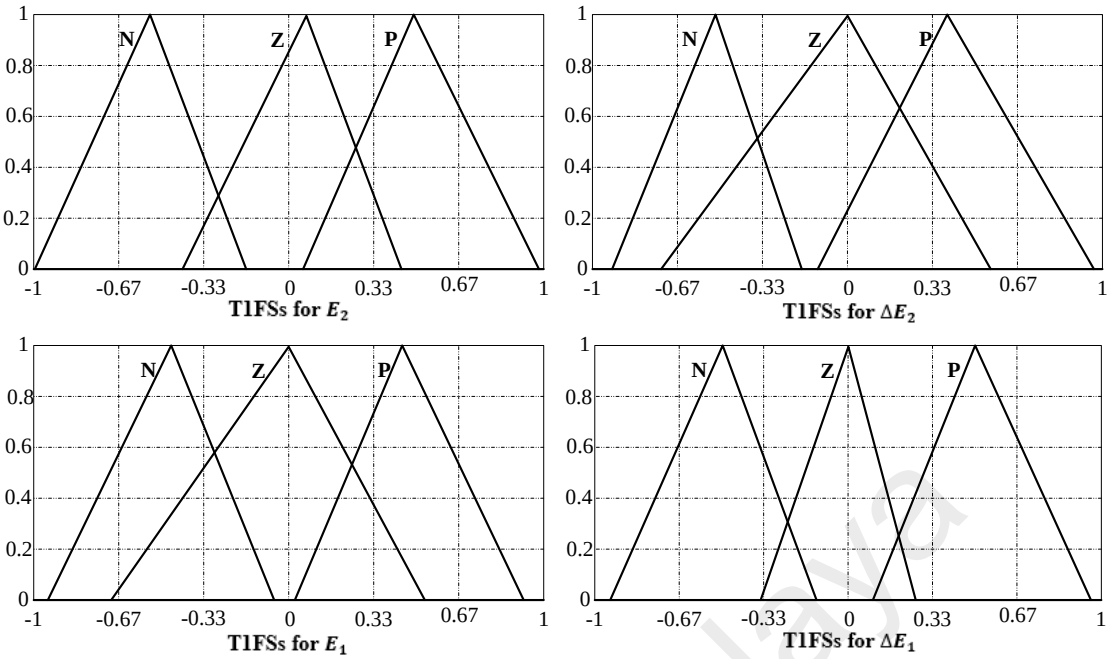

Figure 5.3: Optimized antecedent MFs of T1FPIDC (CS-based), $\gamma = 1$

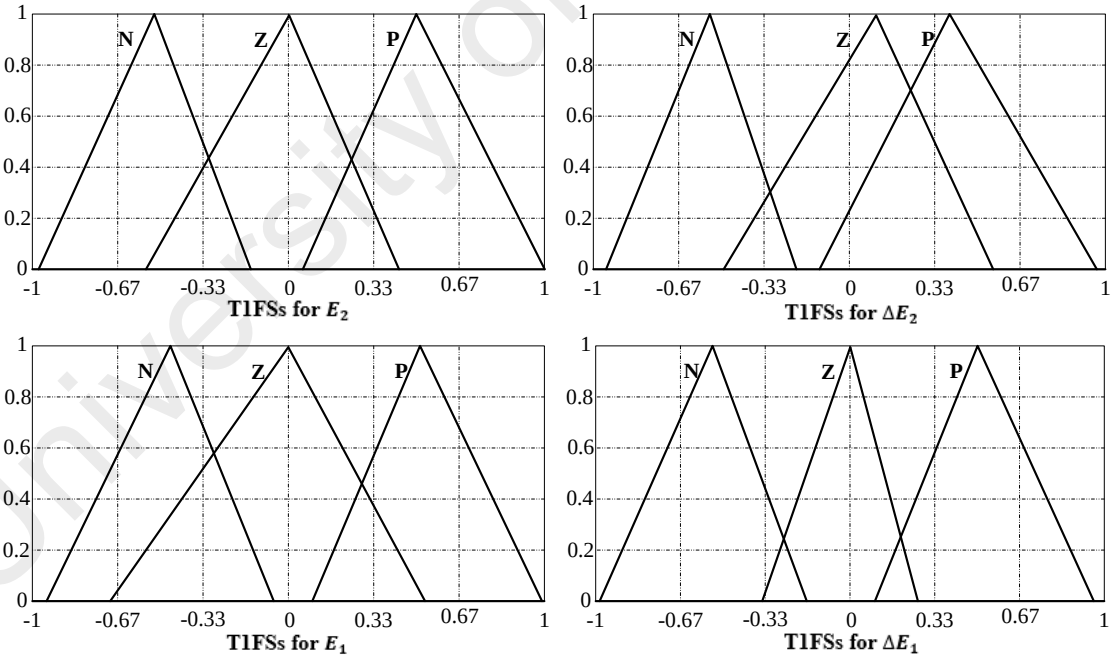

Figure 5.4: Optimized antecedent MFs of T1FPIDC (GA-based), $\gamma = 1.5$

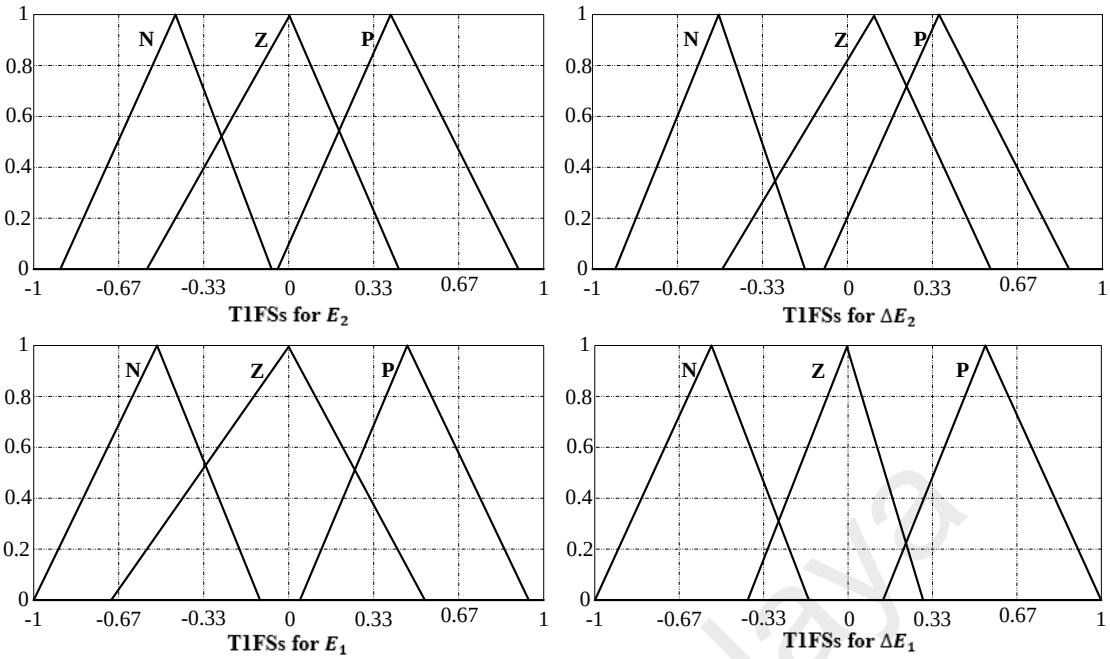

Figure 5.5: Optimized antecedent MFs of T1FPIDC (PSO-based), $\gamma = 1.5$

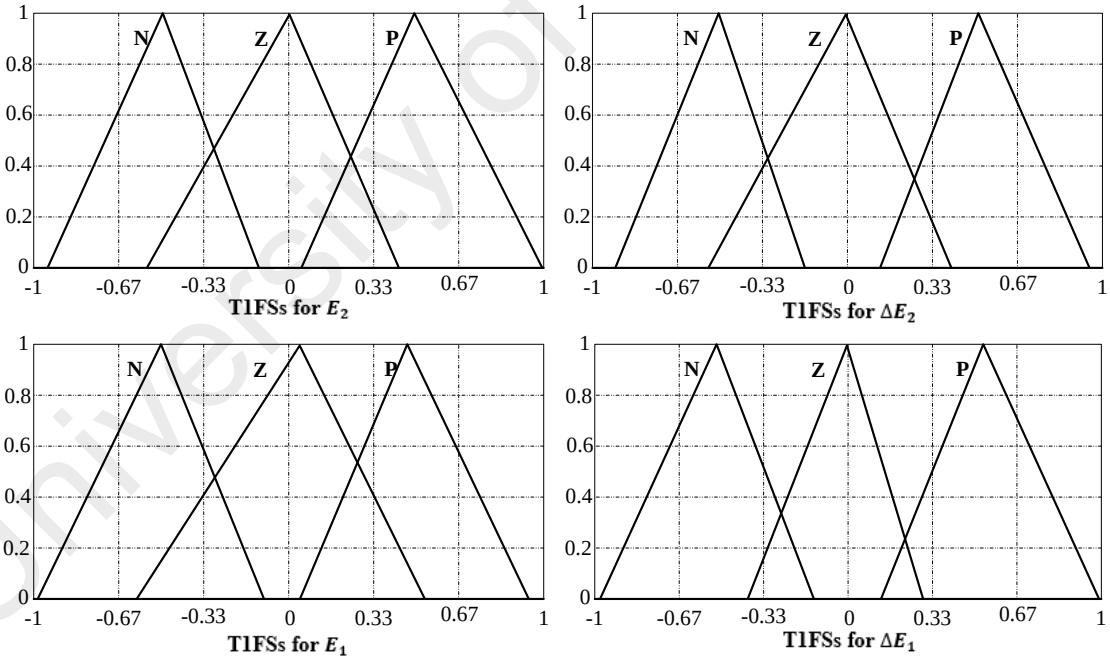

Figure 5.6: Optimized antecedent MFs of T1FPIDC (CS-based), $\gamma = 1.5$

5.2.2 Convergence Characteristics based on T1FPIC

To see the convergence characteristics of the proposed T1FPIDC, two statistical simulations are performed. That is the standard deviation of the coast value and mean value. The standard deviation is used to measure the speed of convergence for a given

algorithm while the mean value is used to indicate the accuracy of the algorithm. (Hassanzadeh & Mobayen, 2011). Figure 5.7 (a) and (b) shows that all T1FPIDC (i.e. GA-based, PSO-based and CS-based) can secure stable mean cost value, for weighing factor $\gamma = 1$ and $\gamma = 1.5$ using the same simulation conditions and cost function. However, CS-based controllers have the best mean value and cost value, which indicate that the CS-based T1FPIDC can achieve best accuracy than PSO-based and GA-based. This is the case for both $\gamma = 1$ and $\gamma = 1.5$. On the other hand, Figure 5.8. (a) and (b) shows that in the tendency of convergence of standard deviation of cost values, CS-based controllers is faster than PSO-based and GA-based controllers. However, PSO-based controllers are faster than GA-based controllers. This indicates that CS method have the best convergence efficiency than PSO and GA, also PSO have better convergence efficiency than GA. The optimized scaling factors for cascade T1FPIDC are shown in Table 5.1. $\gamma = 1$ $\gamma = 1.5$

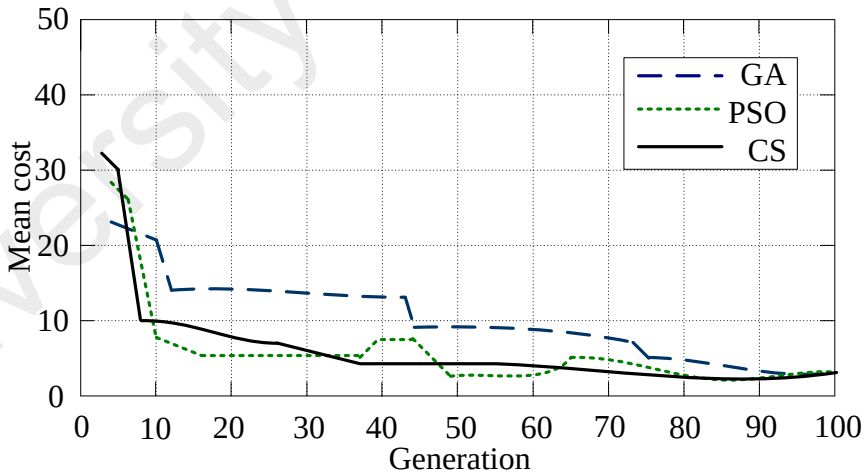

(a) $\gamma = 1$

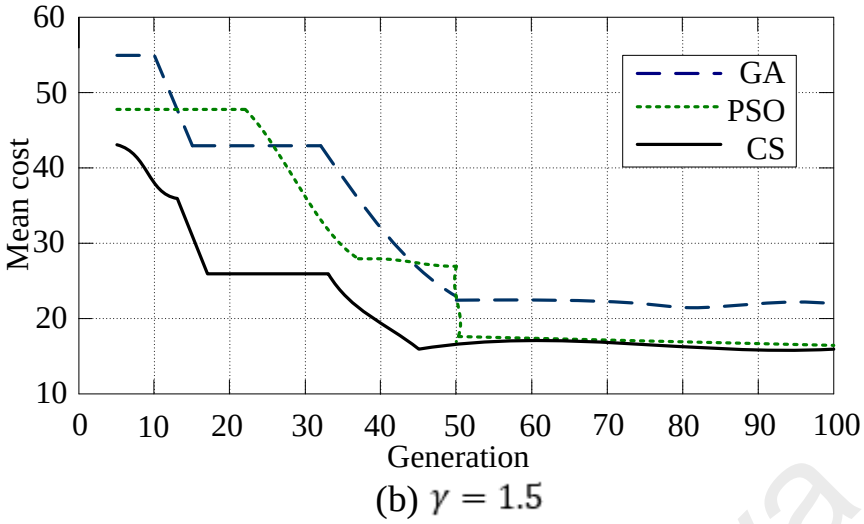

Figure 5.7: Tendency of convergence of mean value of cost function in T1FPIDC

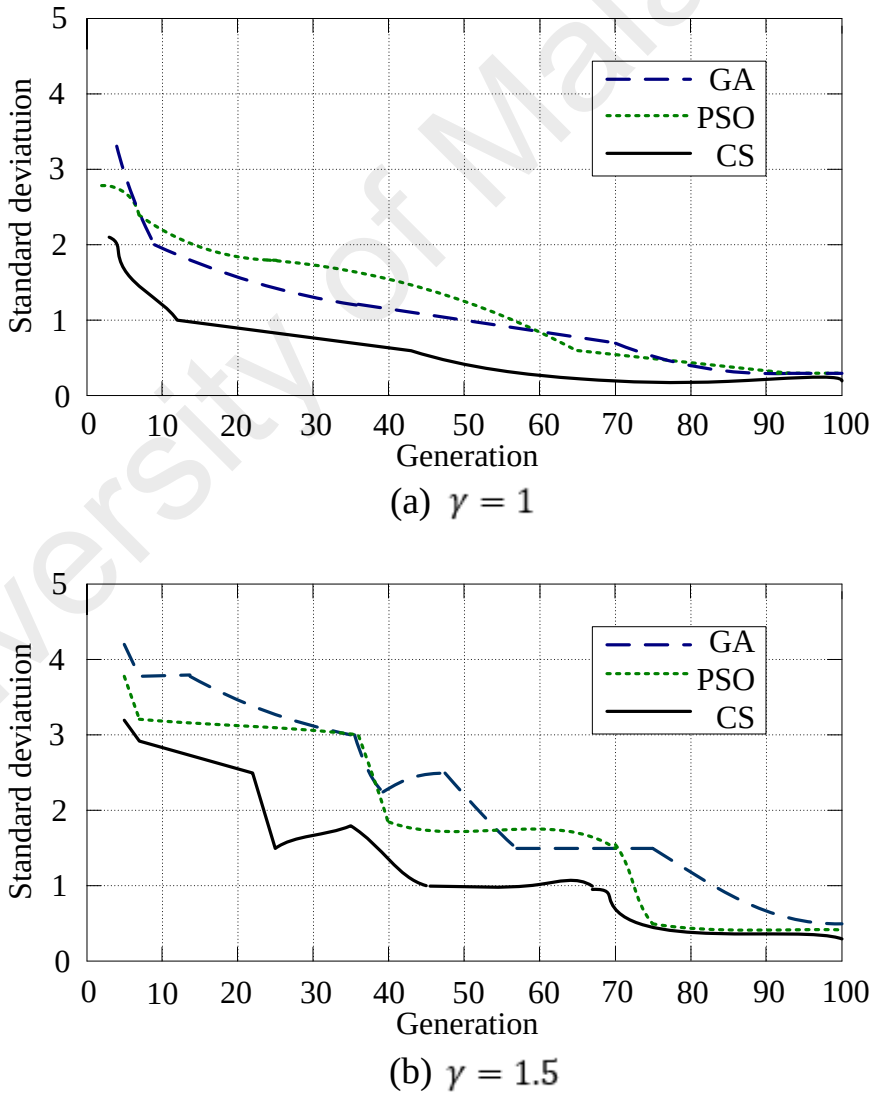

Figure 5.8: Tendency of convergence of standard deviation value of cost function in T1FPIDC

Table 5.1 Optimized scaling factors for cascade T1FPIDC

		Outer controller				Inner Controller			
Algorithms	γ	K_{P_1}	K_{I_1}	K_{D_1}	K_{a_1}	K_{P_2}	K_{I_2}	K_{D_2}	K_{a_2}
GA	1	8.754	6.321	0.0181	1.472	0.8321	0.6981	0.0072	0.4121
	1.5	7.914	5.106	0.0371	2.049	0.7941	0.7124	0.0091	0.3981
PSO	1	9.625	7.769	0.0512	1.638	0.6114	0.5931	0.0065	0.5170
	1.5	9.625	7.485	0.0432	1.906	0.7096	0.5179	0.0049	0.5939
CS	1	7.516	5.594	0.0129	1.516	0.7518	0.5593	0.0068	0.4654
	1.5	7.102	5.918	0.0351	2.319	0.6992	0.6192	0.0052	0.5467

5.2.3 Stabilization control using optimized cascade T1FPIDC

In this section, stabilization control of RIP using optimized cascade T1FPIDC has been analyzed. Figure 5.9 (a), (b), (c) and (d) shows the best simulation results of the pendulum angle, arm angle, output of outer control loop and the output of the inner control loop (i.e. voltage to the servo motor) respectively. These results are the one obtained by setting $\gamma = 1$. To see the effect of γ, its value was change to $\gamma = 1.5$. Figure 5.10 (a), (b), (c) and (d) illustrate the best results for the pendulum angle, arm angle, output of outer control loop and the output of the inner control loop (i.e. voltage to the servo motor) respectively. The summary of the best simulation results in 60 runs for different values of γ are shown in Table 5.2. The best results was only shown because meta-heuristic optimization algorithms is used. The solution can be the absolute best out of other alternative solutions (Martínez-Soto et al., 2014). Different values are found for each run. In some cases, the solutions are far away from the desirable solution that if the average is taken, the whole solutions will be destroyed. Also, the following literature did similar work and the report only the best solution (Hassanzadeh & Mobayen, 2011; Kumbasar & Hagras, 2014;

Nguyen, Khosravi, Creighton, & Nahavandi, 2015; Yao, Hagras, Alghazzawi, & Alhaddad, 2013).

Based on these figures and Table 5.2. It can be seen that the optimized cascade T1FPIDC designed using CS method exhibit better results based on some performance measures such as rise time t_r, settling time t_s (less than 2%), steady state error E_{ss} and maximum overshoot M_p compared with GA and PSO based.

For example, considering the pendulum angle results, the CS-based cascade T1FPIDC with $\gamma = 1$ have some improvements over GA based cascade T1FPIDC by 36.7%, 42.9% and 70.7% in t_r, t_s and M_p respectively and over PSO based T1FPIDC by 12.6%, 45.7% and 69.2% in t_r, t_s and M_p respectively. Similarly, the CS based cascade T1FPIDC pendulum angle results with $\gamma = 1.5$ have some improvement over GA based cascade T1FPIDC of 17.6%, 48.0% and 50.0% in t_r, t_s and M_p respectively and over PSO based T1FPIDC of 23.3%, 49.1% and 20.8% in t_r, t_s and M_p respectively.

Also, considering the arm angle results, the CS-based cascade T1FPIDC with $\gamma = 1$ have some improvements over GA based cascade T1FPIDC of 46.1%, 43.6% and 18.4% in t_r, t_s and M_p respectively and over PSO based T1FPIDC of 29.7%, 32.8% and 3.4% in t_r, t_s and M_p respectively. Similarly, the CS based cascade T1FPIDC pendulum angle results with $\gamma = 1.5$ have some improvement over GA based cascade T1FPIDC of 38.2%, 50.3% and 31.5% in t_r, t_s and M_p respectively and over PSO based T1FPIDC of 58.8%, 32.2% and 17.3% in t_r, t_s and M_p respectively.

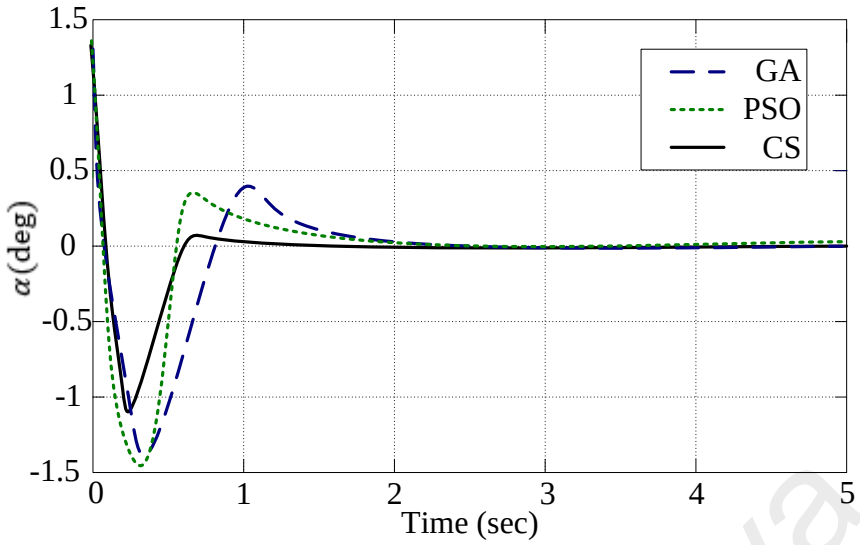

(a) Pendulum angle

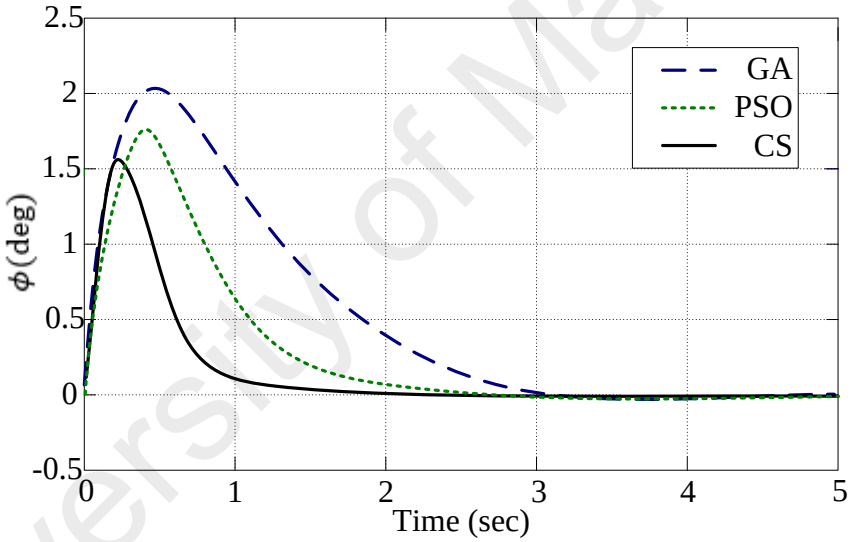

(b) Arm angle

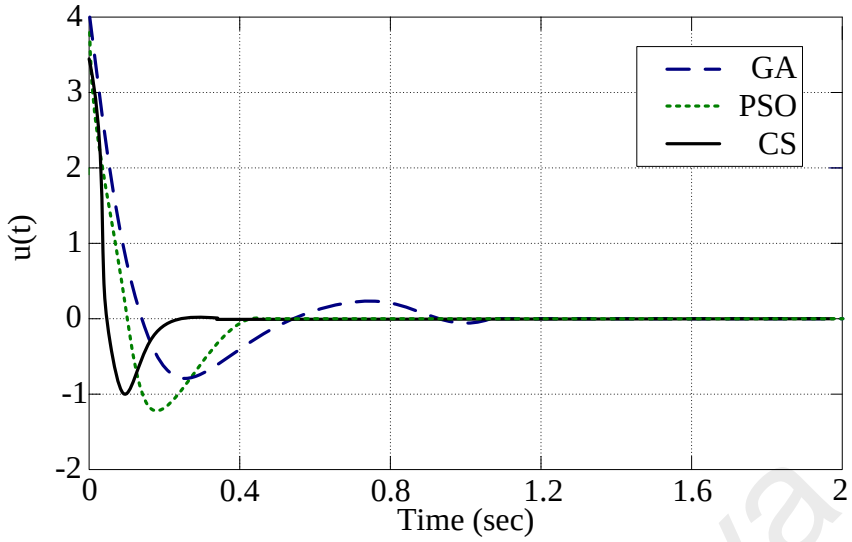

(c) Output of the outer loop controller

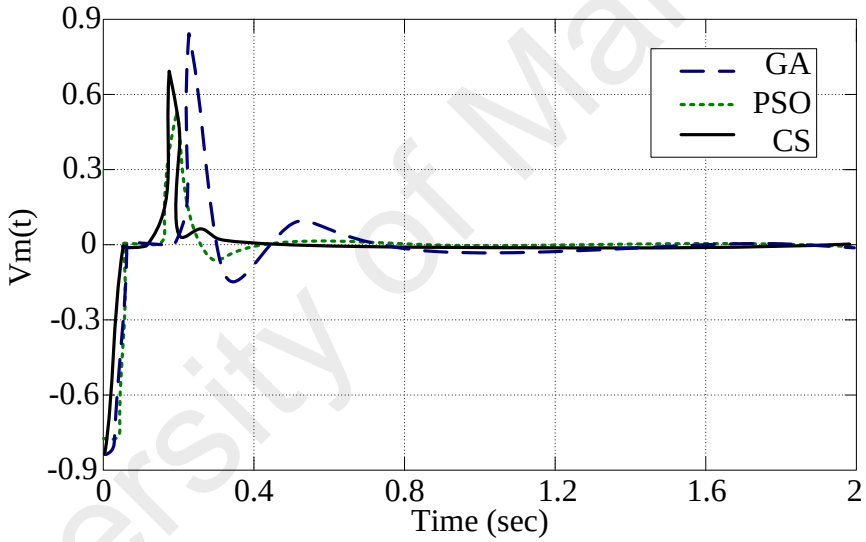

(d) Output of the inner controller

Figure 5.9: Simulation results for cascade optimized T1FPIDC with $\gamma = 1$

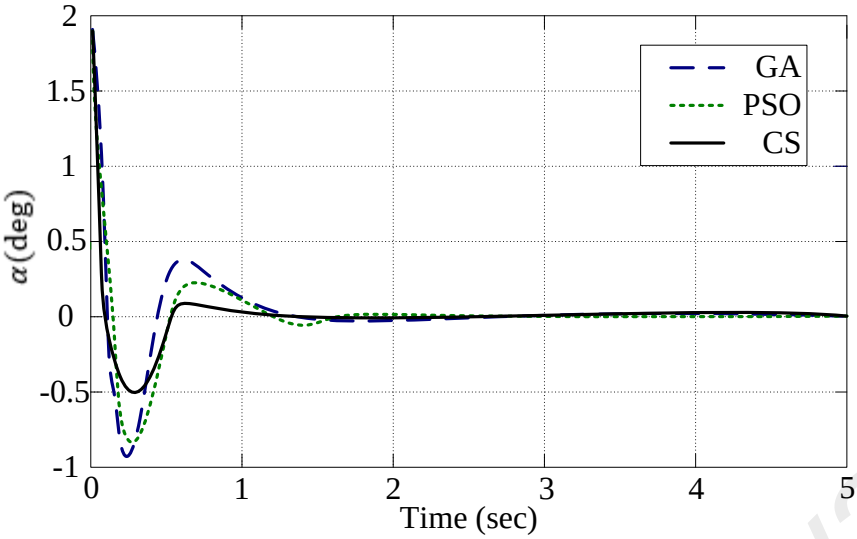

(a) Pendulum angle

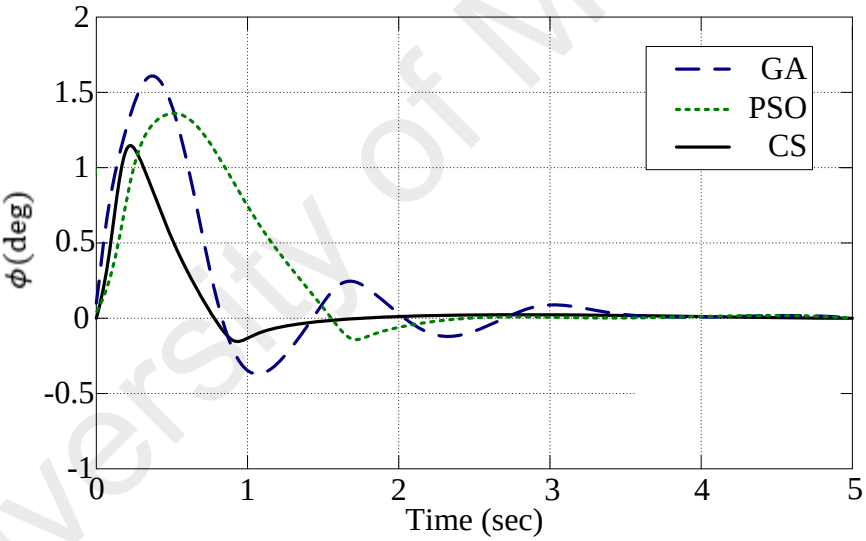

(b) Arm angle

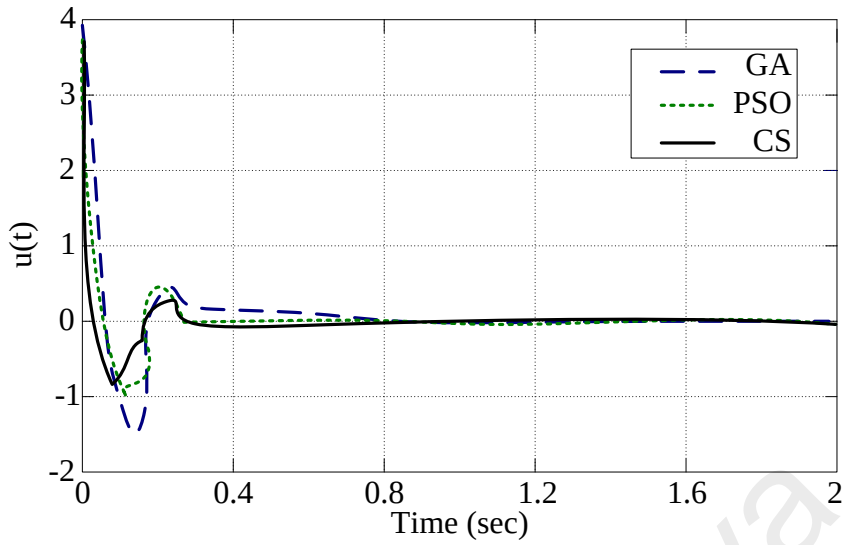

(c) Output of the outer controller

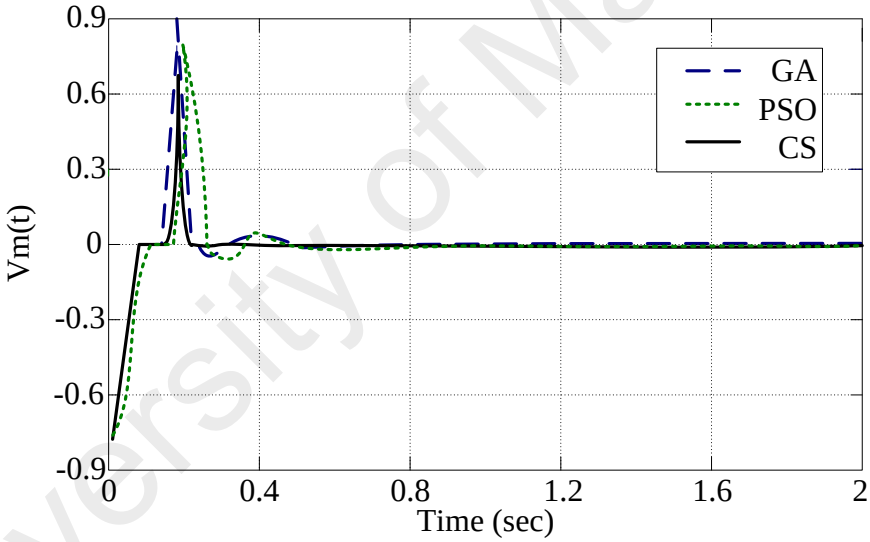

(c) Output of the inner controller

Figure 5.10: Simulation results for cascade optimized T1FPIDC with $\gamma = 1.5$

Table 5.2 Comparative Analysis of results for optimized cascade T1FPIDC

		Based on GA		**Based on PSO**		**Based on CS**	
	γ	1	1.5	1	1.5	1	1.5
t_r(Sec)	Pendulum(α)	0.98	0.68	0.71	0.73	0.62	0.56
	Arm(ϕ)	0.49	0.34	0.37	0.51	0.26	0.21
t_s(Sec)	Pendulum(α)	2.10	2.27	2.21	2.32	1.20	1.18
	Arm(ϕ)	3.12	3.38	2.62	2.48	1.76	1.68
E_{ss}	Pendulum(α)	0.0091	0.0086	0.0089	0.0090	0.0085	0.0085
	Arm(ϕ)	0.0101	0.0088	0.0090	0.0086	0.0084	0.0082
M_p(%)	Pendulum(α)	0.41°	0.38°	0.39°	0.24°	0.12°	0.19°
	Arm(ϕ)	2.06°	1.63°	1.74°	1.39°	1.68°	1.15°
$Coast$		0.338	0.328	0.402	0.274	0.147	0.146

5.2.4 Disturbances rejection analysis in stabilization control for optimized cascade T1FPIDCs

The internal noise and external disturbances are added to the system to test for the robustness of the proposed optimized T1FPIDCs. A load of length 0.1685meter and mass of 0.0635 kg was added to the pendulum. Also, the white noise of 0.00634 power and 10% parameter value changes are added to the process output (feedback) as shown in Figure 5.11. Figure 5.12 (a), (b), (c) and (d) shows the best simulation results of the pendulum angle, arm angle, output of outer control loop and the output of the inner control loop with disturbances for stabilization of RIP. The results indicate the effectiveness and robustness of the proposed controllers in present of noise, disturbances, and plant parameter changes. Though there is some oscillation between -0.2 to 0.2 degrees in arm

angle and -0.05 to 0.05 degrees in pendulum angle which are not a presence in the simulation without the disturbances. However, still all the controllers can stabilize the pendulum in an upright unstable position. Table 5.3 shows the performance of the controller with disturbances. It can be seen from these results that there is some difference in almost all the performance indexes when compared with the simulation results for no disturbances. Also, the optimized cascade T1FPIDC designed using CS method display an improved results based on some considered performance criteria (i.e. t_r, t_s and M_p) compared with the T1FPIDCs designed based using PSO and CS methods.

For the pendulum angle results, the CS-based cascade T1FPIDC in the presence of disturbances have some improvements over GA-based cascade T1FPIDC of 36.7%, 42.9% and 70.7% in t_r, t_s and M_p respectively and over PSO based T1FPIDC of 12.6%, 45.7% and 69.2% in t_r, t_s and M_p respectively. Note that this simulation was done for $\gamma = 1$ only.

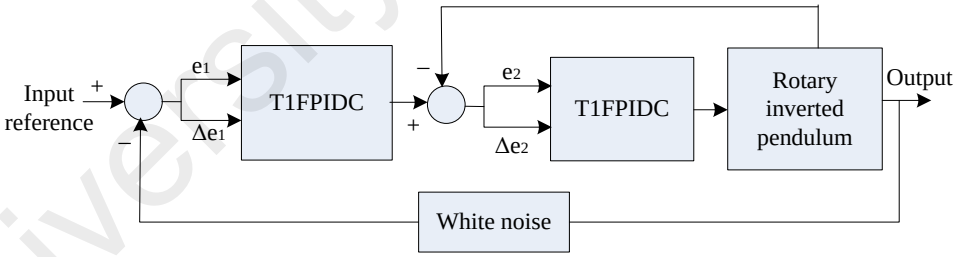

Figure 5.11: T1FPIDC including the source of noise

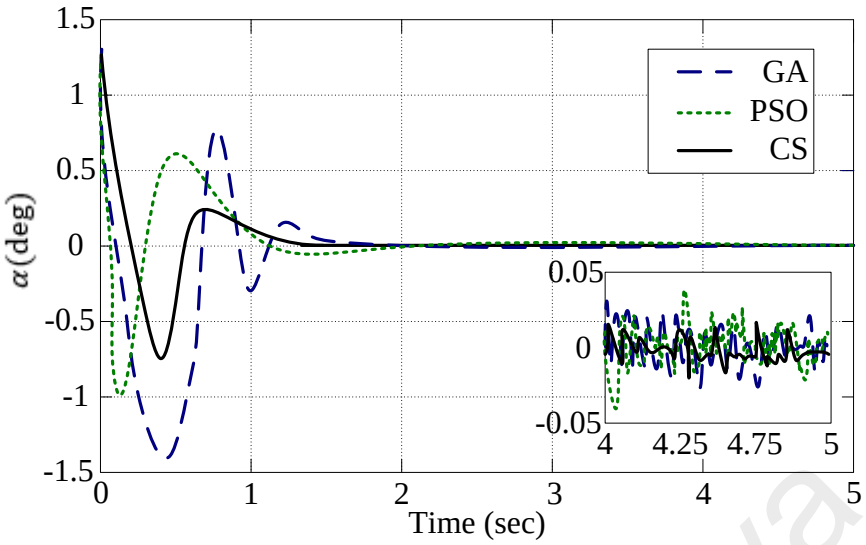

(a) Pendulum angle

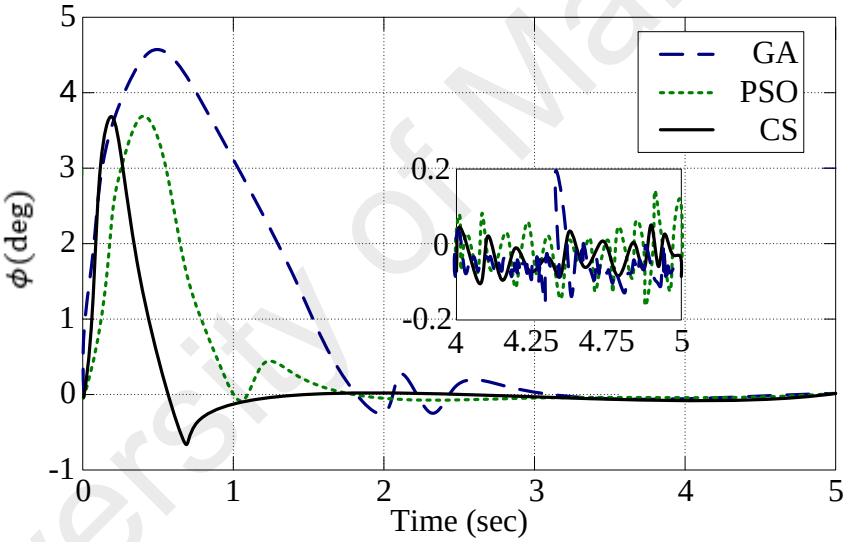

(b) Arm angle

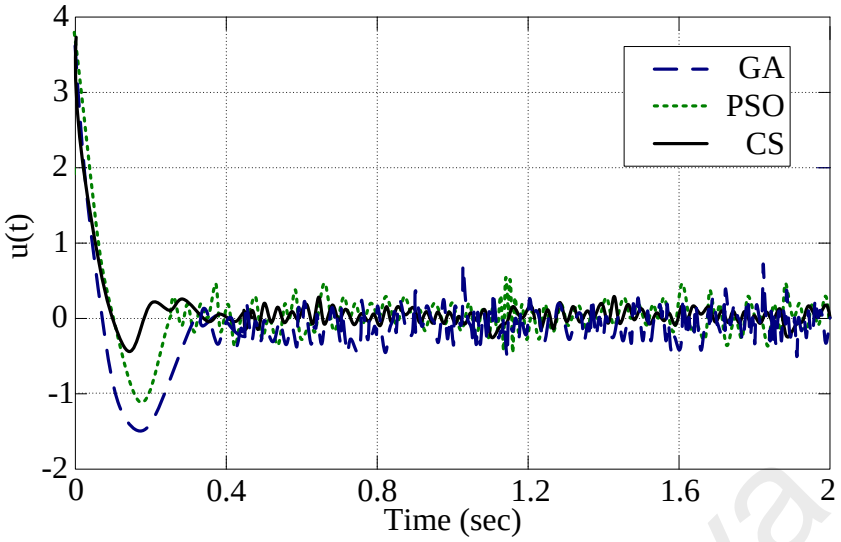

(c) Output of the outer controller

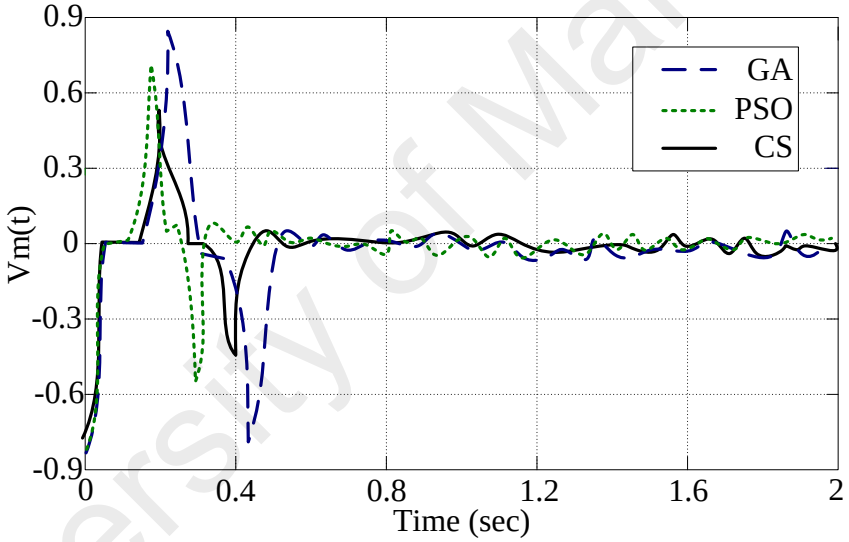

(d) Output of the inner controller

Figure 5.12: Disturbance rejection analysis for cascade optimized T1FPIDC with $\gamma = 1$

Table 5.3 Comparative Analysis of results for disturbance rejection ability of optimized cascade T1FPIDC

		GA based	PSO based	CS based
$t_r(\text{sec})$	Pendulum(α)	0.89	0.78	0.70
	Arm(ϕ)	0.51	0.39	0.26
$t_s(\text{sec})$	Pendulum(α)	2.20	2.10	1.40
	Arm(ϕ)	3.48	2.96	1.89
E_{ss}	Pendulum(α)	0.0100	0.0097	0.0098
	Arm(ϕ)	0.0111	0.0098	0.0096
$M_p(\%)$	Pendulum(α)	0.75°	0.64°	0.24°
	Arm(ϕ)	4.62°	3.74°	3.68°
Coast		0.481	0.448	0.208

5.2.5 Trajectory tracking control for optimized cascade T1FPIDC

Trajectory tracking control is one of the important control objectives of the RIP. It shows the ability of the controller to control the arm of RIP in such a way that the arm tracks the desired time-varying trajectory while the pendulum remains at an unstable position. This problem includes the controller design $\tau \epsilon \mathbb{R}$ in such a way that, the trajectory error $\tilde{\phi}$ and the pendulum angle are uniformly ultimately bounded (Khalil & Grizzle, 1996). That is the design controller guarantees the following:

$$\left\| \begin{matrix} \tilde{\phi}(t_0) \\ \alpha(t_0) \end{matrix} \right\| \leq a \Rightarrow \left\| \begin{matrix} \tilde{\phi}(t) \\ \alpha(t) \end{matrix} \right\| \leq b, \forall t \geq t_0 + T \tag{5.1}$$

where a and b are constant, $T > 0$ and $\tilde{\phi} = \phi_d - \phi$. The desired trajectory function ϕ_d used in this study is the time varying square function. This function is continuous and

differentiable. Beside also, $\phi_d, \dot{\phi}_d,$ and $\ddot{\phi}_d$ are bound for all $t \geq 0$. The output function is define as:

$$y = \tilde{\phi} - \alpha \tag{5.2}$$

The detailed explanation and formulation of RIP trajectory tracking control can be found in (Aguilar-Avelar & Moreno-Valenzuela, 2015) and in chapter three.

The best simulation results for RIP trajectory tracking control of optimized cascade T1FPIDC for $\gamma = 1$ is shown in Figure 5.13 (a) and (b) for pendulum angle and arm angle respectively. Also, the best simulation result for RIP trajectory tracking control by optimized cascade T1FPIDC for $\gamma = 1.5$ is presented in Figure 5.14 (a) and (b) for pendulum angle and arm angle respectively. It can be observed from both Figure 5.13 (a) and 5.14 (a) that the CS based cascade T1FPIDC reaches the set point more quickly compared with the GA based and PSO based cascade T1FPIDC. The detail comparative performance is presented in Table 5.4. It can be seen from that table that the CS based cascade T1FPIDC have some improved performance in terms of t_r, t_s, M_p and delay time t_d. The stability of IT2FLC 's hard to confirm, Unlike sliding mode control (SMC) (Hung, Gao, & Hung, 1993; Utkin, 2013). The stability analysis of IT2FLC can be addressed within an SMC framework. The stability of hybrid IT2FSMC systems can be analyzed using Lyapunov stability theory (Feng, 2006). The common Lyapunov functions that can be used are: Global or common quadratic Lyapunov functions, piecewise quadratic Lyapunov functions and non-quadratic or fuzzy Lyapunov functions (Masumpoor & Khanesar, 2015). The stability analysis of the IT2FLC is not within the scope of the present research.

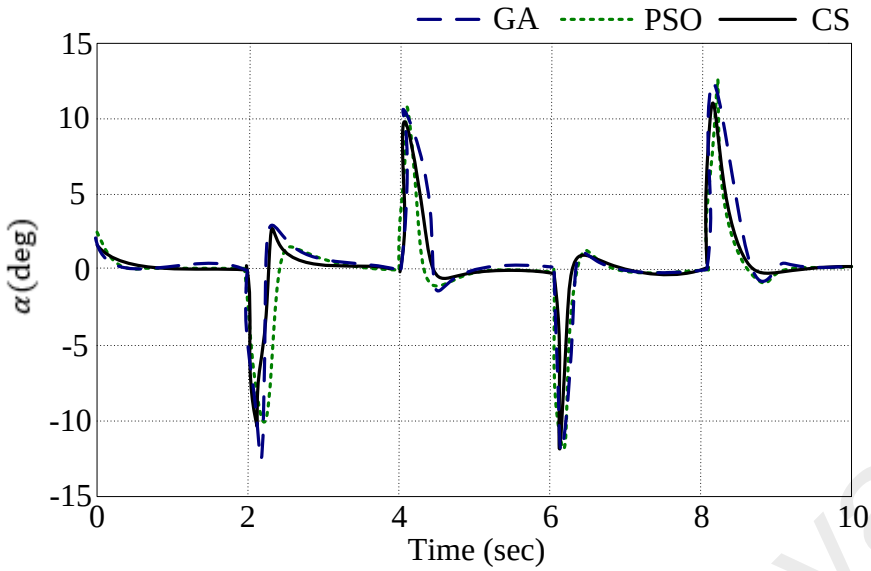

(a) Pendulum angle

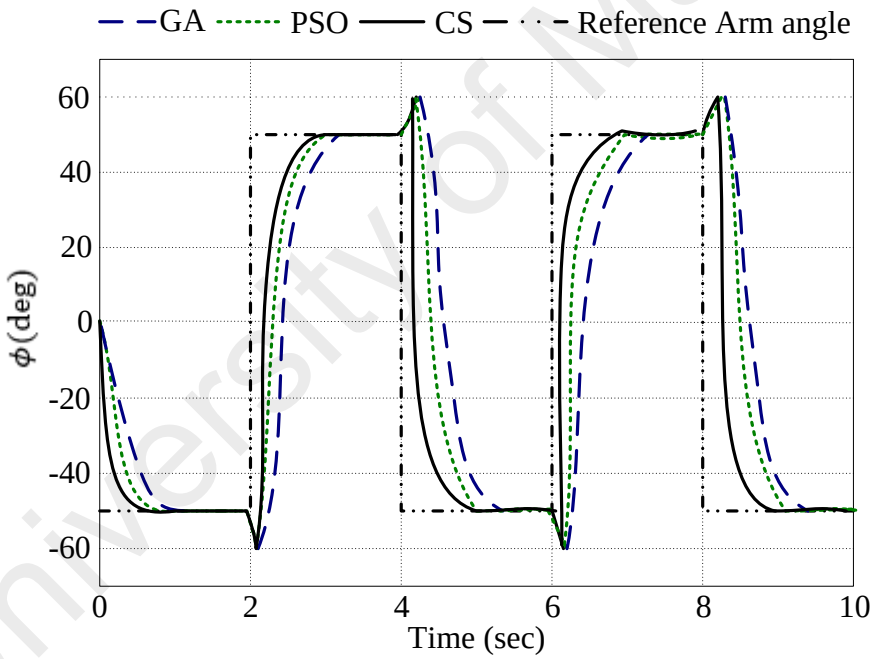

(b) Arm angle

Figure 5.13: Optimized Cascade T1FPIDC simulation result for trajectory tracking control $\gamma = 1$

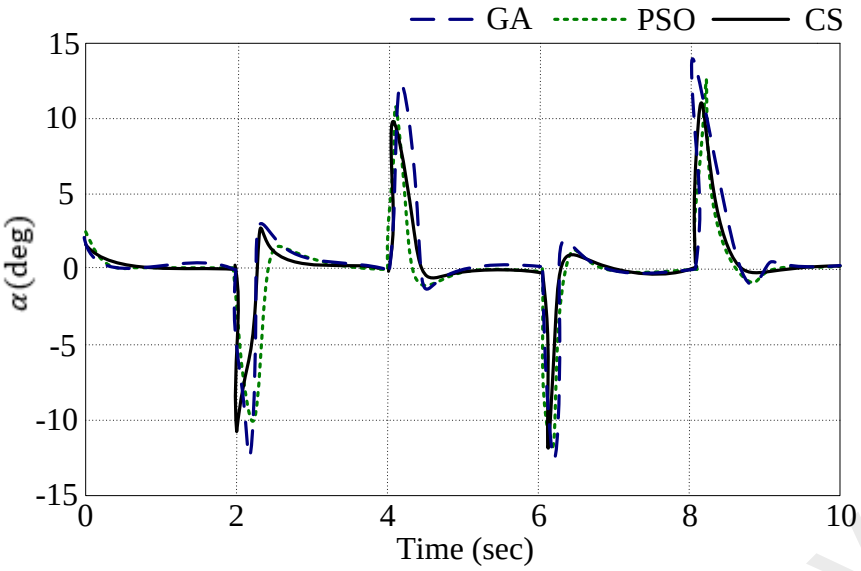

(a) Pendulum angle

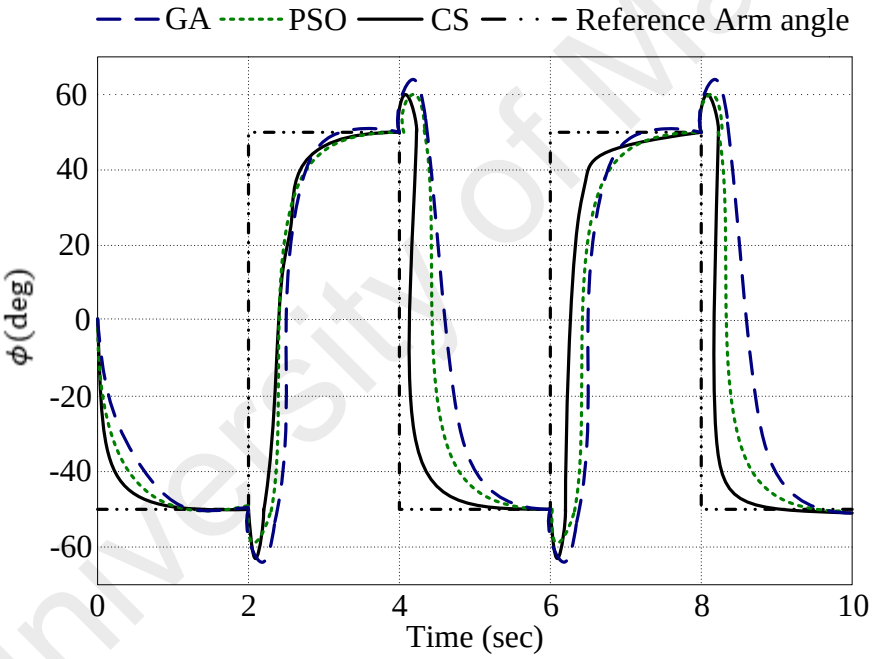

(b) Arm angle

Figure 5.14: Optimized Cascade T1FPIDC simulation result for trajectory tracking control $\gamma = 1.5$

Table 5.4 Comparative trajectory tracking results for optimized cascade T1FPIDC (Simulation)

		Based on GA		**Based on PSO**		**Based on CS**	
	γ	1	1.5	1	1.5	1	1.5
t_r(Sec)	Pendulum(α)	0.58	0.56	0.52	0.57	0.51	0.49
	Arm(ϕ)	0.56	0.53	0.52	0.46	0.39	0.36
t_s(Sec)	Pendulum(α)	1.24	1.40	1.31	1.51	1.02	1.14
	Arm(ϕ)	1.39	1.57	1.41	1.59	1.27	1.42
t_d(Sec)	Pendulum(α)	0.62	0.69	0.58	0.61	0.53	0.55
	Arm(ϕ)	0.59	0.61	0.52	0.56	0.41	0.43
E_{ss}	Pendulum(α)	0	0	0	0	0	0
	Arm(ϕ)	0	0	0	0	0	0
M_p(%)	Pendulum(α)	2.19	2.37	2.05	2.12	1.93	2.01
	Arm(ϕ)	6.24	7.81	4.45	6.48	4.68	6.12

5.3 Simulation results for optimized cascade IT2FPIDC

5.3.1 Optimized Antecedent MFs for IT2FPIDC

Similar to T1FPIDC, the size of the population and the maximum number of iterations for all IT2FPIDC (GA-based, PSO-based and CS-based) design strategies are chosen to be the same. That is the number of iteration and population size are 150 and 100 respectively. This was done to have fair comparisons of the performance of the optimization algorithms as well as the performance of the IT2FPIDC and T1FPIDC. The inner and the outer controllers are optimized to minimized the coast function in equation (4.1). By setting the weighing factor $\gamma = 1$, the optimized antecedent MFs for IT2FPIDC inner loop E_2 and ΔE_2, and outer loop E_1 and ΔE_1 for GA-based, PSO based and CS-

based are shown in Figure 5.15, 5.16 and 5.17 respectively. Also, by setting the weighing factor $\gamma = 1.5$, the optimized antecedent MFs for IT2FPIDC inner loop E_2 and ΔE_2, and outer loop E_1 and ΔE_1 for GA-based, PSO based and CS-based are shown in Figure 5.18, 5.19 and 5.20 respectively.

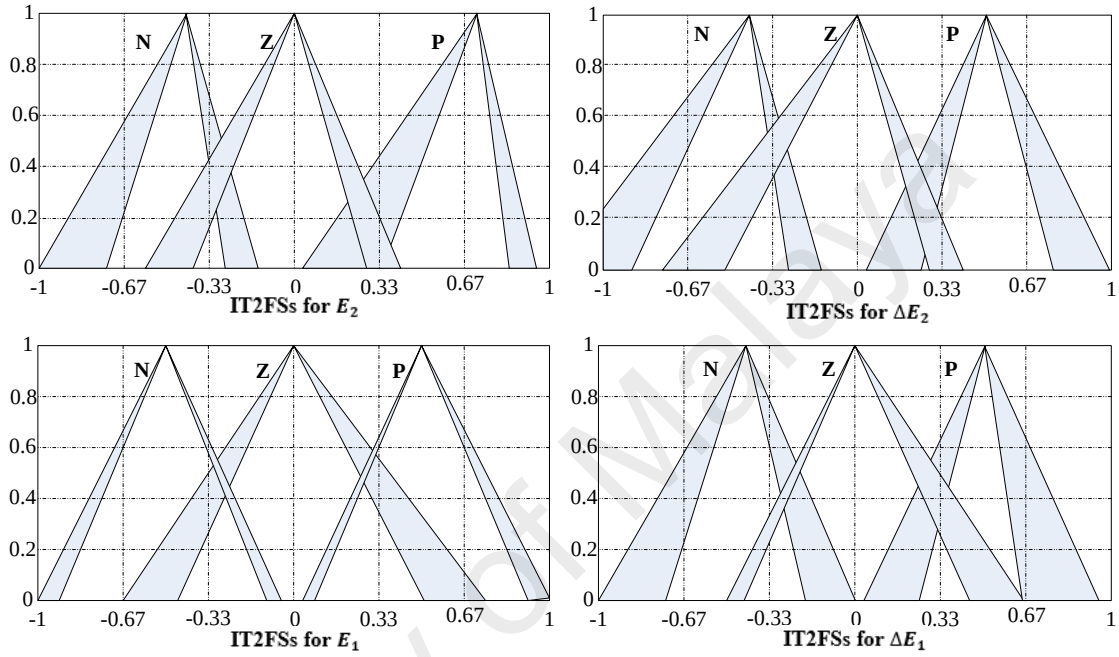

Figure 5.15: Optimized antecedent MFs of IT2FPIDC (GA-based), $\gamma = 1$

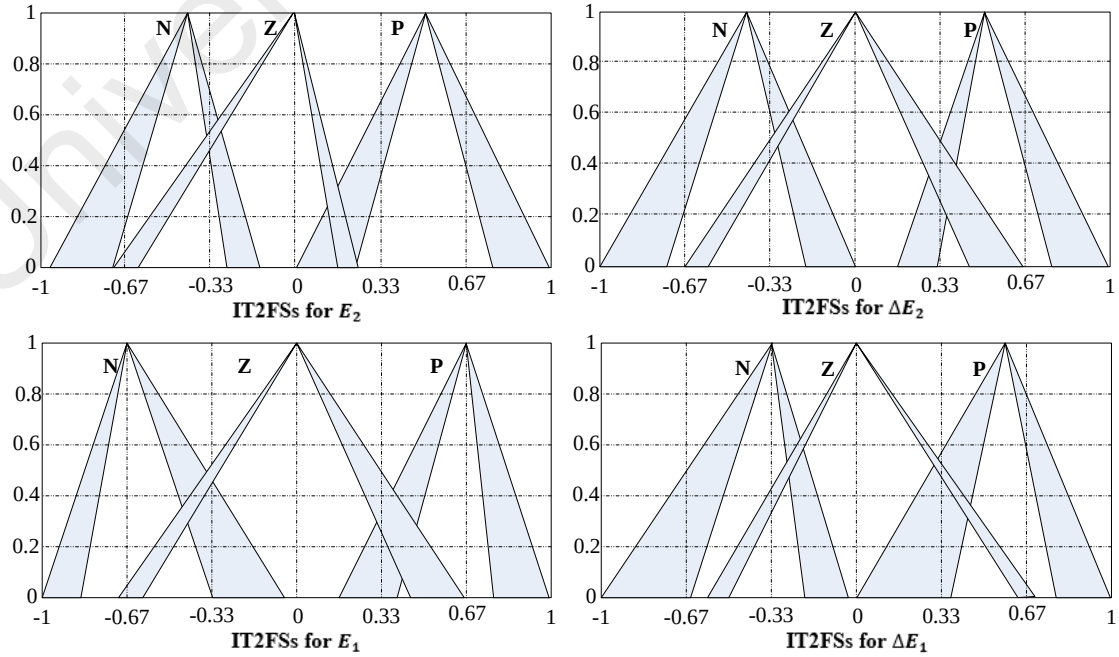

Figure 5.16: Optimized antecedent MFs of IT2FPIDC (PSO-based), $\gamma = 1$

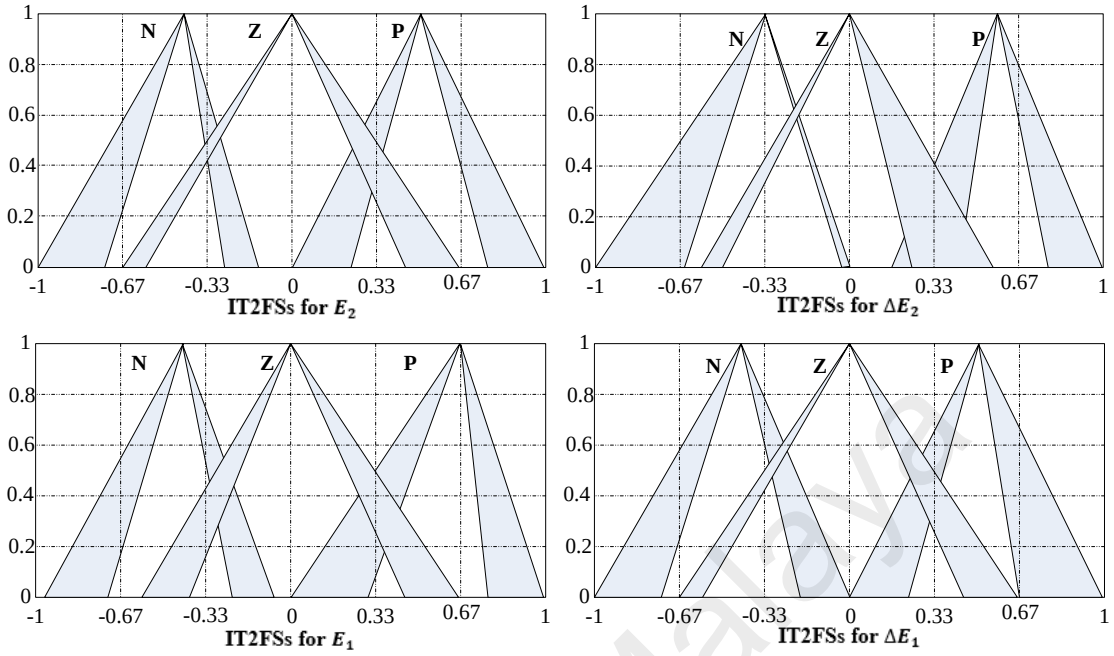

Figure 5.17: Optimized antecedent MFs of IT2FPIDC (CS-based), $\gamma = 1$

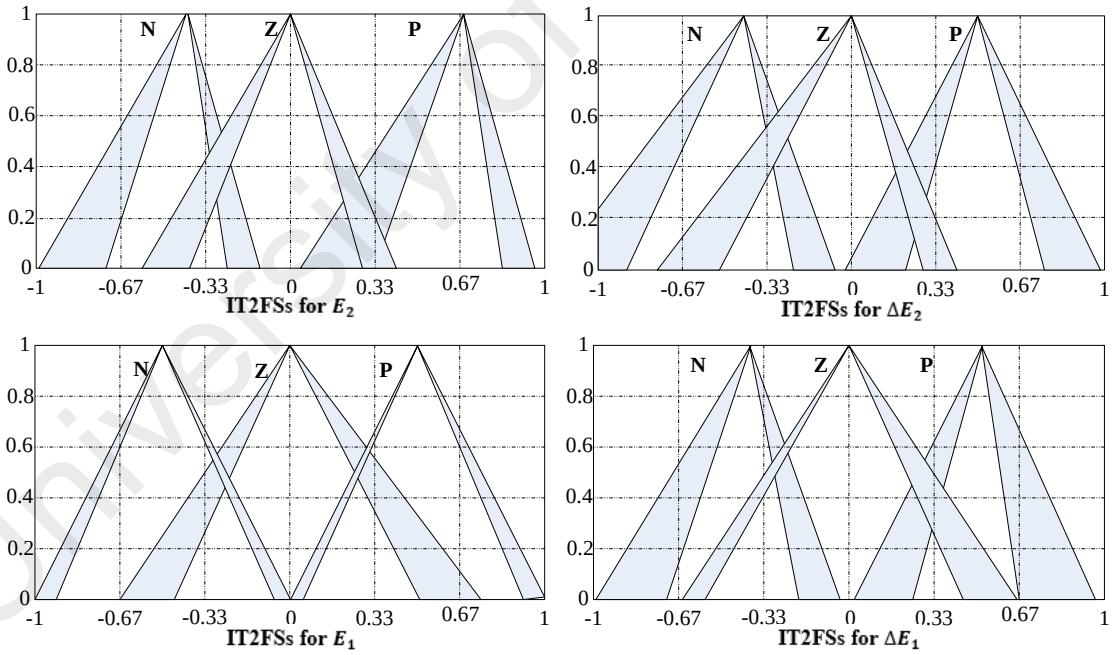

Figure 5.18: Optimized antecedent MFs of IT2FPIDC (GA-based), $\gamma = 1.5$

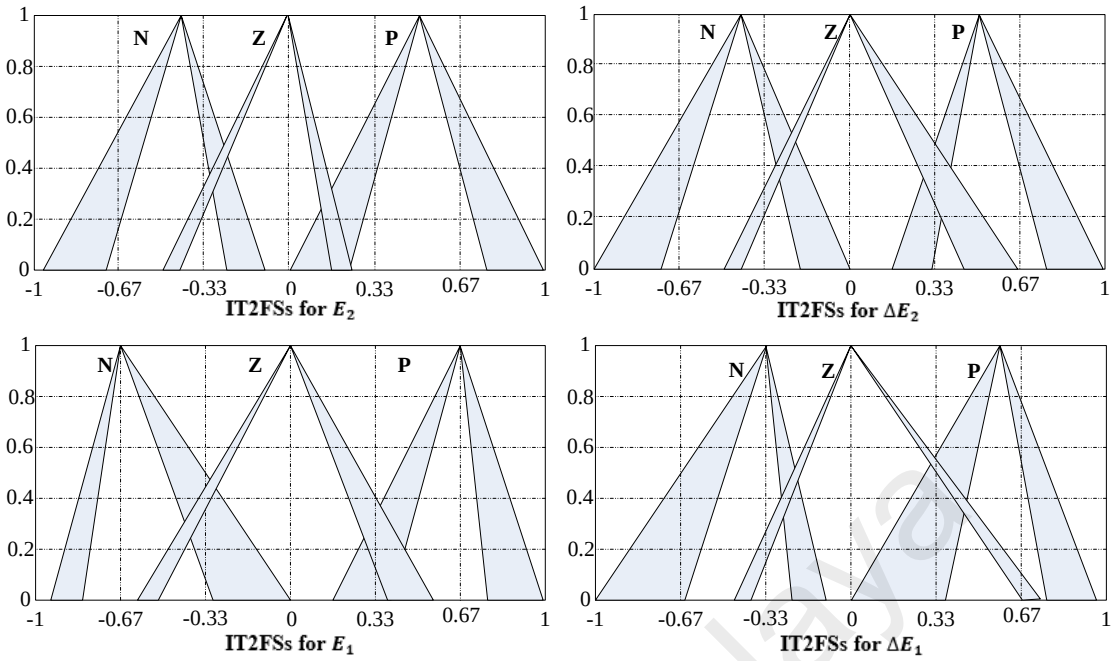

Figure 5.19: Optimized antecedent MFs of IT2FPIDC (PSO-based), $\gamma = 1.5$

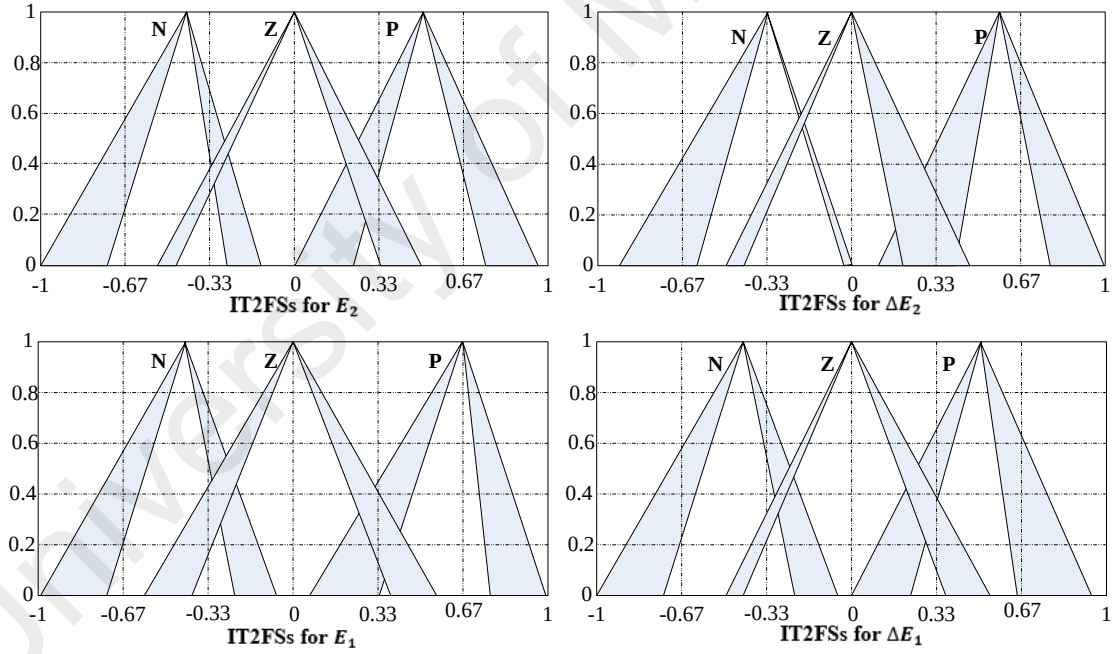

Figure 5.20: Optimized antecedent MFs of IT2FPIDC (CS-based), $\gamma = 1.5$

5.3.2 Convergence Characteristics based on IT2FPIDC

Similar to T1FPIDC, the test for accuracy and speed of convergence was performed for IT2FPIDC. Figure 5.21 (a) and (b) shows that all IT2FPIDC (i.e. GA-based, PSO-based and CS-based) can secure stable mean cost value, for $\gamma = 1$ and $\gamma = 1.5$ using the same simulation conditions and cost function. However, CS-based IT2FPIDC have the

best mean value and cost value compared to PSO and GA based IT2FPIDC. This indicates that the CS-based IT2FPIDC can achieve better accuracy than PSO-based and GA-based It2FPIDCs for both $\gamma = 1$ and $\gamma = 1.5$. On the other hand, Figure 5.22 (a) and (b) show that in the tendency of convergence of standard deviation of cost values, CS-based IT2FPIDC is faster than PSO-based and GA-based IT2FPIDCs. This indicates that CS method have the best convergence efficiency than PSO and GA. Also PSO, have better convergence efficiency than GA. The optimized scaling factors for cascade IT2FPIDC are shown in Table 5.4.

Table 5.5 Optimized scaling factors for cascade IT2FPIDC

		Outer controller				**Inner Controller**			
Algorithms	γ	K_{P_1}	K_{I_1}	K_{D_1}	K_{a_1}	K_{P_2}	K_{I_2}	K_{D_2}	K_{a_2}
GA	1	7.963	6.341	0.0054	1.941	0.7723	0.7052	0.0276	0.3759
	1.5	8.115	6.516	0.0061	2.011	0.7832	0.6982	0.0323	0.3870
PSO	1	9.147	7.947	0.0089	1.798	0.6973	0.6197	0.0512	0.5545
	1.5	8.922	6.072	0.0073	1.394	0.7034	0.5991	0.0281	0.5747
CS	1	8.014	6.136	0.0019	1.563	0.7276	0.5893	0.0205	0.5061
	1.5	7.913	5.862	0.0073	2.087	0.7134	0.6018	0.0393	0.4917

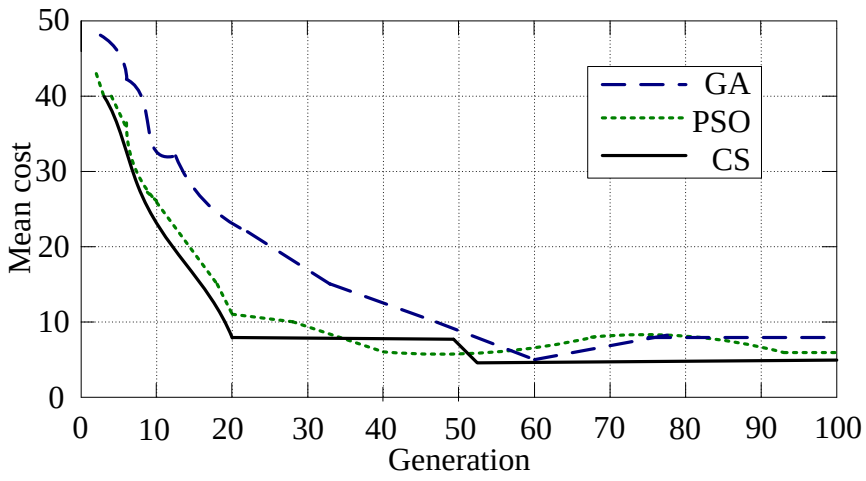

(a) $\gamma = 1$

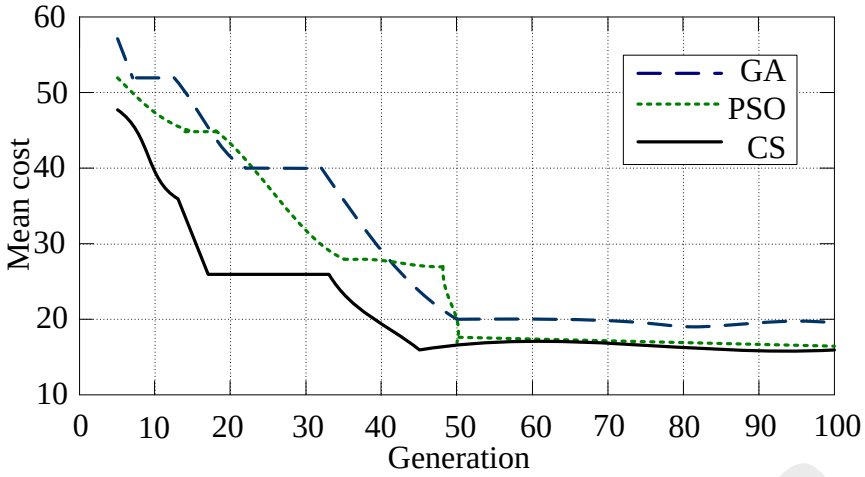

(b) $\gamma = 1.5$

Figure 5.21: Tendency of convergence of mean value of cost function with IT2FPIDC

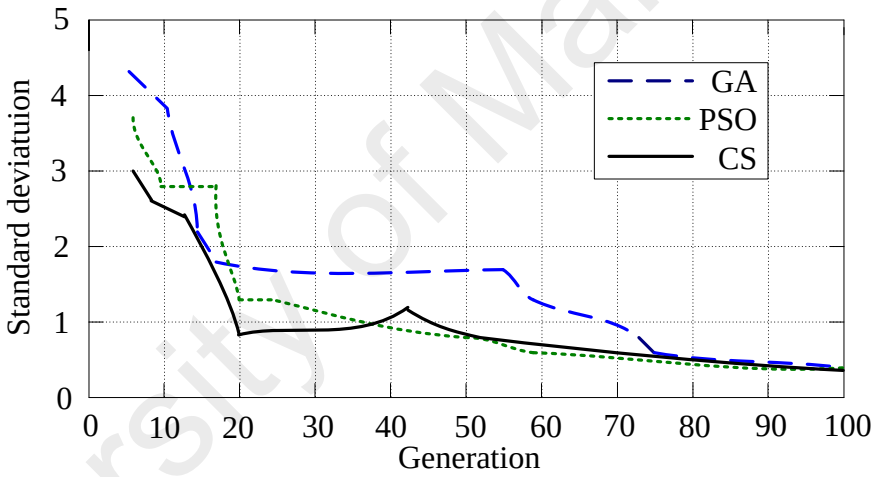

(a) $\gamma = 1$

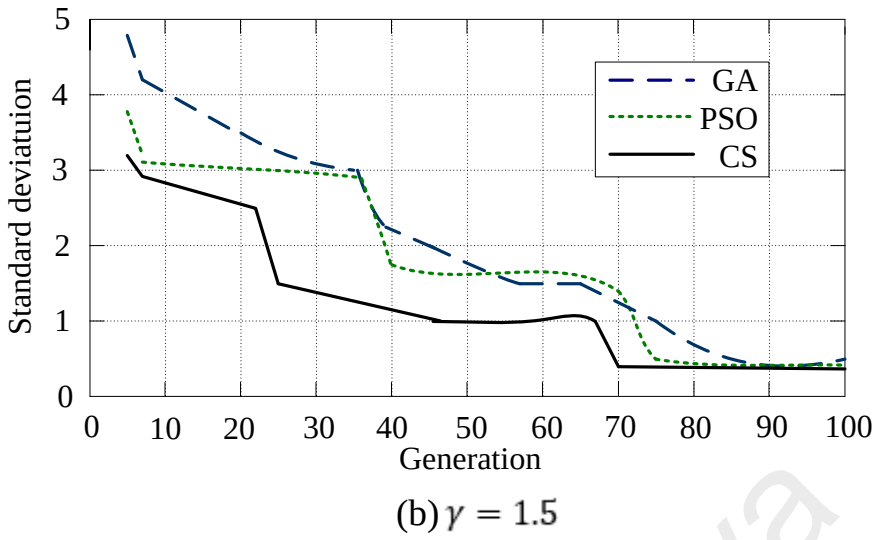

(b) $\gamma = 1.5$

Figure 5.22: Tendency of convergence of standard deviation value of cost function in IT2FPIDC

The best run time for T1FPIDCs and IT2FPIDCs in 100 iterations are shown in Table 5.6. The run time for IT2FPID is higher for each corresponding optimization algorithm in T1FPIDCs. This due to the higher number of optimization parameters in IT2FPIDC compared with T1FPIDC.

Table 5.6 Average computational time for IT2FPIDCs and T1FPIDCs

	$\gamma = 1$		$\gamma = 1.5$	
Algorithms	**T1FPIDC**	**IT2FPIDC**	**T1FPIDC**	**IT2FPIDC**
GA	385.64 minute	453.70 minute	443.41 minute	558.05 minute
PSO	259.21 minute	294.55 minute	375.85 minute	481.10 minute
CS	178.67 minute	196.33 minute	217.97 minute	262.25 minute

5.3.3 Stabilization control using optimized cascade IT2FPIDC

The stabilization control of RIP using optimized cascade IT2FPIDC has been analyzed in this section. The reference pendulum angle α_r was set to zero, assuming $\alpha_r = 0$ is the upright unstable position. The pendulum is need to be stabilized at this position as quickly

as possible. The best results found for the pendulum angle, arm angle, output of outer control loop and the output of the inner control loop (i.e. voltage to the servo motor) for $\gamma = 1$ are shown in Figure 5.23 (a), (b), (c) and (d) respectively. The effect of changing the γ is anlysed in stabilization control by changing its value to $\gamma = 1.5$. Figure 5.24 (a), (b), (c) and (d) demonstrate the best results found for the pendulum angle, arm angle, output the of outer control loop and the output of the inner control loop (i.e. voltage to the servo motor) respectively. The summary of the best simulation results in 60 runs for different values of γ are shown in Table 5.6. Based on these Figures and Table 5.7 it can be stated that the optimized cascade IT2FPIDC designed using CS method exhibit a better results based on some performance indexes such as rise time t_r, settling time t_s (less than 2%), steady state error E_{ss} and maximum overshoot M_p compared with the optimized IT2FPIDC designed based on GA as well as that designed based on PSO.

For the pendulum angle results, the CS-based cascade IT2FPIDC with $\gamma = 1$ have some improvements over GA based cascade IT2FPIDC of 57.1%, 8.2% and 61.6% in t_r, t_s and M_p respectively and over PSO based IT2FPIDC of 7.1%, 4.7% and 28.6% in t_r, t_s and M_p respectively. Similarly, the CS based cascade IT2FPIDC pendulum angle results with $\gamma = 1.5$ have some improvement over GA based cascade IT2FPIDC of 8.8%, 38.7% and 29.2% in t_r, t_s and M_p respectively and over PSO based IT2FPIDC of 32.8%, 16.5% and 22.7% in t_r, t_s and M_p respectively.

For the arm angle results, the CS-based cascade IT2FPIDC with $\gamma = 1$ have some improvements over GA based cascade IT2FPIDC of 57.1%, 41.1% and 33.3% in t_r, t_s and M_p respectively and over PSO based IT2FPIDC of 50%, 35.8% and 20.5% in t_r, t_s and M_p respectively. Similarly, the CS based cascade IT2FPIDC pendulum angle results with $\gamma = 1.5$ have some improvement over GA based cascade IT2FPIDC of 46.4%, 54.7% and 24.5% in t_r, t_s and M_p respectively and over PSO based IT2FPIDC of 60.5%,

46.1% and 11.3% in t_r, t_s and M_p respectively. The steady state error E_{ss} are almost the same in all the controllers and they can be approximated to zero. Both PSO based and CS based IT2FPIDC have lower cost function compared with CS based IT2FPIDC.

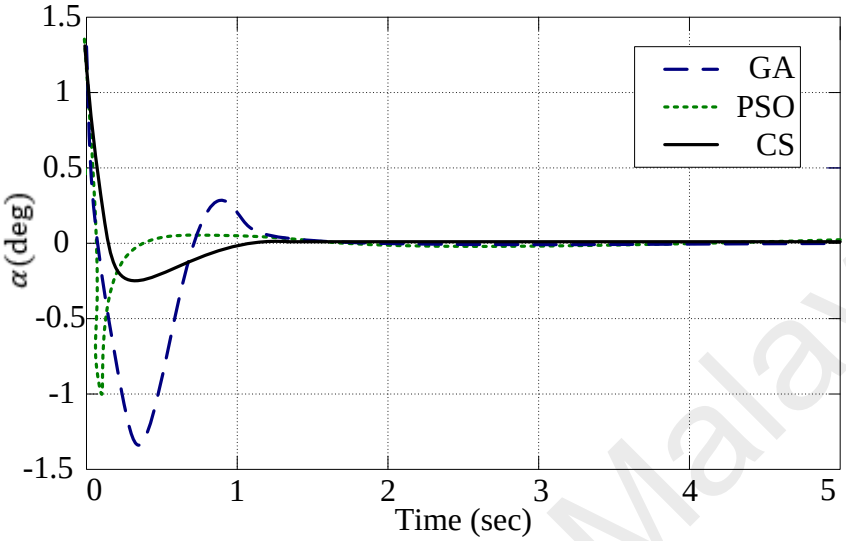

(a) Pendulum angle

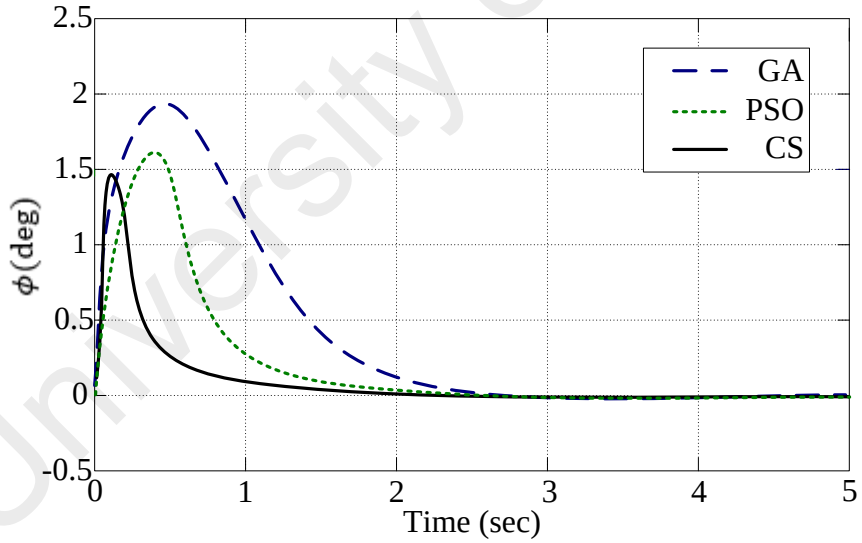

(b) Arm angle

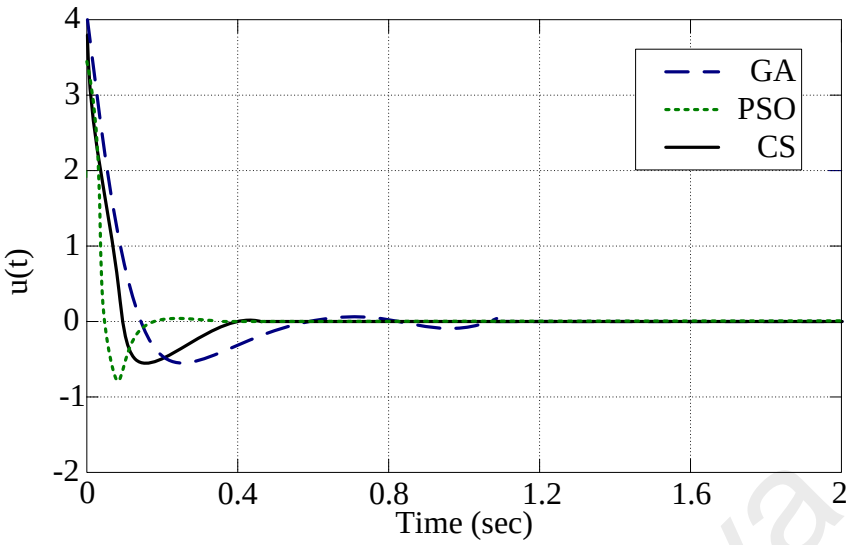

(c) Output of the outer controller

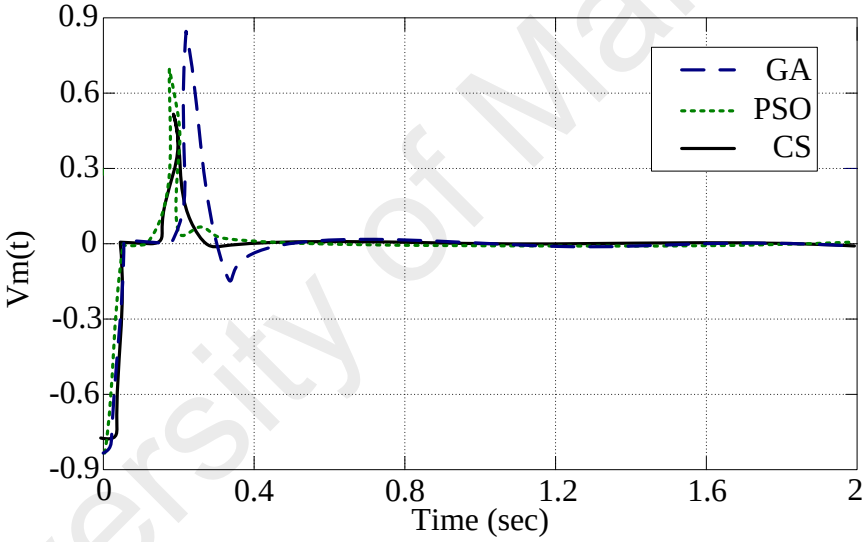

(d) Output of the inner controller

Figure 5.23: Simulation results for cascade optimized IT2FPIDC with $\gamma = 1$

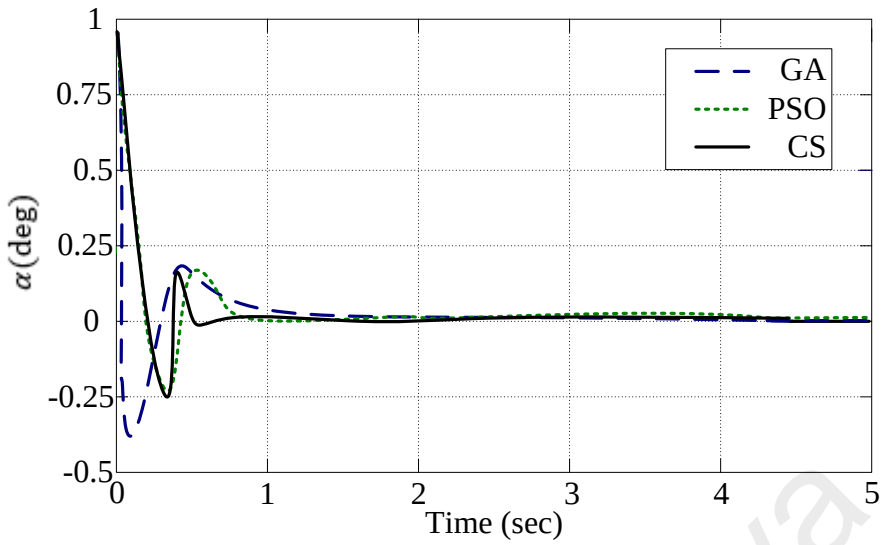

(a) Pendulum angle

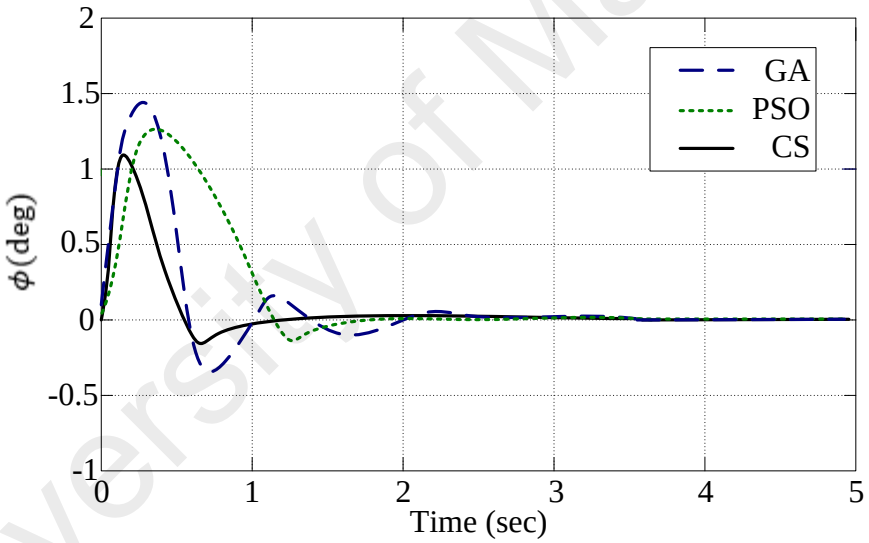

(b) Arm angle

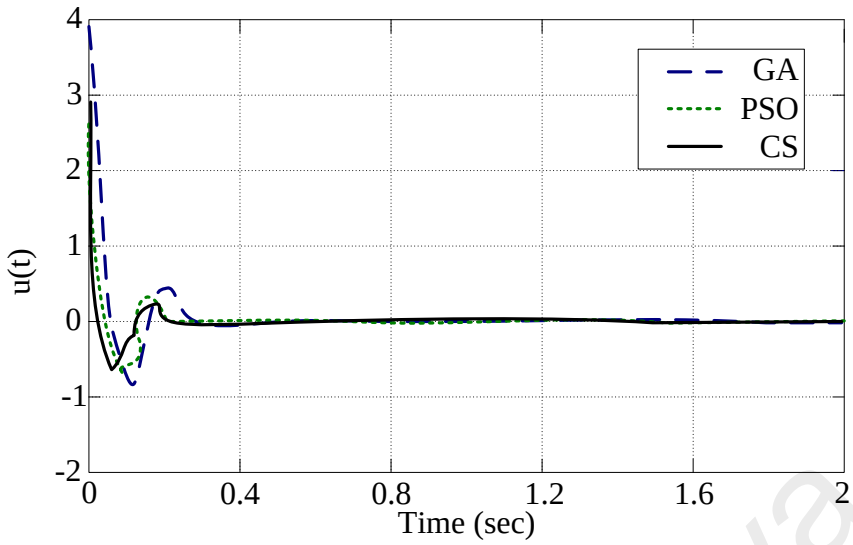

(c) Output of the outer controller

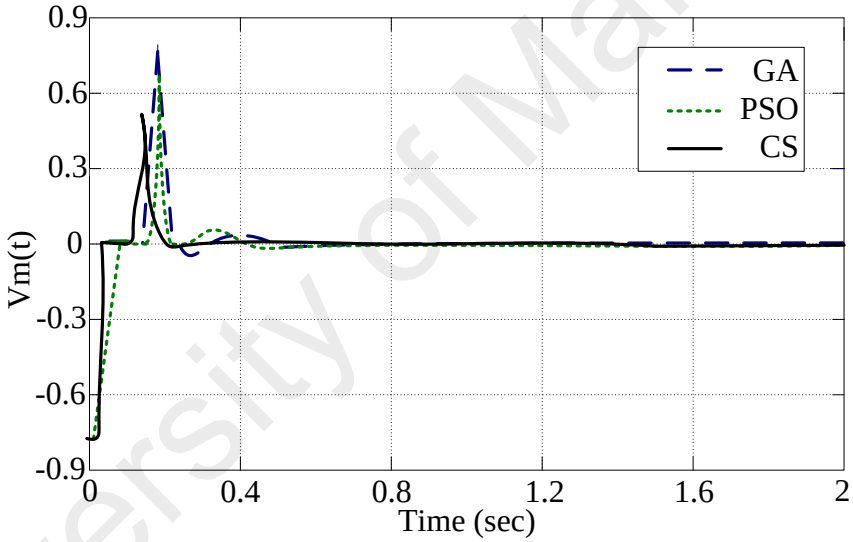

(d) Output of the inner controller

Figure 5.24: Simulation results for cascade optimized IT2FPIDC with $\gamma = 1.5$

Table 5.7 Comparative Analysis of results for optimized cascade IT2FPIDC

		Based on GA		Based on PSO		Based on CS	
	γ	1	1.5	1	1.5	1	1.5
t_r(Sec)	Pendulum(α)	0.88	0.45	0.42	0.61	0.39	0.41
	Arm(ϕ)	0.42	0.28	0.36	0.38	0.18	0.15
t_s(Sec)	Pendulum(α)	1.34	1.24	1.29	0.91	1.23	0.76
	Arm(ϕ)	2.65	2.78	2.43	2.34	1.56	1.26
E_{ss}	Pendulum(α)	0.0089	0.0077	0.0087	0.0086	0.0076	0.0079
	Arm(ϕ)	0.0093	0.0084	0.0085	0.0082	0.0077	0.0086
M_p(%)	Pendulum(α)	0.26	0.24	0.14	0.22	0.10	0.17
	Arm(ϕ)	1.92	1.47	1.61	1.25	1.28	1.11
$Coast$		0.169	0.184	0.207	0.122	0.189	0.108

5.3.4 Disturbances rejection analysis in stabilization control for optimized cascade IT2FPIDCs

Similar to T1FPIDC, the internal noise and external disturbances are added to the RIP system to test for the robustness of the proposed optimized cascade IT2FPIDCs. A load of length 0.1685meter and mass of 0.0635 kg mass was added to the pendulum. Also, the white noise of 0.00634 power and 10% parameter value changes is added to the process output (feedback) as shown in Figure 5.26. Figure 5.27 (a), (b), (c) and (d) shows the best simulation results of the pendulum angle, arm angle, output of outer control loop and the output of the inner control loop with disturbances. The results indicate the effectiveness and robustness of the proposed IT2FPIDCs. Though there is some oscillation between -0.1 to 0.2 degrees in arm angle and -0.04 to 0.04 degrees in pendulum angle which are not present in the simulation without the disturbances but still all the controllers are able

to stabilize the pendulum in an upright unstable position with little vibrations. Table 5.8 shows the performance of the controller with disturbances. The advantage of IT2FPIDC over T1FPIDC can be seen when there result in the presence of disturbances are compared. For example, the performance of optimized cascade IT2FPIDC have some improvement between 6.1% to 33.3%, 5.7% to 35.2% and 6.6% to 20.8% in term of t_r,t_s, and E_{ss} over the optimized cascade T1FPIDC counterpart.

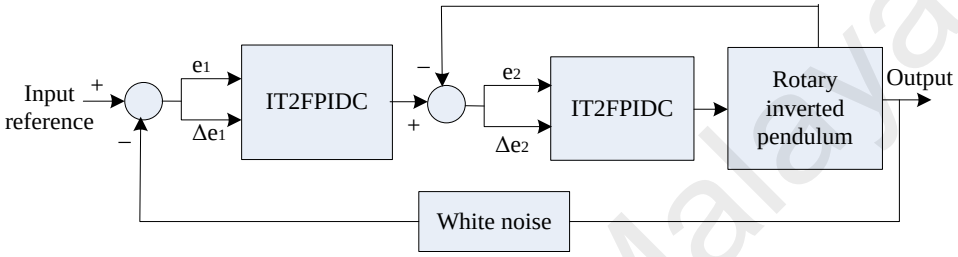

Figure 5.25: IT2FPIDC including the source of noise

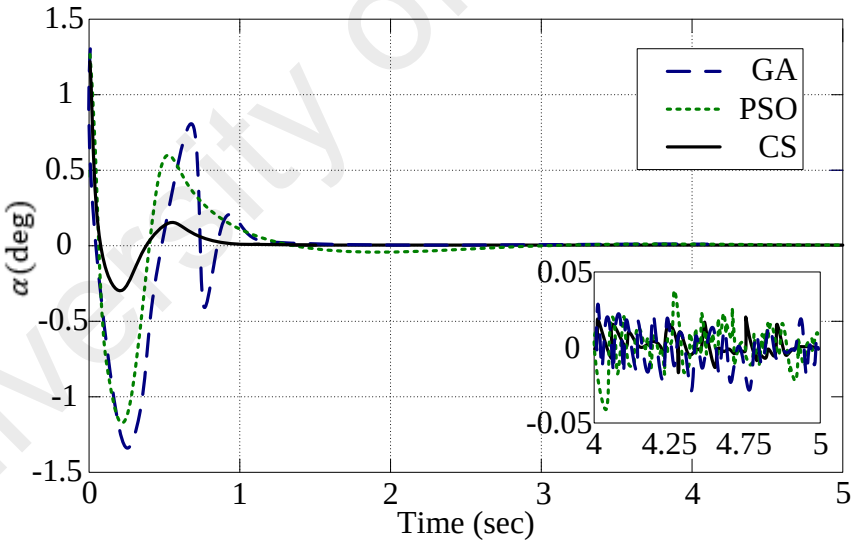

(a) Pendulum angle

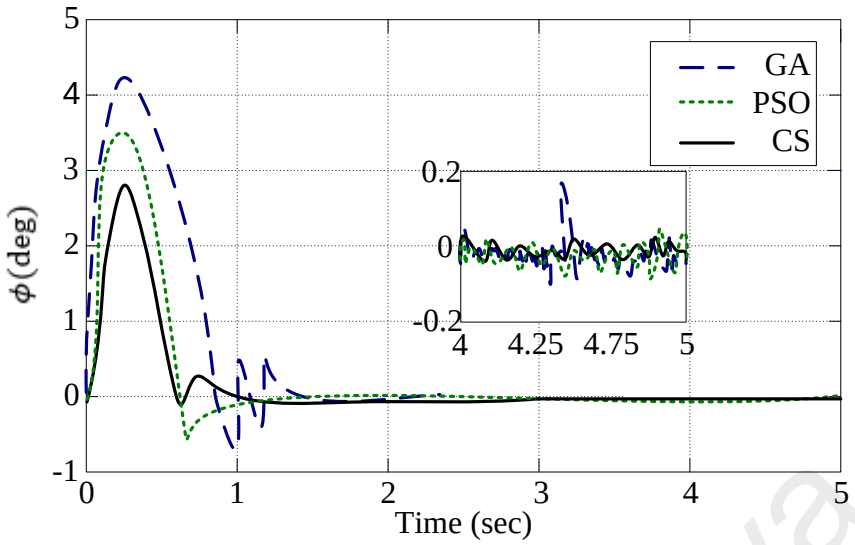

(b) Arm angle

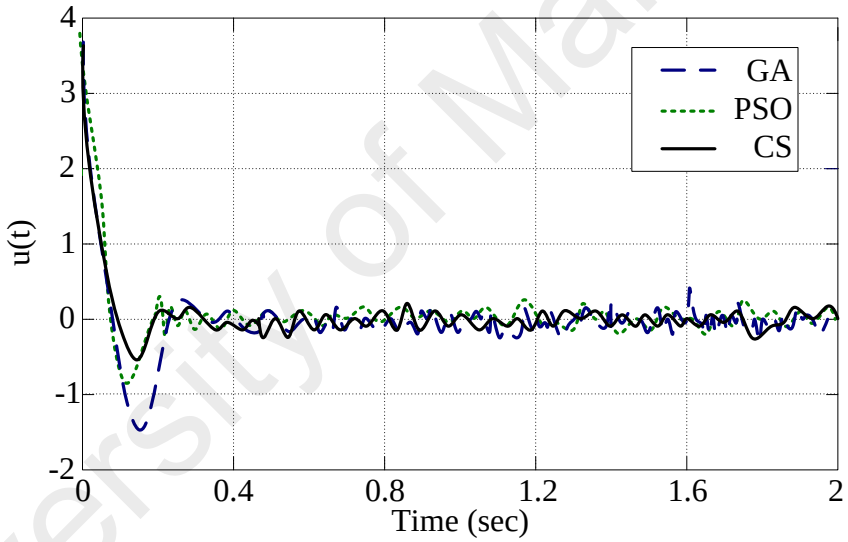

(c) Output of the outer controller

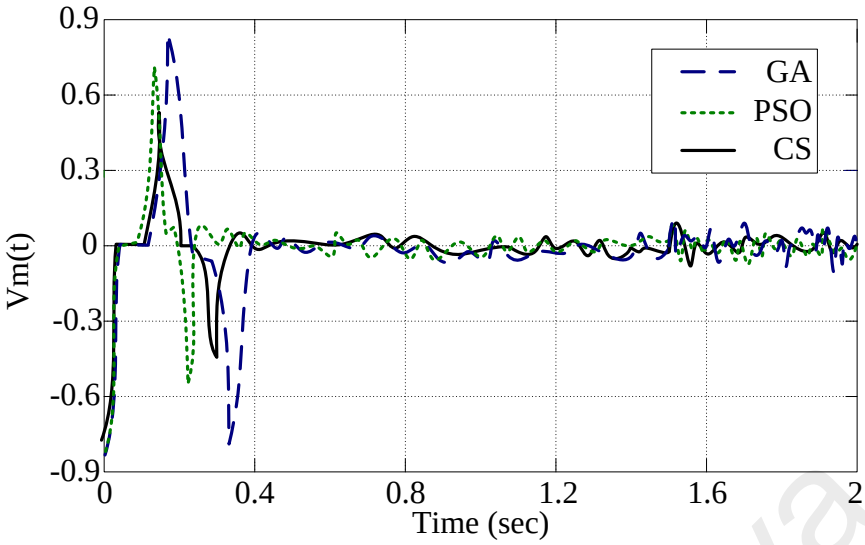

(d) Output of the inner controller

Figure 5.26: Disturbance rejection analysis for cascade optimized IT2FPIDC with $\gamma = 1$

Table 5.8 Comparative Analysis of results for disturbance rejection ability of optimized cascade IT2FPIDC

		GA based	PSO based	CS based
t_r(Sec)	Pendulum(α)	0.89	0.52	0.51
	Arm(ϕ)	0.48	0.37	0.23
t_s(Sec)	Pendulum(α)	1.52	1.36	1.32
	Arm(ϕ)	2.90	2.57	1.62
E_{ss}	Pendulum(α)	0.0092	0.0090	0.0085
	Arm(ϕ)	0.0096	0.0089	0.0088
M_p(%)	Pendulum(α)	0.70°	0.61°	0.19°
	Arm(ϕ)	4.28°	3.41°	2.75°
$Coast$		0.340	0.350	0.212

5.3.5 Trajectory tracking control for optimized cascade T1FPIDC

Similar to optimized cascade T1FPIDC, the best simulation results for RIP trajectory tracking control of optimized cascade IT2FPIDC for $\gamma = 1$ is shown in Figure 5.27 (a) and (b) for pendulum angle and arm angle respectively. Also, the best simulation result for RIP trajectory tracking control by optimized cascade IT2FPIDC for $\gamma = 1.5$ is presented in Figure 5.28 (a) and (b) for pendulum angle and arm angle respectively. It can be observed from both Figure 5.27 (a) and 5.28 (a) that the CS based cascade IT2FPIDC reaches the set point quickly compared with the GA based and PSO based cascade IT2FPIDC. The detail comparative performance is presented in Table 5.9. It can be seen from Table5.9 that the CS based cascade IT2FPIDC have some improved performance in terms of t_r, t_s, M_p and t_d. Also, comparing the performance of optimized cascade IT2FPIDC and optimized cascade T1FPIDCThe pendulum it can be seen based on the results in Table 5.4 and 5.9 that the optimized cascade IT2FPIDC exhibit a better

results in all the corresponding performance measures and corresponding optimization algorithms. This is likely due to the extra DOF that is present in IT2FPIDC.

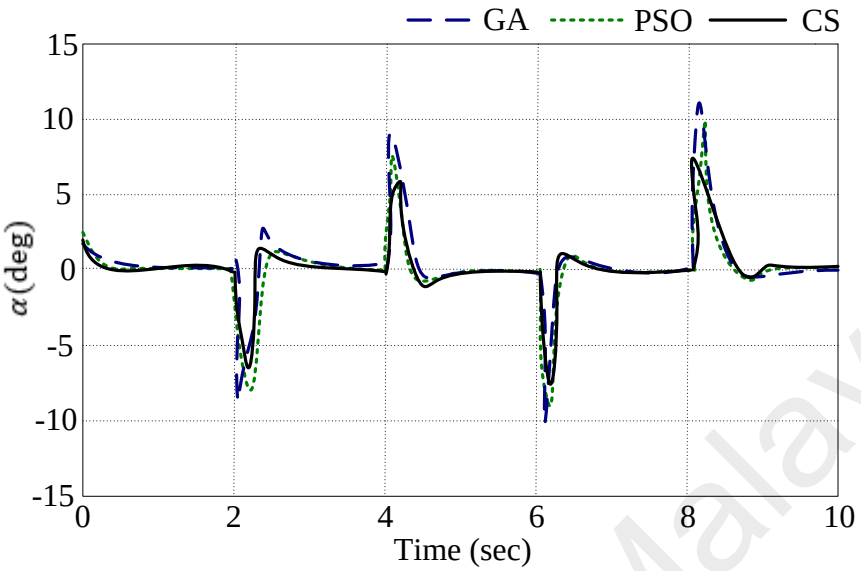

(a) Pendulum angle

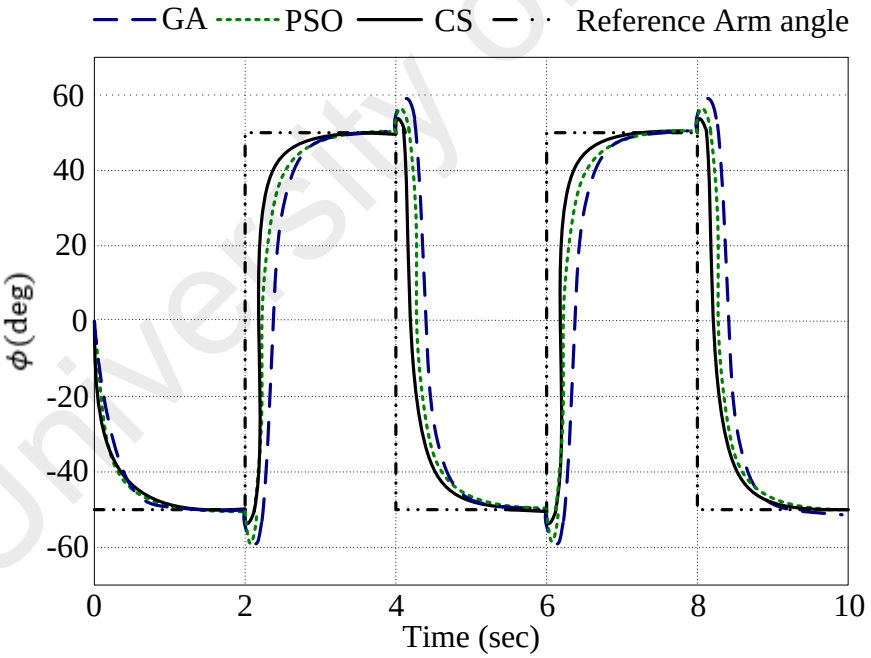

(b) Arm angle

Figure 5.27: Optimized Cascade IT2FPIDC simulation result for trajectory tracking control $\gamma = 1$

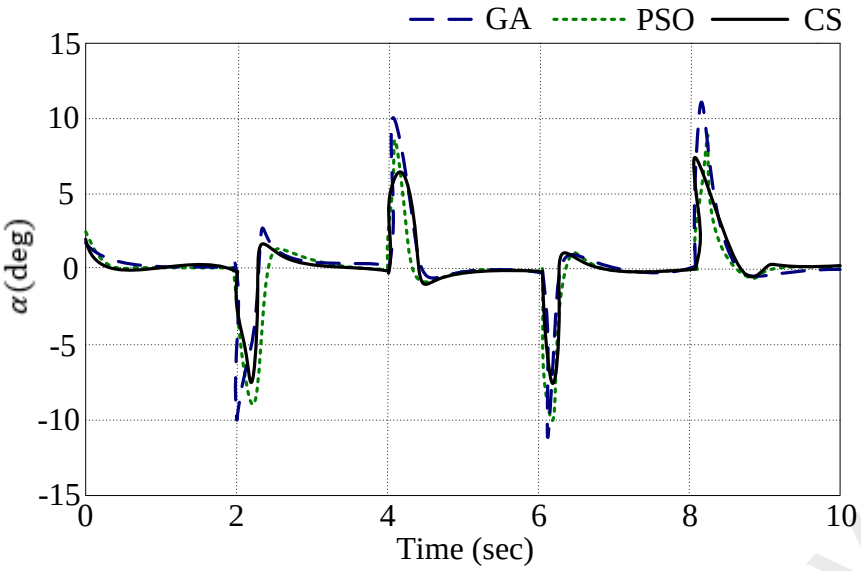

(a) Pendulum angle

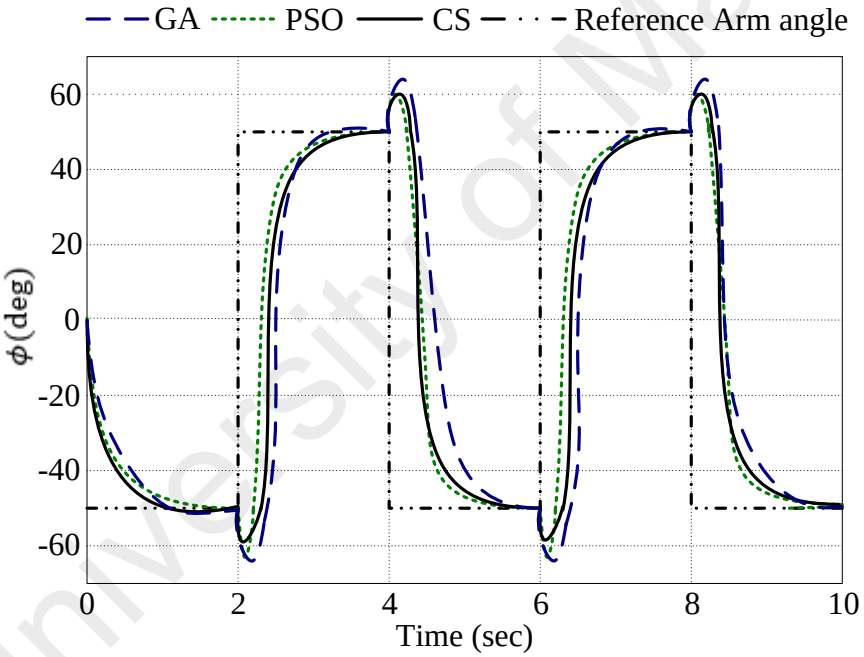

(b) Arm angle

Figure 5.28: Optimized Cascade IT2FPIDC simulation result for trajectory tracking control $\gamma = 1.5$

Table 5.9 Comparative trajectory tracking results for optimized cascade IT2FPIDC (Simulation)

		Based on GA		**Based on PSO**		**Based on CS**	
	γ	1	1.5	1	1.5	1	1.5
t_r(Sec)	Pendulum(α)	0.44	0.43	0.38	0.44	0.38	0.37
	Arm(ϕ)	0.42	0.39	0.40	0.35	0.30	0.26
t_s(Sec)	Pendulum(α)	0.93	1.09	0.97	1.18	0.75	0.86
	Arm(ϕ)	1.04	1.22	1.03	1.19	0.97	1.08
t_d(Sec)	Pendulum(α)	0.55	0.61	0.50	0.54	0.47	0.48
	Arm(ϕ)	0.50	0.54	0.45	0.49	0.35	0.37
E_{ss}	Pendulum(α)	0	0	0	0	0	0
	Arm(ϕ)	0	0	0	0	0	0
M_p(%)	Pendulum(α)	1.64	1.75	1.56	1.53	1.45	1.57
	Arm(ϕ)	5.2	7.1	3.7	5.4	2.2	5.1

5.4 Experimental Validation

The CS-based controllers were proven in real time because in the simulation analysis CS based controllers appear to be better with respect to all the performance index considered to GA-based and CS based. It was stated in the following literature (Castillo & Cervantes, 2014; Hassanzadeh & Mobayen, 2011; Oh, Kim, & Pedrycz, 2012) that whenever the best-simulated controller is validated in the real experiment the other controller are also validated.

The experimental result that validate the simulation results are presented in this section. This include the stabilization control, trajectory tracking control and disturbance rejection analysis. All the results were found for $\gamma = 1$ for both CS based IT2FPIDC and

CS based T1FPIDC. The CS based controllers and weighing factor $\gamma = 1$ are choosed for validation because, in the simulation studies they show the better performance than their comparatives.

5.4.1 Stabilization control (Experiments)

The experimental results that compared the proposed CS based optimized cascade IT2FPIDC, CS based optimized cascade T1FPIDC and conventional energy-based controller for pendulum angle and arm are shown in Figure 5.29 (a) and (b) respectively. The time starts from zero in order to show the performances from the swing-up to the balance mode. Looking at the real plant's results, some initial oscillations were noticed which is due to the swing motion needed to bring the pendulum from stable position to the vertically unstable position. Also, the two controllers (i.e. CS based optimized cascade IT2FPIDC and CS based optimized cascade T1FPIDC) manifest the considerable level of robustness. On the other hand, the conventional energy-based controller manifests many oscillations before it becomes stable. The time taken for conventional energy-based to reach the steady state is 4.6 seconds which is higher compared to the CS based optimized cascade IT2FPIDC with 2.2 seconds and CS based optimized cascade T1FPIDC with 2.5 seconds.

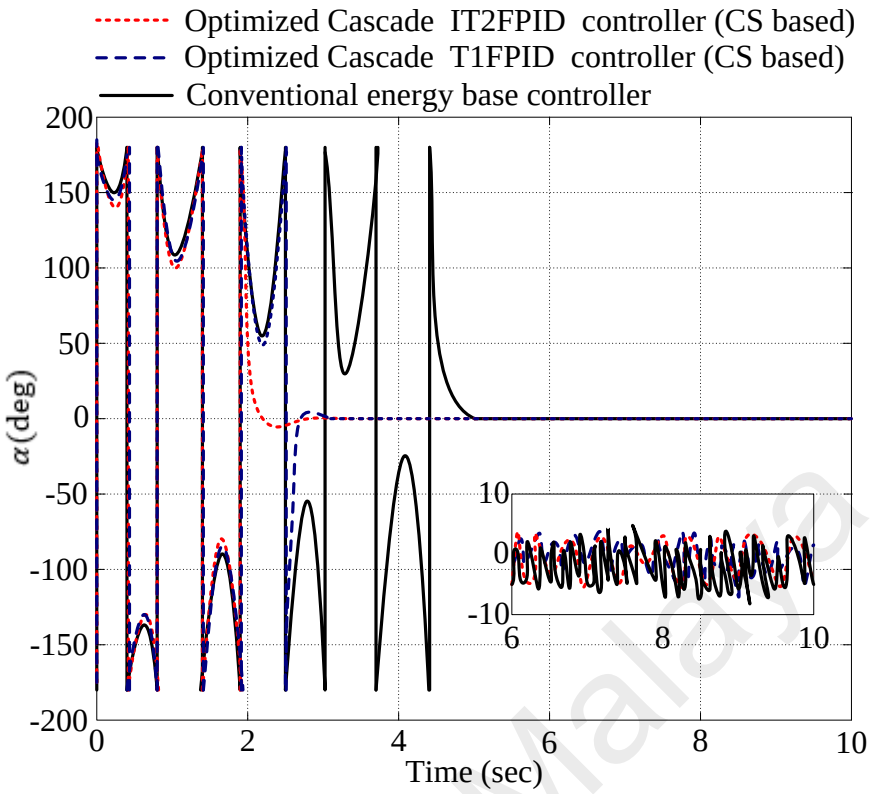

(a) Pendulum angle

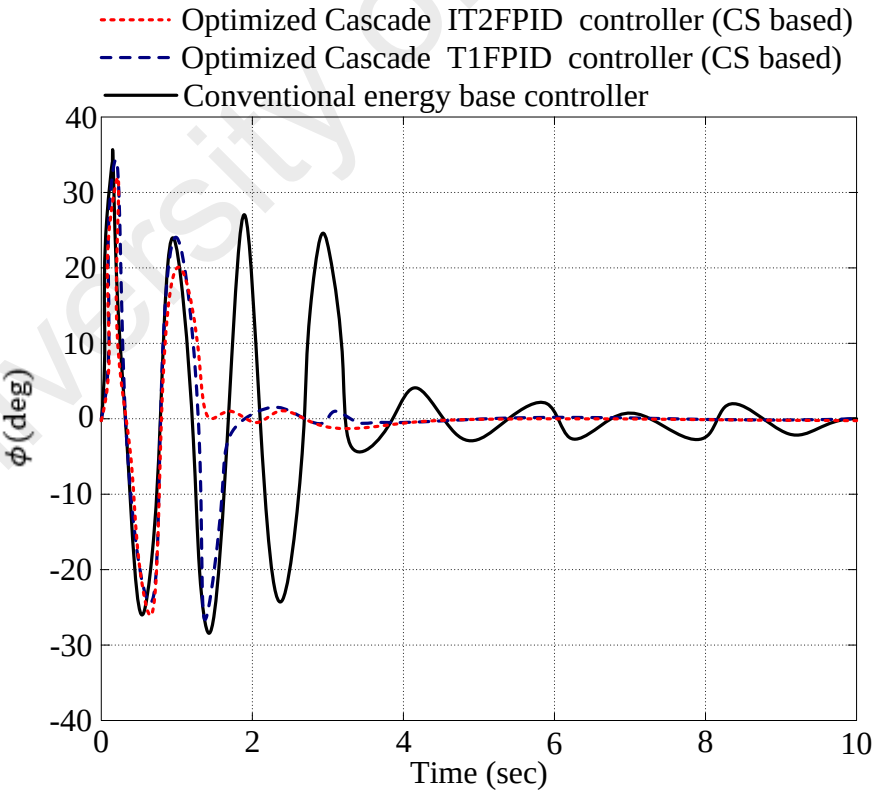

(b) Arm angle

Figure 5.29: Experimental results for stabilization control

5.4.2 Trajectory tracking control (Experiments)

A square wave with an amplitude of $\pm 40°$ is employed as the reference signal that should be followed by the arm. Figure 5.30 (a) and (b) shows the response for the pendulum angle and arm angle respectively. It can be seen that both optimized cascade CS based IT2FPIDC and T1FPIDC can smoothly make the motor shaft to trace the desired trajectories while kept the pendulum stable in an upright position (around 0°) and continuously compensating the necessary mechanical disturbances such as friction.

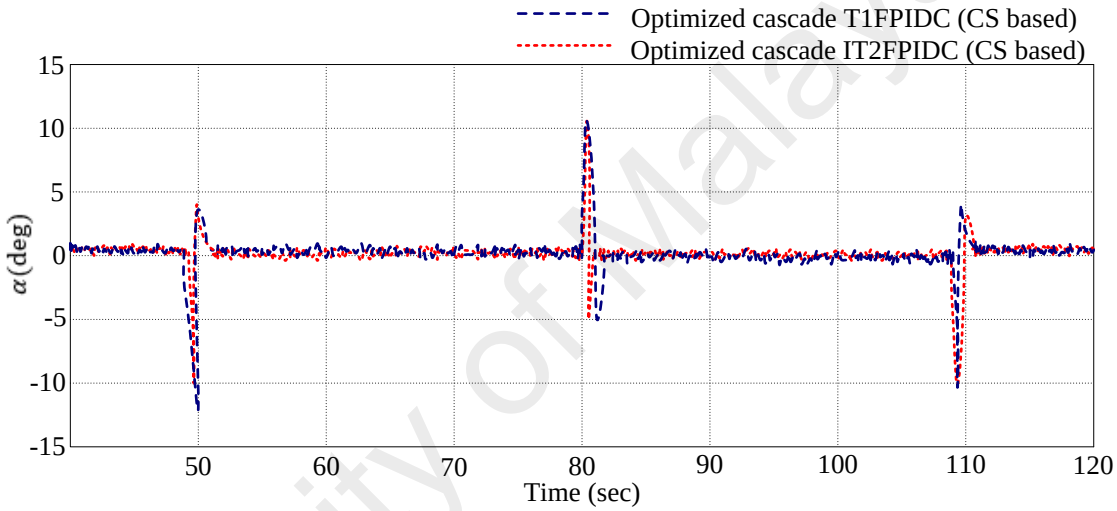

(a) Pendulum angle

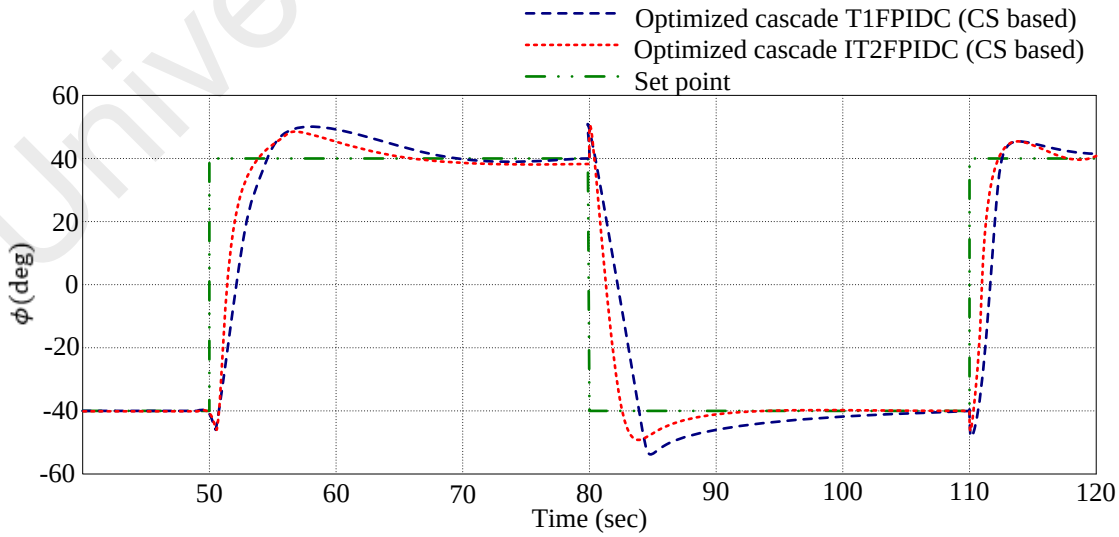

(b) Arm angle

Figure 5.30 Experimental result for trajectory tracking control comparing optimized cascade CS based IT2FPIDC and T1FPIDC

5.4.3 Disturbance rejection analysis (Experiments)

The internal noise and external disturbances are added to the system in the real world to test for the robustness of the proposed cascade optimized CS based IT2FPIDC T1FPIDC. A load of length 0.1685meter and mass of 0.0635 kg mass was added to the pendulum as shown in figure 5.11. Also, the white noise of 0.00634 power and 10% parameter value changes is added to the process output (feedback) as shown in Figure 5.11. The experimental results for trajectory tracking control of RIP system is shown in Figure 5.31 (a) and (b) for pendulum and arm respectively. The experimental and simulation results indicated that the effectiveness and robustness of the proposed optimized cascade IT2FPIDC with respect to load disturbances, parameter variation and noise effects has been improved over the optimized cascade T1FPIDC. Though there is some oscillation between in arm angle and in pendulum angle which are not present in the experimental results for trajectory tracking control without disturbances but still both controllers are able to make the motor shaft to trace the desired trajectories while kept the pendulum stable in upright position (around 0°) and continuously compensating the necessary mechanical disturbances as well as the introduced disturbances with small vibrations. In summary, it can be concluded based on the evidence emanated from the experiment results, that the optimized cascade IT2FPIDC has advanced the performance of the cascade optimized T1FPIDC and conventional energy-based controller on the RIP. The superior performance of optimized cascade IT2FPIDC over the optimized cascade T1FPIDC in the presence of disturbances and no disturbed condition can be seen from Table 5.10.

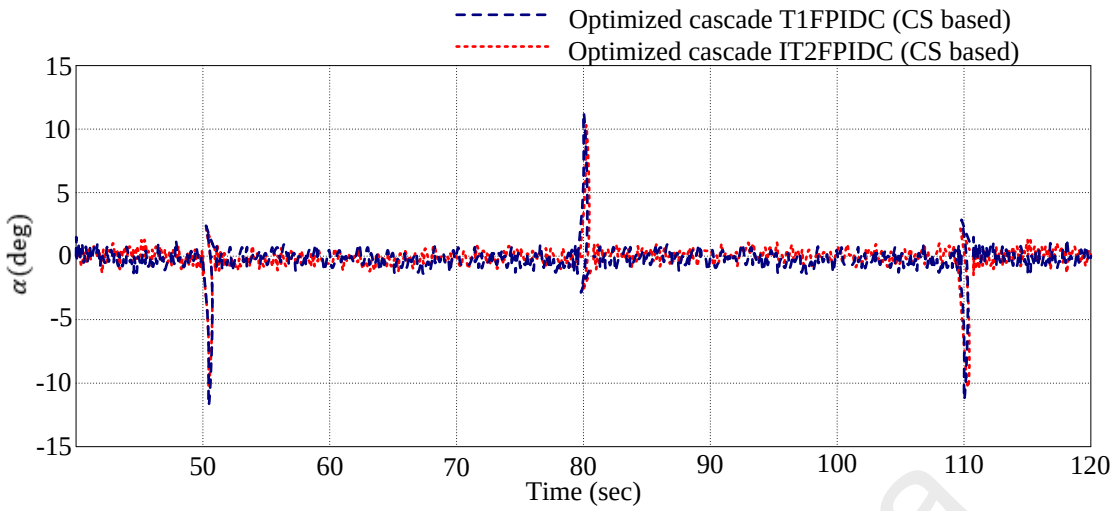

(a) Pendulum angle

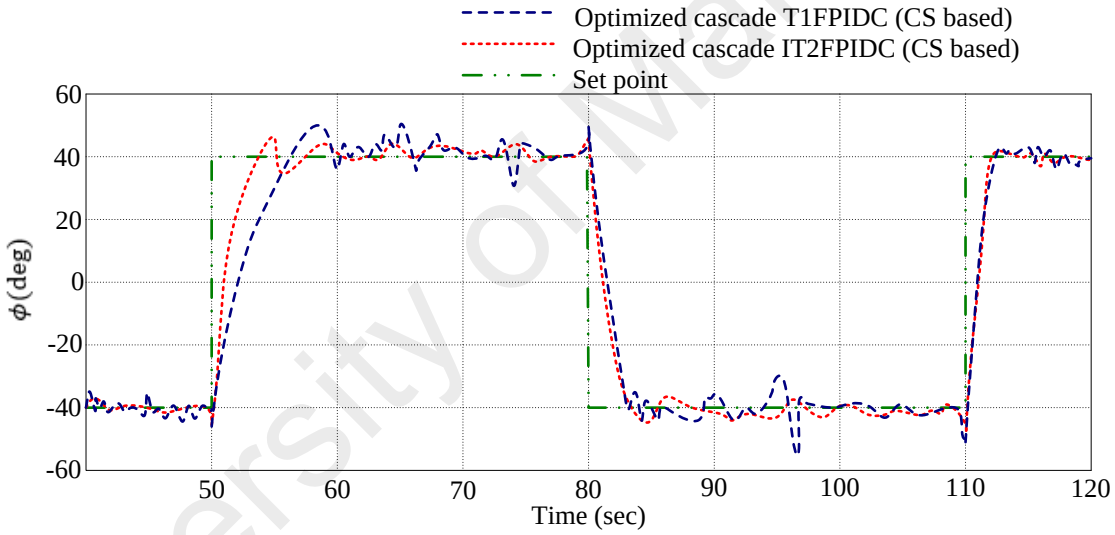

(b) Arm angle

Figure 5.31 Experimental result for disturbed trajectory tracking control comparing optimized cascade CS based IT2FPIDC and T1FPIDC

Table 5.10 Comparative trajectory tracking results for optimized cascade CS based IT2FPIDC and T1FPIDC (Experiment)

Controllers	Disturbances	t_r(sec)	t_s(sec)	t_d(sec)	M_p%	E_{ss}	Cost
IT2FPIDC	No disturbance	1.64	5.16	1.48	10.15	0	3.855
	With disturbance	1.89	6.94	1.66	10.55	0	4.263
T1FPIDC	No disturbance	2.12	7.81	1.39	12.37	0	4.956
	With disturbance	2.39	8.92	1.69	13.28	0	5.398

CHAPTER 6: CONCLUSION AND RECOMMENDATIONS

6.1 Introduction

It has been demonstrated in several research that IT2FLCs have the potential to properly handle high levels of uncertainties and nonlinearities to produce an improved control performance compared to its T1FLCs counterpart. However, finding the appropriate values of parameters and structure of IT2FLCs is a challenging and complex task. The main aim of this study is to examine the application of meta heuristic optimization algorithm methods in designing the IT2FLCs. Also to investigate the advantages of IT2FLC over T1FLC. Considering the higher number of parameters to be optimized in IT2FC, the CS method was employed because of its high convergence speed and less computational cost. The GA and PSO were also used for optimization to enable the comparisons in their performances with CS since GA is the most well-established optimization algorithm in the literature and PSO is also a stochastic global search algorithm. The performances of optimization of the IT2FPIDC in cascade structure is compared with the performances of optimization of the T1FPIDC in cascade structure based on the cost function that comprised four performance measures namely steady state error (E_{ss}), settling time (t_s), rise time (t_r), maximum overshoot (M_p).

The conclusions based on the research objectives and research question would be presented in this section.

6.2 Conclusion

Both nonlinear and linear mathematical models of RIP have been realized using Newton-Euler-Lagrange method and Kane's method. The Matlab model of the developed model for RIP are realized. This was done to exploits the advantages and disadvantages of these modeling methods and to have the accurate model of RIP that would be used to

test the proposed controllers. The RIP system is highly nonlinear, unstable, under-actuated and non-minimum phase system dynamics.

In comparisons with GA and PSO based design method, the obtained results indicated that the CS based design strategy could achieve advanced quality solutions with fewer computational time. For example, for IT2FPIDC, the best computational time for CS, PSO and GA are 196.33minutes, 294.55 minutes and 453.70 minutes respectively. Hence the CS can be used in future designed of more complex IT2FLCs with a higher number of inputs/outputs parameters in the applications that require some excellent results of optimization in the fastest frame of time. To clearly indicate the advantage of FOU present in IT2FPIDC on the response of the system, the rule-based, rule weighing factors and the consequent MFs parameters were kept fixed. Only the scaling factors and the parameters of the antecedent MFs parameters are optimized. The same thing was done to the T1FPIDC for fair comparisons. Furthermore, both experimental and simulation results showed that the optimized cascade IT2FPIDC outperforms the optimized cascade T1FPIDC with respect to the E_{ss}, t_s, t_r, and M_p irrespective of the optimization method used. For example, the performance of optimized cascade IT2FPIDC in present of disturbances have some improvement between 6.1% to 33.3%, 5.7% to 35.2% and 6.6% to 20.8% in term of t_r,t_s, and E_{ss} respectively over the optimized cascade T1FPIDC counterpart. This is likely due to the advantage of FOU present in IT2FPIDC which give it an ability to implement highly sophisticated control that cannot be handle by T1FPIDC with the same rule based as stated in many literatures.

The proposed controllers were implanted in effective and simple cascade architecture that has also been developed in this research. The proposed GA based PSO based and CS based IT2FPIDC and T1FPIDC were evaluated in cascade structures for stabilization and

trajectory tracking control of RIP system using simulation studies before conducting the real-world experiments for validation of the simulation results.

The experiments were performed on Quanser SRV02 RIP set up. Two US Digital S1 single-ended optical shaft encoder that can offer a high resolution of 1024 lines per revolution was used for measuring the pendulum angle and arm angle. The VoltPAQ-X1 power amplifier and Q2-USB data acquisition device were used to evaluate the performance of the proposed IT2FPIDC in this research.

The results from experiments and simulations support the effectiveness and robustness of the proposed optimized cascade IT2FPIDC design method. It has been demonstrated that the reference tracking and the disturbances rejection performance of the optimized cascade IT2FPIDC is better in the presence of uncertainties, parameter variation and noise, especially in experiments, compared with optimized cascade T1FPIDC. The experimental results agreed with the simulation results shown which justifies the availability of the proposed nonlinear model of RIP and confirm the performance of the proposed methods. The experimental results also validate the simulation results. The detailed on the limitations of the state of art controllers applied to RIP are discussed.

Since the RIP systems perform in an extensive range of real life applications like aerospace systems, robotics, marine systems, mobile systems, flexible systems, pointing control, and locomotive systems and simplified industry crane application, the proposed control strategy can be regarded as a promising strategy for controlling such kind of systems especially in the presence of noise and disturbances.

6.3 Recommendation

The recommendation for future research divided in two namely proposed controller and the test benchmark.

6.3.1 Proposed controller

In future work, the optimization parameters would be extended to both antecedent and consequent MFs parameters, scaling factors, inference mechanism, fuzzy rule, type of MFs, fuzzy linguistic set and input/output variables to the fuzzy inference. This may need the optimization method with lower complexity in computation, faster convergence speed and global optimization such as hybrid optimization and some other optimization techniques that are yet to be applied in T2FLC design like Grid search, genetic programming, harmony computing, membrane computing, bat algorithm.

It was also intended to apply the GT2FLC in future work since the FLC are the parametric controller, and GT2FLC has more design parameter than IT2FLC. Therefore, it has extra DOF in design more sophisticated controller than IT2FLCs. That is to say, GT2FLC has the potential to provide better and certainly not worst control performance over IT2FCs.

The comparisons with another controller with extra DOF would be made so as to clearly understand the reason why the T2FLC is having good performance in the presence of noise and uncertainties. Is it because of extra DOF? Or it is in the way it deals with noise and uncertainties presents in real time implementation. In this context, the T1FLC tuning with error based rule Weighting Adjustment (EBW) would be investigated in future work. The structure of self-tuning in EBW adjust the weight of each rule online on the signal error. This mean, additional DOF is produced by taking the weight of the rule as tuning parameters.

6.3.2 Testing benchmark

The controller that is intelligent enough to implement all the control objective is intended to be produced in the future work. This may avoid the oscillation due to the switching between different controllers in RIP. We would like to propose more general

inverted pendulum named Two Wheeled Rotary Inverted Pendulum (TWRIP). The TWRIP has all the futures in RIP with a two-wheeled robot. It is 5 DOF consisting of all what is in RIP and all that is in two-wheeled robot as shown in figure 14. For the stabilization, the TWRIP will need two controllers; one to stabilize the RIP pendulum and the other to stabilize the whole body of TWRIP on the two tires. Also, the two trajectory tracking control may be applied; one for the navigation of the whole TWRIP and the other for the RIP arm. The TWRIP can be used for testing intelligent and complex controllers. The TWRIP have many real life applications particularly in an industry where a robot that can move and transport the load in the form of crane is needed. It can also find application in the military sector where the transportation and pointing are needed. The development of TWRIP model is an open research in this field of research.

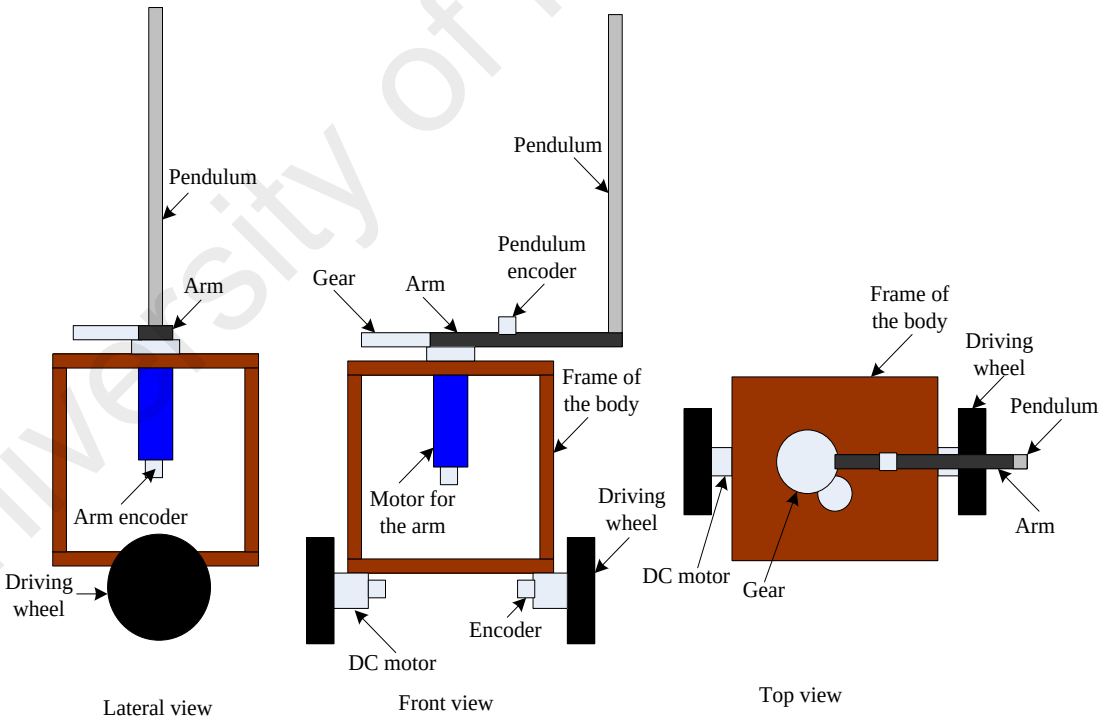

Figure 6.1: Proposed TWRIP

REFERENCES

Abdelaziz, A., & Ali, E. (2015). Cuckoo Search algorithm based load frequency controller design for nonlinear interconnected power system. *International Journal of Electrical Power & Energy Systems, 73*, 632-643.

Acosta, J. (2010). Furuta's Pendulum: A Conservative Nonlinear Model for Theory and Practise. *Mathematical Problems in Engineering, 2010*.

Agrawal, R., & Mitra, R. (2013) Adaptive neuro fuzzy inference structure controller for rotary inverted pendulum. *Vol. 174 AISC. Advances in Intelligent Systems and Computing* (pp. 1163-1170).

Aguilar-Avelar, C., & Moreno-Valenzuela, J. (2014). *A feedback linearization controller for trajectory tracking of the Furuta pendulum.* Paper presented at the Proceedings of the American Control Conference.

Aguilar-Avelar, C., & Moreno-Valenzuela, J. (2015). A composite controller for trajectory tracking applied to the Furuta pendulum. *ISA Transactions*.

Ahangar-Asr, H., Teshnehlab, M., Mansouri, M., & Pazoki, A. (2011). *A hybrid strategy for the control of Rotary Inverted Pendulum.* Paper presented at the Electrical and Control Engineering (ICECE), 2011 International Conference on.

Al-Jodah, A., Zargarzadeh, H., & Abbas, M. K. (2013). Experimental Verification and Comparison of Different Stabilizing Controllers for a Rotary Inverted Pendulum. *2013 Ieee International Conference on Control System, Computing and Engineering (Iccsce 2013)*, 417-423.

Aliasghary, M., Eksin, I., Guzelkaya, M., & Kumbasar, T. (2013). A design methodology and analysis for interval type-2 fuzzy PI/PD controllers. *Int. J. Innov. Comput. Inf. Control, 9*(10), 4215-4230.

Allawi, Z. T., & Abdalla, T. Y. (2014, 2-5 Sept. 2014). *A PSO-optimized type-2 fuzzy logic controller for navigation of multiple mobile robots.* Paper presented at the Methods and Models in Automation and Robotics (MMAR), 2014 19th International Conference On.

Almaraashi, M., & Hedar, A. R. (2014, July 30 2014-Aug. 1 2014). *Optimization of interval type-2 fuzzy logic systems using tabu search algorithms.* Paper presented at the Nature and Biologically Inspired Computing (NaBIC), 2014 Sixth World Congress on.

Alt, B., Hartung, C., & Svaricek, F. (2011). *Robust fuzzy cascade control revised: application to the rotary inverted pendulum.* Paper presented at the Control & Automation (MED), 2011 19th Mediterranean Conference on.

Altpeter, F. (1999). Friction modeling, identification and compensation.

Antonio-Cruz, M., Silva-Ortigoza, R., Sandoval-Gutierrez, J., Merlo-Zapata, C. A., Taud, H., Marquez-Sanchez, C., & Hernandez-Guzman, V. M. (2015). *Modeling,*

simulation, and construction of a furuta pendulum test-bed. Paper presented at the Electronics, Communications and Computers (CONIELECOMP), 2015 International Conference on.

Apkarian, J., Levis, M & Gurocak H. (2011) *User manual SRV02 rotary servo based unit, set up and configration.* Quanser innovate educate 1-23

Aracil, J., Acosta, J. Á., & Gordillon, F. (2013). A nonlinear hybrid controller for swinging-up and stabilizing the Furuta pendulum. *Control Engineering Practice, 21*(8), 989-993. doi:10.1016/j.conengprac.2013.04.001

Ashrafiuon, H., & Whitman, A. M. (2012). Closed-loop dynamic analysis of a rotary inverted pendulum for control design. *Journal of Dynamic Systems, Measurement and Control, Transactions of the ASME, 134*(2). doi:10.1115/1.4005358

Astolfi, A., Ortega, R., & Venkatraman, A. (2010). A globally exponentially convergent immersion and invariance speed observer for mechanical systems with non-holonomic constraints. *Automatica, 46*(1), 182-189.

Astudillo, L., Melin, P., & Castillo, O. (2012, 5-9 Nov. 2012). *Nature optimization applied to design a type-2 fuzzy controller for an autonomous mobile robot.* Paper presented at the Nature and Biologically Inspired Computing (NaBIC), 2012 Fourth World Congress on.

Astudillo, L., Melin, P., & Castillo, O. (2013). Nature Inspired Chemical Optimization to Design a Type-2 Fuzzy Controller for a Mobile Robot. *Proceedings of the 2013 Joint Ifsa World Congress and Nafips Annual Meeting (Ifsa/Nafips)*, 1423-1428.

Awtar, S., King, N., Allen, T., Bang, I., Hagan, M., Skidmore, D., & Craig, K. (2002). Inverted pendulum systems: rotary and arm-driven-a mechatronic system design case study. *Mechatronics, 12*(2), 357-370.

Azar, A. T., & Serrano, F. E. (2015) Adaptive sliding mode control of the furuta pendulum. *Vol. 576. Studies in Computational Intelligence* (pp. 1-42).

Baklouti, N., & Alimi, A. M. (2013, 15-17 Dec. 2013). *Real time PSO based adaptive learning type-2 fuzzy logic controller design for the iRobot Create robot.* Paper presented at the Individual and Collective Behaviors in Robotics (ICBR), 2013 International Conference on.

Barbosa, D. I., Castillo, J. S., & Combita, L. F. (2011). *Rotary inverted pendulum with real time control.* Paper presented at the Robotics Symposium, 2011 IEEE IX Latin American and IEEE Colombian Conference on Automatic Control and Industry Applications (LARC).

Bedford, A., Fowler, W. L., & Ahmad, Y. (2008). *Engineering mechanics: dynamics*: Pearson Prentice Hall.

Bellman, R. E., & Zadeh, L. A. (1970). Decision-making in a fuzzy environment. *Management science, 17*(4), B-141-B-164. Retrieved from

Bemporad, A., Morari, M., Dua, V., & Pistikopoulos, E. N. (2002). The explicit linear quadratic regulator for constrained systems. *Automatica, 38*(1), 3-20.

Bi, Y. R., Srinivasan, D., Lu, X. B., & Sun, Z. (2013). Single Intersection Signal Control Based on Type-2 Fuzzy Logic. *Proceedings of the 2013 Ieee Symposium on Computational Intelligence in Vehicles and Transportation Systems (Civts)*, 25-31.

Brown, C. T., Liebovitch, L. S., & Glendon, R. (2007). Lévy flights in Dobe Ju/'hoansi foraging patterns. *Human Ecology, 35*(1), 129-138.

Casanova, V., Alcaína, J., Salt, J., Pizá, R., & Cuenca, Á. (2015). Control of the rotary inverted pendulum through threshold-based communication. *ISA Transactions*. doi:10.1016/j.isatra.2016.01.009

Castillo, O. (2012). Introduction to Type-2 Fuzzy Logic Control *Type-2 Fuzzy Logic in Intelligent Control Applications* (pp. 3-5): Springer.

Castillo, O., & Cervantes, L. (2014). Genetic Design of Optimal Type-1 and Type-2 Fuzzy Systems for Longitudinal Control of an Airplane. *Intelligent Automation and Soft Computing, 20*(2), 213-227. doi:Doi 10.1080/10798587.2014.902913

Castillo, O., Martinez-Marroquin, R., Melin, P., Valdez, F., & Soria, J. (2012). Comparative study of bio-inspired algorithms applied to the optimization of type-1 and type-2 fuzzy controllers for an autonomous mobile robot. *Information Sciences, 192*, 19-38. doi:DOI 10.1016/j.ins.2010.02.022

Castillo, O., & Melin, P. (2012). Optimization of type-2 fuzzy systems based on bio-inspired methods: A concise review. *Information Sciences, 205*, 1-19. Retrieved from doi:10.1016/j.ins.2012.04.003

Castillo, O., & Melin, P. (2014). A review on interval type-2 fuzzy logic applications in intelligent control. *Information Sciences, 279*, 615-631. doi:DOI 10.1016/j.ins.2014.04.015

Cervantes, L., & Castillo, O. (2013). Statistical Comparison of Type-1 and Type-2 Fuzzy Systems design with Genetic Algorithms in the Case of Three Tank Water Control. *Proceedings of the 2013 Joint Ifsa World Congress and Nafips Annual Meeting (Ifsa/Nafips)*, 1056-1061.

Cervantes, L., & Castillo, O. (2015). Type-2 fuzzy logic aggregation of multiple fuzzy controllers for airplane flight control. *Information Sciences, 324*, 247-256.

Chakravarty, S., & Dash, P. K. (2012). A PSO based integrated functional link net and interval type-2 fuzzy logic system for predicting stock market indices. *Applied Soft Computing, 12*(2), 931-941. doi:DOI 10.1016/j.asoc.2011.09.013

Chan, R. P. M., Stol, K. A., & Halkyard, C. R. (2013). Review of modelling and control of two-wheeled robots. *Annual Reviews in Control, 37*(1), 89-103.

Chandran, D., Krishna, B., George, V. I., & Thirunavukkarasu, I. (2015). *System Identification of Rotary Double Inverted Pendulum using Artificial Neural*

Networks. Paper presented at the 2015 International Conference on Industrial Instrumentation and Control, ICIC 2015.

Chaparro, B., Thuillier, S., Menezes, L., Manach, P.-Y., & Fernandes, J. (2008). Material parameters identification: Gradient-based, genetic and hybrid optimization algorithms. *Computational Materials Science, 44*(2), 339-346. Retrieved from

Chen, W.-H., Ballance, D. J., Gawthrop, P. J., & O'Reilly, J. (2000). A nonlinear disturbance observer for robotic manipulators. *Industrial Electronics, IEEE Transactions on, 47*(4), 932-938.

Chen, Y.-F., & Huang, A.-C. (2014). Adaptive control of rotary inverted pendulum system with time-varying uncertainties. *Nonlinear Dynamics, 76*(1), 95-102.

Chiluvuri, N. T., Harshe, O. A., Patterson, C. D., & Baumann, W. T. (2015). *Using heterogeneous computing to implement a trust isolated architecture for cyber-physical control systems.* Paper presented at the CPSS 2015 - Proceedings of the 1st ACM Workshop on Cyber-Physical System Security, Part of ASIACCS 2015.

Chiou, J.-S., & Liu, M.-T. (2009). Numerical simulation for fuzzy-PID controllers and helping EP reproduction with PSO hybrid algorithm. *Simulation Modelling Practice and Theory, 17*(10), 1555-1565.

Chou, K., & Chen, Y. (2014). *Energy based swing-up controller design using phase plane method for rotary inverted pendulum.* Paper presented at the Control Automation Robotics & Vision (ICARCV), 2014 13th International Conference on.

Civicioglu, P., & Besdok, E. (2013). A conceptual comparison of the Cuckoo-search, particle swarm optimization, differential evolution and artificial bee colony algorithms. *Artificial Intelligence Review, 39*(4), 315-346.

Clerc, M., & Kennedy, J. (2002). The particle swarm - explosion, stability, and convergence in a multidimensional complex space. *Evolutionary Computation, IEEE Transactions on, 6*(1), 58-73. doi:10.1109/4235.985692

Cordón, O., Herrera, F., Gomide, F., Hoffmann, F., & Magdalena, L. (2001). *Ten years of genetic fuzzy systems: current framework and new trends.* Paper presented at the IFSA World Congress and 20th NAFIPS International Conference, 2001. Joint 9th.

Cortes-Rios, J. C., Gomez-Ramirez, E., Ortiz-de-la-Vega, H. A., Castillo, O., & Melin, P. (2014). Optimal design of interval type 2 fuzzy controllers based on a simple tuning algorithm. *Applied Soft Computing, 23*, 270-285. doi:DOI 10.1016/j.asoc.2014.06.015

Dang, Q. V., Allouche, B., Vermeiren, L., Dequidt, A., & Dambrine, M. (2014). *Design and implementation of a robust fuzzy controller for a rotary inverted pendulum using the Takagi-Sugeno descriptor representation.* Paper presented at the Computational Intelligence in Control and Automation (CICA), 2014 IEEE Symposium on.

Dash, P., Saikia, L. C., & Sinha, N. (2015). Comparison of performances of several FACTS devices using Cuckoo search algorithm optimized 2DOF controllers in multi-area AGC. *International Journal of Electrical Power & Energy Systems, 65*, 316-324.

Davies, N. B. (2010). *Cuckoos, cowbirds and other cheats*: A&C Black.

De Jong, K. (1988). Learning with genetic algorithms: An overview. *Machine Learning, 3*(2-3), 121-138.

Dehuri, S., Ghosh, S., & Coello, C. A. C. (2009). An Introduction to Swarm Intelligence for Multi-objective Problems in Data Mining. In Satchidananda Dehuri, Susmita Ghosh, & C. A. C. Coello (Eds.), *Swarm Intelligence for Multi-objective Problems in Data Mining*: Springer.

Dongrui, W. (2013). Approaches for Reducing the Computational Cost of Interval Type-2 Fuzzy Logic Systems: Overview and Comparisons. *Fuzzy Systems, IEEE Transactions on, 21*(1), 80-99.

Doostparast Torshizi, A., & Fazel Zarandi, M. H. (2014). Alpha-plane based automatic general type-2 fuzzy clustering based on simulated annealing meta-heuristic algorithm for analyzing gene expression data. *Computers in Biology and Medicine*. Retrieved from http://www.ncbi.nlm.nih.gov/pubmed/25035233 doi:10.1016/j.compbiomed.2014.06.017

Driver, J., & Thorpe, D. (2004). Design, build and control of a single/double rotational inverted pendulum. *The University of Adelaide, School of Mechanical Engineering, Australia, 4*.

Dulikravich, G. S., & Colaço, M. J. (2015). Hybrid Optimization Algorithms and Hybrid Response Surfaces *Advances in Evolutionary and Deterministic Methods for Design, Optimization and Control in Engineering and Sciences* (pp. 19-47): Springer.

Eberhart, R. C., & Kennedy, J. (1995). *A new optimizer using particle swarm theory.* Paper presented at the Proceedings of the sixth international symposium on micro machine and human science.

Eberhart, R. C., & Shi, Y. (2001). *Particle swarm optimization: developments, applications and resources.* Paper presented at the Evolutionary Computation, 2001. Proceedings of the 2001 Congress on.

El-Nagar, A. M., & El-Bardini, M. (2014). Interval type-2 fuzzy neural network controller for a multivariable anesthesia system based on a hardware-in-the-loop simulation. *Artificial Intelligence in Medicine, 61*(1), 1-10. doi:DOI 10.1016/j.ar tm ed.2 01 4.03.002

Elazim, S. A., & Ali, E. (2016). Optimal Power System Stabilizers design via Cuckoo Search algorithm. *International Journal of Electrical Power & Energy Systems, 75*, 99-107.

Ernest, P., & Horacek, P. (2011). *Algorithms for control of a rotating pendulum.* Paper presented at the Proceeding of the 19th IEEE Mediterranean Conference on Control and Automation (MED'11). Athens: National Technical University.

Fabbri, T., Fenucci, D., Falasca, S., Gamba, M., & Bicchi, A. (2013, 25-28 June 2013). *Packet-based dynamic control of a Furuta Pendulum over Ethernet.* Paper presented at the Control & Automation (MED), 2013 21st Mediterranean Conference on.

Fairus, M., Mohamed, Z., & Ahmad, M. (2013). *Fuzzy modeling and control of rotary inverted pendulum system using LQR technique.* Paper presented at the IOP Conference Series: Materials Science and Engineering.

Fairus, M., Mohamed, Z., Ahmad, M., & Loi, W. (2015). LMI-based Multiobjective Integral Sliding Mode Control for Rotary Inverted Pendulum System Under Load Variations. *Jurnal Teknologi, 73*(6).

Faradja, P., Qi, G., & Tatchum, M. (2014). *Sliding mode control of a Rotary Inverted Pendulum using higher order differential observer.* Paper presented at the International Conference on Control, Automation and Systems.

Faradja, P., Qi, G., & Tatchum, M. (2014). *Sliding mode control of a Rotary Inverted Pendulum using higher order differential observer.* Paper presented at the Control, Automation and Systems (ICCAS), 2014 14th International Conference on.

Fayek, H. M., Elamvazuthi, I., Perumal, N., & Venkatesh, B. (2014). A controller based on Optimal Type-2 Fuzzy Logic: Systematic design, optimization and real-time implementation. *ISA Transactions, 53*(5), 1583-1591. doi:DOI 10.1016/j.isat ra.2 014.06.001

Feng, G. (2006). A survey on analysis and design of model-based fuzzy control systems. *Fuzzy Systems, IEEE Transactions on, 14*(5), 676-697.

Ferreira, A., Bejarano, F. J., & Fridman, L. M. (2011). Robust control with exact uncertainties compensation: With or without chattering? *Ieee Transactions on Control Systems Technology, 19*(5), 969-975. doi:10.1109/TCST.2010.2064168

Fister Jr, I., Yang, X.-S., Fister, D., & Fister, I. (2014). Cuckoo search: a brief literature review *Cuckoo search and firefly algorithm* (pp. 49-62): Springer.

Fujita, Y., Izutsu, M., & Hatakeyama, S. (2014). *Swing-up and stabilization control of twin furuta pendulums by energy control.* Paper presented at the Proceedings, IECON 2014 - 40th Annual Conference of the IEEE Industrial Electronics Society.

Furuta, K., Yamakita, M., & Kobayashi, S. (1992). Swing-up control of inverted pendulum using pseudo-state feedback. *Proceedings of the Institution of Mechanical Engineers, Part I: Journal of Systems and Control Engineering, 206*(4), 263-269.

Gäfvert, M. (1999). *Dynamic model based friction compensation on the Furuta pendulum.* Paper presented at the Control Applications, 1999. Proceedings of the 1999 IEEE International Conference on.

Gafvert, M., Svensson, J., & Astrom, K. J. (2015). *Friction and friction compensation in the Furuta pendulum.* Paper presented at the European Control Conference, ECC 1999 - Conference Proceedings.

Gaing, Z.-L. (2004). A particle swarm optimization approach for optimum design of PID controller in AVR system. *Energy Conversion, IEEE Transactions on, 19*(2), 384-391.

Gandomi, A. H., Yang, X.-S., & Alavi, A. H. (2013). Cuckoo search algorithm: a metaheuristic approach to solve structural optimization problems. *Engineering with Computers, 29*(1), 17-35.

Gaxiola, F., Melin, P., & Valdez, F. (2013a). Neural Network with Lower and Upper Type-2 Fuzzy Weights using the Backpropagation Learning Method. *Proceedings of the 2013 Joint Ifsa World Congress and Nafips Annual Meeting (Ifsa/Nafips)*, 637-642.

Gaxiola, F., Melin, P., & Valdez, F. (2013b). Type-2 Fuzzy Weight Adjustment for Backpropagation in Prediction Time Series and Pattern Recognition. *Soft Computing Applications in Optimization, Control, and Recognition, 294*, 187-213. doi:Doi 10.1007/978-3-642-35323-9_8

Gaxiola, F., Melin, P., Valdez, F., & Castillo, O. (2013). Optimization of type-2 Fuzzy Weight for Neural Network using Genetic Algorithm and Particle Swarm Optimization. *2013 World Congress on Nature and Biologically Inspired Computing (Nabic)*, 22-28.

George, J., Krishna, B., George, V. I., Shreesha, C., & Menon, M. K. (2012). Stability analysis and design of PI controller using Kharitnov polynomial for rotary inverted pendulum. *Sensors and Transducers, 138*(3), 104-113.

Ghaemi, M., Akbarzadeh-T, M., & Jalaeian-F, M. (2012, 18-19 Oct. 2012). *Adaptive Interval Type-2 Fuzzy PI Sliding Mode Control with optimization of membership functions using genetic algorithm.* Paper presented at the Computer and Knowledge Engineering (ICCKE), 2012 2nd International eConference on.

Ghorbani, F., Shooredeli, M. A., & Teshnehlab, M. (2013). *Fault tolerant improvement with chaos synchronization using Fuzzy-PID control.* Paper presented at the 13th Iranian Conference on Fuzzy Systems, IFSC 2013.

Goldberg, D. E. (2002). The design of competent genetic algorithms: Steps toward a computational theory of innovation: Kluwer Academic Publishers, Dordrecht.

Hassan, M. U., Kadri, M. B., & Amin, I. (2013). Proficiency of Fuzzy Logic Controller for Stabilization of Rotary Inverted Pendulum based on LQR Mapping *Fuzzy Logic and Applications* (pp. 201-211): Springer.

Hassanzadeh, I., & Mobayen, S. (2011). Controller design for rotary inverted pendulum system using evolutionary algorithms. *Mathematical Problems in Engineering, 2011*.

Hassibi, B., Sayed, A. H., & Kailath, T. (1999). *Indefinite-Quadratic Estimation and Control: A Unified Approach to H2 and H-Infinity Theories* (Vol. 16): SIAM.

Haupt, R. L., & Haupt, S. E. (2004). *Practical genetic algorithms*: John Wiley & Sons.

Hercus, R., Wong, K. Y., & Ho, K. F. (2013) Balancing of a simulated inverted pendulum using the neurabase network model. *Vol. 8131 LNCS. Lecture Notes in Computer Science (including subseries Lecture Notes in Artificial Intelligence and Lecture Notes in Bioinformatics)* (pp. 527-536).

Hercus, R., Wong, K. Y., Shee, S. K., & Ho, K. F. (2013) Control of an inverted pendulum using the NeuraBase network model. *Vol. 8227 LNCS. Lecture Notes in Computer Science (including subseries Lecture Notes in Artificial Intelligence and Lecture Notes in Bioinformatics)* (pp. 605-615).

Hernandez, M. D., Melin, P., Mendez, G. M., Castillo, O., & Lopez-Juarez, I. (2015). A hybrid learning method composed by the orthogonal least-squares and the back-propagation learning algorithms for interval A2-C1 type-1 non-singleton type-2 TSK fuzzy logic systems. *Soft Computing, 19*(3), 661-678. doi:DOI 10.10 07/s00500-014-1287-8

Herrera, F. (2008). Genetic fuzzy systems: taxonomy, current research trends and prospects. *Evolutionary Intelligence, 1*(1), 27-46.

Hidalgo, D., Melin, P., & Castillo, O. (2012). An optimization method for designing type-2 fuzzy inference systems based on the footprint of uncertainty using genetic algorithms. *Expert Systems with Applications, 39*(4), 4590-4598. doi:DOI 10.1016/j.eswa.2011.10.003

Hosseini, R., Qanadli, S. D., Barman, S., Mazinani, M., Ellis, T., & Dehmeshki, J. (2012). An Automatic Approach for Learning and Tuning Gaussian Interval Type-2 Fuzzy Membership Functions Applied to Lung CAD Classification System. *Ieee Transactions on Fuzzy Systems, 20*(2), 224-234. doi:Doi 10.1109/Tfuzz.2011.2172616

Hsu, C. H., & Juang, C. F. (2013). Evolutionary Robot Wall-Following Control Using Type-2 Fuzzy Controller With Species-DE-Activated Continuous ACO. *Ieee Transactions on Fuzzy Systems, 21*(1), 100-112. doi:Doi 10.1109/Tfu zz.20 12.2202665

Hung, J. Y., Gao, W., & Hung, J. C. (1993). Variable structure control: a survey. *Industrial Electronics, IEEE Transactions on, 40*(1), 2-22.

Ileš, Š., Matuško, J., & Kolonić, F. (2011). *TP transformation based control of rotary pendulum.* Paper presented at the MIPRO, 2011 Proceedings of the 34th International Convention.

Jadlovska, S., & Sarnovsky, J. (2013). A complex overview of modeling and control of the rotary single inverted pendulum system. *Advances in Electrical and Electronic Engineering, 11*(2), 73-85. doi:10.15598/aeee.v11i2.773

Jadlovská, S., & Sarnovský, J. (2013). *Application of the state-dependent Riccati equation method in nonlinear control design for inverted pendulum systems.* Paper presented at the SISY 2013 - IEEE 11th International Symposium on Intelligent Systems and Informatics, Proceedings.

Jadlovský, S., & Sarnovský, J. (2013). Modelling of Classical and Rotary Inverted Pendulum Systems–a Generalized Approach. *Journal of Electrical Engineering, 64*(1), 12-19.

Juang, C. F., & Jang, W. S. (2014). A type-2 neural fuzzy system learned through type-1 fuzzy rules and its FPGA-based hardware implementation. *Applied Soft Computing, 18*, 302-313. doi:DOI 10.1016/j.asoc.2014.01.006

Kao, Y.-T., & Zahara, E. (2008). A hybrid genetic algorithm and particle swarm optimization for multimodal functions. *Applied Soft Computing, 8*(2), 849-857. Retrieved from

Karnik, N. N., & Mendel, J. M. (1998a, 4-9 May 1998). *Introduction to type-2 fuzzy logic systems.* Paper presented at the Fuzzy Systems Proceedings, 1998. IEEE World Congress on Computational Intelligence., The 1998 IEEE International Conference on.

Karnik, N. N., & Mendel, J. M. (1998). *Introduction to type-2 fuzzy logic systems.* Paper presented at the Fuzzy Systems Proceedings, 1998. IEEE World Congress on Computational Intelligence., The 1998 IEEE International Conference on.

Karnik, N. N., & Mendel, J. M. (1998b, 11-14 Oct 1998). *Type-2 fuzzy logic systems: type-reduction.* Paper presented at the Systems, Man, and Cybernetics, 1998. 1998 IEEE International Conference on.

Karnik, N. N., Mendel, J. M., & Qilian, L. (1999). Type-2 fuzzy logic systems. *Fuzzy Systems, IEEE Transactions on, 7*(6), 643-658. Retrieved from doi:10.1109/91.811231

Khalil, H. K., & Grizzle, J. (1996). *Nonlinear systems* (Vol. 3): Prentice hall New Jersey.

Khooban, M. H., Abadi, D. N. M., Alfi, A., & Siahi, M. (2014). Optimal Type-2 Fuzzy Controller For HVAC Systems. *Automatika, 55*(1), 69-78. doi:DOI 10.7305/automatika.2014.01.219

Khosla, M., Sarin, R. K., & Uddin, M. (2012, 11-13 May 2012). *Identification of Type-2 Fuzzy Models for Time-Series Forecasting Using Particle Swarm Optimization.* Paper presented at the Communication Systems and Network Technologies (CSNT), 2012 International Conference on.

Kiani, M., Mohammadi, S. M. A., & Gharaveisi, A. A. (2013). A bacterial foraging optimization approach for tuning type-2 fuzzy logic controller. *Turkish Journal of*

Electrical Engineering and Computer Sciences, 21(1), 263-273. doi:Doi 10.3906/Elk-1107-10

Kim, D. H. (2007). GA–PSO based vector control of indirect three phase induction motor. *Applied Soft Computing, 7*(2), 601-611.

Kim, D. H., Abraham, A., & Cho, J. H. (2007). A hybrid genetic algorithm and bacterial foraging approach for global optimization. *Information Sciences, 177*(18), 3918-3937.

Kim, W. D., Oh, S. K., Seo, K. S., & Pedrycz, W. (2013). A Design of FCM-based Interval Type-2 Fuzzy Neural Network Classifier with the Aid of PSO. *Proceedings of the 2013 Joint Ifsa World Congress and Nafips Annual Meeting (Ifsa/Nafips)*, 1209-1214.

Knutson, A. J. (2012). Application of Kane's method to incorporate attitude dynamics into the circular restricted three-body problem.

Komistek, R. D., Stiehl, J. B., Dennis, D. A., Paxson, R. D., & Soutas-Little, R. W. (1997). Mathematical model of the lower extremity joint reaction forces using Kane's method of dynamics. *J Biomech*, *31*(2), 185-189.

Krohling, R., Jaschek, H., & Rey, J. (1997). *Designing PI/PID controllers for a motion control system based on genetic algorithms.* Paper presented at the Intelligent Control, 1997. Proceedings of the 1997 IEEE International Symposium on.

Kumbasar, T., & Hagras, H. (2014). Big Bang-Big Crunch optimization based interval type-2 fuzzy PID cascade controller design strategy. *Information Sciences, 282*, 277-295. doi:DOI 10.1016/j.ins.2014.06.005

Kumbasar, T., & Hagras, H. (2015). Interval Type-2 Fuzzy PID Controllers. In J. Kacprzyk & W. Pedrycz (Eds.), *Springer Handbook of Computational Intelligence* (pp. 285-294): Springer Berlin Heidelberg.

Kuo, T., Huang, Y., & Hong, B. (2009). *Adaptive PID with sliding mode control for the rotary inverted pendulum system.* Paper presented at the Advanced Intelligent Mechatronics, 2009. AIM 2009. IEEE/ASME International Conference on.

Kurode, S., Chalanga, A., & Bandyopadhyay, B. (2011). *Swing-Up and Stabilization of Rotary Inverted Pendulum using Sliding Modes.* Paper presented at the Preprints of the 18th IFAC World Congress Milano (Italy) August.

Lee, W.-c., Lyu, Y.-Y., Hsu, T.-Y., & Wei, C.-c. (2014). *Using the Taguchi methods to study the balance control of a rotary inverted pendulum.* Paper presented at the Advanced Robotics and Intelligent Systems (ARIS), 2014 International Conference on.

Li, C., Zhang, X., & Yi, J. (2012, 25-27 July 2012). *SIRMs connected type-2 fuzzy-genetic backing up control of the truck-trailer system.* Paper presented at the Control Conference (CCC), 2012 31st Chinese.

Li, C. D., Zhang, G. Q., Wang, M., & Yi, J. Q. (2013). Data-driven modeling and optimization of thermal comfort and energy consumption using type-2 fuzzy method. *Soft Computing, 17*(11), 2075-2088. doi:DOI 10.1007/s00500-013-1117-4

Li, C. T., Lee, C. H., Chang, F. Y., & Lin, C. M. (2014). An Interval Type-2 Fuzzy System with a Species-Based Hybrid Algorithm for Nonlinear System Control Design. *Mathematical Problems in Engineering*. Doi 10.1155/2014/735310

Li, J. H. (2013). *Composite fuzzy control of a rotary inverted pendulum.* Paper presented at the IEEE International Symposium on Industrial Electronics.

Liu, P., Yang, L. X., Wang, L., & Li, S. K. (2014). A solid transportation problem with type-2 fuzzy variables. *Applied Soft Computing, 24*, 543-558. doi:DOI 10.1016/j.asoc.2014.08.005

Liu, S. (2014). *Stable synchronization of two Furuta pendulums network based on the method of controlled Lagrangian.* Paper presented at the Proceedings of the 33rd Chinese Control Conference, CCC 2014.

Long, N. C., & Meesad, P. (2014). An optimal design for type-2 fuzzy logic system using hybrid of chaos firefly algorithm and genetic algorithm and its application to sea level prediction. *Journal of Intelligent & Fuzzy Systems, 27*(3), 1335-1346. doi:Doi 10.3233/Ifs-131101

Long, Z. Q., Yuan, Y., & Long, W. (2014). Designing fuzzy controllers with variable universes of discourse using input-output data. *Engineering Applications of Artificial Intelligence, 36*, 215-221. doi:DOI 10.1016/j.engappai.2014.07.011

Lu, T.-C. (2015). Genetic-algorithm-based type reduction algorithm for interval type-2 fuzzy logic controllers. *Engineering Applications of Artificial Intelligence, 42*, 36-44. Retrieved from

Mahmoodian, H. (2012). Predicting the continuous values of breast cancer relapse time by type-2 fuzzy logic system. *Australasian Physical & Engineering Sciences in Medicine, 35*(2), 193-204. doi:DOI 10.1007/s13246-012-0147-z

Maldonado, Y., & Castillo, O. (2012, 6-8 Aug. 2012). *Comparison between multiobjective GA and PSO for parameter optimization of AT2-FLC for a real application in FPGA.* Paper presented at the Fuzzy Information Processing Society (NAFIPS), 2012 Annual Meeting of the North American.

Maldonado, Y., & Castillo, O. (2012). Genetic Design of an Interval Type-2 Fuzzy Controller for Velocity Regulation in a DC Motor. *International Journal of Advanced Robotic Systems, 9*. Doi 10.5772/51188

Maldonado, Y., Castillo, O., & Melin, P. (2013). Particle swarm optimization of interval type-2 fuzzy systems for FPGA applications. *Applied Soft Computing, 13*(1), 496-508.doi:DOI 10.1016/j.asoc.2012.08.032

Maldonado, Y., Castillo, O., & Melin, P. (2014). A multi-objective optimization of type-2 fuzzy control speed in FPGAs. *Applied Soft Computing, 24*, 1164-1174. doi:DOI 10.1016/j.asoc.2014.04.041

Man, K.-F., TANG, K. S., & Kwong, S. (2012). *Genetic algorithms: Concepts and designs*: Springer Science & Business Media.

Mandić, P., Lazarević, M., Stojanović, S., & Ristanović, M. (2014). REAL TIME CONTROL OF ROTARY INVERTED PENDULUM. *Annals of the Faculty of Engineering Hunedoara-International Journal of Engineering, 12*(2).

Mandic, P., Lazarevic, M. P., & Sekara, T. B. (2014). *Fractional order PD control of Furuta pendulum: D-decomposition approach.* Paper presented at the 2014 International Conference on Fractional Differentiation and Its Applications, ICFDA 2014.

Martínez-Soto, R., Castillo, O., & Aguilar, L. T. (2014). Type-1 and Type-2 fuzzy logic controller design using a Hybrid PSO–GA optimization method. *Information Sciences, 285*, 35-49. doi:10.1016/j.ins.2014.07.012

Martinez-Soto, R., Castillo, O., Aguilar, L. T., & Rodriguez, A. (2015). A hybrid optimization method with PSO and GA to automatically design Type-1 and Type-2 fuzzy logic controllers. *International Journal of Machine Learning and Cybernetics, 6*(2), 175-196. doi:DOI 10.1007/s13042-013-0170-8

Mary, P. M., & Marimuthu, N. (2009). Minimum time swing up and stabilization of rotary inverted pendulum using pulse step control. *Iranian Journal of Fuzzy Systems, 6*(3), 1-15.

Mathew, N. J., Rao, K. K., & Sivakumaran, N. (2013). *Swing up and stabilization control of a rotary inverted pendulum.* Paper presented at the IFAC Proceedings Volumes (IFAC-PapersOnline).

Melendez, A., Castillo, O., & Melin, P. (2013, 24-28 June 2013). *Genetic optimization of interval type-2 fuzzy reactive controllers for mobile robots.* Paper presented at the IFSA World Congress and NAFIPS Annual Meeting (IFSA/NAFIPS), 2013 Joint.

Melin, P., Astudillo, L., Castillo, O., Valdez, F., & Garcia, M. (2013). Optimal design of type-2 and type-1 fuzzy tracking controllers for autonomous mobile robots under perturbed torques using a new chemical optimization paradigm. *Expert Systems with Applications, 40*(8), 3185-3195.

Melin, P., & Pulido, M. (2014). Optimization of Ensemble Neural Networks with Type-2 Fuzzy Integration of Responses for the Dow Jones Time Series Prediction. *Intelligent Automation and Soft Computing, 20*(3), 403-418. doi:Doi 10.1080/10798587.2014.893047

Melin, P., Sanchez, D., & Castillo, O. (2012). Genetic optimization of modular neural networks with fuzzy response integration for human recognition. *Information Sciences, 197*, 1-19. doi:DOI 10.1016/j.ins.2012.02.027

Mendel, J., Hagras, H., Tan, W.-W., Melek, W. W., & Ying, H. (2014). *Introduction to Type-2 Fuzzy Logic Control: Theory and Applications*: John Wiley & Sons.

Mendel, J. M. (2001). Uncertain rule-based fuzzy logic system: introduction and new directions. Retrieved from

Mendel, J. M. (2007). Advances in type-2 fuzzy sets and systems. *Information Sciences, 177*(1), 84-110. Retrieved from

Mendel, J. M. (2007). Type-2 fuzzy sets and systems: an overview. *Computational Intelligence Magazine, IEEE, 2*(1), 20-29. doi:10.1109/MCI.2007.380672

Mendel, J. M. (2014). General type-2 fuzzy logic systems made simple: a tutorial. *Fuzzy Systems, IEEE Transactions on, 22*(5), 1162-1182.

Mendel, J. M. (2014). General Type-2 Fuzzy Logic Systems Made Simple: A Tutorial. *Ieee Transactions on Fuzzy Systems, 22*(5), 1162-1182. doi:Doi 10.1109/Tfuzz.2013.2286414

Mendel, J. M. (2015). On Type-Reduction Versus Direct Defuzzification for Type-2 Fuzzy Logic Systems *Fifty Years of Fuzzy Logic and its Applications* (pp. 387-399): Springer.

Mendel, J. M., John, R. I., & Feilong, L. (2006). Interval Type-2 Fuzzy Logic Systems Made Simple. *Fuzzy Systems, IEEE Transactions on, 14*(6), 808-821. Retrieved from doi:10.1109/TFUZZ.2006.879986

Mendel, J. M., & Rajati, M. R. (2015). Critique of "Footprint of uncertainty for type-2 fuzzy sets"[9]. *Information Sciences, 308*, 1-2.

Moreno-Valenzuela, J., Aguilar-Avelar, C., Puga-Guzman, S. A., & Santibanez, V. (2016). Adaptive Neural Network Control for the Trajectory Tracking of the Furuta Pendulum. *Ieee Transactions on Cybernetics*. doi:10.1109/TCYB.2015.2509863

Muske, K. R., Ashrafiuon, H., Nersesov, S., & Nikkhah, M. (2012). Optimal Sliding Mode Cascade Control for Stabilization of Underactuated Nonlinear Systems. *Journal of Dynamic Systems Measurement and Control-Transactions of the Asme, 134*(2). doi:Artn 021020Doi 10.1115/1.4005367

Nath, V., & Mitra, R. (2014). Swing-up and Control of Rotary Inverted Pendulum using Pole Placement with Integrator. *2014 Recent Advances in Engineering and Computational Sciences (Raecs).*

Nath, V., & Mitra, R. (2014). *Swing-up and control of Rotary Inverted Pendulum using pole placement with integrator.* Paper presented at the Engineering and Computational Sciences (RAECS), 2014 Recent Advances in.

Nguyen Cong, L., & Meesad, P. (2013, 13-13 July 2013). *Meta-heuristic algorithms applied to the optimization of type-1 and type 2 TSK fuzzy logic systems for sea water level prediction.* Paper presented at the Computational Intelligence & Applications (IWCIA), 2013 IEEE Sixth International Workshop on.

Nguyen, H. C. T., & Shen, A. W. (2011). Using Hybrid And LQR Method Control Of A Self-Erecting Rotary Inverted Pendulum System Based On PIC 18F4431. *International Journal of Computer Science and Information Technologies, 2*(6), 2548-2553.

Nguyen, S. D., Choi, S. B., & Nguyen, Q. H. (2014). An optimal design of interval type-2 fuzzy logic system with various experiments including magnetorheological fluid damper. *Proceedings of the Institution of Mechanical Engineers Part C-Journal of Mechanical Engineering Science, 228*(17), 3090-3106. doi:Doi 10.1177/0954406214526585

Nguyen, T., Khosravi, A., Creighton, D., & Nahavandi, S. (2015). Medical data classification using interval type-2 fuzzy logic system and wavelets. *Applied Soft Computing, 30*, 812-822.

Nguyen, T., Khosravi, A., Nahavandi, S., & Creighton, D. (2013). Neural Network and Interval Type-2 Fuzzy System for Stock Price Forecasting. *2013 Ieee International Conference on Fuzzy Systems (Fuzz - Ieee 2013)*.

Niknam, T., Khooban, M. H., Kavousifard, A., & Soltanpour, M. R. (2014). An optimal type II fuzzy sliding mode control design for a class of nonlinear systems. *Nonlinear Dynamics, 75*(1-2), 73-83. doi:DOI 10.1007/s11071-013-1050-1

NøRgaard, M., Poulsen, N. K., & Ravn, O. (2000). New developments in state estimation for nonlinear systems. *Automatica, 36*(11), 1627-1638.

Nukulwuthiopas, W., Laowattana, S., & Maneewarn, T. (2002). *Dynamic modeling of a one-wheel robot by using Kane's method.* Paper presented at the Industrial Technology, 2002. IEEE ICIT'02. 2002 IEEE International Conference on.

Ogata, K. (1998). *System dynamics* (Vol. 3): Prentice Hall New Jersey.

Oh, S.-K., Jang, H.-J., & Pedrycz, W. (2011). Optimized fuzzy PD cascade controller: A comparative analysis and design. *Simulation Modelling Practice and Theory, 19*(1), 181-195. doi:http://dx.doi.org/10.1016/j.simpat.2010.06.004

Oh, S.-K., Jung, S.-H., & Pedrycz, W. (2009). Design of optimized fuzzy cascade controllers by means of Hierarchical Fair Competition-based Genetic Algorithms. *Expert Systems with Applications, 36*(9), 11641-11651. doi:http://dx.doi.org/10.1016/j.eswa.2009.03.027

Oh, S. K., Jang, H. J., & Pedrycz, W. (2011). A comparative experimental study of type-1/type-2 fuzzy cascade controller based on genetic algorithms and particle swarm optimization. *Expert Systems with Applications, 38*(9), 11217-11229. doi:DOI 10.1016/j.eswa.2011.02.169

Oh, S. K., Kim, W. D., & Pedrycz, W. (2012). Design of optimized cascade fuzzy controller based on differential evolution: Simulation studies and practical insights. *Engineering Applications of Artificial Intelligence, 25*(3), 520-532. doi:DOI 10.1016/j.engappai.2012.01.002

Oltean, S.-E. (2014). Swing-up and Stabilization of the Rotational Inverted Pendulum Using PD and Fuzzy-PD Controllers. *Procedia Technology, 12*, 57-64.

Oltean, S.-E., & Duka, A.-V. (2014). Balance Control System Using Microcontrollers for a Rotational Inverted Pendulum. *Procedia Technology, 12*(0), 11-19. doi:http://dx.doi.org/10.1016/j.protcy.2013.12.450

Ordaz, P., & Poznyak, A. (2012). *The Furuta's pendulum stabilization without the use of a mathematical model: Attractive Ellipsoid Method with KL-adaptation.* Paper presented at the Proceedings of the IEEE Conference on Decision and Control.

Ordaz, P., & Poznyak, A. (2016). Adaptive-Robust Stabilization of the Furuta's Pendulum Via Attractive Ellipsoid Method. *Journal of Dynamic Systems, Measurement and Control, Transactions of the ASME, 138*(2). doi:10.1115/1.4032130

Pan, F., Xue, D., Chen, D., & Jia, X. (2012). *Sliding mode variation structure network controller design based on inverted pendulum.* Paper presented at the Proceedings of the 2012 24th Chinese Control and Decision Conference, CCDC 2012.

Panda, M. K., Pillai, G. N., & Kumar, V. (2012). Power System Stabilizer Design: Interval Type-2 Fuzzy logic controller Approach. *2012 2nd International Conference on Power, Control and Embedded Systems (Icpces 2012)*.

Pavlyukevich, I. (2007). Lévy flights, non-local search and simulated annealing. *Journal of Computational Physics, 226*(2), 1830-1844.

Petchithai, V., Chitra, V. S., Manimaran, M., & Senthilrajan, T. (2015). Design of multivariable systems controlled by novelty based techniques. *Indian Journal of Science and Technology, 8*(5), 407-412. doi:10.17485/ijst/2015/v8i5/60471

Pulido, M., Melin, P., & Castillo, O. (2013, 12-14 Aug. 2013). *Optimization of ensemble neural networks with type-2 fuzzy response integration for predicting the Mackey-Glass time series.* Paper presented at the Nature and Biologically Inspired Computing (NaBIC), 2013 World Congress on.

Pulido, M., Melin, P., & Castillo, O. (2014). Particle swarm optimization of ensemble neural networks with fuzzy aggregation for time series prediction of the Mexican Stock Exchange. *Information Sciences, 280*, 188-204. doi:DOI 10.1016/j.ins.2014.05.006

Qi-Ye, Z., Ze-Ming, S., & Feng, Z. (2014, 6-11 July 2014). *A clustering routing protocol for wireless sensor networks based on type-2 fuzzy logic and ACO.* Paper presented at the Fuzzy Systems (FUZZ-IEEE), 2014 IEEE International Conference on.

Qilian, L., & Mendel, J. M. (2000). Interval type-2 fuzzy logic systems: theory and design. *Fuzzy Systems, IEEE Transactions on, 8*(5), 535-550. Retrieved from doi:10.1109/91.873577

Qin, H., Shao, W., & Guo, L. (2014). *Research and verification on swing-up control algorithm of rotary inverted pendulum.* Paper presented at the Control and Decision Conference (2014 CCDC), The 26th Chinese.

Quyen, N., Thuyen, N., Hoc, N. Q., & Hien, N. (2012). *Rotary inverted pendulum and control of rotary inverted pendulum by artificial neural network.* Paper presented at the Proceeding National Conference Theory Physics.

Ramírez-Neria, M., Sira-Ramírez, H., Garrido-Moctezuma, R., & Luviano-Juarez, A. (2014). Linear active disturbance rejection control of underactuated systems: The case of the Furuta pendulum. *ISA Transactions, 53*(4), 920-928.

Ramírez-Neria, M., Sira-Ramírez, H., Garrido-Moctezuma, R., & Luviano-Juarez, A. (2014). *On the linear active disturbance rejection control of the Furuta pendulum.* Paper presented at the Proceedings of the American Control Conference.

Ramírez-Neria, M., Sira-Ramírez, H., Garrido-Moctezuma, R., & Luviano-Juárez, A. (2014). Linear active disturbance rejection control of underactuated systems: The case of the Furuta pendulum. *ISA Transactions, 53*(4), 920-928. doi:http://dx.doi.org/10.1016/j.isatra.2013.09.023

Ren, Q., Baron, L., & Balazinski, M. (2006). *Type-2 Takagi-Sugeno-Kang fuzzy logic modeling using subtractive clustering.* Paper presented at the Fuzzy Information Processing Society, 2006. NAFIPS 2006. Annual meeting of the North American.

Rubio, J. d. J., Zamudio, Z., Pacheco, J., & Mújica Vargas, D. (2013). Proportional derivative control with inverse dead-zone for pendulum systems. *Mathematical Problems in Engineering, 2013*.

Rudra, S., Barai, R., Maitra, M., Mandal, D., Ghosh, S., Dam, S., . . . Bhattacharyya, P. (2013). *Stabilization of Furuta Pendulum: A backstepping based hierarchical sliding Mode approach with disturbance estimation.* Paper presented at the Intelligent Systems and Control (ISCO), 2013 7th International Conference on.

Ryalat, M., & Laila, D. S. (2013). IDA-PBC for a Class of Underactuated Mechanical Systems with Application to a Rotary Inverted Pendulum. *2013 Ieee 52nd Annual Conference on Decision and Control (Cdc)*, 5240-5245.

S.N.Sivanandam, & S.N.Deepa. (2008). *Introduction to Genetic Algorithms*: Springer.

Sanchez, D., & Melin, P. (2013a, 24-28 June 2013). *Hierarchical Genetic Algorithm for Type-2 fuzzy Integration applied to Human Recognition.* Paper presented at the IFSA World Congress and NAFIPS Annual Meeting (IFSA/NAFIPS), 2013 Joint.

Sanchez, D., & Melin, P. (2013b). Multi-Objective Hierarchical Genetic Algorithm for Modular Granular Neural Network Optimization. *Soft Computing Applications in Optimization, Control, and Recognition, 294*, 157-185.

Sánchez, D., Melin, P., & Castillo, O. (2015). Fuzzy system optimization using a hierarchical genetic algorithm applied to pattern recognition *Intelligent Systems' 2014* (pp. 713-720): Springer.

Sanchez, M. A., Castro, J. R., Perez-Ornelas, F., & Castillo, O. (2013, 24-28 June 2013). *A hybrid method for IT2 TSK formation based on the principle of justifiable granularity and PSO for spread optimization.* Paper presented at the IFSA World Congress and NAFIPS Annual Meeting (IFSA/NAFIPS), 2013 Joint.

Sayed, M. M., Saad, M. S., Emara, H. M., & Abou El-Zahab, E. E. (2013a). Improving the performance of the Egyptian second testing nuclear research reactor using interval type-2 fuzzy logic controller tuned by modified biogeography-based optimization. *Nuclear Engineering and Design, 262*, 294-305. doi:DOI 10.1016/j.nucengdes.2013.04.035

Sayed, M. M., Saad, M. S., Emara, H. M., & Abou El-Zahab, E. E. (2013b, 25-28 Feb. 2013). *A novel method for type-2 fuzzy logic controller design using a modified biogeography-based optimization.* Paper presented at the Industrial Technology (ICIT), 2013 IEEE International Conference on.

Seman, P., Rohal'-Ilkiv, B., & Salaj, M. (2013). Swinging up the Furuta pendulum and its stabilization via model predictive control. *Journal of Electrical Engineering, 64*(3), 152-158.

Shahsadeghi, M., Khooban, M. H., & Niknam, T. (2014). A robust and simple optimal type II fuzzy sliding mode control strategy for a class of nonlinear chaotic systems. *Journal of Intelligent & Fuzzy Systems, 27*(4), 1849-1859. doi:Doi 10.3233/Ifs-141151

Shamsudin, M. A., Mamat, R., & Nawawi, S. W. (2013). Dynamic modelling and optimal control scheme of wheel inverted pendulum for mobile robot application. *International Journal of Control Theory and Computer Modeling, 3*(6), 1-20.

Shill, P. C., Amin, M. F., Akhand, M. A. H., & Murase, K. (2012, 10-15 June 2012). *Optimization of interval type-2 fuzzy logic controller using quantum genetic algorithms.* Paper presented at the Fuzzy Systems (FUZZ-IEEE), 2012 IEEE International Conference on.

Singh, P., & Borah, B. (2014). Forecasting stock index price based on M-factors fuzzy time series and particle swarm optimization. *International Journal of Approximate Reasoning, 55*(3), 812-833. doi:DOI 10.1016/j.ijar.2013.09.014

Singh, Y., Kumar, A., & Mitra, R. (2012). *Design of ANFIS controller based on fusion function for rotary inverted pendulum.* Paper presented at the Advances in Power Conversion and Energy Technologies (APCET), 2012 International Conference on.

Son, L. H. (2014). Enhancing clustering quality of geo-demographic analysis using context fuzzy clustering type-2 and particle swarm optimization. *Applied Soft Computing, 22*, 566-584. doi:DOI 10.1016/j.asoc.2014.04.025

Soto, J., Melin, P., & Castillo, O. (2014, 9-12 Dec. 2014). *Optimization of the type-1 and interval type-2 fuzzy integrators in Ensembles of ANFIS models for prediction of the Dow Jones time series.* Paper presented at the Computational Intelligence and Data Mining (CIDM), 2014 IEEE Symposium on.

Stamnes, Ø. N., Aamo, O. M., & Kaasa, G. O. (2011). A constructive speed observer design for general EulerLagrange systems. *Automatica, 47*(10), 2233-2238. doi:10.1016/j.automatica.2011.08.006

Sun, X., Sun, W., Wang, J., Zhang, Y., & Gao, Y. (2016). Using a Grey–Markov model optimized by Cuckoo search algorithm to forecast the annual foreign tourist arrivals to China. *Tourism Management, 52*, 369-379.

Sun, Z., Wang, N., & Bi, Y. R. (2015). Type-1/type-2 fuzzy logic systems optimization with RNA genetic algorithm for double inverted pendulum. *Applied Mathematical Modelling, 39*(1), 70-85.doi:DOI 10.1016/j.apm.2014.04.035

Taskin, A., & Kumbasar, T. (2015, December). An Open Source Matlab/Simulink Toolbox for Interval Type-2 Fuzzy Logic Systems. In*Computational Intelligence, 2015 IEEE Symposium Series on* (pp. 1561-1568). IEEE.

Tewari, A. (2002). MODER CONTROL DESIGN.

Tsuge, Y., Kawanishi, M., Narikiyo, T., & Jennawasin, T. (2014). *Nonlinear controller design based on polynomial and non-polynomial representation.* Paper presented at the IEEE International Conference on Control and Automation, ICCA.

Turker, T., Gorgun, H., & Cansever, G. (2013). Stabilisation of a class of 2-DOF underactuated mechanical systems via direct Lyapunov approach. *International Journal of Control, 86*(6), 1137-1148. doi:10.1080/00207179.2013.784809

Türker, T., Görgün, H., & Cansever, G. (2012). Lyapunov's direct method for stabilization of the Furuta pendulum. *Turkish Journal of Electrical Engineering and Computer Sciences, 20*(1), 99-110. doi:10.3906/elk-1007-653

Ufnalski, B., Kaszewski, A., & Grzesiak, L. M. (2015). Particle Swarm Optimization of the Multioscillatory LQR for a Three-Phase Four-Wire Voltage-Source Inverter With an Output Filter. *Industrial Electronics, IEEE Transactions on, 62*(1), 484-493.

Ul Hassan, M., Kadri, M. B., & Amin, I. (2013) Proficiency of fuzzy logic controller for stabilization of rotary inverted pendulum based on LQR mapping. *Vol. 8256 LNAI. Lecture Notes in Computer Science (including subseries Lecture Notes in Artificial Intelligence and Lecture Notes in Bioinformatics)* (pp. 201-211).

van Kats, C. (2004). Nonlinear control of a Furuta Rotary inverted pendulum. *DCT report*(2004.69).

Videcoq, E., Girault, M., Bouderbala, K., Nouira, H., Salgado, J., & Petit, D. (2015). Parametric investigation of Linear Quadratic Gaussian and Model Predictive Control approaches for thermal regulation of a high precision geometric measurement machine. *Applied Thermal Engineering, 78*, 720-730.

Wei, X., Mottershead, J. E., & Ram, Y. M. (2016). Partial pole placement by feedback control with inaccessible degrees of freedom. *Mechanical Systems and Signal Processing, 70*, 334-344.

Xia, W., & Wu, Z. (2005). An effective hybrid optimization approach for multi-objective flexible job-shop scheduling problems. *Computers & Industrial Engineering, 48*(2), 409-425. Retrieved from

Yan, Q. (2003). *Output tracking of underactuated rotary inverted pendulum by nonlinear controller.* Paper presented at the Decision and Control, 2003. Proceedings. 42nd IEEE Conference on.

Yang, X.-S., & Deb, S. (2009). *Cuckoo search via Lévy flights.* Paper presented at the Nature & Biologically Inspired Computing, 2009. NaBIC 2009. World Congress on.

Yang, X.-S., & Deb, S. (2010). Engineering optimisation by cuckoo search. *International Journal of Mathematical Modelling and Numerical Optimisation, 1*(4), 330-343.

Yang, X.-S., & Deb, S. (2014). Cuckoo search: recent advances and applications. *Neural Computing and Applications, 24*(1), 169-174.

Yao, B., Hagras, H., Alghazzawi, D., & Alhaddad, M. J. (2013). A Big Bang-Big Crunch Optimization for a Type-2 Fuzzy Logic based Human Behaviour Recognition System in Intelligent Environments. *2013 Ieee International Conference on Systems, Man, and Cybernetics (Smc 2013)*, 2880-2886. doi:Doi 10.1109/Smc.2013.491

Yesil, E. (2014). Interval type-2 fuzzy PID load frequency controller using Big Bang-Big Crunch optimization. *Applied Soft Computing, 15*, 100-112. doi:DOI 10.1016/j.asoc.2013.10.031

Zadeh, L. A. (1965). Fuzzy sets. *Information and control, 8*(3), 338-353.

Zadeh, L. A. (1974). *The concept of a linguistic variable and its application to approximate reasoning*: Springer.

Zhang, J., & Zhang, Y. P. (2011). Optimal Linear Modeling and its Applications on Swing-up and Stabilization Control for Rotary Inverted Pendulum. *2011 30th Chinese Control Conference (Ccc)*, 493-500.

Zhang, Z., & Zhang, S. (2012). Type-2 fuzzy soft sets and their applications in decision making. *Journal of Applied Mathematics, 2012*.

PUBLICATIONS

(a) *ISI INDEX JOURNALS*

1. Hamza, M. F., Yap, H. J., & Choudhury, I. A. (2015). Recent advances on the use of meta-heuristic optimization algorithms to optimize the type-2 fuzzy logic systems in intelligent control. *Neural Computing and Applications*, 1-21.
2. Hamza, M. F., Yap, H. J., & Choudhury, I. A. (2015). Genetic algorithm and particle swarm optimization based cascade interval type 2 fuzzy PD controller for rotary inverted pendulum system. *Mathematical Problems in Engineering, 2015*.
3. Hamza, M. F., Yap, H. J., & Choudhury, I. A. (2016). Advances on the Use of Meta-Heuristic Algorithms to Optimize Type-2 Fuzzy Logic Systems for Prediction, Classification, Clustering and Pattern Recognition. *Journal of Computational and Theoretical Nanoscience, 13*(1), 96-109.

(b) *SCOPUS JOURNAL*

Hamza, M. F., Yap, H. J., Choudhury, I. A., Isa, A. & Zimit, A. Y. (2016). Simulation studies for stabilization control of Furuta Pendulum System using Cascade Fuzzy PD controller. *International Journal of Simulation- Systems, Science and Technology (SCOPUS Cited Publication*)

(c) **CONFERENCE**

Hamza, M. F., Yap, H. J., Choudhury, I. A., & Isa, A. I. (2016, 1-3 March.). Application of Kane's Method for Dynamic Modeling of Rotary Inverted Pendulum System. Paper presented at the micro and nano technologies, modelling and simulation (MNTMSIM 2016), 1st International Conference On.